A Mathematical Study of Environmental Effects and Genetic Drug Resistance on the Life Cycle of the Nematode *Teladorsagia circumcincta*

Andrea Sherriff

Ph.D. Thesis

Department of Statistics and Modelling Science
University of Strathclyde
Glasgow, U.K.

1996

Abstract

The parasitic nematode, *Teladorsagia (Ostertagia) circumcincta* is the primary cause of Parasitic Gastro-Enteritis (PGE) in lambs in Britain. Control of this parasite has largely depended on the use of broad spectrum anthelmintic drugs since their inception three decades ago. Widespread and unconstrained use of anthelmintics has resulted in selection for resistant strains of nematode, particularly within the *T. circumcincta* species.

Control of PGE now involves optimizing parasite control whilst preserving the susceptibility of the parasites to the anti-parasitic drugs.

Two aspects of the epidemiology of *T. circumcincta* are investigated in this thesis. First, the effect of temperature on the development and survival of the free-living stages is investigated. The conventional nematode development models are replaced by more sophisticated and biologically meaningful methods of describing temperature-dependent development rate phenomena in nematodes. The effect of geographical, temporal and developmental variation on the population dynamics of *T. circumcincta* are explored to determine possible sources of observed variability in infection levels in the field.

Next, a suite of models generic to most direct life cycle parasites undergoing intensive drug therapy, is constructed and analysed. Provision is made within these models to explore the impact of important life history events such as refugia and immigration on the evolution of resistance. A novel technique in resistance control involving overwhelming a resistant strain of nematode with a susceptible strain is modelled and suggestions made for the practical implementation of such a method.

Acknowledgements

I would like to thank my supervisor, Professor George Gettinby for his encouragement, enthusiasm, patience and support over the past five years both academically and personally.

Many thanks to my friends, Louise, Gordon, Pauline, Kieran, Shahid, Michael, Ian, David, Iain, Tina, Ray and Isla, who kept their heads when I was losing mine, and without whom, this wouldn't have been so much fun.

A special thanks to Gary for being a soulmate throughout.

Finally, I want to thank all my family for their practical and emotional support, but particularly to my mum and dad, Liz and Eric, who gave me this wonderful opportunity and whose unconditional love and understanding made it all possible. I dedicate this thesis to them.

This research was supported by the Engineering and Physical Sciences Research Council.

Contents

Chapter 1

Introduction

1.1 Parasites and Parasitic Diseases

Parasitism, as defined by Soulsby (1969), is

> "... a state in which an organism, (the parasite), is metabolically dependent to a greater or lesser extent on another, (the host)".

An eloquent description of this dependency is given by Gordon (1948),

> "... a parasites existence is usually an elaborate compromise between extracting sufficient nourishment to maintain and propagate itself, and not impairing too much the vitality, or reducing the numbers of its host which is providing it with a home and a free ride."

Parasitic diseases of domestic livestock in the temperate, tropical and sub-tropical regions of the world impose massive constraints on economic growth and prosperity. In developing countries, such diseases can have devastating effects on animal and human populations. For example, it is estimated that approximately one third of the 150 million cattle distributed over 37 countries in Africa are at risk of trypanosomiasis, (Nagana), predominantly a cattle disease of sub-Saharan Africa. The causal agent of trypanosomiasis is the protozoal parasite of the genus *Trypanosoma* and is transmitted to the bovine host by the tsetse, (*Glossina* spp.). Consequently, 50 million humans risk contracting sleeping sickness, the human form of trypanosomiasis. After rabies, human trypanosomiasis is the most infectious of all communicable diseases on the African sub-continent. Losses in meat

production are estimated to be in the region of $5 billion per year. This figure does not include losses in milk production or bi-products of the cattle industry (ILRAD publication, 1988).

In the developed world, parasitic diseases pose less of a threat to humans. Good public health facilities and education programmes help to prevent infection and highly effective anti-parasitic drugs are widely available to treat infection.

Nevertheless, nematode parasitic diseases of domestic livestock in Western Europe, Australia and the U.S.A. are considered serious economic threats to the agricultural industry world-wide. Taylor (1938) stated that

> "...with the sole exception of the bacterial diseases of dairy cattle, the diseases of farm animals caused by parasitic worms are of greater economic importance than are any other group of diseases with which the husbandsman has to contend."

In Britain, gastro-intestinal trichostrongylid nematode parasites of sheep are considered one of the major threats to agriculture production, and cause significant economic loss. Directly measurable losses as a result of parasitic diseases include losses due to animal death, decreased meat, wool, and milk production and the cost of anti-parasitic drugs. It is estimated that reductions in wool yield, milk yield and liveweight gain in sheep infested with worms is around 26%, 17% and 52%, respectively (MAFF, 1991). Additional costs are incurred when produce from a treated animal cannot be used due to the enforcement of drug withdrawal periods, and when pastures cannot be grazed due to high levels of infection. In lambs alone, it has been estimated that losses of £30-40 million per year result from worm infestation (MAFF, 1991). Furthermore, animal welfare concerns coupled with environmental worries over chemical residues in the environment are mounting.

Three species of nematode are commonly considered to pose the most serious threat to sheep populations around Britain. These are the abomasal parasite *Teladorsagia circumcincta*, and the intestinal parasites *Trichostrongylus vitrinus* and *Nematodirus battus*. In Northern Britain, particularly during the summer months, sheep suffering from Parasitic Gastro-Enteritis, (PGE) would invariably be infested by a single species of nematode, namely *T. circumcincta* , (Jackson, 1989). This parasite is primarily responsible for PGE in lambs and is regarded as being one of the most important causes of losses in sheep flocks in Britain,

(Crofton, 1963).

1.2 The Life Cycle of *T. circumcincta*

The trichostrongylid nematode, *T. circumcincta* , like most helminths of sheep, has a direct life cycle consisting of free-living and intra-host stages. This life cycle is given in Figure 1.1.

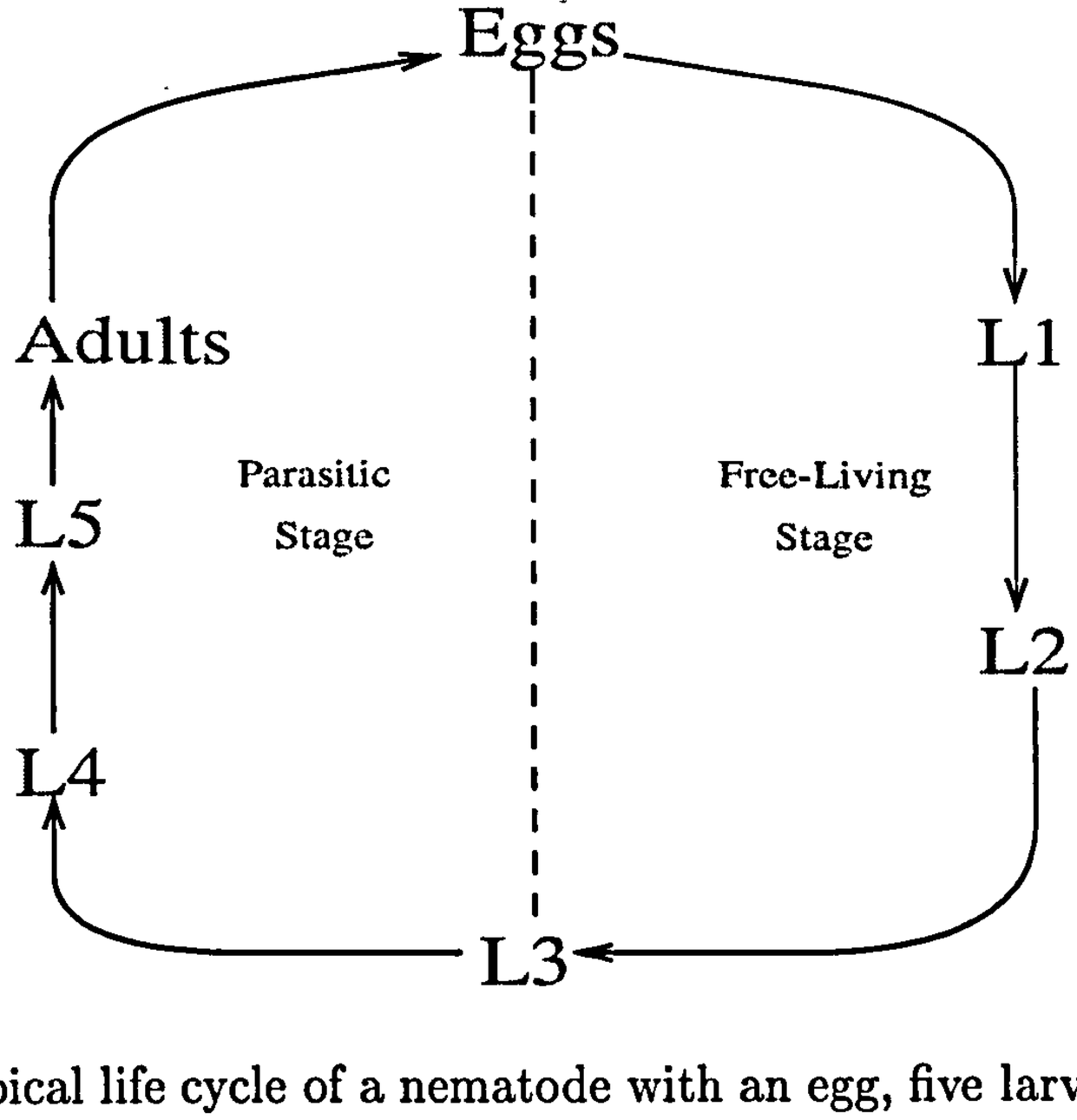

Figure 1.1: Typical life cycle of a nematode with an egg, five larval and an adult stage split into a free-living and a parasitic stage with a possibility of inhibition in the fourth larval stage.

Free-Living Stages of the Life Cycle

Eggs from the sexually mature female worms are expelled in the faeces of the sheep onto pasture and remain within the faecal mat during development to the first and second larval stages, namely L1 and L2.

Environmental factors play an influential role in the development and survival of the larval stages on pasture. Temperature is the primary factor governing the rate of development of individuals free-living on pasture, (Levine, 1963; Kates, 1965; Crofton, 1963; Young *et al*, 1980; Salih and Grainger, 1981; Pandey, 1993). In countries with warmer climates, such as Australia and South Africa, development

from the egg to the infective stage (L3) is more rapid than in the UK for all nematode species. This causes shorter generation times which in turn leads to higher infection levels on the pasture. The presence of moisture films on the grass swards facilitate the vertical migration of infective L3s, as they await ingestion by a suitable host. Therefore the relative humidity within the microhabitat is also an important factor in the development and survival of the free-living stages. Other factors such as soil type, herbage constituents, size, consistency and location of the faecal mat play a secondary role in influencing development and survival of the free-living stages (Crofton, 1963).

Intra-Host Stages of the Life Cycle

Grazing sheep will unknowingly ingest the questing larvae, which then pass through the alimentary canal of the animal. After exsheathment of the L3, further development takes place in the lumen of an abomasal gland, (Urquhart *et al*, 1991). Inhibition in the early fourth larval stage, (EL4), may occur for any period up to 6 months, usually if larvae are ingested near the end of the season (Urquhart *et al*, 1991), after which normal development is resumed. A final moult occurs to produce the fifth larval stage, (or immature adult). Sexual maturation occurs on emergence of the L5 onto the mucosal lining. It is at this stage that the deleterious effect on the infected animal, resulting in digestive disturbances characterised by inappetance, poor growth and diarrhoea occurs (MAFF, 1983).

1.3 Parasitic Gastro-Enteritis

Parasitic Gastro-Enteritis, (PGE) is the collective term for the complex of diseases caused by parasitic helminths. It was originally diagnosed in sheep in 1895, (Soulsby, 1969). On average since 1983, 2.26% of total ovine submissions to the Veterinary Investigation Diagnosis Analysis (VIDA) were diagnosed as PGE. It is suspected that the actual figure is much higher as many cases are treated locally, or go undiagnosed (Jackson, 1989). Figure 1.2 shows the number of reported cases of PGE in sheep and cattle in the whole of Britain, presented to VIDA over the last 20 years. Clearly, there appears to be a decreasing trend in the number of cattle diagnosed with PGE. In sheep populations there is some evidence of a decline in cases. However, the decline is much more gradual. This may be an indication of the problems associated with ovine nematodes developing resistance

to anthelmintics, not yet experienced to the same extent in cattle populations.

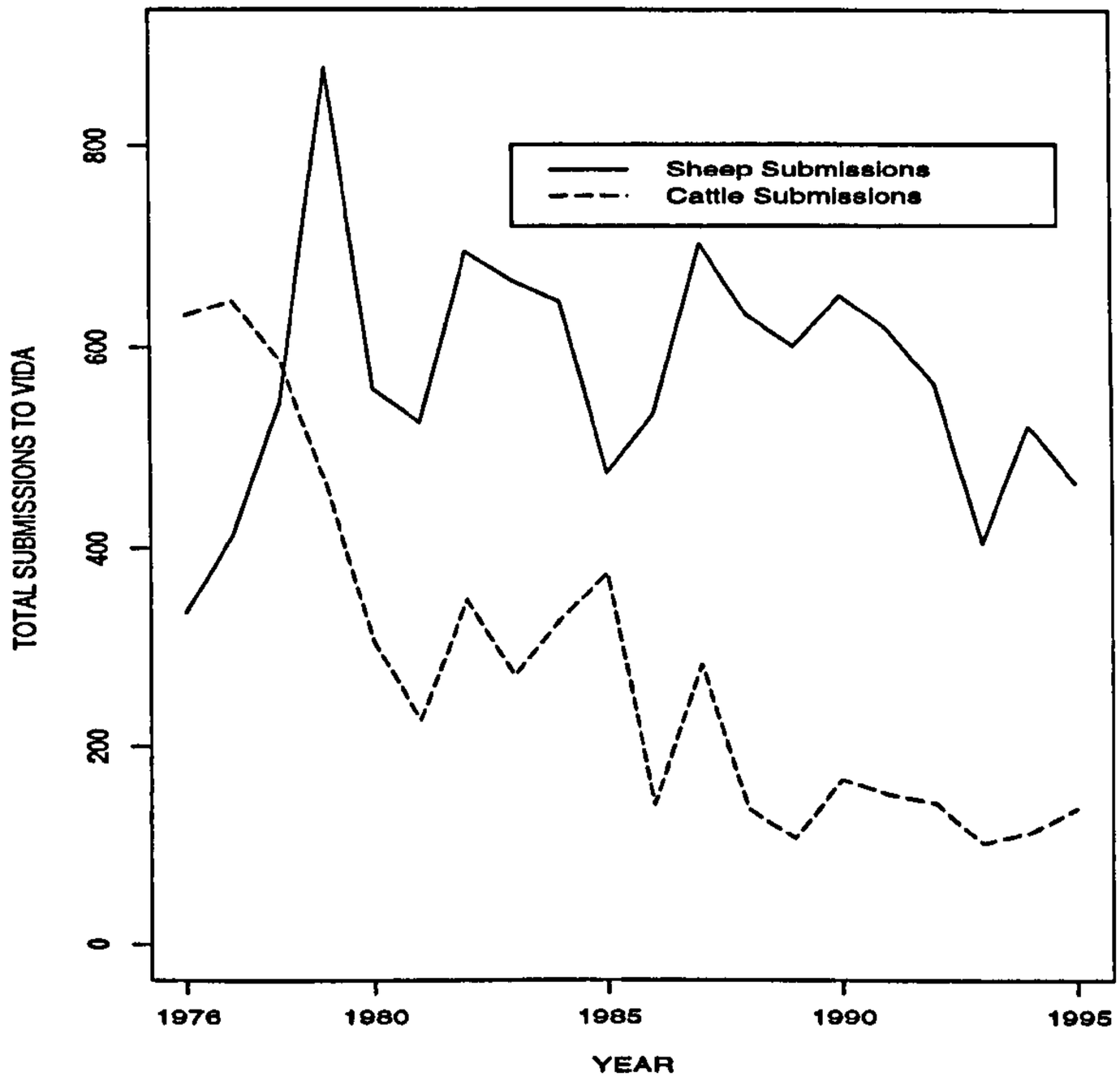

Figure 1.2: Total submissions to VIDA of PGE in cattle and sheep between 1976 and 1995.

It is very difficult to attribute an outbreak of PGE to any one species of nematode. However, in Britain, the timing of the outbreak may indicate which species is likely to predominate due to the distinctive seasonality in emergence patterns of the three main species.

1.4 Epidemiology of *T. circumcincta* in Britain

In the temperate regions of Western Europe, a periparturient rise in the levels of infective *T. circumcincta* larvae is observed between the months of July and October. This is as a result of ewe egg deposition from around two weeks prior to lambing until about 6 weeks after (Urquhart *et al*, 1991). Also contributing to this periparturient rise are the larvae descended from overwintered L3s, picked up by the new lambs at the start of the season. Type I ostertagiasis is commonly diagnosed during this period as a result of the development of L4 to immature adults within lambs during their first season of grazing. Type II ostertagiasis

occurs in animals who harbour inhibited EL4s near the end of one season that subsequently resume development early in the next season.

1.5 Parasitic Control

Since their introduction in the 1960s, anthelmintic drugs have been used exhaustively to treat parasitic helminths of sheep. There are seven main drug groups (Urquhart *et al*, 1991) three of which are most commonly used: the benzimadazoles, the imidazothiazoles and the most recently developed avermectins. In general the mode of action is to target the adult and developing larval stages within the host. Coyne and Smith (1994) give figures for lamb mortality and quote results from Barger (1982) and Gulland (1991). They compare treated and untreated lambs parasitized with several nematode species. Mortality in treated lambs ranged from 0 to 10%, but rose considerably in untreated lambs from 10% to 68%. Live weight gain and fleece weight were higher in treated sheep.

For a period in the 1970s, it appeared that parasitic diseases were controllable. However, disturbingly, the events of the following decade closely mirrored the situation in the insect domain where pesticide resistance had rapidly evolved, rendering the majority of those drugs ineffective.

1.6 Anthelmintic Resistance

The introduction of broad spectrum anthelmintic drugs in the 1960s was heralded as the beginning of the end for parasites and their associated diseases. However, this euphoria was short lived.

In Australia, initial reports of resistance to anthelmintics in 1962 were confined to research stations and were regarded as "parasitological curiosities" (Waller, 1994). Unfortunately, under the broad acre husbandry regimes common in the Southern Hemisphere, resistance spread to commercial farms. By 1994, benzimadazole resistance in *T. circumcincta* in Australia had reached levels of between 50% and 98% (Waller, 1994).

Resistance to an anthelmintic compound is described as the ability of a strain to tolerate therapeutic doses of the drug that normal members of the population cannot. In addition, resistance must be heritable in order that frequencies of the

gene conferring resistance increase over time due to selection for those individuals which survive supposed lethal exposures to the drug (Prichard *et al*, 1980; LeJambre, 1977).

The first case of anthelmintic resistance in the UK was in a commercial farm in Cheshire in 1981 (Britt, 1982). *T. circumcincta* was the species implicated and the drug was a member of the benzimadazole group. A further two reported cases of benzimadazole resistant strains of *T. circumcincta* in Southern England followed in 1983, one at the Ministry of Agriculture Central Veterinary Laboratories, Weybridge and the other on a commercial farm in the surrounding area. In Scotland around the same time the Moredun Research Institute, Edinburgh and the Hill Farming Research Organisation, Hartwood, reported *T. circumcincta* resistance to benzimadazoles (Scott *et al*, 1990). Since then, resistance has rapidly disseminated throughout the country.

1.6.1 Anthelmintic Resistance Surveys

Recently, a review of anthelmintic resistance in nematode parasites of sheep in the UK was undertaken (Hazelby *et al*, 1994). The results of a number of surveys on the prevalence of anthelmintic resistance were summarised (Cawthorne and Cheong, 1984; Taylor and Hunt, 1989; Coles, 1992; Hong *et al*, 1992). The majority of these surveys were carried out in southern England where the farming is more intensive and hence more favourable to selection for resistance than anywhere else in the country. Here it was discovered that levels of resistance to benzimadazoles in *T. circumcincta* was around 36%, an increase in prevalence of more than 20% in five years. Further north however, in Newcastle, Evans (1988), found no evidence of benzimadazole resistance. In Scotland, the incidence was found to be 24.3%, the equivalent of 1 out of 4 farms surveyed revealing evidence of anthelmintic resistance, (Scott *et al*, 1990).

These figures illustrate that the problems of anthelmintic resistance are no longer solely a concern for the countries in the Southern Hemisphere, it is now a problem of international significance (Waller, 1993).

Whilst immediate action is being taken to avoid the worst excesses of drug use, such as avoiding underdosing, using dose and move strategies, rotating drugs and treating imported stocks, alternative methods of control are being considered. The most promising include the development of novel vaccines, the breeding of resistant hosts and the discovery of nematophagouss fungi as a means of biological

control (Barnes and Dobson, 1995; Waller, 1993; Stear, 1996).

1.7 Mathematical Modelling

Despite the existence of mathematical models for human disease since the 18^{th} century, it has only been in the last three decades of this century that veterinary mathematical modelling has been recognised as an important tool in the understanding of animal disease (Thrusfield, 1995). Models are being used to assess the risk, control and impact of disease, and to provide a deeper understanding of disease dynamics.

A wide range of modelling methods are currently practised with respect to animal management systems. Here, we shall discuss a broad range of models encompassing many of the modelling techniques currently in use today, paying particular attention to models of parasites and parasitic diseases.

1.7.1 Index Models

In 1959, Olleranshaw and Rowlands developed a very simple index model to predict the risk of fascioliasis, (liver fluke), in sheep and cattle populations around Britain. *Fasciola hepatica* has an indirect life cycle. This means that the parasite develops in three different environments: on pasture, within a snail and within a sheep.

Observations made on the bionomics of *F. hepatica* revealed two significant factors limiting the development and survival of the parasite. The first was the discovery that below a temperature of 10^oC, development of the parasite is negligible. Consequently, there was little danger of high infection levels in the months between November and April in Britain. Secondly, the importance of moisture during the egg and intra-host stage was identified, without this film of moisture the eggs and metacecariae would desiccate. These important observations facilitated the construction of the M_t, or wetness index.

This index determined the suitability of the habitat for development of the parasite using meteorological data between the months of May and October. The wetness score,

$$M_t = (R - P + 5)n$$

where R is the monthly rainfall in inches, P is potential transpiration, and n is the number of rain days, was calculated each month. The monthly M_t indices were weighted and summed. The wetness score fell into one of three risk categories: no loss, some loss and heavy loss. From this, preventative measures could be taken by farmers to minimise the levels of infection on pasture and the exposure of their sheep to infection.

The model predictions were made available to farmers all over Britain, and monthly wetness scores for different regions were broadcast over the radio.

Following the success of the M_t index in relating weather conditions to the bionomics of the liver fluke, a similar method was adopted by Thomas and Starr (1978), to forecast peak infection levels of nematodes in lambs. The Wet Score Unit, W_p over a 12-hour period depended on certain rainfall limits as well as historical information on rainfall. The limits were based on individual experience and a consideration of the rainfall data available to agriculture. Critical levels and a warning index were given so that prophylactic measures could be taken to minimise infection levels on pasture.

In relating historical climatic data to infection levels or morbidity, index models are empirical and make no attempt to model the dynamical behaviour of a parasite population or its interaction with the host or environment. The following group of models, broadly described as analytical models work on the philosophy that complex physical or biological phenomena have simple underlying mathematical laws.

1.7.2 The Spherical Cow

An approach described as the reductionist principle by Harte (1988) in his book, "Consider a Spherical Cow", involves extracting simple key factors within a complex system and constructing a model that can be analysed quickly so that immediate action can be taken as a consequence.

As more realism is introduced to the model, the mathematical complexity increases and simple on the "back of envelope" solutions cannot be obtained.

1.7.3 Differential/Difference Equations

The rate of change of numbers in parasite and host populations can be conveniently represented using calculus equations. The strength of this approach lies in the ease with which complex biological systems, such as host-vector-parasite systems can be represented by a finite set of equations for the interaction between the various populations.

Formulation of the equations differ depending on whether changes to population numbers are considered to be a continuous or discrete process. Differential equations describe rates of change of numbers in the population whereas difference equations update the population numbers at discrete equally spaced points in time.

Bacterial models are easily represented by differential equations where the possible states of the host individual, such as susceptible, infectious, immune, death, are thought of as compartments within which an individual can remain, migrate from or migrate to with specific probabilities or rates (Renshaw, 1993).

Smith (1990) proposed a mathematical model for the evolution of anthelmintic resistance in a direct life cycle nematode parasite. A system of paired differential equations was developed to predict changes in the genotype distribution of free-living and parasitic stages,

$$\begin{aligned} \frac{dP_i}{dt} &= \beta I_i - (a + bP)P_i \\ \frac{dI_i}{dt} &= \lambda P_i \phi_i - \mu_i I_i - \beta I_i \end{aligned} \tag{1.1}$$

where $i = 1, 2, 3$ represents the genotypes, RR, (resistant), RS, (heterozygote), and SS, (susceptible), respectively,

I_i and P_i are the numbers of free-living and intra-host parasites of genotype i,

μ_i is the free-living mortality,

λ is the female fecundity,

β is the rate of infection, and

ϕ_i is the genetic component of the model determining the offspring genotype distribution from the parent genotype distribution.

1.7.4 Stability Analysis

The non-linear effects due to genetic mixing in the model means that conventional methods of solution used for linear differential equations cannot be used. Analysis of non-linear models involves examining the behaviour of the system in a region around the steady states using local linearisation techniques. A steady state is said to be locally stable if small perturbations about the equilibrium return the system to that equilibrium. Otherwise the steady state is said to be unstable. This is quite a powerful method of analysis which provides stability criteria with respect to different permutations of the model parameters (Nisbet and Gurney, 1982; Renshaw, 1993).

Using this technique, Smith assessed whether simultaneous use of two drugs, that is mixtures, or the sequential use of two drugs, would impede the evolution of resistance greater. The model favoured the use of mixtures as opposed to the sequential use of two drugs as a means of impeding resistance. This is in general agreement with other nematode models (Barnes and Dobson, 1995) and insect models (Mani, 1985). The fact that only a proportion of the entire parasite population are exposed to treatment at any one time, given the remainder remain on pasture, means that some susceptibility is conserved. Within the host, the mixture of drugs kills more individuals than the sequential use of the same drugs. This means that the surviving population contributes relatively fewer progeny to the next generation, resulting in the increase in the gene conferring resistance being minimised.

1.7.5 Stochastic Models

Models, such as that of Smith (1990), described previously are considered deterministic in nature, in that the behaviour of the model in the future can be predicted from prior/historical knowledge of the system in the past. In contrast, stochastic models work on the assumption that the future behaviour of the system is not predictable from the present or previous states, but is based on a set of probabilistic rules. Recently, stochastic models have been formulated to describe host-parasite interactions, particularly for describing the relationship between the levels of immunity in the host, variation in infection rates and observed levels of parasitism in the field, (Isham, 1995; Grenfell, Dietz and Roberts, 1995).

1.7.6 Matrix Models

Describing changes in human demography using matrices was pioneered by Leslie in 1945 for age-classified populations and was subsequently extended by Lefkovitch in 1965 for stage-classified populations. In essence, a state vector containing numbers of individuals at time t, split by age or stage is multiplied by a transition matrix containing the relevant demographic parameters such as fecundity, mortality and transition probabilities, to give the corresponding state vector in the next time unit.

Gettinby and McLean (1979) formulated the life cycle of the liver fluke, *F. hepatica* as a matrix model to assess different methods of controlling fluke infection levels in sheep. The state vector contained the life stages of the liver fluke and the transition matrix contained all the relevant life history parameters of the fluke. The model was extended to investigate possible population control measures on infection numbers. The principal conclusion from the analysis of this matrix model was that good drainage is an effective means of control, so that an initial investment in installing a good drainage system would eliminate the need for the use of long term expensive drug treatments.

Matrix properties can be exploited in these circumstances to determine limiting behaviour of the population provided reliable parameter estimates are used.

1.7.7 Simulation Models

The life cycles of infectious agents, vectors and hosts can be integrated with environmental factors that vary from site to site and season to season to model the dynamics of a disease over time. Representation of such a complex system as a finite number of equations would be impossible, but simulation of the system using a computer model is relatively simple.

There are many examples of computer simulation models for parasitic diseases. Paton, Thomas and Waller (1984) present a simulation model that successfully predicts infection levels of parasites on pasture over a two year period using historical climatic data. Mathematical models for development of the free-living stages, for adult establishment and for ewe egg output, in addition to site specific data such as stocking rate, pasture area, herbage density and initial contamination levels are integrated into this model, and the dynamics of the parasite population simulated.

Results from this model indicated that the lamb contribution to infection may be greater than once suspected. The summer wave of infection had previously been attributed to the post-parturient rise in ewe egg output. However when the lamb contribution to infection was examined in isolation, it proved to be quite significant. In addition, it was noted that if climatic conditions were right, up to three generations of parasites could pass through the lambs during one season, contrary to common belief that at most two generations would get through. These conclusions had practical implications for the control of parasite infection levels. Subsequently provision was made in the model for assessing the impact of different control regimens on infection levels. As a result, it was recommended that the lambs were dosed early in the season to minimise their contribution to the summer wave of infection.

In the wake of large scale resistance to anthelmintics, simulation modelling has made it possible to investigate the long term exposure of parasite populations to drugs. Information on the genetic fitness of the parasite, climatic conditions, animal response and pasture management have been combined with anthelmintic control regimens to determine how rapidly there would be selection for a resistant strain (Gettinby *et al*, 1989; Barnes and Dobson, 1995).

The model of Barnes and Dobson (1995) was used to answer a set of concise questions pertaining to the effectiveness of current measures of impeding the dissemination of resistance throughout a population. Although the authors addressed a wide range of topical issues, three points emerged as being most relevant. Firstly, the model highlighted the importance of acquired immunity in lambs, suggesting that some exposure of lambs to infection shortly after birth would be desired. Using the model, two ways of conserving susceptibility to drugs were recommended. The first involves using a grazing management scheme and the second improved use of the available drugs. Finally, the model was used to examine alternative, non-chemotherapeutic methods of parasite control. In comparing the performance of novel vaccines with anthelmintic drugs, it was discovered that efficacies required for successful vaccination of sheep are well below the efficacies required for anthelmintics.

1.7.8 Future Modelling Trends

Currently, epidemiological modelling is moving towards a holistic approach that incorporates mathematical models, expert rules, environmental data and litera-

ture into a powerful integrated knowledge management tool. It is hoped that through the use of hypertext knowledge bases, this approach will bridge the gap between the model and the user. Successful integrated models have been developed for the study of equine welfare, (Revie *et al*, 1994) and currently a generic modelling approach has been adopted for the control of epizootic diseases, in the first instance, theileriosis and trypanosomiasis in Eastern Africa.

1.8 Thesis Outline

During its lifetime, the nematode parasite *T. circumcincta* spends a period free-living on pasture and the remainder inside a sheep host.

On the pasture, the free-living stages are exposed to external environmental stimuli. Chapters 2 and 3 examine the effect of temperature on the free-living development rate of *T. circumcincta* . A development rate temperature model is proposed in Chapter 2 that is both flexible and biologically interpretable. In Chapter 3, this model is incorporated into a simulation model of the population dynamics of *T. circumcincta* called **Osterant** and the concept of developmental variability is explored as a means of explaining observed variation in infection levels on pasture.

Chapter 4 presents a theoretical modelling framework for the entire life cycle of *T. circumcincta* incorporating developmental variability and genetical mixing together with other important epidemiological aspects of the nematodes life history, such as areas of refugia and host ingestion.

Chapters 5, 6 and 7 focus on an important aspect of the parasitic stages of the nematode life cycle, that of anthelmintic resistance. A basic modelling structure is presented in Chapters 5 and 6 that describes the evolution of drug resistance in a parasite population undergoing intensive drug treatment, and a model is given that assesses the impact of different life history parameters on the time to significant resistance within such a population. In Chapter 7, a novel method of resistance control is addressed and the previous models used to assess the effect of this control technique on the resistance status of a typical nematode population. Practical advice is given on the optimal way to suppress resistance and control parasitism.

Chapter 2

The Effect of Temperature on the Free-Living Development of Nematodes of Sheep

2.1 Introduction

It has long been recognised that the development and survival of the free-living stages of poikilothermic organisms such as nematodes is governed by the surrounding environment. The effect of environmental factors on the development and survival of organisms has been documented in the book *Temperature and Life* (Precht *et al*, 1973). Temperature, relative humidity, photoperiodicity, soil and vegetation types are the main environmental factors governing the complex developmental process of such organisms. It has been concluded, however that temperature exerts the primary influence on development and survival of the free-living stages of nematodes (Crofton, 1963; Soulsby, 1969; Kates, 1965). Several attempts have been made to quantify this relationship for certain species of nematode within specific climatic zones (Paton, 1983; Leathwick *et al*, 1992; Barnes and Dobson, 1995), however no serious attempt has been made to accurately model this temperature-dependent relationship over the entire temperature range in both temperate and tropical regions.

In the insect domain, it has been recognised that the quantification of the relationship between development and temperature is of great practical importance for accurate scheduling of census samples and in the control of insect populations (Wagner *et al*, 1984).

Early accounts of models of this dependency have been recorded as far back

as the last century. These models have their origins in chemistry where they were used to determine the effect of temperature on the rate of enzyme-catalysed biochemical reactions.

In the last two decades advances have been made in the mathematical treatment of this phenomenon in insect populations to produce quite sophisticated and in some cases, quite complex models.

It is the intention here to give a brief guide through the modelling literature on this subject over the past twenty years, and then to arrive at the most recent models. From these, it is hoped to apply similar techniques to nematode populations in a bid to solve some of the problems that have arisen in agriculture as a result of these parasites.

2.2 A Review of Mathematical Models for Temperature Dependent Development Rate

Three models of insect development will be discussed in the order that they appear in the literature. The chronology of these models reflects the evolution and sophistication of ideas developed through years of collaboration between entomologists and modellers seeking to explain insect behaviour.

In addition, a model of nematode development will be reviewed alongside the three for insect development in an attempt to see if recent techniques in the insect domain can be adapted to improve current nematode models.

2.2.1 Temperature Dependent Development Modelled Using the Degree - Days Method

The Degree-Day concept (Sanderson and Peairs 1913; Arnold 1960; Baskerville and Emin 1969; Abrami 1972; Allen 1976; Sevacherian *et al* 1977), has been around since the beginning of the century and has probably enjoyed the longest and most varied usage out of the three models under discussion. It assumes a linear relationship between temperature and the development rate of an organism between two temperature bounds. A threshold temperature, T_{base}, below which, development does not occur, is incorporated into the equation. The degree-days

on day i are calculated to be

$$DD_i = T_i - T_{base} \tag{2.1}$$

where T_i is the average temperature on day i.

Within certain temperature boundaries, it is accepted that as temperature rises, the rate of development increases. For each species there exists an optimal temperature, such that development time is minimal. Experimentally, this optimum can be found and the minimum time in which an organism may develop fully to the next stage can be established. Development is said to be complete once

$$\sum_{i=1}^{n} DD_i \geq DD_{opt} \tag{2.2}$$

where DD_{opt} is the minimum number of degree-days taken for an organism to develop to the next stage under optimum temperature conditions.

Within certain temperature bounds, the development rate of most organisms varies linearly with temperature, in agreement with this model. Historically, development at temperatures outwith these boundaries was either modelled empirically or ignored. With the increasing prevalence in diseases of crops and livestock in both temperate and tropical climates, comes an increasing need to use these models over a broader range of temperatures. They are of no practical use if they cannot model the development of organisms at temperature extremes, as it may be that in these extreme conditions the most interesting and important behaviour occurs.

In most poikilothermic organisms, development rate rises either exponentially or sigmoidally between a base and an optimum temperature. Beyond the optimum temperature, a sharp decline in development rate is observed until a lethal maximum temperature is reached and the life of the organism can no longer be sustained (Andrewartha and Birch, 1954).

The following models attempt to address development outwith the previously imposed temperatures boundaries.

2.2.2 Temperature Dependent Development Modelled as an Inverted Logistic Equation

Stinner *et al* (1974), modelled the development rate of the insect, *Trichoplusia ni* as a function of temperature using a sigmoid curve which was inverted once

an optimal temperature was exceeded. The form that the sigmoid curve takes is derived from the following differential equation for the rate of change of the development rate with temperature

$$\frac{dD_T}{dT} = aD_T\left[1 - \frac{D_T}{D_{opt}}\right] \tag{2.3}$$

where D_T is the development rate at temperature T,

D_{opt} is the optimum development rate, and

a is the natural uninhibited growth rate.

The development rate at temperature T is then calculated to be

$$D_T = \frac{D_{opt}\left[e^{aT_{opt}+b}\right]}{1 + e^{a\tau'+b}} \tag{2.4}$$

where

$$\tau' = \begin{cases} T & T \leq T_{opt} \\ 2T_{opt} - T & T > T_{opt} \end{cases} \tag{2.5}$$

and T_{opt} is the optimum temperature.

Effectively, once the temperature exceeds the optimum level, that temperature is mirrored about this optimum to determine the development rate. Figure 2.1 illustrates this model graphically.

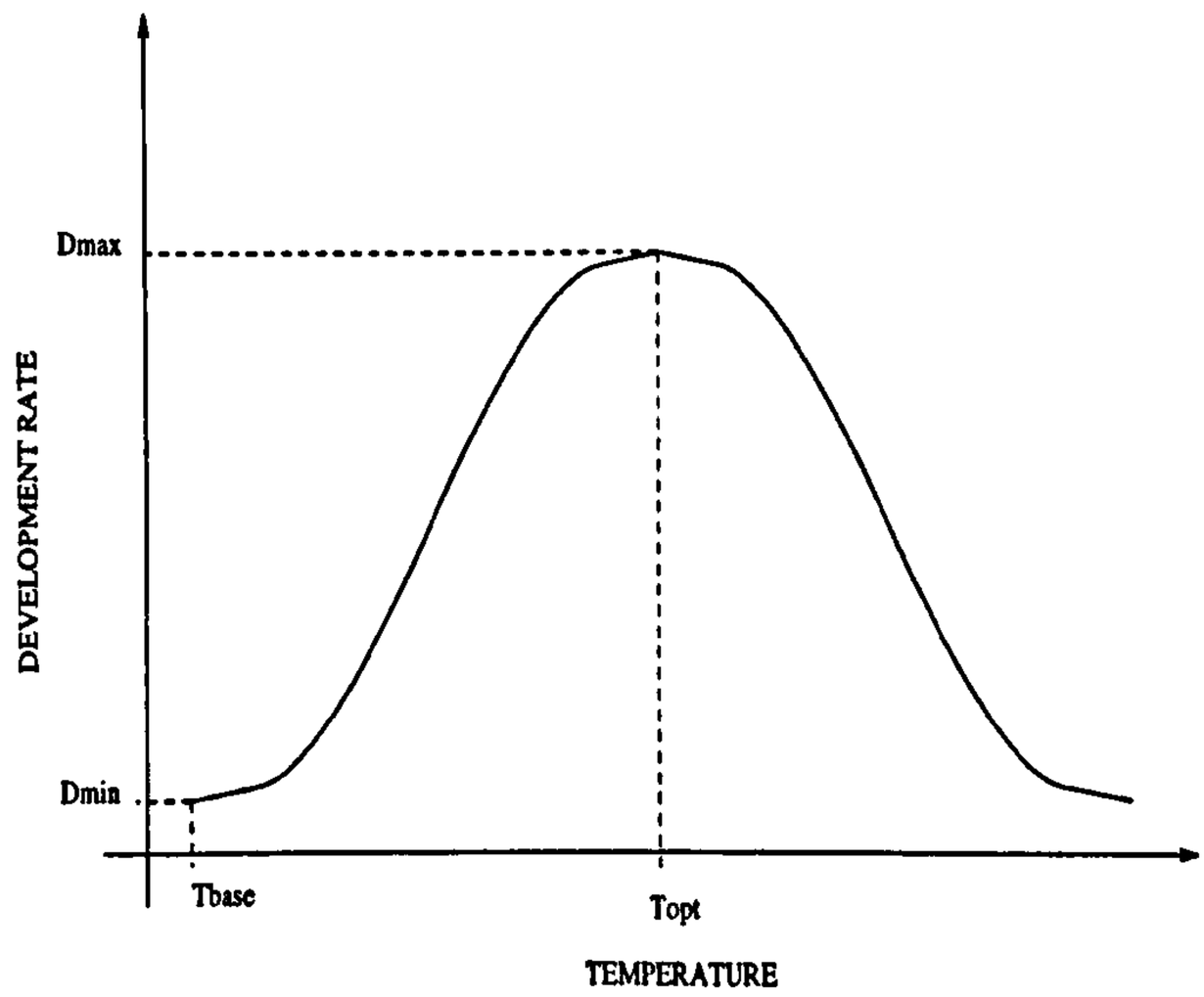

Figure 2.1: Illustration of the inverted sigmoid curve of Stinner *et al* (1974), where growth is logistic from a base to an optimum temperature, $(T_{base} - T_{opt})$, and inversion of the function beyond the thermal optimum, T_{opt}.

2.2.3 Temperature Dependent Development Modelled by Matching Two Independent Solutions with a Common Limit

Logan *et al* (1976), acknowledged that two distinct relationships exist between development rate and temperature, which they demonstrated for the McDaniel spider mite, *Tetranychus mcdanieli McGregor*. The first relationship, which they called *Phase 1*, describes the development rate of an individual when exposed to temperatures between a threshold and an optimum temperature ($T_{base} - T_{opt}$). For many species this is in the form of a sigmoid or exponential growth curve (Andrewartha and Birch, 1954). Once the temperature has exceeded this optimum level, the associated development rate decreases rapidly until a lethal maximum temperature is reached whereby the life of the organism cannot be sustained, which they called *Phase 2*. Figure 2.2 gives an illustration of this.

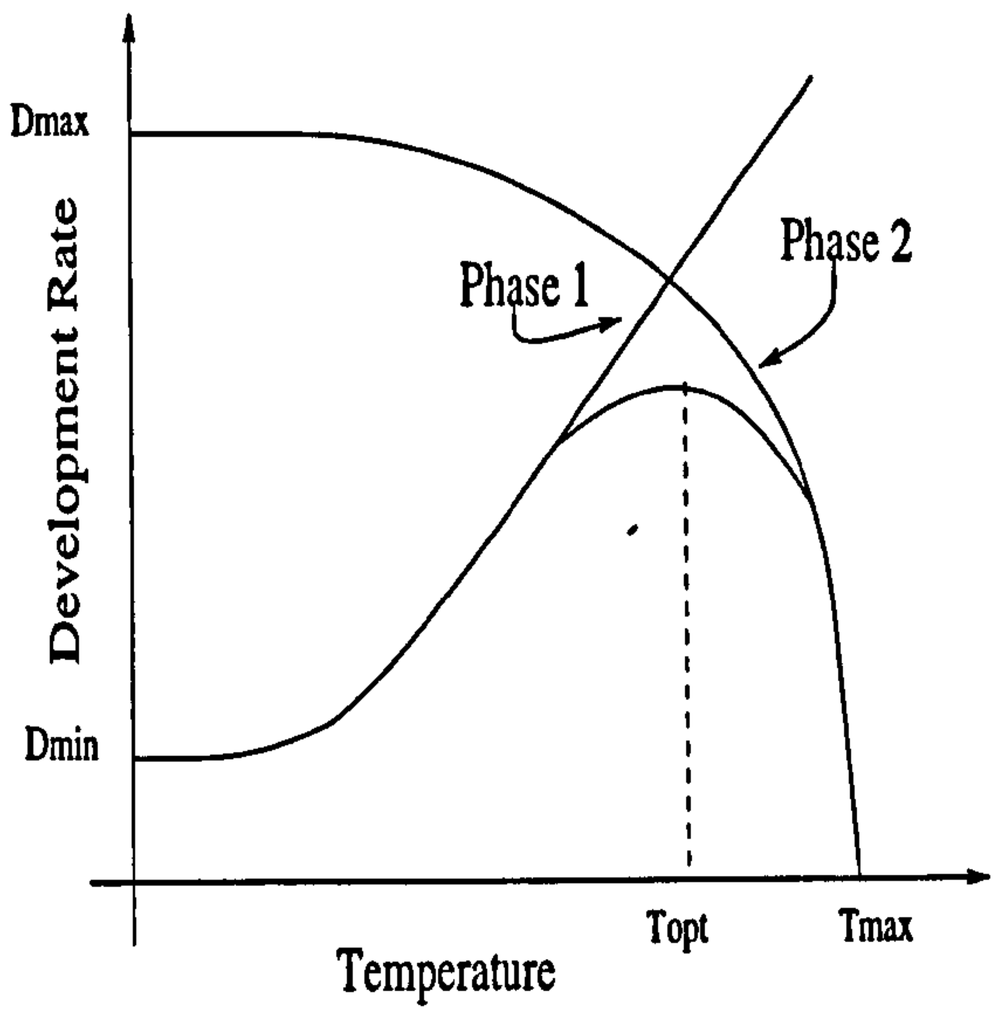

Figure 2.2: Illustration of the matched asymptote method of Logan *et al* (1976).

The challenge here was to produce a single analytic equation describing the behaviour of the development rate of an organism over the entire range of temperatures ($T_{base} - T_{max}$).

Logan *et al* (1976) recognised that their problem could be approached as a boundary layer problem. Boundary layer problems arise in situations where the behaviour of the system changes very quickly over a relatively small area. Using singular perturbation methods, solutions for *Phases 1* and 2 were found.

For this particular case, the solution to *Phase 1*, called the outer solution and denoted $D_o(T)$, represented the increase in development rate with increasing

temperature from a base to an optimum level, and for the parasite under study, was exponential in nature

$$D_o(T) = D_0 e^{\rho T} \tag{2.6}$$

where D_0 represents the development rate at base temperature, and
ρ is the natural rate of increase in development rate.

The solution to *Phase 2*, called the inner solution, described the behaviour of the development rate within the high temperature boundary layer, denoted by $D_i(\tau)$. A special scaling factor, τ, was introduced to take account of relative distances within the boundary layer. This equation took the form

$$D_i(\tau) = C_0(1 - e^{-\tau}) \tag{2.7}$$

where $\tau = \frac{T_M - T}{T_M - T_{opt}}$, and
C_0 is a constant yet to be determined.

By matching the asymptotes of these solutions, the common limit was found to be

$$D_o(T_M) = \lim_{\tau \to \infty} D_i(\tau) = C_0 = D_0 e^{\rho T_M} \tag{2.8}$$

Adding the equations for the inner and outer solutions (2.6) and (2.7) and subtracting their common limit in equation (2.8) yields a uniform approximation to the required solution valid over the entire range of temperatures ($T_{base} - T_{max}$)

$$D_u(T) = D_0 \left[e^{\rho T} - e^{\rho T_M - \tau} \right] \tag{2.9}$$

This provided the most flexible modelling technique to date as it addressed the change in behaviour of development rate once an optimum temperature had been exceeded. It could be adapted for any species inhabiting any climatic region, as all that needed altering was the nature of the inner and outer solutions, provided a common limit existed between them.

2.2.4 Temperature Dependent Development of Nematodes Modelled as a Step Function

Paton (1983), developed a model for the free-living development of *O. circumcincta* as a function of temperature, which was incorporated into a population simulation model called **Osterant**. Development was seen to occur in three distinct phases

- development at low temperatures from $4^oC - 10^oC$,
- development in the mid temperatures from $11^oC - 21^oC$, and
- development at high temperatures from 21^oC upwards.

Three separate equations were formulated using the data provided by Christie (pers.comm), and Salih and Grainger (1982), to estimate the parameters. The step function model took the following form

$$D_T = \begin{cases} \frac{1}{a_1 T + b_1} & 4 \leq T \leq 10 \\ \frac{1}{a_2 T + b_2} & 10 < T \leq 21 \\ 1 & T > 21 \end{cases} \tag{2.10}$$

where $D_1(T)$, $D_2(T)$ and $D_3(T)$ represent the development rate within the three temperature ranges and $a_{1,2}$ and $b_{1,2}$ are parameters to be estimated. Figure 2.3 illustrates this model graphically.

This model was one of only a few models of temperature-dependent development of free-living nematodes. It was adequate for the purpose of simulation, however, analytically, it provided no insights into the biology of the parasite system, and was not flexible enough to incorporate high temperature development. Clearly a model that was analytic, rather than empirical in nature, and explained development over a wider range of temperatures using a single equation with biologically meaningful parameters was desirable.

2.3 An Analytic Model for the Temperature Dependent Development Rate of *T. circumcincta*

An investigative study was undertaken to develop an analytical model that accurately described the effect of temperature on the free-living stages of the abomasal nematode *T. circumcincta* . The step model of Paton (1983), the inverted logistic model of Stinner *et al* (1974), and the matched asymptote model of Logan *et al* (1976), were fit to data on the development of the free-living stages of *T. circumcincta* exposed to constant temperature stimuli. The resultant models were compared in order to obtain the best fitting model for this species.

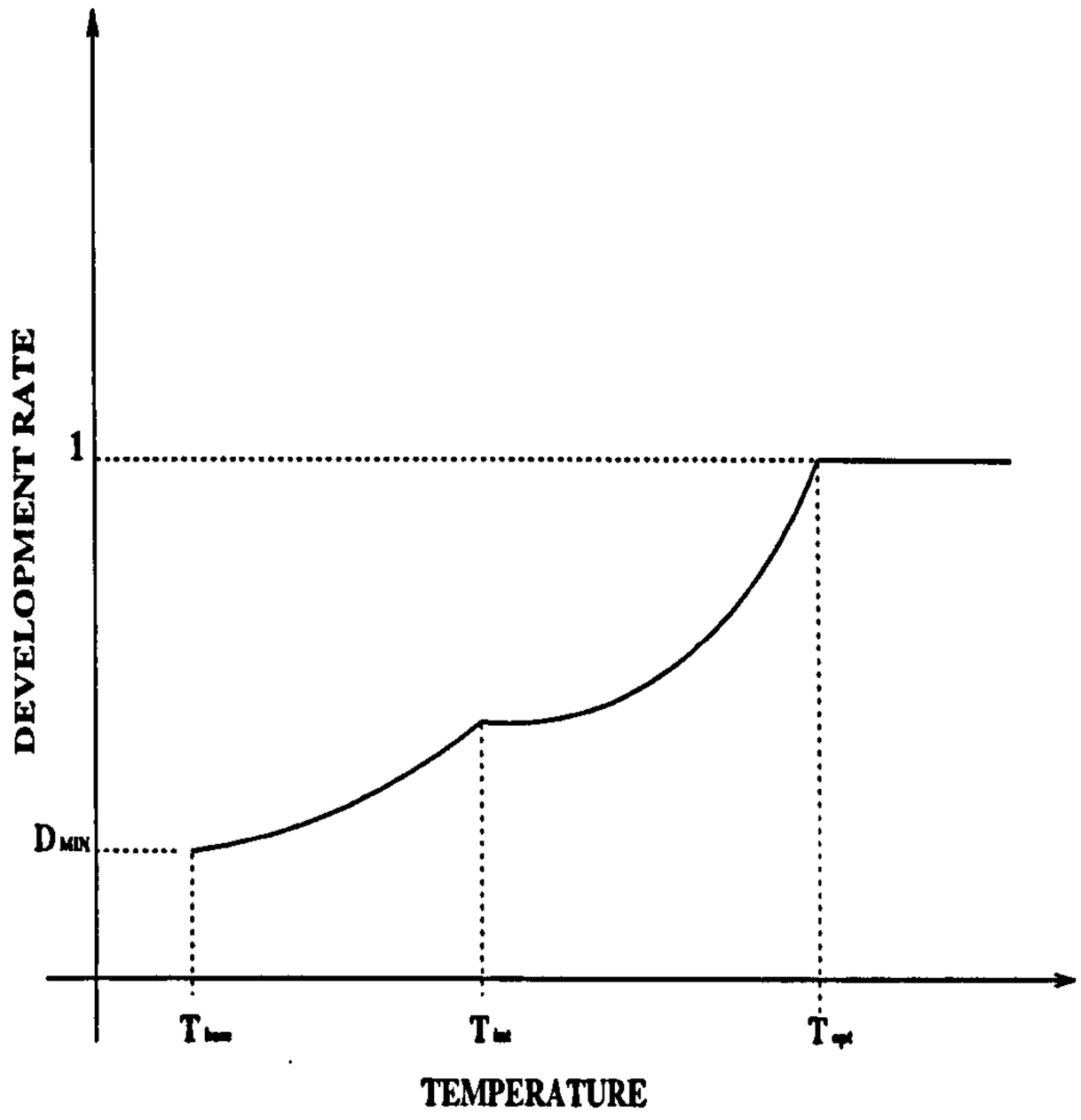

Figure 2.3: Illustration of the step function of Paton, 1983.

2.3.1 Development Data for *T. circumcincta* Under Constant Temperatures

Mean Time To Hatching of *T. circumcincta* Eggs

Table 2.1 gives data on the mean hatching times of *T. circumcincta* eggs under constant temperatures from three different studies. The data provided by Christie (pers.comm), covered the lower end of the temperature scale, ranging from 4^oC to 21^oC, whereas the data generated by Salih and Grainger (1981), covered a broader temperature range, from 5^oC to 35^oC in 5^oC intervals. The third data set, that of Young *et al* (1980), gave a distribution of hatching times over a range of constant temperatures from 6^oC to 20^oC. The mean hatching times in all three data sets were in broad agreement and followed a similar pattern. Development time decreases as temperatures rise from a base to an optimum. Development at very high temperatures was only recorded by Salih and Grainger (1981). This data showed that development times began to increase once an optimum temperature was exceeded until a lethal maximum was reached and the organism died. There was general agreement that the base temperature, or developmental zero, appeared to be about 4^oC, and hatching would not occur at 40^oC or beyond.

Table 2.1: Mean hatching times (in days) of eggs and development times of L1 to L3 *T. circumcincta* for a range of data sets.

	Egg to L1 Stage			L1 to L3 Stage	
Temperature (°C)	Salih and Grainger (1981)	Christie (pers.comm.)	Young *et al* (1980)	Salih and Grainger (1981)	Christie (pers.comm)
4	-	17	-	-	62
5	11.745	15	-	-	46
6	-	-	12.6	-	35
8	-	8	-	-	24
10	4.016	5	3.958	20	20
12	-	4	-	-	18
14	-	3	-	-	14
15	2.058	-	2.135	13.14	-
20	1.495	-	1.1854	10.41	-
21	-	1	-	-	1
25	0.9916	-	-	8.11	-
30	1.000	-	-	4.89	-
35	1.245	-	-	-	-
40	∞	-	-	-	-

Mean Development Time of *T. circumcincta* L1 to L3

Table 2.1 also gives the mean development times of *T. circumcincta* L1 to L3 life stages from two separate data sets (Salih and Grainger, 1981; Christie (pers.comm)). The data provided by both were not really comparable as different temperature ranges were investigated. Christie provided data on temperatures at the low end of the scale, from 4^oC to 21^oC, and Salih and Grainger (1981) gave data on temperatures ranging from 10^oC to 30^oC at 5^o intervals. Again, the developmental zero appeared to be about 4^oC. Neither of the studies investigated development at very high temperatures, although Salih and Grainger (1981) stated that there was negligible development at 35^oC.

2.3.2 A Model for the Mean Hatching Time from Egg to L1

The step function (Paton, 1983), the inverted logistic (Stinner *et al*, 1974), and the matched asymptote model (Logan *et al*, 1976) were fit to the data of mean hatching times in Table 2.1 in an attempt to determine the best predictive model of hatching times of *T. circumcincta* in the field. Non-linear parameter estimation using the standard non-linear least squares routine, the Levenberg-Marquardt method (Press *et al*, 1992), was carried out. The parameter estimates are given

in Table 2.2.

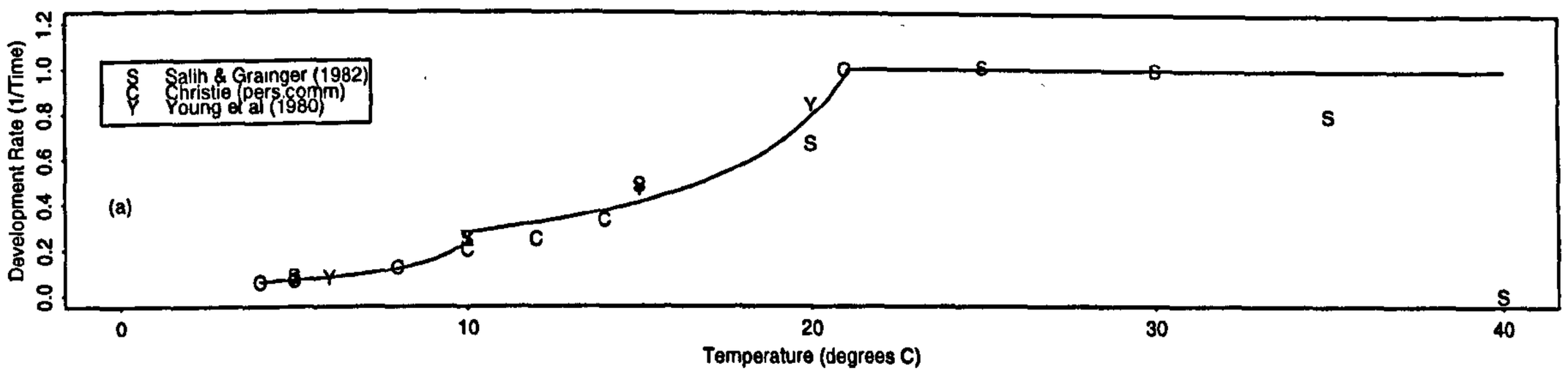

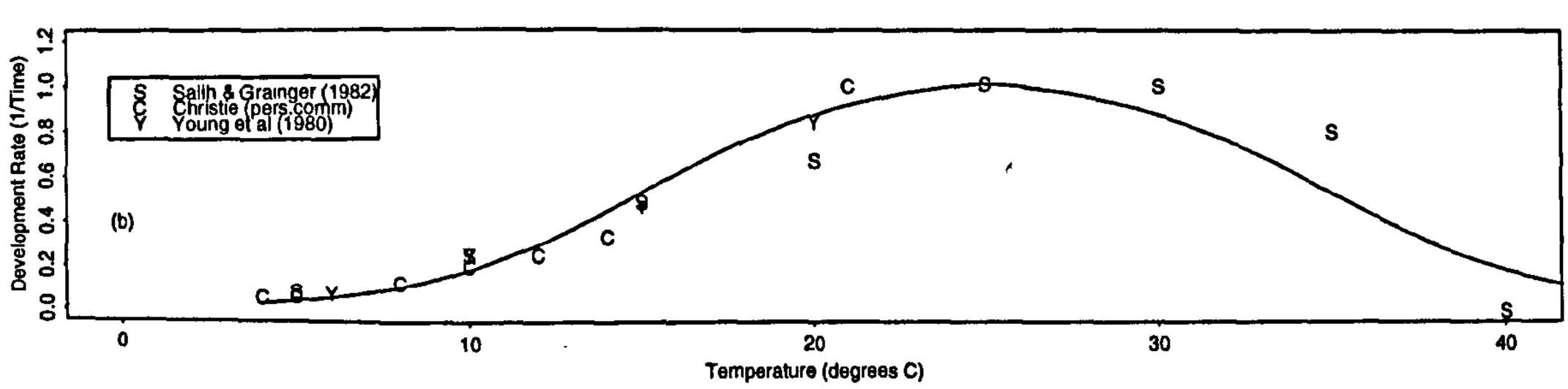

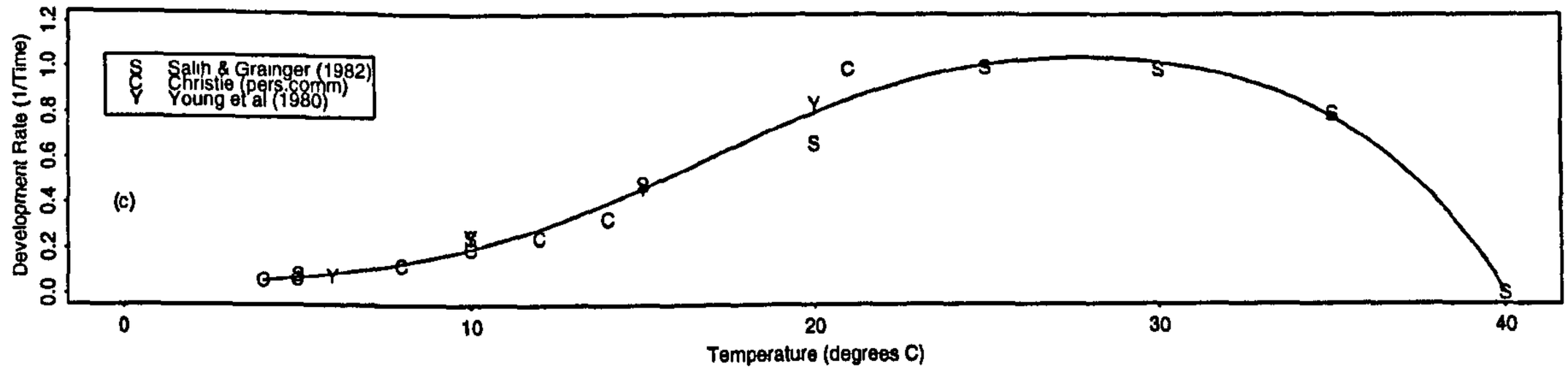

Figure 2.4: Fitting (a) step function (Paton, 1983) (b) inverted logistic function (Stinner *et al*, 1974), and (c) matched asymptote function (Logan *et al*, 1976) to mean hatching time (in days) of *T. circumcincta* eggs given in Table 2.1.

The Step Function

The step function of Paton (1983), for the mean hatching times of *T. circumcincta* egg to L1, given in Table 2.1, takes the following form

$$D_T = \begin{cases} \frac{1}{-2.12T+25.43} & 4 \leq T \leq 10 \\ \frac{1}{-2.36T+5.99} & 10 < T \leq 21 \\ 1 & T > 21 \end{cases} \qquad (2.11)$$

Figure 2.4(a) shows that this function (Paton, 1983), fits the data quite well between 4^oC and 21^oC. However, no attempt was made to model the behaviour of the development rate beyond 21^oC. This becomes a problem certainly in

tropical climates where temperatures can exceed 21^oC throughout the year, and more often than not in temperate climates where it is not unusual to experience temperatures above this level. As a consequence, using this model to predict development times in the field could cause serious errors in the prediction of peak infection levels.

The Inverted Logistic Model

The inverted logistic function (Stinner *et al*, 1974) was next fit to the data for mean hatching times, given in Table 2.1, at different temperatures. Figure 2.4(b) graphically presents the following equation

$$D_T = \frac{24.23\left[e^{-0.31T_{opt}+4.69}\right]}{1+e^{-0.31\tau'+4.69}} \tag{2.12}$$

where

$$\tau' = \begin{cases} T & T \leq T_{opt} \\ 2T_{opt} - T & T > T_{opt} \end{cases} \tag{2.13}$$

It is clear that the fit was good over the initial temperature range $(T_{base} - T_{opt})$. However, due to the assumption of symmetry about the thermal optimum, the function did not fit the data well over the final temperature range $(T_{opt} - T_{max})$. Despite addressing the problem of development at high temperatures, the inverted logistic model was unsuccessful in modelling this phenomenon due to the assumed symmetry about the thermal optimum, which in reality does not exist.

The Logistic-Exponential Model

The final model fit to the mean hatching times of *T. circumcincta* eggs was that of Logan *et al* (1976). A function representing development over the initial temperature range, *Phase 1*, was proposed and asymptotically matched to the function for development over the final range of temperatures, *Phase 2*. A common limit was subtracted from the sum of the two functions to produce a single analytic equation uniformly valid over the entire temperature range, $(T_{base} - T_{max})$.

On examination of the plotted data, *Phase 1* it appears, is well described by a sigmoidal curve. This means that the outer solution is of the form

$$D_o(T) = \frac{\rho/\gamma}{[1+ke^{-\rho T}]} \tag{2.14}$$

where $k = \frac{\alpha - \phi}{\phi}$ and

ρ and γ are defined as before.

The behaviour of the data in *Phase 2* from an optimum to a lethal maximum temperature is characterised by a rapid declining function such as an exponentially decaying function, given by the inner solution,

$$D_i(T) = C_0 \left[1 - e^{-\tau}\right] \tag{2.15}$$

where $\tau = \frac{T_M - T}{T_M - T_{opt}}$.

The asymptotes of equations (2.14) and (2.15) were matched and the common limit subtracted from the sum of the inner and outer solutions to produce a single analytic function uniformly valid over the entire temperature range

$$D_u = \frac{\rho}{\gamma}\left\{\left[1 + ke^{-\rho T}\right]^{-1} - e^{-\tau}\right\} \tag{2.16}$$

Non-linear parameter estimation, (Press *et al*, 1990), resulted in the following equation for the mean hatching rate of *T. circumcincta* eggs at any temperature, T

$$D_T = \frac{0.23}{0.18}\left[\left[1 + \frac{\frac{0.23}{0.18} - 0.06}{0.057}e^{-0.23T}\right]^{-1} - e^{-\frac{40.03 - T}{40.03 - 35.16}}\right] \tag{2.17}$$

It is clear from Figure 2.4(c) that this function gave a very good fit over the entire range of temperatures. It was a continuous function, uniformly valid between T_{base} and T_{max}, and many of the parameter values, given in Table 2.2, had biological significance. For example, ϕ represents the developmental threshold, ρ is the unconstrained growth rate, and γ is a heat denaturization effect triggered by high temperatures.

The final column in Table 2.2 gives the associated final sum of squares (FSS) for each model fit to the data sets. The final sum of squares for the step function (Paton, 1983) was the highest at 1.0747. This was due to the inadequacy of the model to predict development rates at above optimal temperatures. The inverted logistic model of Stinner *et al* (1974) yielded a final sum of squares of 0.2083

Table 2.2: Table containing parameter estimates obtained when comparing the step function (Paton, 1983), the inverted logistic function (Stinner *et al*, 1974) and the logistic-exponential model of Logan *et al*, 1976 for hatching rates of *T. circumcincta* eggs and the logistic-exponential model of Logan *et al* (1976), for the development of *T. circumcincta* L1 to L3.

Life Stage	Function	Parameter Estimates					FSS
Egg to L1	Inverted Logistic Stinner *et al*, 1974	D_{opt}	α	β			0.2083
		24.2324	-0.3129	4.6917			
Egg to L1	Step Function Paton, 1983	a_1	a_2	b_1	b_2		1.0747
		-1.91332	-2.36308	23.4669	5.99449		
Egg to L1	Logistic-Exponential Logan *et al*, 1976	ρ	γ	ϕ	T_{opt}	T_{max}	0.0526
		0.23087	0.18431	0.05747	35.15831	40.03	
L1 to L3	Logistic-Exponential Logan *et al*, 1976	ρ	γ	ϕ	T_{opt}	T_{max}	0.0008
		0.07435	0.0005	0.02895	36.82324	37.1711	

suggesting that it gave a better fit to the data than the step function of Paton, (1983). However, the final sum of squares for the logistic-exponential model of Logan *et al*, (1976), 0.0526, was markedly lower than the other two. It was concluded that this model represented the best fitting model to the data.

A more sensitive test of goodness of fit involving the residual mean square deviances could have been used, however, for our purposes, the differences in the fits of the various models was so great that visual comparisons could be made.

By far, this modelling technique provided the most flexible and best fitting model to the available data for *T. circumcincta* egg hatching rates as a function of temperature.

Description of the temperature development rate relation using the technique of matching asymptotes of two curves (Logan *et al*, 1976), for the remainder of the free-living stages of *T. circumcincta* now follows.

2.3.3 A Model for the Mean Development Time of *T. circumcincta* L1 to L3

As was mentioned previously, there was little data available on the development times of L1 to L3 life stages of *T. circumcincta* at high temperatures. From the data on the mean development time of L1 to L3 at lower temperatures (*Phase 1*), the relationship appears sigmoidal in nature. Generally at high temperature levels, small changes in temperature are characterised by more rapid changes in development times which suggests that as a preliminary step, *Phase 2* behaviour may assume an exponentially decaying function. Using the data from Table 2.1, the parameters were estimated in the same way as before and the function,

$$D_T = \frac{0.07}{0.0005}\left[\left[1 + \frac{\frac{0.07}{0.0005} - 0.028}{0.028}e^{-0.07T}\right]^{-1} - e^{-\frac{37.17-T}{37.17-36.82}}\right] \tag{2.18}$$

was fit to the data for mean development times of *T. circumcincta* L1 to L3. From Figure 2.5 it is clear that the function fits the data well. Table 2.2 gives the parameter estimates derived from the non-linear parameter estimation routine. As data was not provided for temperatures above 30^oC, the function was used to estimate the behaviour of the development rate beyond this temperature. Initial estimates of the optimum and maximum temperatures were provided, and were then used by the estimation procedure to estimate optimum and maximum temperatures.

2.4 Variation In Response to Temperature

Comparison of the most recent practical nematode temperature development model with two of the commonly used insect development models revealed that the model of Logan *et al*, (1976) had greater success in modelling the temperature dependent rate phenomena in nematode populations than the others, both for the egg to L1 and L1 to L3 stage.

Traditionally, the next step from here would be to incorporate the best fitting model into a population dynamics model in order to predict parasite emergence levels in the field so that control measures could be optimised in terms of efficacy and safety.

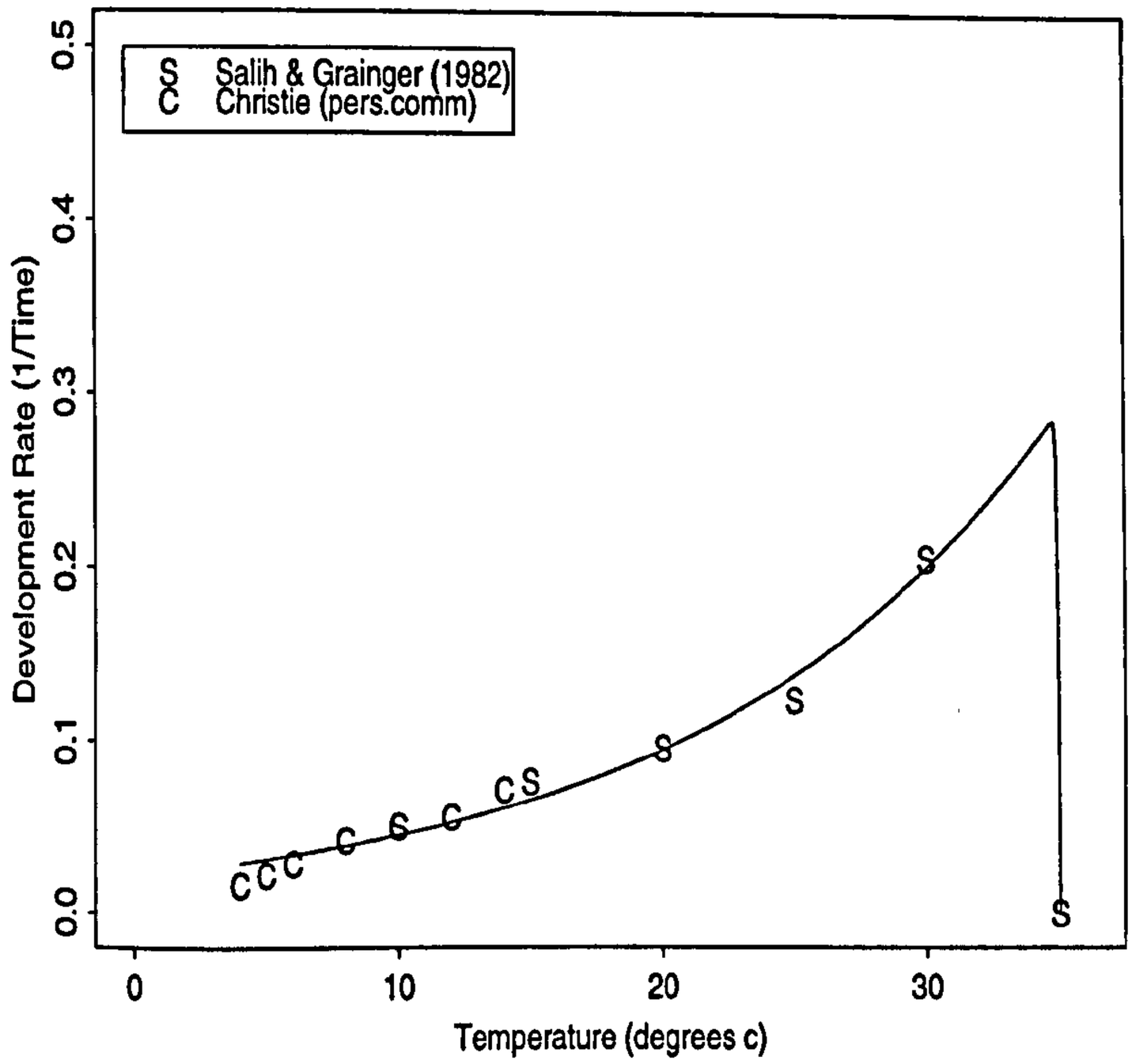

Figure 2.5: Fitting the logistic boundary layer function (Logan *et al*, 1976), in equation (2.18), to mean development time (in days) of *T. circumcincta* L1 to L3.

The timing and magnitude of peak pasture contamination levels is seen to fluctuate geographically and temporally, and there has been much difficulty in accounting for these fluctuations. Changes in climate cause much of this variation, however changes in temperature, precipitation and relative humidity do not explain all of it. Another source of this variation may come directly from the parasites in their individual response to temperature.

Experiments to determine development rates at various constant temperatures yield a distribution of development times within a population ranging from those who develop quickly to those who take a good deal longer to develop. However, more often than not, it is only mean development rates (or times) that are reported, and those individuals in the tails of the distribution that develop significantly faster or slower than the average developers are generally omitted from further analysis.

The effect that variation in developmental response to temperature stimuli has on the population dynamics of the sheep nematode *T. circumcincta* is unknown. Only one publication that we know of provides a distribution of development times

with temperature (Young *et al*, 1980). Experiments have since been undertaken at the Moredun Research Institute, Edinburgh, to provide additional data. Despite this lack of data, it is clear from these initial findings that there is a great deal of variation in response to temperature stimuli between individuals in a population.

From here, it is necessary to quantify this variation using the data available to us to assess the impact that within-population variation may have on the population dynamics of *T. circumcincta* .

The data provided by the various authors was the distribution of hatching times and development times of *T. circumcincta* eggs and L1 to L3, respectively, under different constant temperatures. To get an idea of the range in development times exhibited in a single population, three percentile groups were chosen from the distribution:

- The time until 1% of the population had completed their stage development provided data for the *fast* developers,
- the time until 50% of the population had completed stage development provided data for the *average* developers, and finally,
- the time until 80% of the population had completed their stage development provided data for the *slow* developers.

The 50^{th} percentile was chosen here to represent the *average* behaviour in the population. The 80^{th} percentile was chosen here to represent *slow* developers as it was quite unusual that 100% of the population would develop to the next stage. There was always a few individuals that would not survive. On average, just under 90% of the population would complete stage development (Young *et al*, 1980).

In the last two sections of this chapter, prediction models have been given for the development rate as a function of temperature for mean development times, representing some average behaviour in the population.

In the following two sections, prediction models for the development rate of *fast* and *slow* egg to L1 and L1 to L3 stages, respectively, are given using the technique devised by Logan *et al* (1976).

2.4.1 A Model for *Fast* Developers

An individual is categorised as a *fast* developer if the time to completion of a specific life stage at a constant temperature corresponds to the time when 1% of the experimental population under the same constant temperature completes that life stage.

Hatching Times of *Fast T. circumcincta* Eggs

The first two columns of Table 2.3 gives data on the hatching times of *fast* developing *T. circumcincta* eggs, provided by Crofton (1963) and Young *et al* (1980).

Table 2.3: Hatching times (in days) of *fast* eggs and development times of *fast* L1 to L3 *T. circumcincta* .

	Egg to L1 Stage		L1 to L3 Stage
Temperature(°C)	Crofton, (1963)	Young *et al*, (1980)	Young *et al*, (1980)
4	9	-	-
5	-	-	-
6	7	9	-
10	-	1.979	33.33
13	2	-	-
15	-	-	8
20	1	1.06	5
34	0.708	-	-
35	-	-	∞
40	∞	∞	-

Using a logistic function for *Phase 1*, and an exponentially decaying function for *Phase 2*, the following equation was formulated by matching the asymptotes of both curves

$$D_T = \frac{0.19}{0.13}\left[\left[1 + \frac{\frac{0.19}{0.13} - 0.14}{0.14} e^{-0.19T}\right]^{-1} - e^{-\frac{40-T}{40-39.81}}\right] \tag{2.19}$$

to give the development rate of *fast T. circumcincta* eggs at temperature T.

The fit of the data in Table 2.3 to this curve is shown graphically in Figure 2.6. The final sum of squares for this model is 0.0351.

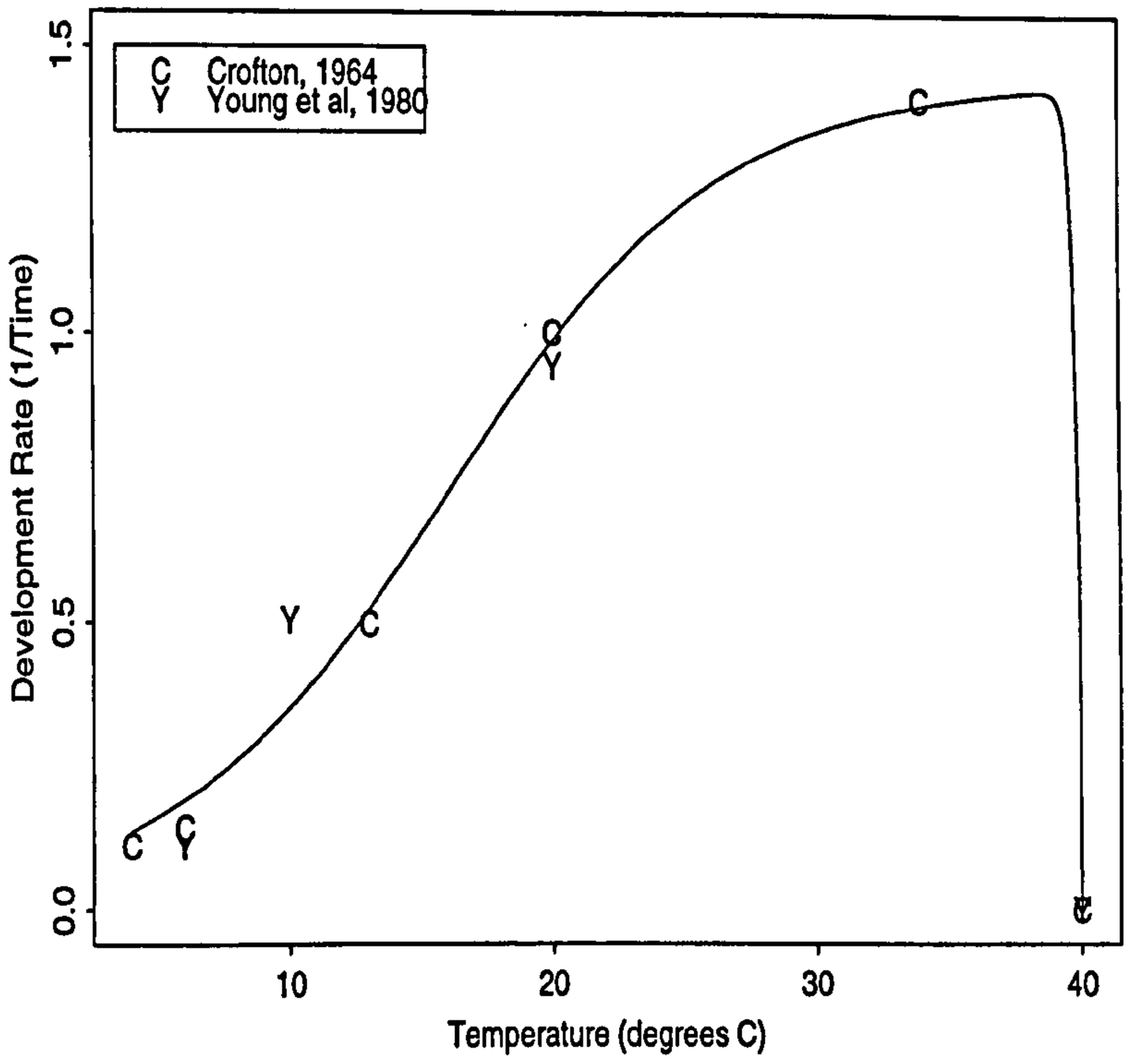

Figure 2.6: Fitting logistic-exponential function (Logan *et al*, 1976), to *fast* hatching times (in days) of *T. circumcincta* eggs given by Crofton, (1963) and Young *et al*, (1980).

Development Times of *Fast T. circumcincta* L1 to L3

The final column of Table 2.3 gives data on development of *fast* L1 to L3 parasites under different constant temperatures. Due to the difficulty in obtaining data for this percentile category in the population, dummy data points had to be introduced into the parameter estimation routine. This provided the routine with sufficient degrees of freedom to obtain parameter estimates. The use of dummy data points is common in mathematical modelling of data sets (Press *et al*, 1992). Generation of dummy data points when real data is unavailable can be done by simulating data points from a specified curve with the assumption that the development rate at temperature T is normally distributed with mean μ_T and variance σ_T. Random numbers are then generated to give development rates at each temperature, T, representing the departure of that generated data point at temperature T from the mean μ_T.

Identical forms for the equations in *Phases 1* and 2 were used to model development of *fast* L1 to L3 as a function of temperature. The data in Table 2.3 were

used to estimate the parameters given in the equation for the development rate of *fast T. circumcincta* L1 to L3 at temperature T

$$D_T = \frac{0.15}{0.59}\left[\left[1 + \frac{\frac{0.15}{0.59} - 0.041}{0.041}e^{-0.15T}\right]^{-1} - e^{-\frac{31.073-T}{31.073-29.634}}\right] \tag{2.20}$$

Figure 2.7 is a plot of the equation in (2.20) fit to the data points in Table 2.3. The final sum of squares for this particular data set is 0.000007.

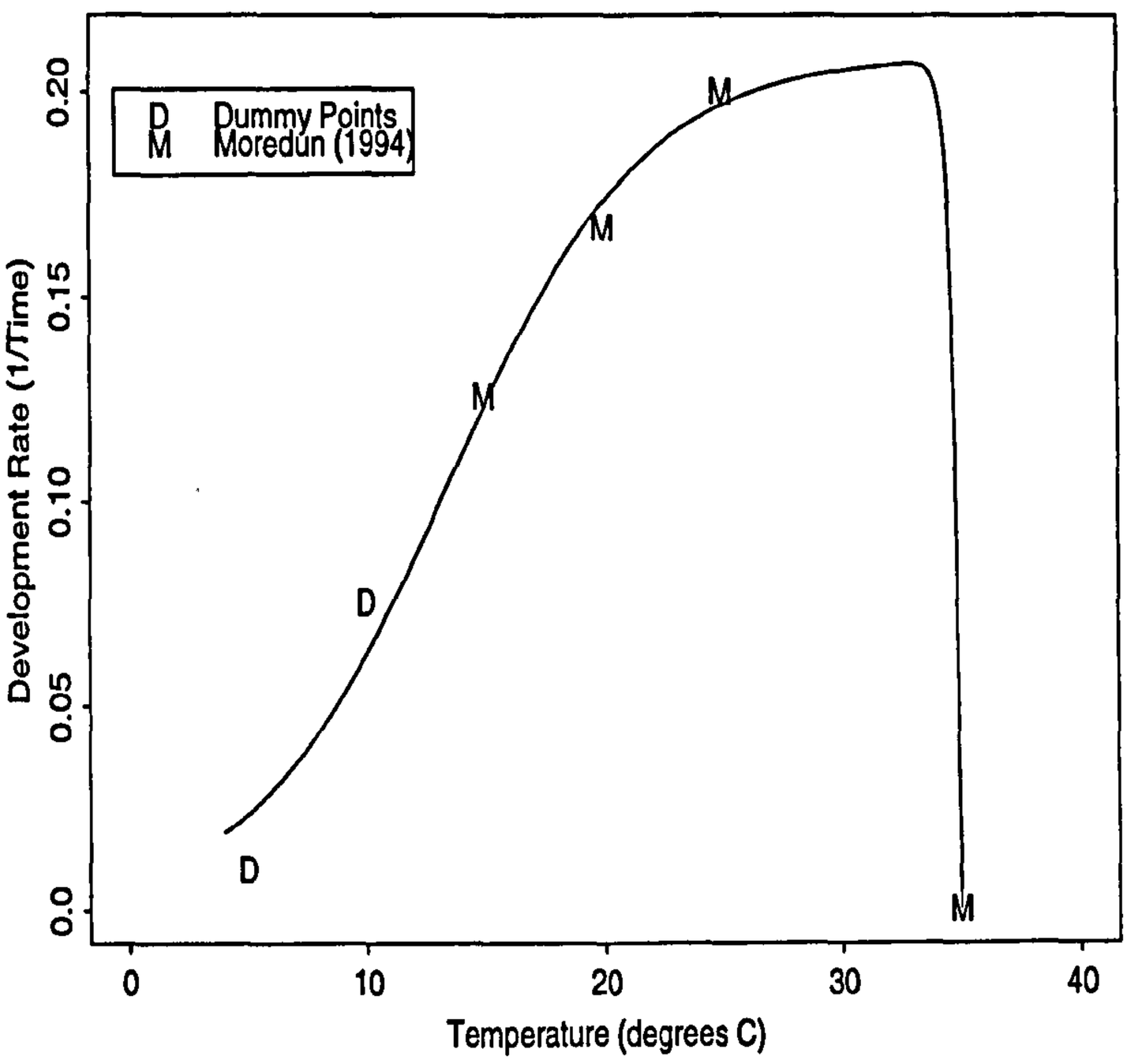

Figure 2.7: Fitting logistic-exponential function (Logan *et al*, 1976), to development time (in days) of *fast T. circumcincta* L1 to L3 using data generated at the Moredun Research Institute, Edinburgh.

2.4.2 A Model For *Slow* Developers

An individual is categorised as a *slow* developer if the time to completion of a specific life stage at a constant temperature corresponds to the time when 80% of an experimental population under the same constant temperature develops from one life stage to the next.

Table 2.4: Development times (in days) of *slow T. circumcincta* egg to L1 and L1 to L3, respectively.

Temperature(^{o}C)	Egg to L1	L1 to L3
	(Crofton, 1963)	(Young *et al*, 1980)
4	-	-
5	-	100(D)
6	27.3333	-
10	4.6875	33.3(D)
15	2.5	20
20	1.291666	12
25	-	10
35	-	∞
40	∞	-

Hatching Times of *Slow T. circumcincta* Eggs

The second column in Table 2.4 gives data on the hatching times of *slow* developing *T. circumcincta* eggs provided by Crofton (1964) and Young *et al* (1980).

Using a logistic function for *Phase 1*, and an exponentially decaying function for *Phase 2*, the following equation was formulated by matching the asymptotes of both curves

$$D_T = \frac{0.22}{0.16}\left[\left[1 + \frac{\frac{0.22}{0.16} - 0.05}{0.05}e^{-0.22T}\right]^{-1} - e^{-\frac{40-T}{40-39.36}}\right] \tag{2.21}$$

The fit of the data in the second column of Table 2.4 to this curve is shown graphically in Figure 2.8. The final sum of squares for this model is 0.0035.

Development Times of *Slow T. circumcincta* L1 to L3

The third column in Table 2.4 gives data on development of *slow* L1 to L3 parasites under different constant temperatures. Unfortunately, very little data of this type is available and dummy data points were introduced in order that parameter

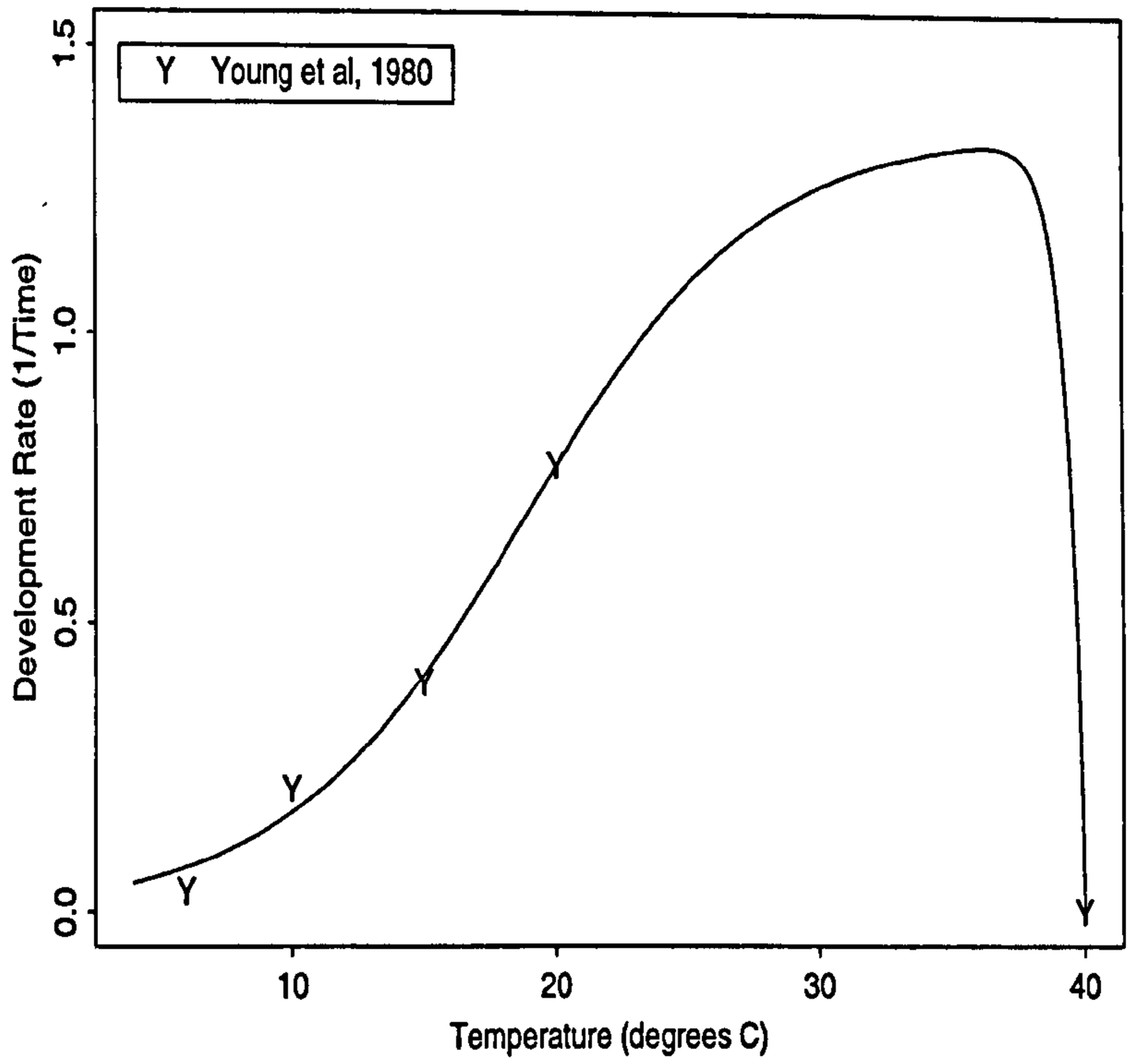

Figure 2.8: Fitting Logistic-Exponential Function (Logan *et al*, 1976), to hatching times (in days) of *slow T. circumcincta* eggs.

estimates could be made. The following models were constructed and fit to the data.

Identical forms for the equations in *Phase 1* and *Phase 2* were used to model development of *slow* L1 to L3 as a function of temperature. The data in Table 2.4 were used in the parameter estimation algorithm to estimate the parameters in the following equation

$$D_T = \frac{0.17}{0.77}\left[\left[1 + \frac{\frac{0.17}{0.77} - 0.014}{0.014}e^{-0.17T}\right]^{-1} - e^{-\frac{31.55-T}{31.55-23.61}}\right] \tag{2.22}$$

The fit of the data in the third column of Table 2.4 to this curve is shown graphically in Figure 2.9. The final sum of squares for this model is 0.000012.

Biological Significance of Estimated Parameter Values

From Table 2.5 of the estimated parameter values obtained when fitting logistic-exponential models to data of *fast*, *average* and *slow* hatching and development

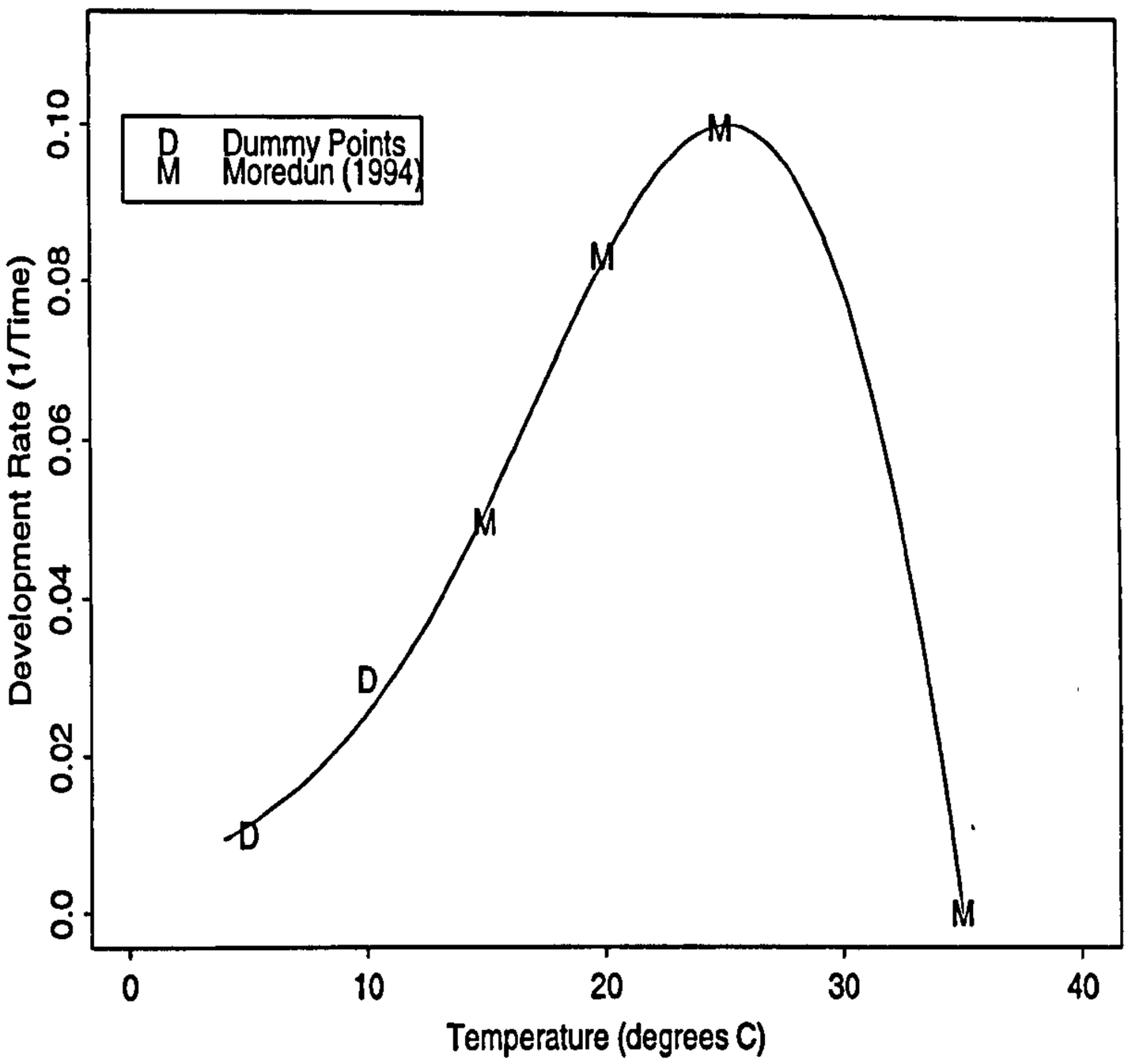

Figure 2.9: Fitting logistic-exponential function (Logan *et al*, 1976), to development times (in days) of *slow T. circumcincta* L1 to L3.

rates, it is clear that each parameter has a biological meaning. For example, ϕ represents the developmental zero, that is, the development rate at a certain base temperature below which life of the organism cannot be sustained. The estimated ϕ for the hatching rate of eggs at a base temperature is greater than the estimated ϕ for the development rate of L1 to L3 in all three development groups. This is consistent with the data, where development from egg to L1 is faster at 4^oC than development from L1 to L3 at the same temperature. The growth rate ρ, of the exponential part of the logistic curve is consistently greater for the egg to L1 life stage than the L1 to L3 life stage for all three development groups. This is in broad agreement with the data as over all temperatures, L1s take longer to develop to L3s compared to the time taken for eggs to hatch to L1s.

2.5 Discussion

Two separate issues have been addressed in this chapter. The first is concerned with developing an accurate mathematical description of the relationship between

Table 2.5: Table of estimated parameter values for both life stages and three development groups, *fast*(F), *average*(M) and *slow*(S), with final sum of squares after the non-linear parameter estimation.

Life Stage	**F,M,S**	ρ	γ	φ	T_{opt}	T_{max}	**FSS**
Egg to L1	Fast	0.1889	0.1305	0.1361	39.8079	40.0021	0.0351
Egg to L1	Average	0.2309	0.1843	0.0575	35.1583	40.0345	0.0526
Egg to L1	Slow	0.2199	0.1616	0.0509	39.3656	40.0060	0.0035
L1 to L3	Fast	0.173447	0.7736	0.013628	23.608	31.5472	0.000007
L1 to L3	Average	0.0744	0.00186	0.02893	31.2262	31.2839	0.0008
L1 to L3	Slow	0.1467	0.5981	0.041438	29.6337	31.0729	0.000012

the development rate of nematodes when free-living and the temperatures they are exposed to in the environment. The second is concerned with quantifying the variation in response to temperature within a nematode population.

Temperature-Dependent Development Models

Typically when modelling the life cycle of nematodes, the free-living period is split into two distinct stages for convenience, the egg to L1 and the L1 to L3 stage, as distinguishing between the first and second larval stage is quite difficult (Urquhart *et al*, 1991).

A comparative analysis of the development models of Paton (1983), Stinner *et al* (1974), and Logan *et al* (1976) was undertaken by fitting each equation to a sequence of temperature-development data sets produced under controlled experiments. The final (residual) sum of squares, (FSS), for each fit is given in Table 2.5 and can be used to determine the goodness of fit of each model.

The step function developed by Paton (1983) for *T. circumcincta* , was not easily adaptable to different species or climatic zones as development at high temperatures was not addressed. The inverted logistic model of Stinner *et al* (1974) was unsuccessful in predicting development rate at high temperatures as the true

behaviour of development rate beyond an optimum temperature was not symmetrical to the development rate at lower temperatures.

The technique used by Logan *et al* (1976), to model temperature dependent development was by far the most flexible to date. With the exception of those models that simulate the physiological processes involved in development and so consequently are very complex (Sharpe and DeMichel, 1977), this model provides the most accurate description of the developmental process.

The technique of matching the asymptotes of two curves to produce a single analytic function has been successfully used in describing the relationship of development time and temperature for insects and now in this thesis, nematodes. This relationship in poikilotherm populations has two distinct phases, the first typically characterised by a logistic growth equation from a threshold temperature to an optimum, the second by some rapid decaying function from the optimal to lethal maximum temperature. Previous attempts at modelling this relationship have fallen short of describing the full behaviour over the entire temperature range.

Very little is known about the biological mechanisms governing *Phase 2*. There have been suggestions that the heat denaturization effect may manifest itself by slowing down the metabolic rate, causing a rapid decline in development rate at high temperatures. More information must be gathered with respect to the mechanisms of development at high environmental temperatures, particularly now with suggestions that temperatures are increasing globally.

Variation In Response to Temperature

The second issue addressed in this chapter was concerned with quantifying the variation in response to temperature within a nematode population.

In order to obtain an indication of the magnitude of developmental variation within a population, three percentile points from the developmental distribution were identified for investigation. These percentile points were labelled *fast*, *average* and *slow*, respectively, and models for both free-living stages were constructed for each, producing 6 models in total.

The variation between the three percentile categories in the population was considerable and would surely have implications for the dynamics of the entire population. For example, the hatching times of *T. circumcincta* eggs under a constant

temperature of 10^oC varies from 47.5 hours for 1% of the population to hatch to 113 hours when 80% of the population have hatched. This is a difference of more than three days between the fastest and slowest individuals hatching to the first larval stage. At 15^oC, development from first larval stage to third takes around 8 days for *fast* developers compared to 20 days for *slow* developers. Not accounting for this kind of variation may seriously affect the success of any control strategy due to the inability to accurately predict peak emergence times.

Developmental variability has, to date, never been addressed for nematode populations. As a result of, or because of this, there is a distinct shortage of data for the response of the entire population to external stimuli, such as temperature. For our purposes, the non-linear parameter estimation could only be undertaken in some cases by including dummy data points for temperatures where data was unavailable. This shortcoming highlighted the need for good quality data over entire temperature ranges for the whole population.

2.6 Conclusion

Previous models predicted mean development times at a range of different temperatures, which encompassed only a subsection of the individuals in a population. Those individuals that developed slower or faster than average were unaccounted for, yet their inclusion in any predictive model may have far reaching consequences for the dynamics of the population.

In this chapter, six models of development were constructed and fit to experimental data on development times under different constant temperature levels. These models were for *fast*, *average* and *slow* development from egg to L1 and *fast*, *average* and *slow* development from L1 to L3. Despite the shortage of data for some parameter estimation, each model fitted well.

The final sum of squares, (FSS), gave a very good indication of the goodness of fit of each model to the available data and were consistently lower when the technique developed by Logan *et al* (1976) was used to develop temperature dependent development rate models for this data.

This investigation has provided a sophisticated technique for modelling temperature dependent development and has introduced the concept of within population variation with respect to individual response to temperature. To date, this is the first time that this aspect of the population dynamics of nematodes has been ex-

plored despite a substantial amount of work having been carried out in the insect domain (Regniere *et al*, 1981; Wagner *et al*, 1984a; Stinner *et al*, 1974).

Before this work can be taken into the continuous domain by fitting some distribution to our models rather than having distinct groups, additional experimental data is required to validate the models we have now. There are concerns here, especially when fitting the functions to the *fast* and *slow* data, that too few data points were available to obtain accurate parameter estimates. Visually, the functions fit the available data well, but at temperatures where data are missing, we need to clarify that the model is making accurate predictions through experimental effort.

Chapter 3

Exploring The Effect of Geographical, Temporal and Developmental Variation on the Population Dynamics of *T. circumcincta*

3.1 Introduction

It was proposed in the previous chapter that variation in the development rate of individual nematode parasites within a population may contribute to the observed variation in pasture contamination levels recorded between locations and within locations from year to year. Mathematical models of development as a function of temperature for the three development groups, *fast*, *average* and *slow* were presented. From the experimental data, it was clear that there was a significant difference in the development times of the three groups, however, the effect that this has on the population dynamics of the parasite is as yet unknown.

In the past, nematode population models assumed uniform development of the population and sought to explain the observed variation in emergence patterns through changes in climate.

The aim of this chapter is to investigate whether variation in emergence patterns both geographically and temporally may be explained to some extent by developmental differences within the parasite population which may arise from genetic variability rather than by changes in the environment experienced by a uniform

parasite population.

This theory was investigated using a population dynamics model first developed by Gettinby and Paton at the University of Strathclyde in the 1980s and is discussed in detail in the following section.

3.2 Osterant

Osterant (©STAMS) is a menu-driven simulation model, written in the Pascal programming language, developed to predict outbreaks of parasitic gastroenteritis, (PGE), in lambs in Britain. One of the main causal organisms of PGE in lambs in Britain is *T. circumcincta* (Jackson, 1989). In addition, **Osterant** incorporates a drug selection model that simulates the evolution of anthelmintic resistance in a parasite population undergoing drug therapy. The model operates in discrete time at a particular location using site-specific climatic data and offers the user a choice of management strategies for the control of parasite populations.

The model provides the user with an effective way of inputting this data via a sequence of menus and outputs the results to a text file. Each menu represents a different aspect of the model. The following sections describe each menu and it's role in the overall model.

3.2.1 The Population Data

Information on the epidemiology of the disease, including daily survival probabilities for each of the life stages of *T. circumcincta* , the frequency of the gene conferring resistance in the population initially output by the ewes, and the fitness of the anthelmintic drug are determined by the user.

Daily survival probabilities are site-specific and are typically determined from laboratory experiments, where the percentage of individuals that hatch and survive from day to day are calculated under constant temperatures. Survival is multiplicative in that the probability that an individual survives for n days given that the daily survival probability is p, is p^n.

When the ewes are initially introduced to the pasture at the beginning of the grazing season, they may be harbouring parasites in their abomasum. In **Osterant**, the user defines the genetic status of this population with relation to

drug resistance. That is, the proportion of rr, rs and ss genotypes, representing resistant homozygotes, heterozygotes and susceptible homozygotes, respectively, within the host are specified, with the constraint that $rr + rs + ss = 1$.

The fitness of an individual undergoing drug treatment depends on the genotype of that individual and the anthelmintic preparation used. The user is able to specify the proportion of each genotype, rr,rs and ss that the drug is expected to kill.

3.2.2 The Meteorological Data

The free-living population dynamics of *T. circumcincta* are principally climate driven. Given that at least half of the parasites life is spent free-living, temperature, rainfall and relative humidity will all have an effect on the epidemiology of the disease. The development of the parasite is modelled in **Osterant** using meteorological data obtained from weather stations. This data consists of minimum, average and maximum daily temperatures and total daily rainfall levels. The average daily temperature is entered into an equation that determines development rate at different temperatures. The method of development fractions is used, whereby the daily development rates for a particular life stage are summed until unity is reached or exceeded, whence that life stage is said to be complete, and development to the next life stage can then proceed using another development-temperature function. The particular development-temperature functions used in **Osterant** were developed and discussed in Chapter 2. A weight was incorporated into the daily development fraction to account for times during the day when temperatures fell below the threshold temperature. This weight was the estimated proportion of the day when temperatures were such that development proceeded normally.

Not only is development temperature dependent, it is also known that rainfall plays an important part in the free-living stages of nematodes, particularly in the migration of newly hatched eggs from the faecal mat and infective L3s up the grass swards. Two moisture effects have been incorporated into the model.

The first moisture effect involves the development from the first larval stage, L1, to the third, L3. One of three conditions pertaining to the rainfall history and herbage density must be satisfied for the pasture to be regarded as moist on a specific day. Either, rain must have fallen on that day or on either of the two days preceding it, or 10mm (or 15mm) of rain must have fallen over the preceding

week (or 15 days) with herbage density exceeding 2500 (or 3000) kdm per hectare. Herbage density is regarded as being important for migration as a high density of herbage on pasture means that surface moisture is retained in higher quantities for a longer time.

The development rate for an individual on a particular day would be weighted according to the moisture index. The weight would be zero if none of the above moisture conditions were satisfied and one if at least one of the conditions were satisfied.

The second moisture effect involves the migration of the infective L3s from the mat up the grass sward. A single days rainfall is required for newly developed infective L3s to be available for ingestion by the sheep host. This follows from the frequently observed appearance of large numbers of parasites on the pasture immediately after rainfall.

The Julian date of commencement and end of the simulation is input by the users as is the area of land in hectares on which the parasite and host populations inhabit.

3.2.3 Grass Sample Data

If samples of herbage density taken at the site of simulation are available, the model will incorporate these and interpolate over the simulation period using established methods to determine daily herbage density levels on that particular pasture. This aids in the calculation of the moisture index discussed above. The grass sample data is easily entered into the program from the menu.

3.2.4 The Site of Simulation

Data specific to the site or location being simulated must be entered by the user. This includes the number of ewes and lambs initially introduced onto pasture, the faecal output of ewes and lambs respectively, the date of lamb movement, the stocking rate, and the number of years which the simulation is to be run for.

The faecal output of ewes and lambs will be different, however obtaining actual figures is likely to be difficult due to the variation in experimental methods. It is necessary to know the expected daily faecal output of ewes and lambs respectively as the parasite egg output is conventionally measured in terms of eggs per gram

of faeces.

Movement of lambs to clean pasture has long been used as a control strategy in the fight against resistance. To move lambs onto clean pasture in the simulation, all that is needed is the date on which this is to happen, the program will then set up a second clean pasture and move the lambs accordingly.

3.2.5 Nematode Treatment Data

Details of the treatment regimen operating at a particular site may be entered into the model at this point. The days on which treatment is to be administered must be specified. From this information, the model will reduce parasite numbers on the days stated according to the efficacy of the drug.

3.2.6 L3 Sample Data

The genotype distribution of parasites harboured in the ewes is input by the user. On initially contaminated pasture, the genotype distribution of overwintered L3s is also required. It is assumed that infective L3s from the previous year will have overwintered and re-emerge at the start of the new grazing season. There is also the opportunity for the user to enter sample data collected from a particular site. This data is then used by the model as real estimates of initial and intermediate contamination levels on the pasture.

3.2.7 The Results Menu

The results menu provides the user with a resumé of the input data and the genetical results from each simulation. This includes the final genotype distribution, and the time taken to reach this distribution.

3.3 Dynamics of Osterant

All of the above factors are under the control of the user. However certain aspects of the epidemiology of the disease, the dynamics of the parasite population and the genetical changes to the population cannot be altered, as to do so would undermine the foundations of the model. These include the development func-

tions, the genetic assumptions, the rate of adult establishment in the host, the estimated herbage intake of ewes and lambs and the egg output of ewes and lambs respectively. Development of the free-living stages of *T. circumcincta* has been discussed in section (3.2.2), and the derivation of the equations can be found in Chapter 2. The development-temperature functions used in this model are particular to each life stage. Each is a single analytic equation that calculates the development rate of an individual in that life stage over the entire temperature range which that individual would expect to be exposed to.

Using results from tracer lamb experiments, pasture larval contamination levels were compared to adult worm burdens in the tracer lambs after slaughter. These experiments indicated that an increased larval intake led to lower adult worm burdens. This phenomenon was modelled using a step function that yielded the proportion of ingested L3 that established as adults sixteen days later in the host.

Egg output of adult worms in lambs is thought to be governed by the hosts immune response and whether the pasture is initially clean or contaminated.

Simple Mendellian principles govern the segregation and recombination of genes within the population. Resistance is assumed to be conferred by two alleles at a single locus on the chromosome, denoted r(resistant) and s(susceptible). Mating of parasites is random and the resultant offspring are assumed to occur in Hardy-Weinberg equilibrium, that is, if the frequency of the gene conferring resistance in a parent population is r, then the resultant offspring genotypes will occur in the ratio $r^2 : 2rs : s^2$ for $rr : rs : ss$, respectively.

3.4 Validation of Osterant

The output from the model was validated by comparing the results obtained from an observational study at an experimental station in Cockle Park in Northumberland (Waller, 1982) over a period of two years. Meteorological and epidemiological data from that site were input into the model. The emergence patterns of infective L3s on pasture for the two years generated by **Osterant** were compared to those generated experimentally. Predicted emergence patterns followed the observed results very closely (Paton, 1983) for both of the years despite very different levels of parasitism in 1973 compared with 1974. That is, predicted initial emergence dates of L3 coincided with the observed emergence dates at very similar levels. Observed and predicted peak pasture contamination levels were

very similar and the timing of the peaks occur within days of each other. The declines after the summer peak for both years follow a similar path for observed and predicted, with predictions of a second autumnal peak in 1973 as observed, but none in 1974, as observed. It can be concluded that at least for the prediction model, despite the myriad of factors involved in the complex dynamics of the population and its interaction with the host and the environment, the results have been validated and the output of the model can be trusted at least as an indicator of events in the field.

The integration of the drug selection model added another dimension to the prediction model by presenting a way to examine the effect of various management control strategies on the growth and evolution of anthelmintic resistance in a population of nematodes at a particular site.

Ten management programmes were examined to reflect the variety of control strategies in use around Britain. These were split into three categories. The first category involved control via the transfer of lambs to safe pasture at different times over the grazing season. The second category contained those strategies involving control by moving both ewes and lambs to safe pasture, and the third category contained those strategies where both ewes and lambs remained permanently on the original pasture throughout the grazing season.

To examine the effect of different drug groups, the fitnesses of the genotypes were varied. Five fitness sets were simulated. It was assumed that all drugs killed all the susceptible homozygotes. The proportion of the heterozygotes and the resistant homozygotes that are killed by the drug varied according to whether the drug selected for dominance, recessiveness, incomplete dominance or heterozygote superiority.

Having carried out the simulations (Gettinby *et al*, 1989), it was concluded that switching to clean pasture and reducing the dosing frequency of the anthelmintics would slow the drug selection process quite significantly. If frequent dosing was unavoidable then it was recommended that it take place early on in the season rather than late and that the drug used selected for dominance of the resistant allele.

These general results have since been backed up by experimental effort and they are now widely established methods of controlling or at least slowing down the growth and evolution of anthelmintic resistance in nematode populations.

3.5 Implementation of Osterant

Osterant as a predictive tool to be used at the farm level on a daily basis is still a long way away. For the moment, its strength lies in its flexibility to change scenarios very easily in order to answer What If ? questions. Such questions provide a broad speculative view on the effect of certain changes to the system, such as a global increase in temperature, a drop in average rainfall levels, the effect of a new drug or control strategy on the population. Predictions for the future primarily require accurate meteorological forecasts, due to the parasites dependence on climate for survival.

In this chapter **Osterant** will be used experimentally to address whether variations arising from within the parasite population can contribute to the variation in infection levels and effects thereof observed in the field, or whether geographical or temporal variations cause these observed fluctuations in the field.

The population dynamics of *T. circumcincta* were simulated by **Osterant** at four different climatic sites in Scotland: Paisley, Mylnefield, Kinloss and Dumfries, over a period of six years from 1985 to 1990, respectively. The locations were chosen to reflect the diversity in climate experienced in Scotland. The development functions derived in Chapter 2 were substituted into the model in place of the step function originally used. The data were taken from the AFRC Meteorological Database, AGREMET.

At each location in each year the model was run for *fast*, *average* and *slow* developers, respectively. The emergence patterns were analysed to determine the sources of variation in peak pasture contamination levels and timing. Initial contamination levels were kept constant at the beginning of each simulation in order to retain as much uniformity as possible.

3.6 Results

From these simulations, three sources of variation were identified

- Geographical : variation observed between locations over each year.
- Temporal : variation observed between years at a single location.
- Developmental : variation observed between development groups within a single location in a single year.

3.6.1 Comparison of Emergence Patterns

In order to compare emergence patterns produced from the simulations, the following criteria were identified:

- Initial Emergence Date : the first day in the season when infective L3s are observed.
- Peak Pasture Contamination Level : the highest number of infective L3s observed on pasture on any one day.
- Timing of peak : the date when peak pasture contamination is observed.

Figures 3.5-3.12 present the emergence profiles obtained and Table 3.1 gives initial emergence dates, peak pasture contamination levels and timing, for each of the simulations.

Emergence Profiles of *Fast* Developers

The emergence profiles of *fast* developers at each location in each year are presented in the first column of Figures 3.5-3.12.

In general, *fast* developing parasites are seen to emerge onto pasture before the *medium* and *slow* developers. As these parasites accumulate daily, the infection level grows steadily to a peak around the middle of July. There follows a gradual decline in infection levels until the end August when a second much smaller peak occurs, possibly as a result of the lamb contribution to infection. Infection levels are then seen to drop steadily until November when a sharp increase in infection levels is observed.

Emergence Profiles of *Medium* Developers

The emergence profiles of the *medium* developers at each location in each year are presented in the second column of Figures 3.5-3.12.

Initial emergence of the *medium* developers occurs slightly later in the season than the *fast* developing parasites as does the peak pasture contamination level. A small second peak possibly as a result of the lamb contribution to infection is observed around the end of September, after which infection levels decline until the end of November, where they are then seen to exhibit a similarly sharp increase as observed when the *fast* developing population were simulated. The overall magnitude of infection on pasture with a *medium* developing population is greatly reduced from the infection levels in a simulated population of *fast* developers.

Emergence Profiles of *Slow* Developers

The emergence profiles of the *slow* developers at each location in each year are presented in the final column of Figures 3.5-3.12.

Slow developing infective L3s take a longer time to develop from eggs than the other two groups. Typically, they will begin to emerge around the middle of June. In many cases, a very small peak is observed at the end of August. The main peak of infection is observed in September, the magnitudes of which are much reduced from the other two groups. Again, a decline in infection levels occurs with a sharp increase after the end of October.

3.6.2 Geographical Variation

The geographical locations simulated were chosen to represent areas in the north, south, east and west of Scotland, to give a sample of the range of climatic behaviour experienced in this country. Within each year, in each development group, the emergence patterns at each location were very similar, with the exception of Dumfries in 1985.

In order to determine the effect of geographical location on the population dynamics of the *T. circumcincta* population, all other sources of variation were held constant. That is, the emergence profiles produced in Dumfries, Kinloss, Paisley and Mylnefield were compared within each development group within each year.

Differences in Initial Emergence Dates Between Locations

Differences in the initial emergence dates within development groups in a single year at each location can be attributed to climatic fluctuations between the four locations. For example, from Table 3.1, the initial emergence date for *fast* developers in Dumfries in 1985 is much later than the initial emergence date in this year at the other locations. In Dumfries, infective L3 were initially detected on pasture on the 31^{st} of May compared to the 9^{th} of May in Paisley and Kinloss, respectively, and the 14^{th} of May in Mylnefield. From the bioclimatographs in Figures 3.1-3.2, this difference in timing of initial emergence may be attributed to the fact that that although Dumfries experienced average temperature levels in April, 1985, the rainfall levels were not adequate for the migration of the infective L3 up the grass sward. In April 1985, the rainfall totalled only 13.5mm over a period of 8 days in Dumfries, compared to 50.8mm in 23 days, 61mm in 19 days and 62.5mm in 25 days recorded in Paisley, Mylnefield and Kinloss, respectively.

Differences in Peak Pasture Contamination Levels and Timing Between Locations

It was suggested previously that below average rainfall levels in April, 1985, caused later than usual initial emergence times in Dumfries for the *fast* and *medium* developers. This has had a knock-on effect for the general emergence pattern during this year. Peak pasture contamination levels in Dumfries in 1985 for the *fast* developers did not occur until the end of the year, with a magnitude of 9543 L3 per kdm, compared to peak levels of 15128 and 15069 L3 per kdm for Paisley and Kinloss, both on the 12^{th} of July, and 15128 L3 per kdm on 17^{th} July in Mylnefield. For *medium* developers, peak pasture contamination levels in Dumfries in 1995 were reached on the 18^{th} November at a magnitude of 4678 L3 per kdm, compared to peak levels of 8532, 7463 and 8124 L3 per kdm in Paisley on the 27^{th} July, in Mylnefield on the 1^{st} August and in Kinloss on the 29^{th} July respectively. The *slow* developers in Dumfries in 1985 were not as severely affected by the shortage of moisture in April, as newly voided eggs in April did not develop to infective L3 until 16^{th} of June, thus avoiding the drought conditions in April that hampered migration of the *fast* and *medium* infective L3s up the grass sward.

Although there were slight differences between the time of initial emergence and of peak pasture contamination levels for all of the locations over the six years,

it was discovered that within each of the development groups, *fast*, *medium* and *slow*, the average time between initial emergence date and peak pasture contamination timing, was approximately the same for each of the locations. The climate determines at what point in time infective L3s will initially emerge on pasture, however, the time interval that passes until peak pasture contamination occurs appears only to depend on what development group the individual belongs.

It is clear from this that climatic differences between geographical locations do not produce sufficient variation in parasite emergence levels to account for the variation observed.

3.6.3 Temporal Variation

Comparisons of emergence profiles were made within development groups at a single location in order to determine the effect of time on the population dynamics of *T. circumcincta* .

Six years of climatic data were simulated in order to determine if changes in climate from year to year would account for the observed fluctuations in emergence patterns in the field.

When the *fast* population were simulated at each location over the six years, similar emergence profiles were produced for the years 1985, 1986, 1987 and 1990. In 1988 at Paisley, Mylnefield and Kinloss (no data for Dumfries in this year was available), and 1989 at Mylnefield, Kinloss and Dumfries, peak pasture contamination levels were much reduced, ranging from 8715 to 10541 L3 per kdm compared to 13997 to 17309 L3 per kdm in the other years.

In contrast, when *medium* and *slow* populations were simulated, there was only a single emergence profile that differed considerably from the others, that of Dumfries in 1985. All other profiles at each location over each of the six years were very similar. Because *fast* developers are changing faster, there is bound to be more variation inherent than the *medium* and *slows*.

From this it can be concluded that observed variation in parasite emergence levels from year to year at a single site cannot be solely attributed to changes in climate from year to year.

3.6.4 Developmental Variation

The final source of variation identified is that of variation between the *fast*, *medium* and *slow* development groups. For each development group: *fast*, *medium* and *slow*, the model was run at each location over all six years. The results for each group were compared at each site within each year. Effectively, the model was run initially assuming that the entire parasite population were *fast*, then *medium* and them *slow* developers, respectively. The emergence profiles produced when simulating a *fast* developing population were quite different to those emergence profiles produced when *medium* and *slow* developing populations were simulated. In turn, the profiles produced by the *medium* development group were quite different to those produced from simulating the *slow* developing population. This variation is consistently observed across the four locations over the six years.

Initial Emergence Times

When the *fast* developing population were simulated over the six years and four locations, the date of initial emergence extended from the 3^{rd} to the 31^{st} May. In comparison, when the *medium* developing population were simulated, they initially emerged between the 12^{th} May and the 12^{th} June, whereas when the *slow* developing population was simulated, the initial emergence dates ranged from 28^{th} May to the 25^{th} June.

There is approximately nine days lag between initial emergence of the *fast* and *medium* developers and sixteen days between initial emergence between *medium* and *slow* developers. It follows that there is almost 4 weeks difference in initial emergence dates between *fast* and *slow* developers.

With a few notable exceptions the variation in initial emergence dates within each development group occurred between locations rather than between years within locations.

Peak Pasture Contamination Levels and Timing

For the *fast* developing population over the six years and four locations, peak pasture contamination of infective L3s typically occurred between 24^{th} June and the 19^{th} July. In a few of the years, peak levels did not occur until the end of the grazing season. In those simulations where this was the case, peak levels were

Table 3.1: Table containing initial emergence dates, peak contamination levels and timing over four locations, six years and three development groups. * represents missing data.

Location	Year	Emergence Day			Peak Level (in L3 per kdm)(Day)		
		Fast	Med	Slow	Fast	Med	Slow
Paisley	1985	129	143	158	15128.54 (193)	8532.967 (208)	4793.949 (213)
	1986	126	138	159	14326.62 (175)	7029.296 (210)	4011.963 (233)
	1987	129	133	148	17309.96 (198)	10600.04 (209)	4695.484 (237)
	1988	123	132	150	10361.01 (197)	7956.819 (220)	5717.840 (239)
	1989	129	144	153	16848.12 (191)	5891.488 (217)	4515.047 (235)
	1990	125	134	148	15438.31 (177)	9184.295 (208)	5289.488 (226)
Mylnefield	1985	134	144	159	15219.69 (198)	7463.317 (213)	3436.476 (255)
	1986	129	142	159	14982.35 (185)	6250.264 (213)	3000.810 (235)
	1987	130	148	156	16498.42 (193)	8893.417 (215)	5845.449 (247)
	1988	123	136	151	8715.036 (325)	7957.883 (213)	4757.301 (254)
	1989	135	148	163	9876.848 (191)	7221.019 (237)	4887.796 (250)
	1990	129	142	158	15724.45 (196)	5268.384 (210)	5788.589 (248)
Dumfries	1985	151	163	169	9543.193 (315)	4678.26 (323)	3950.76 (324)
	1986	134	143	158	15692.61 (191)	7633.822 (213)	3964.887(232)
	1987	129	143	160	13997.94 (175)	6438.044 (213)	3073.298 (234)
	1988	*	*	*	*	*	*
	1989	128	139	153	8465.832 (325)	7071.79 (209)	3455.681 (254)
	1990	135	153	176	16002.09 (191)	4529.039 (226)	4487.525 (240)
Kinloss	1985	129	142	158	15069.29 (193)	8124.095 (210)	3386.219 (247)
	1986	129	145	155	15806.50 (184)	9330.083 (211)	2775.585 (219)
	1987	131	148	158	15945.49 (192)	8759.948 (213)	4153.342 (252)
	1988	130	137	152	10541.54 (197)	8001.106 (218)	5345.077 (254)
	1989	128	143	155	9566.886 (315)	8051.306 (216)	5230.353 (238)
	1990	135	144	157	15461.53 (200)	7414.890 (215)	4713.913 (228)

much reduced. Peak pasture contamination levels for *fast* developing parasites varied from 9876.848 L3 per kdm in Mylnefield in 1989, to 17309.96 L3 per kdm in Paisley in 1989.

The peak pasture levels produced by the *medium* developers were lower than those produced by the *fast* developers, ranging from 4529.039 L3 per kdm in Dumfries in 1990, to 10600.04 L3 per kdm in Paisley in 1987.

Slow developers experienced much reduced peak pasture levels, occurring later in the year than the *medium* and *fast* developers. Peak levels were recorded between 1^{st} August and the 12^{th} September, ranging from 2775.585 L3 per kdm in Kinloss in 1986, to 5845.449 L3 per kdm in Mylnefield in 1987.

Conclusion

As was expected, large differences were observed in the emergence patterns of *fast*, *medium* and *slow* developers. Initial emergence dates were earliest for the *fast* developers. This meant that the parasites would emerge, be ingested by a host and complete intra-host development at an earlier stage than the *medium* and *slow* developers. Completion of the life cycle after reproduction would then lead to the emergence of *fast* developing parasite eggs onto pasture. This cycle would continue with up to three generations of *fast* developers being produced in a single season from April to October, leading to a rapid build-up of infective L3s on pasture to a peak level. After this, temperatures would drop and ewe egg production would cease, leading to a decrease in the abundance of parasites on pasture.

The *medium* developers began to emerge approximately nine days after the *fast* developers and did not attain such high levels of infection on pasture. These parasites develop slower than the *fast* developers under identical climatic conditions. They will have longer generation times and so fewer generations in a single season, which explains the reduction in magnitude of parasite infection on pasture.

The *slow* developers began emerging approximately three weeks after the initial emergence of the *fast* population. Generation time was long for the *slow* developers. When the optimal development and survival conditions occurred during July, the majority of the *slow* developers were completing their intra-host development, and so were unable to take advantage of the good conditions for optimal

development. Therefore the culmination of long generation times and spending the optimal development period inside their host led to low levels of pasture contamination being produced much later on in the year.

3.7 Discussion

The hypothesis that climate is solely responsible for observed variation in parasite contamination levels was tested by simulating the population dynamics of *T. circumcincta* at four different sites, Paisley, Mylnefield, Kinloss and Dumfries, over a period of six years from 1985 to 1990, using the appropriate climatic data. If climate was the main source of variation, it would be expected that yearly fluctuations in temperature and precipitation would have an effect on the emergence patterns of these parasites.

The previous sections explored the effect of geographical, temporal and developmental variation on the population dynamics of *T. circumcincta* . It appears that with the exception of those times when extreme climatic conditions impeded development and survival of parasites, in general, the variation produced between locations and from year to year was not sufficient to explain the observed variation. This suggested that another source of variation may produce the fluctuations in pasture contamination levels observed.

Consistently, over the four locations and six years, *fast* developers emerged earlier in the season and were in greater abundance then the *medium* or *slow* developers. This suggested that differences between individuals within a population may be an important source of the observed variability in infection levels on pasture from year to year. Previously each member of a population was treated as behaving in a uniform manner-any inherent variability in developmental response to temperature stimuli was ignored.

This reinforces the idea that individuals in a population do not behave in a uniform manner with respect to development and so consideration of this genetic diversity within such a population must be made.

It appears from this that the *fast* developing parasite has an advantage over the *medium* and *slow* developer in terms of producing progeny in sufficient numbers to ensure the continuation of this group into future generations. If this was an unconditional advantage the *fast* population would ultimately be selected for. This clearly does not happen to any great extent in reality. This suggests that some

mechanism exists to prevent *fast* developers ultimately taking over. Two hypotheses are given here, one, a physiological, the other, an environmental hypothesis. The first is that the *fast* developers may be exposed to higher natural mortality rates due to "burn-out". The second reason is that although *fast* developers have an obvious advantage when the climate is favourable, when environmental conditions are harsh, the *medium* and *slow* developers are likely to be still within the host sheltered from climatic extremes and so avoid desiccation due to dry weather or flooding out due to wet weather. Therefore the *medium* and *slow* developers may have a better chance of survival during periods of adverse weather conditions.

The results from this chapter are important not only from a theoretical point view, but also practically. For any form of chemotherapeutic drug to be effective, the time when the greatest number of parasites are most likely to be exposed to the drug needs to be known. Mathematical models have been used to advise on the optimal timing of peak parasite levels in the field, (Barnes and Dobson, 1995; Paton, 1983). The optimal time is the time when the optimal number of parasites are targeted by the drug, simultaneously ensuring the dosing strategy does not encourage the evolution of anthelmintic strains of parasite. Predicting the optimal time to administer treatment to a host has been difficult for the conventional mathematical models. This chapter has highlighted a major source of variation coming from within the parasite population, which has previously been omitted from the most recent models of nematode population dynamics to date. By effectively removing climate as a source of variation, it was possible to gauge the effect of developmental variation from within the parasite population on the dynamics of that population.

It is acknowledged that in reality there are not three distinct groups of developers but a continuum beginning with *fast* through *average* to *slow*. However, to develop this theory, it is initially assumed that the population is either *fast*, *medium* or *slow* developers to explore the effect that this variation may have on the population dynamics of *T. circumcincta* .

It is hoped in the next chapter to deal with mixing between the three genotypes to establish conditions under which an equilibrium gene frequency exists.

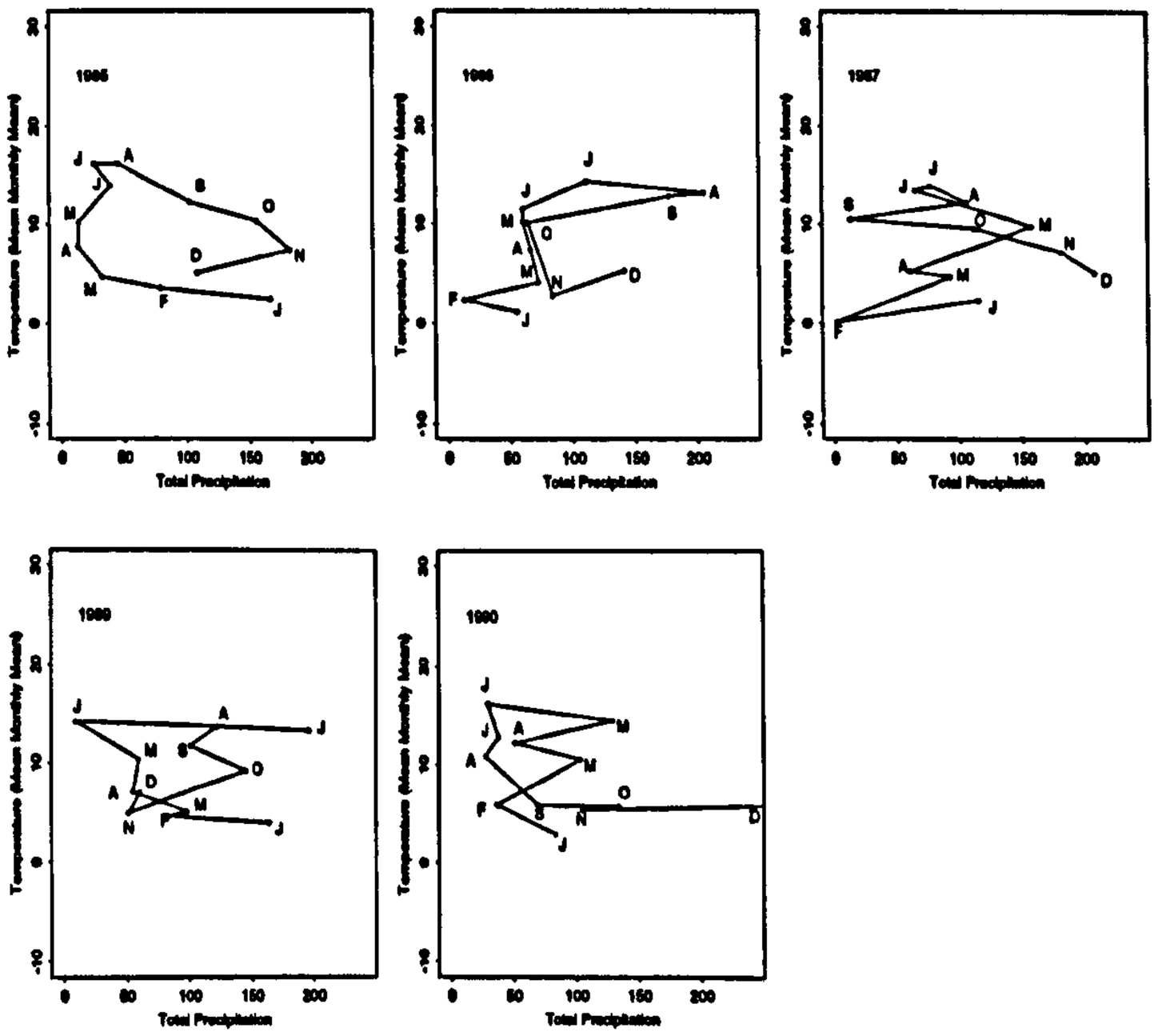

Figure 3.1: Bioclimatograph of total rainfall against mean monthly mean temperatures for Dumfries over the years 1985-1990.

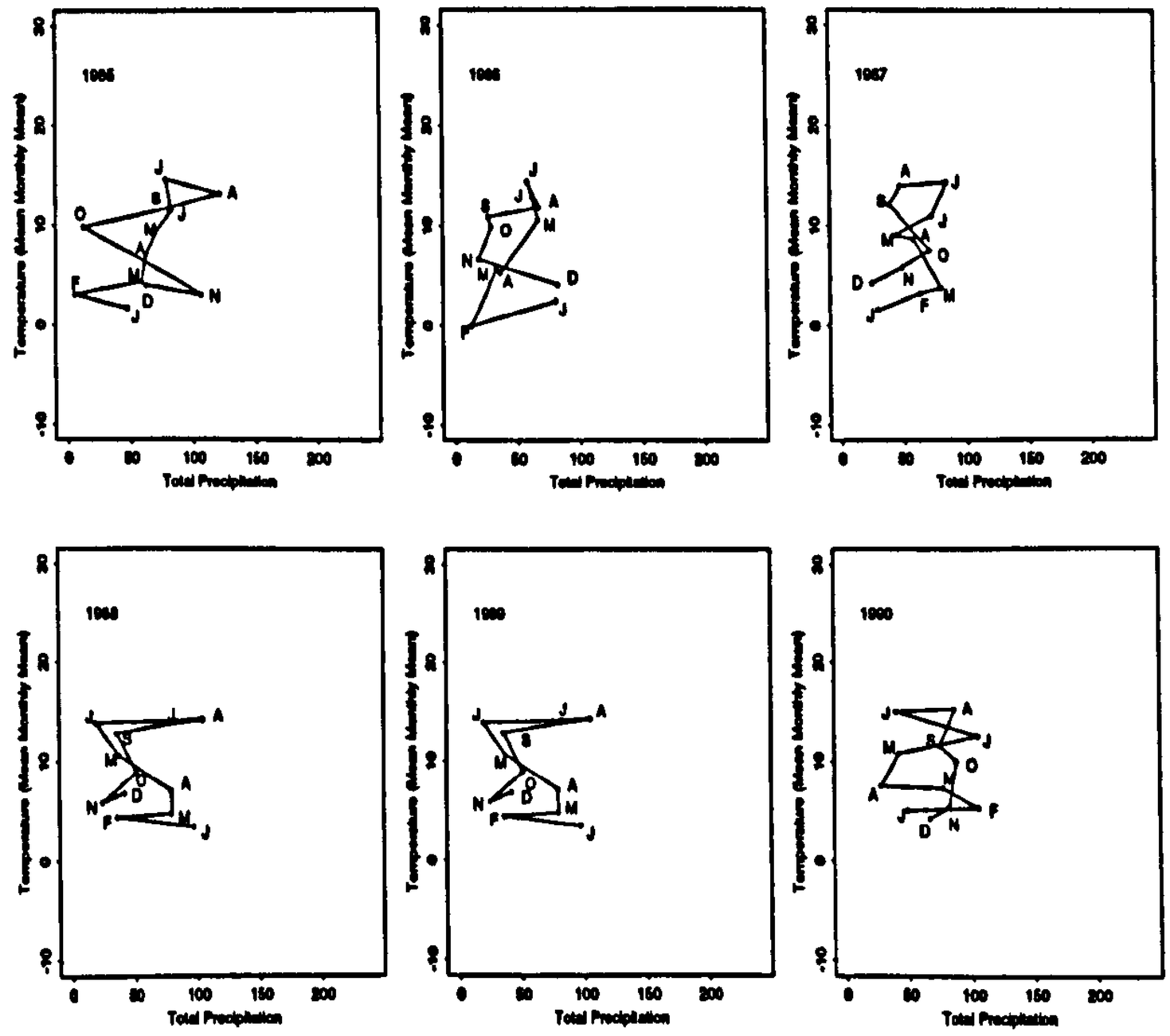

Figure 3.2: Bioclimatograph of total rainfall against mean monthly mean temperatures for Kinloss over the years 1985-1990.

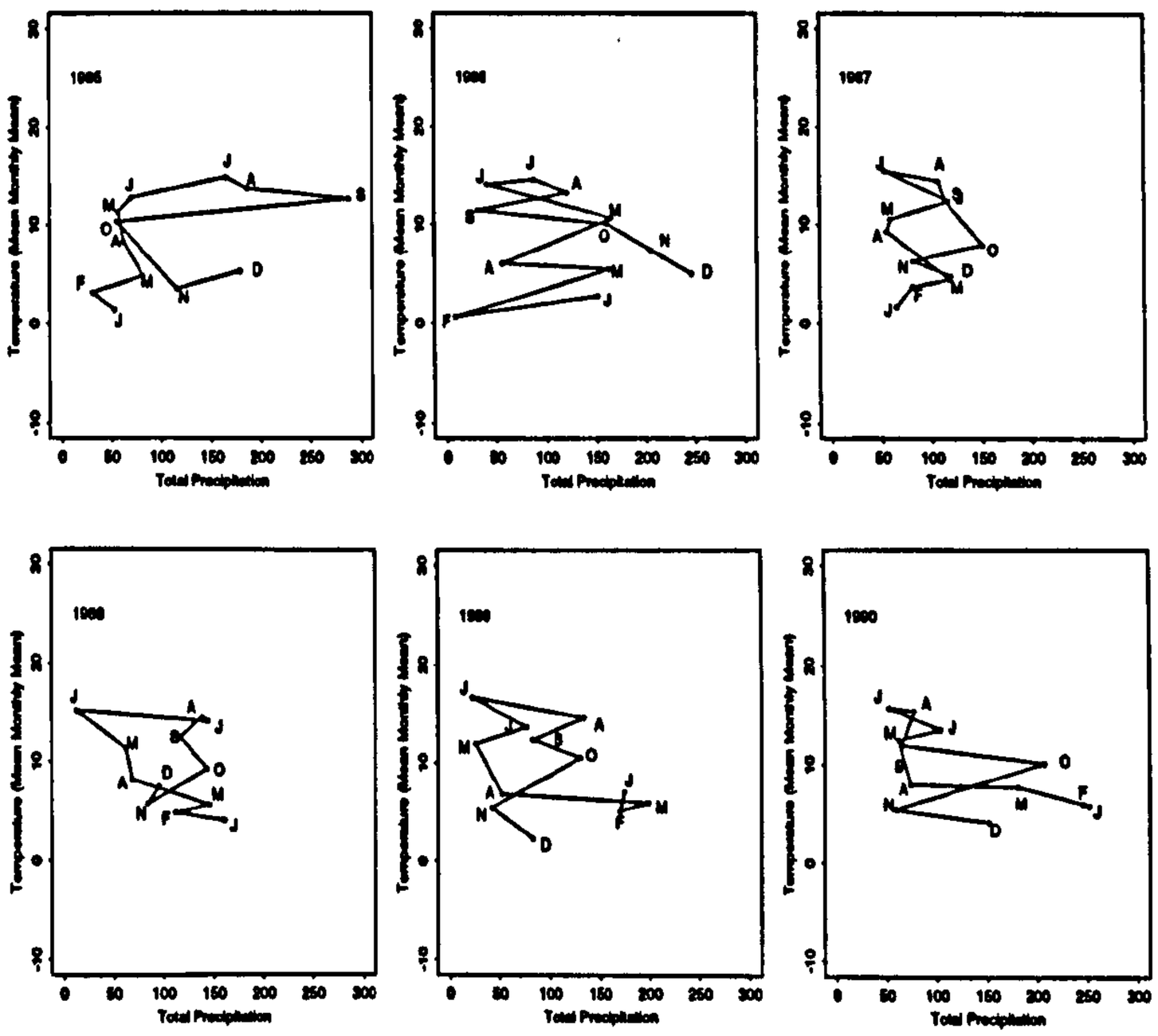

Figure 3.3: Bioclimatograph of total rainfall against mean monthly mean temperatures for Paisley over the years 1985-1990.

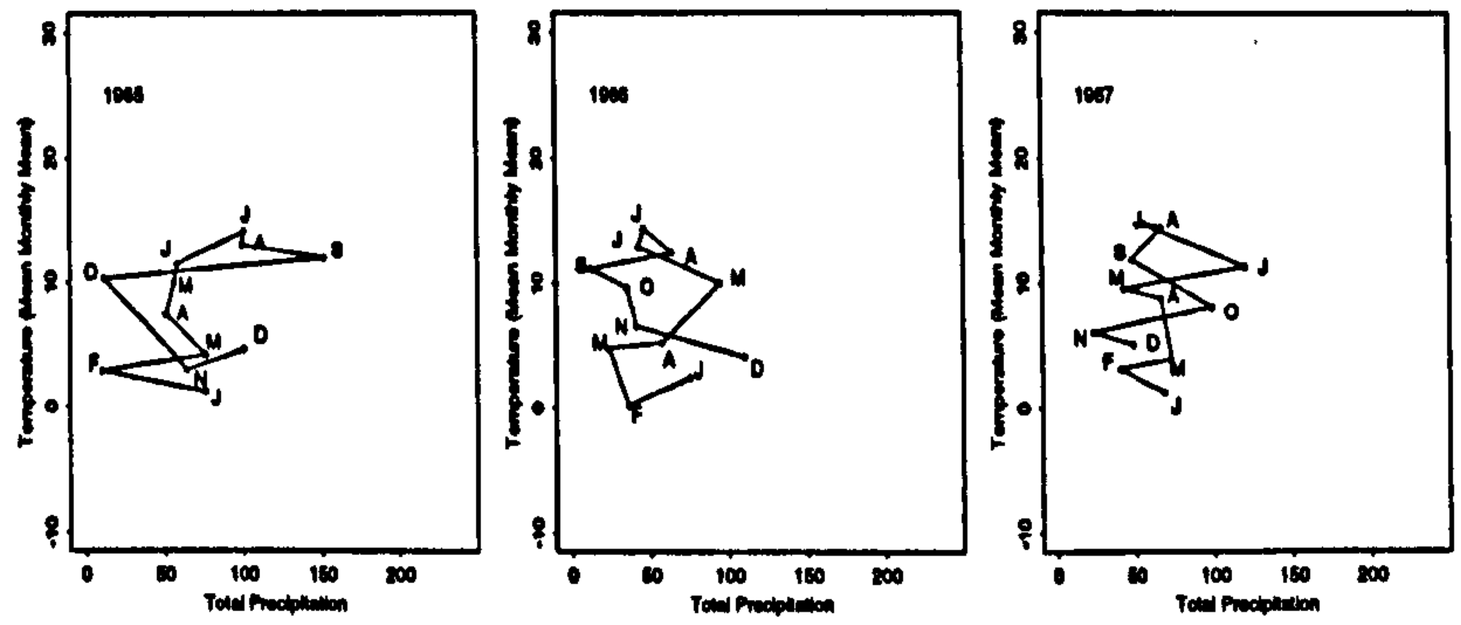

Figure 3.4: Bioclimatograph of total rainfall against mean monthly mean temperatures for Mylnefield over the years 1985-1990.

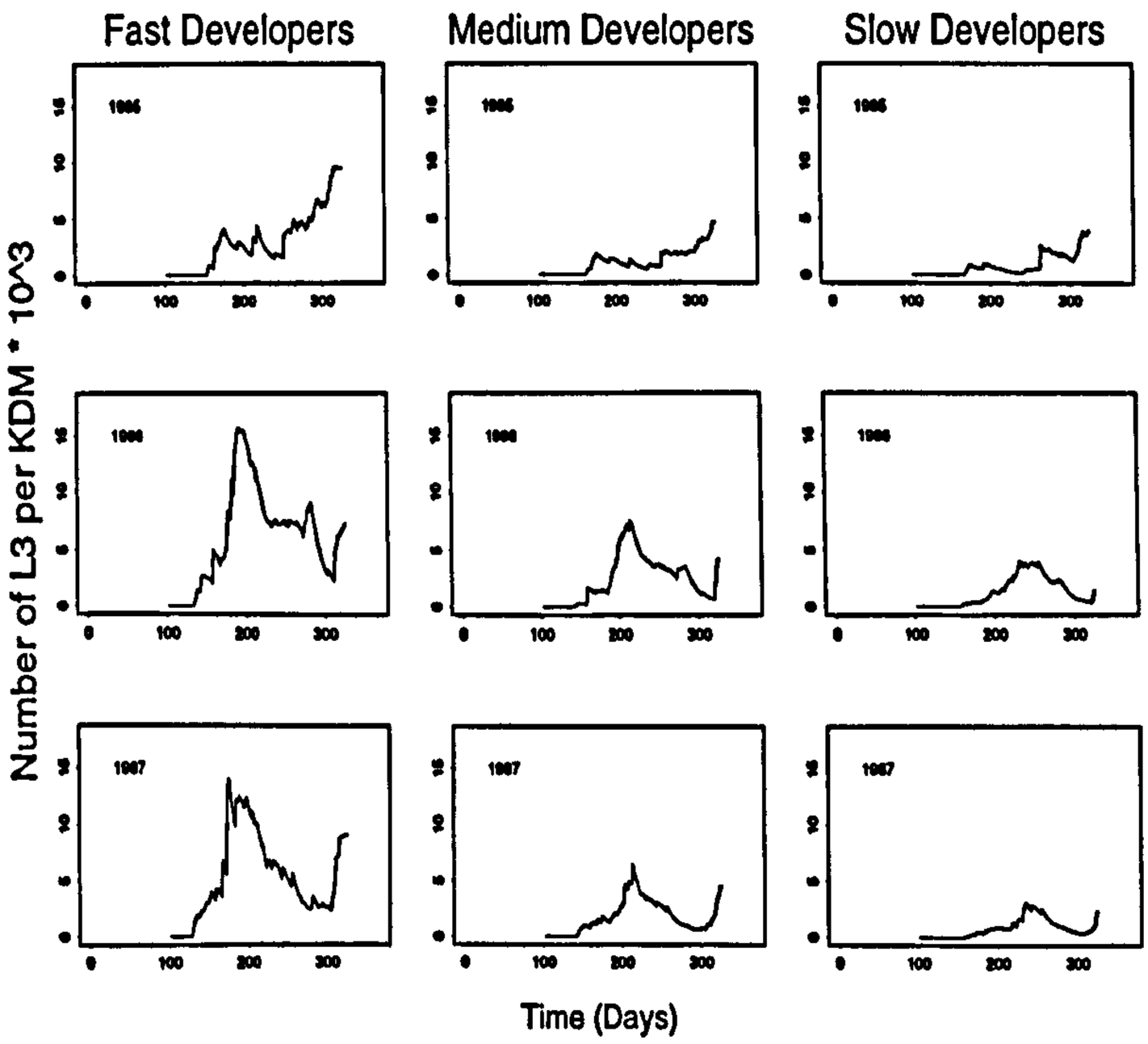

Figure 3.5: Emergence profiles for Dumfries for *fast*, *medium* and *slow* developers for 1985, 1986 and 1987.

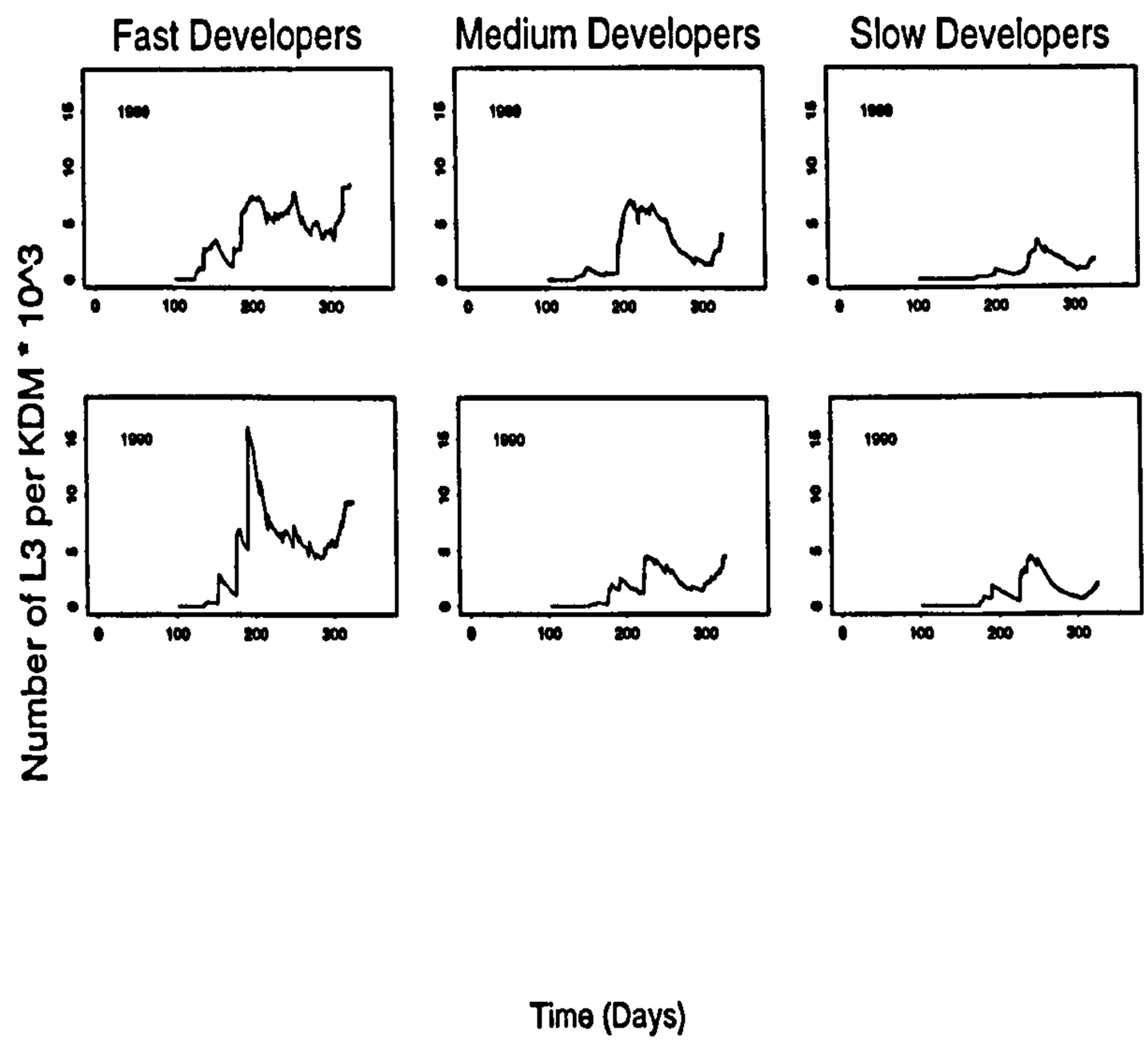

Figure 3.6: Emergence profiles for Dumfries for *fast*, *medium* and *slow* developers for 1989 and 1990. Data is missing for 1988.

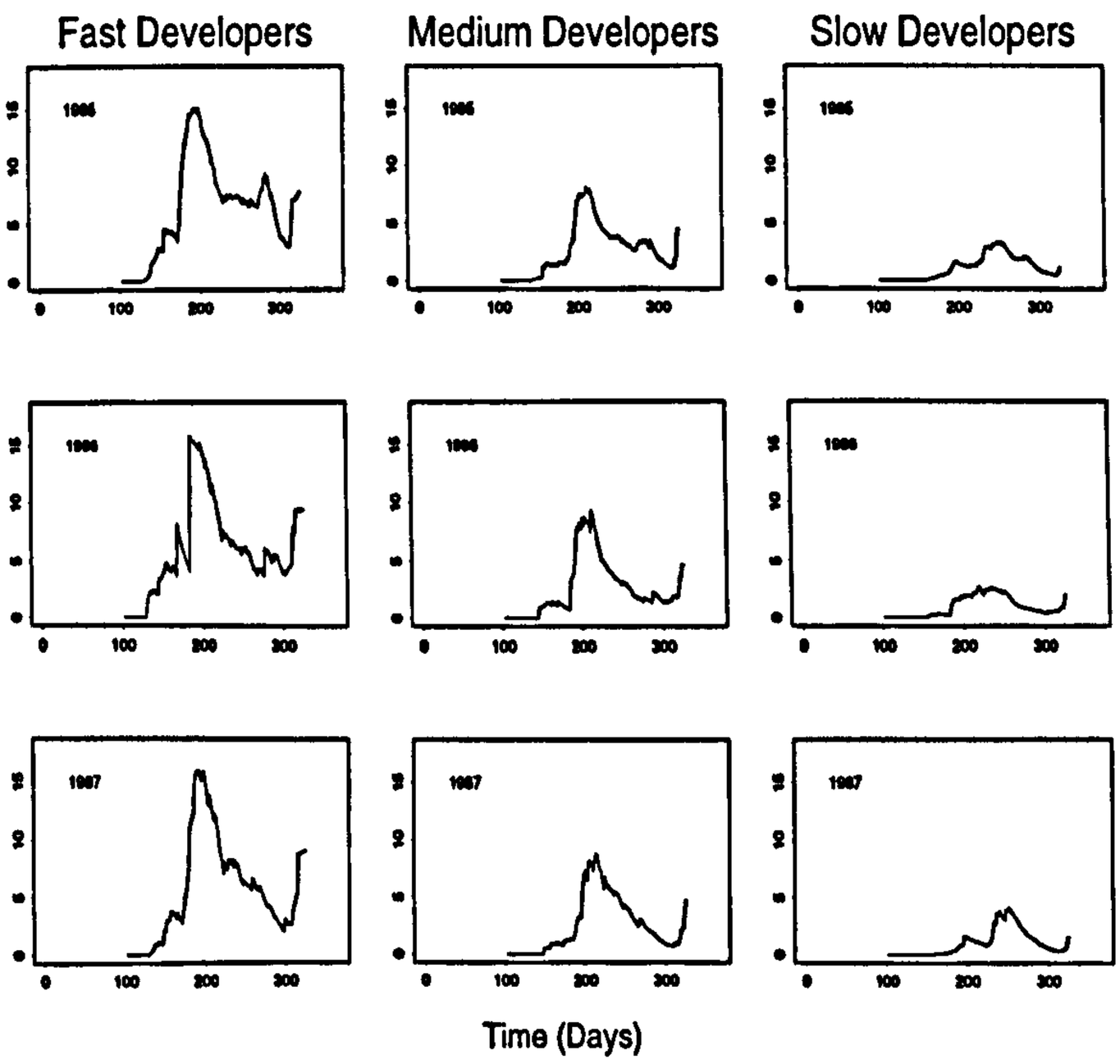

Figure 3.7: Emergence profiles for Kinloss for *fast*, *medium* and *slow* developers for 1985, 1986 and 1987.

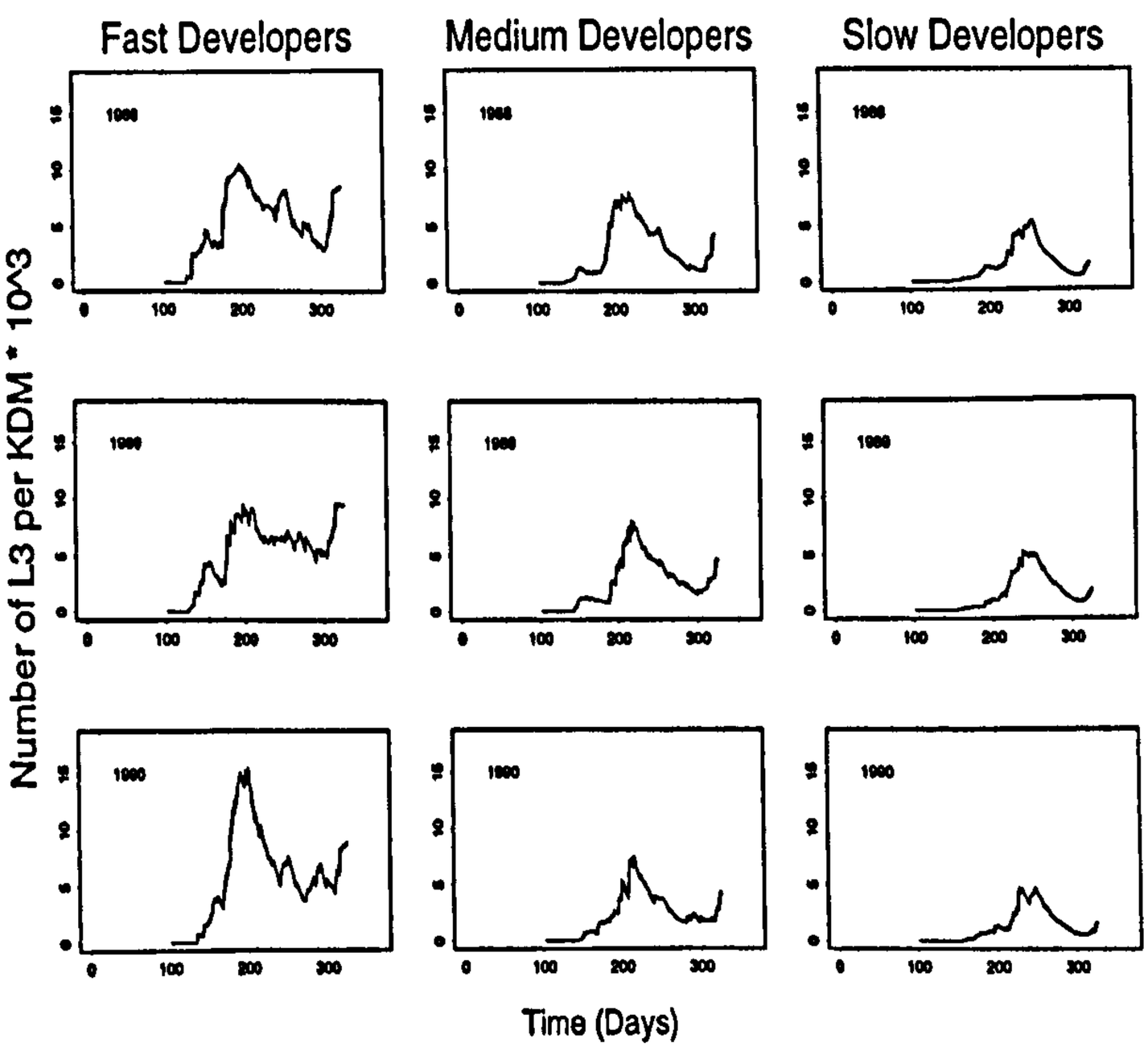

Figure 3.8: Emergence profiles for Kinloss for *fast*, *medium* and *slow* developers for 1988, 1989 and 1990.

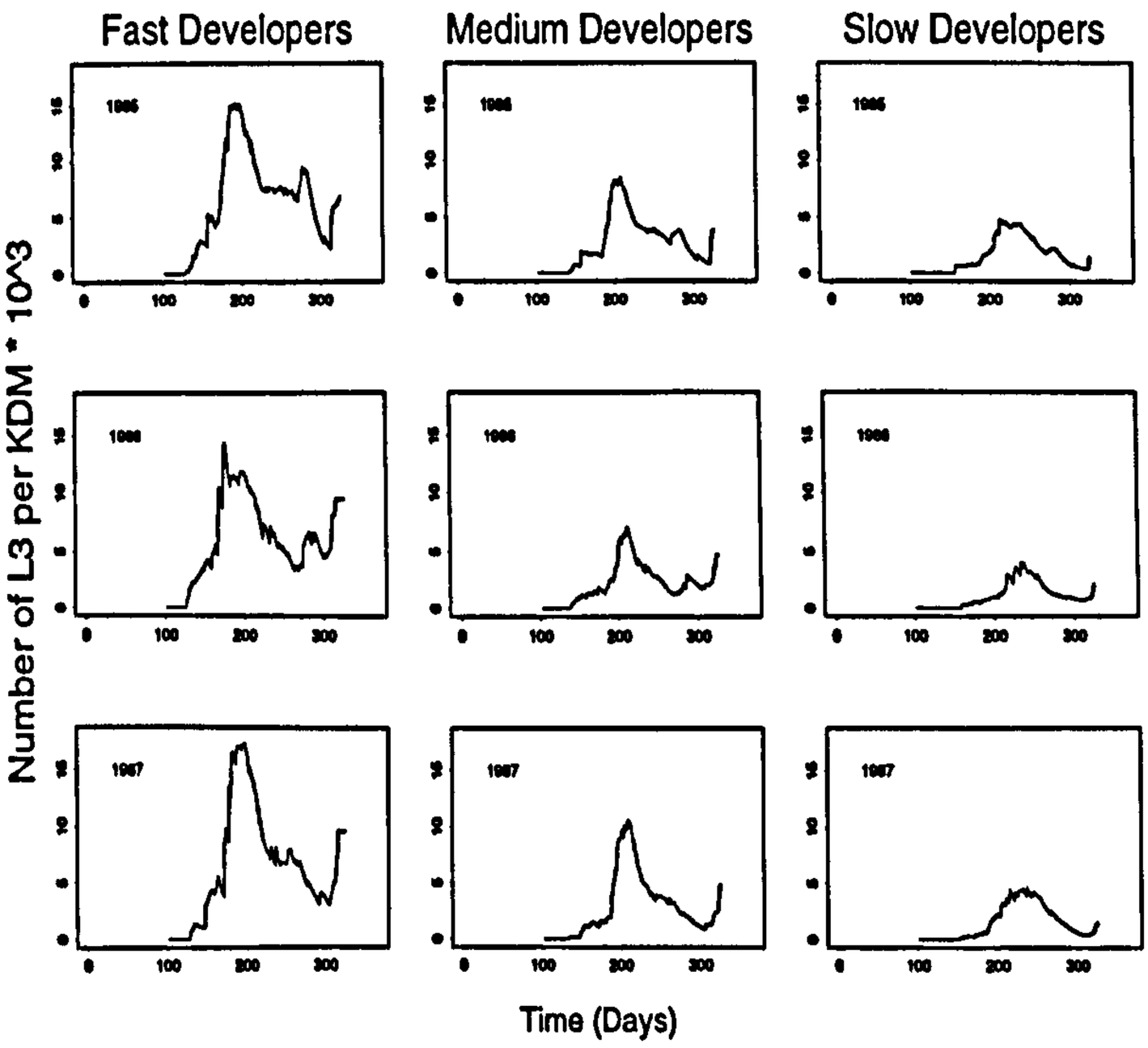

Figure 3.9: Emergence profiles for Paisley for *fast*, *medium* and *slow* developers for 1985, 1986 and 1987.

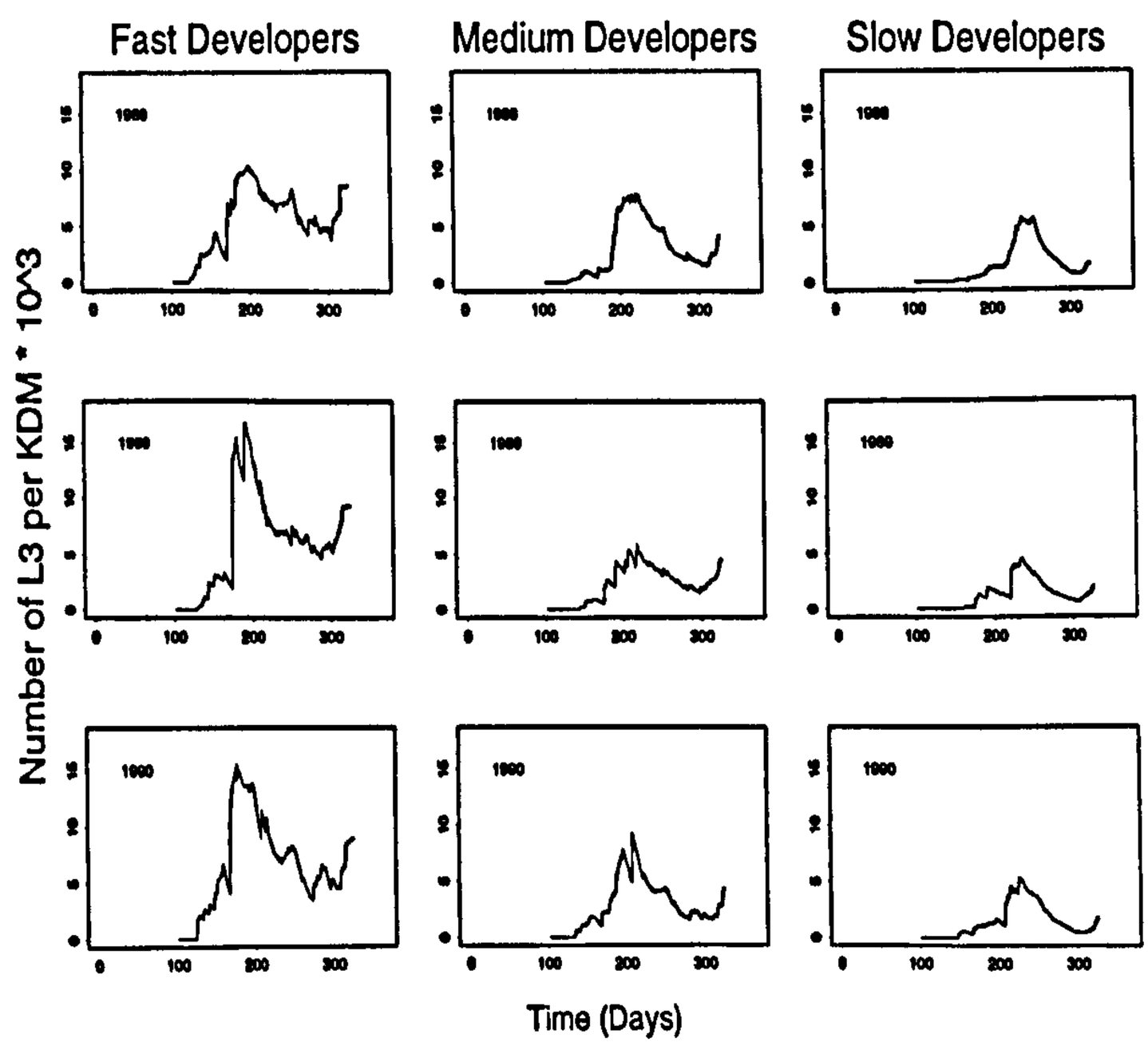

Figure 3.10: Emergence profiles for Paisley for *fast*, *medium* and *slow* developers for 1988, 1989 and 1990.

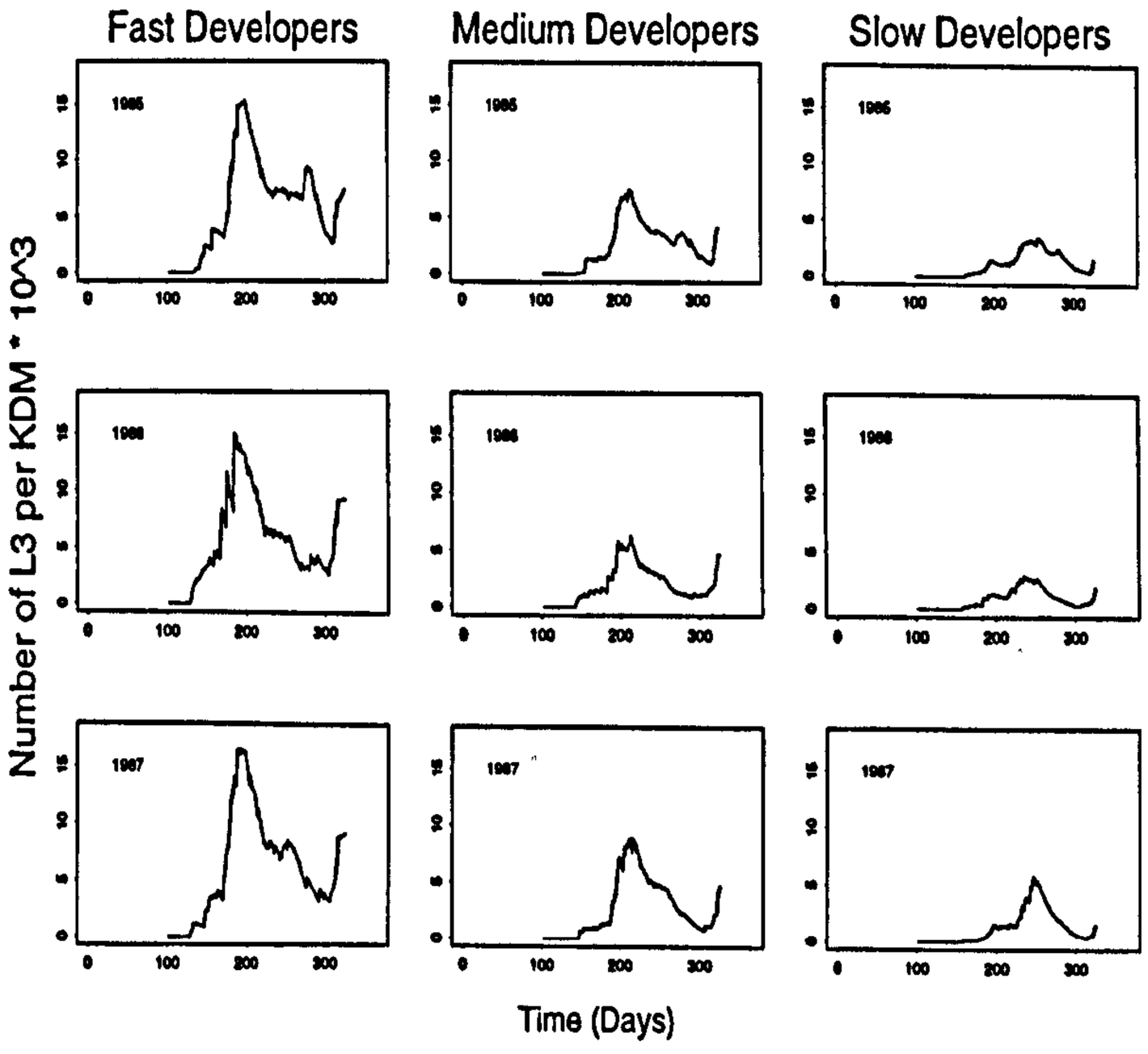

Figure 3.11: Emergence profiles for Mylnefield for *fast*, *medium* and *slow* developers for 1985, 1986 and 1987.

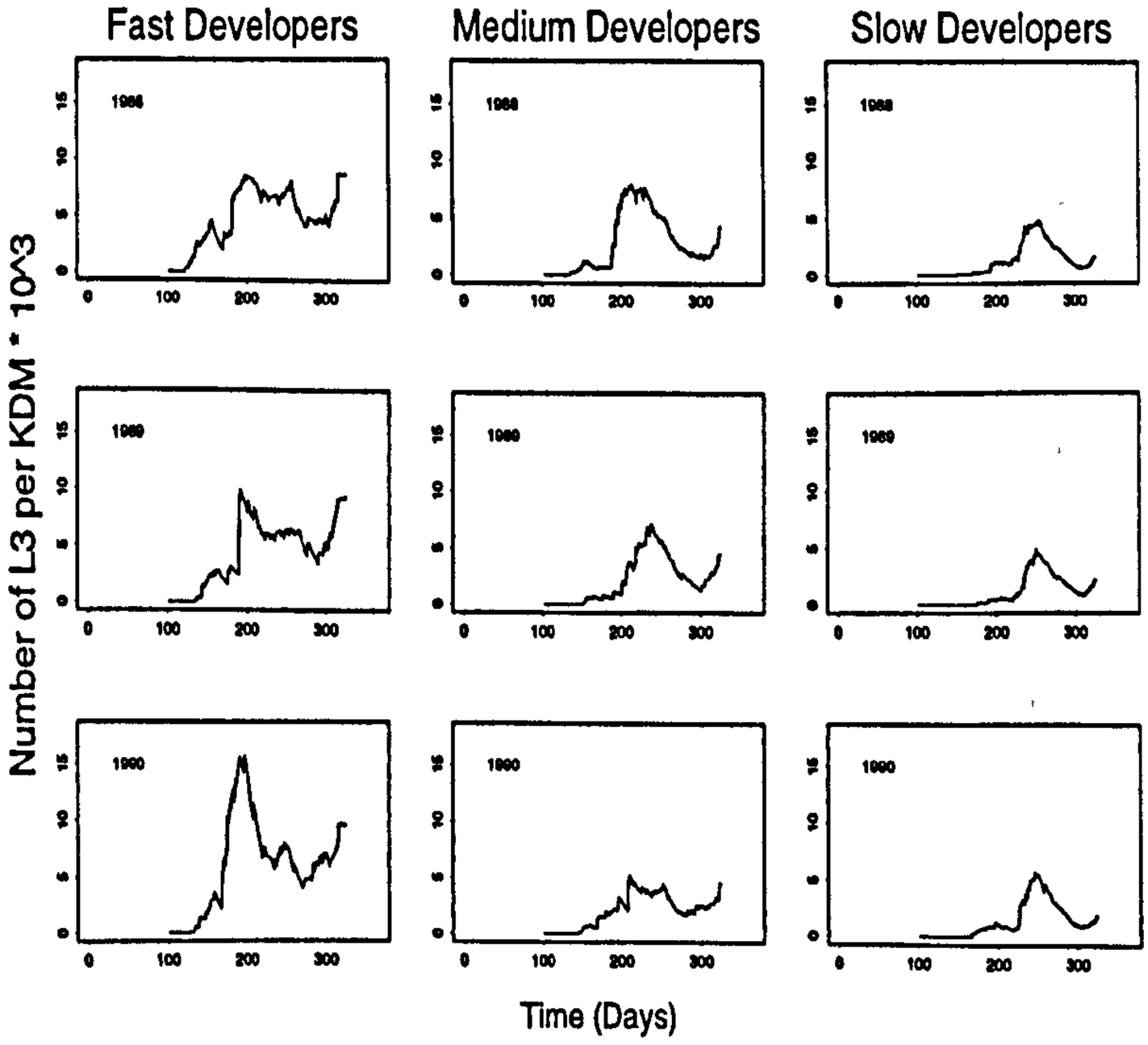

Figure 3.12: Emergence profiles for Mylnefield for *fast*, *medium* and *slow* developers for 1988, 1989 and 1990.

Chapter 4

Modelling the Life Cycle of *T. circumcincta* with Variable Development Times

4.1 Introduction

In Chapter 2, three models were constructed from empirical data that described the free-living development rate of *fast*, *average* and *slow* developing nematodes, respectively, over a range of temperatures. In Chapter 3, these models were incorporated into **Osterant**, a prediction model for PGE in lambs, to explore the impact of development rate on the population dynamics of *T. circumcincta* when the entire nematode population was assumed to be either *fast*, *average* or *slow* developers.

The first model in this Chapter, the non-mixing model, describes the dynamics of a nematode population divided into three development groups that are assumed not to mix at reproduction. Classification into these groups is according to the rate at which an individual develops whilst free-living on pasture.

A genetic component is then integrated into the basic model representing the more realistic situation where the three subgroups interact and mix at reproduction. This adds considerably to the complexity of the model, as interactions between subpopulations give rise to non-linear components. We demonstrate the intractability of such models, outline possible methods of analysis and present a model for the genetic mixing of a simple single staged population.

4.2 The Life Cycle of *T. circumcincta* Without Random Mixing

The Non-Mixing Model

4.2.1 Assumptions

1. The rate at which an individual develops whilst free-living on pasture is assumed to be conferred by two alleles at a single locus on the chromosome, F (*fast* development) and S (*slow* development). This results in three genotypes for development: FF, FS and SS. FF individuals are *fast* developers, SS are *slow*, and FS develop at a rate somewhere between *fast* and *slow* depending on the dominance of the F gene.

2. There are five larval stages, an adult and egg stage in the life cycle of *T. circumcincta* . Three of the larval stages are spent free-living, the remaining two intra-host. For simplicity, the life cycle will be reduced to three life stages only - an egg stage, an infective larval stage and an adult stage, as shown in Figure 4.1. Lewis (1977a) has shown that life cycle graphs can be reduced in this way to simplify analysis.

3. Within a life stage, each individual is classified as being either FF, FS or SS. The genotype of an individual defines the length of time it spends free-living on the pasture before becoming infective to a host.

4. For the moment, the time spent in the parasitic phase inside the host, is not genotype-dependent and is assumed to be constant.

5. At reproduction, it is assumed that no mixing occurs between genotypes. Effectively, individuals within a genotype group are confined to that group at reproduction.

Thus, the population is divided by life stage, by genotype within stage and by age within genotype.

4.2.2 Synthesis of the Non-Mixing Model

This section describes the reduced life cycle of *T. circumcincta* as a system of linear difference equations. Figure 4.1 is a graphical description of this model.

The number of newly voided eggs of genotype i (with $i = 1, 2, 3$, representing FF, FS and SS respectively), in the first age group, at time $t + 1$ is

$$E_{i,1}(t+1) = \Theta_i P_{34} Ad_i(t) \tag{4.1}$$

where P_{34} is the transition probability from adult to egg stage,

Θ_i is the fecundity of female worms of genotype i, and

$Ad_i(t)$ is the number of female adult worms of genotype i at time t.

Development time from egg to the third larval stage, (L3), is genotype dependent, where those individuals with SS genotypes have a longer free-living development period than those with FS genotypes, and likewise, individuals with FS genotypes spend a longer time free-living on pasture than those with FF genotypes.

The number of eggs of genotype i ($i = 1, 2, 3$), in age group n_i, ($n_i = 2...\tau_i$), where τ_i is the genotype dependent development time from egg to L3, is determined by

$$E_{i,n_i}(t+1) = E_{i,n_i-1}(t)\alpha \tag{4.2}$$

where α is the daily survival probability of eggs from one age class to the next.

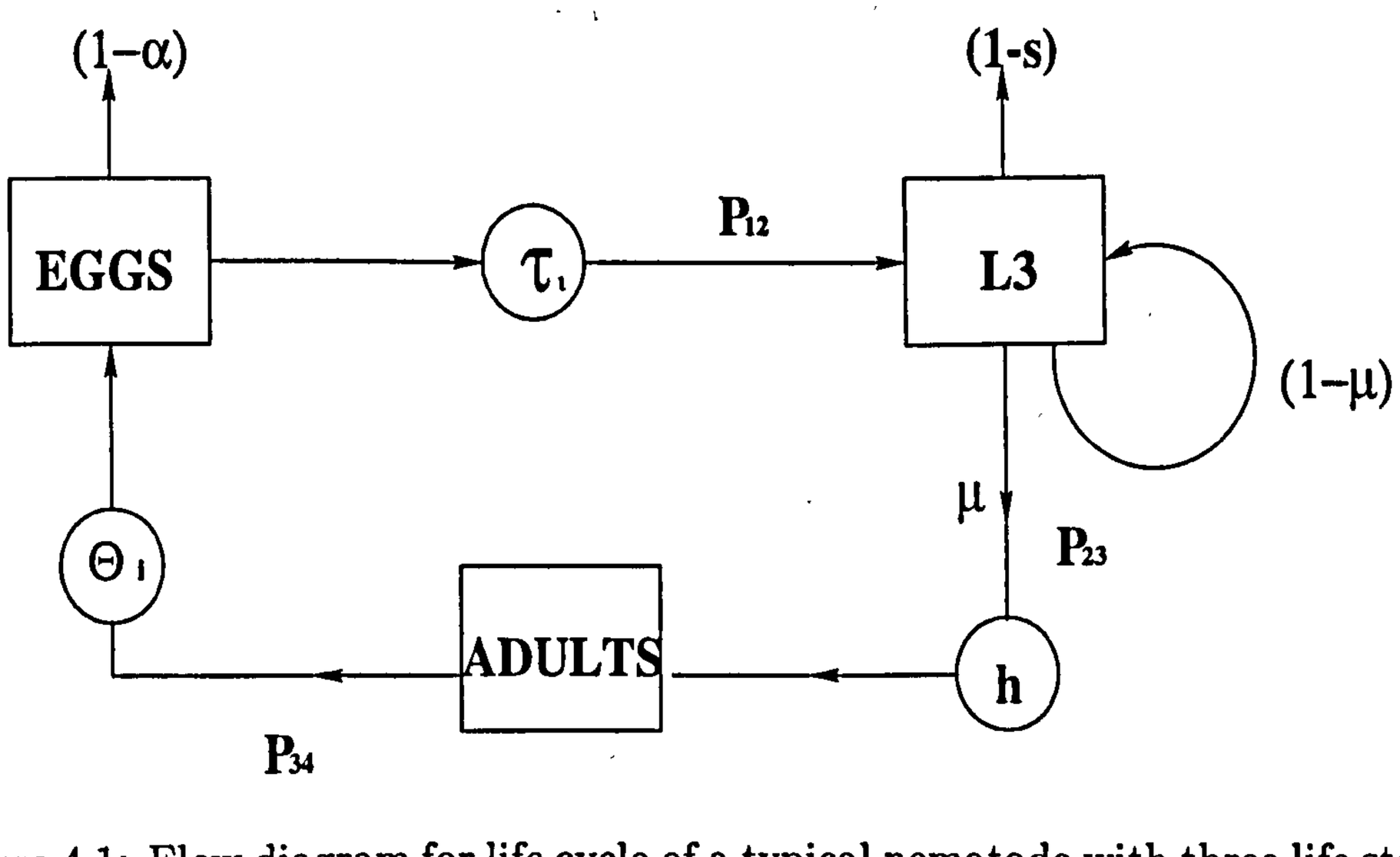

Figure 4.1: Flow diagram for life cycle of a typical nematode with three life stages without random mixing.

Once individuals have developed to the third larval stage (L3), they are either ingested immediately by a host or may spend up to m days on the pasture, uningested, after which they die. Hence

$$L3_{i,1}(t+1) = E_{i,\tau_i}(t)P_{12} \tag{4.3}$$

$$L3_{i,k}(t+1) = (1-\mu)sL3_{i,k-1}(t) \tag{4.4}$$

where $k = 2..m$,

P_{12} is the transition probability of eggs to L3,

μ is the daily ingestion rate of the host, and

s is the daily survival rate of L3 on pasture.

Once ingested by a host, the parasites (irrespective of genotype), spend h days in development to adults, after which they mate at random and offspring are produced. It is assumed that no mixing between genotypes occurs at reproduction and so each member of the population may only mate with another member within the same genotype group. The number of newly developed adults of genotype i at time $t+1$ is then

$$Ad_i(t+1) = \mu P_{23} \sum_{k=1}^{m} L3_{i,k}(t+1-h) \tag{4.5}$$

where P_{23} is the transition probability from L3 to adults, and μ, k and m are defined above.

For explanatory purposes we shall assume that infective L3s can remain on pasture for up to $m = 3$ days, after which, they die. This assumption serves only to reduce the complexity of the model and in no way reflects events in the field.

This system of linear difference equations can be reduced to a single linear difference equation by direct substitution of equations (4.2) to (4.5) into equation (4.1) to give

$$\begin{aligned} E_{i,1}(t) &= P_{12}P_{23}P_{34}\mu\Theta_i\alpha^{\tau_i-1} \\ &\times [E_{i,1}(t-(\tau_i-1)-h-2) \\ &+ E_{i,1}(t-\tau_i-h-2)(1-\mu)s \\ &+ E_{i,1}(t-(\tau_i+1)-h-2)(1-\mu)^2s^2] \end{aligned} \tag{4.6}$$

Biological Interpretation of Equation (4.6)

This equation can be explained using, as an example, changes in the FS population (that is , $i = 2$). The number of newly voided eggs with genotype FS at time t, denoted by $E_{2,1}(t)$, is equal to the number of newly voided eggs of genotype FS at time $(t-(\tau_2-1)-h-2)$, $(t-\tau_2-h-2)$ and $(t-(\tau_2+1)-h-2)$ days ago that developed to L3 and were immediately ingested, ingested after one day as L3, and ingested after two days as L3, respectively, by a host, became adults, mated and produced FS offspring. Similar explanations apply to genotypes FF and SS.

4.3 Linear Difference Equations

A set of simple recurrence relations with associated time delays, τ_i, $(i = 1, 2, 3)$, representing the development times from the egg stage to L3 of the three genotype groups, FF, FS, SS, was formulated in the previous section to describe changes in the egg population on pasture for the three genotype groups, assuming no mixing occurs between groups. Before an analysis of this model is undertaken, some notation must be defined.

A linear difference equation is defined to be

$$f_0(k)y_{k+n} + f_1(k)y_{k+n-1} + \cdots + f_{n-1}(k)y_{k+1} + f_n(k)y_k = g(k) \qquad (4.7)$$

Here, $f_0, f_1, ..., f_n$ and g are functions of k, but not y_k, defined for all values of k in the set S. If the coefficients, $f_0, f_1, ..., f_n$, do not vary with k, the above equation is a linear difference equation with constant coefficients. In addition, provided f_0 and f_n are not zero, equation (4.7) is said to be of order n over S. Finally, if $g(k) = 0$, the equation is said to be a linear n^{th} order homogeneous difference equation with constant coefficients.

4.4 Methods of Solution for Linear Difference Equations

4.4.1 General Solution of the Homogeneous Equation

Returning to equation (4.6) in the previous section

$$
\begin{aligned}
E_{i,1}(t) &= P_{12}P_{23}P_{34}\mu\Theta_i\alpha^{\tau_i-1} \\
&\times [E_{i,1}(t-(\tau_i-1)-h-2) \\
&+ E_{i,1}(t-\tau_i-h-2)(1-\mu)s \\
&+ E_{i,1}(t-(\tau_i+1)-h-2)(1-\mu)^2s^2] \qquad (4.8)
\end{aligned}
$$

This equation is a homogeneous $(\tau_i+1+h+2)^{th}$ order linear difference equation. For illustration purposes, the daily ingestion rate of the sheep host is assumed to be equal to one ($\mu = 1$). In the field, this would mean that an individual would spend only a single time unit as infective L3 on pasture before ingestion. Consequently, equation (4.6) becomes, in standard form

$$e_{t+l_i} - Ce_t = 0 \qquad (4.9)$$

where $C = \alpha^{\tau_i-1}P_{12}P_{23}P_{34}\Theta_i$, and

$$l_i = \tau_i + h + 1,$$

which has the auxiliary equation

$$m^{l_i} - Cm = 0 \qquad (4.10)$$

This is an algebraic equation of degree l_i. This equation has exactly l_i roots that may be real or complex and either repeated or distinct. A set of l_i solutions, $e_i^{(1)}, e_i^{(2)}, ..., e_i^{(n)}$ form the fundamental set of solutions where the n^{th} order determinant,

$$
\begin{vmatrix}
e_0^{(1)} & e_0^{(2)} & \cdots & e_0^{(l_i)} \\
e_1^{(1)} & e_1^{(2)} & \cdots & e_1^{(l_i)} \\
\cdots & \cdots & \cdots & \cdots \\
e_{l_i-1}^{(1)} & e_{l_i-1}^{(2)} & \cdots & e_{l_i-1}^{(l_i)}
\end{vmatrix} \qquad (4.11)
$$

must be different to zero. Each solution in the fundamental set is then summed to form the general solution to the homogeneous equation with l_i arbitrary constants. A unique solution is found by obtaining particular solutions of the complete equation using prescribed initial conditions.

Having obtained a solution to the linear difference equation in (4.9), the limiting behaviour of that solution can be investigated. The largest root of the auxiliary equation (4.10), denoted ρ, determines the behaviour of the solution in the future.

- If $\rho < 1$, the solution will converge to zero, irrespective of initial conditions.
- If $\rho > 1$, divergent solution sequences are to be expected.
- If ρ is complex or negative, the limiting behaviour of the solution will be oscillatory.
- Damped oscillations will occur if $\rho < 1$.

Unfortunately, an auxiliary equation of degree five or more is analytically intractable and numerical methods of solution have to be employed. In the next section an alternative method of solution is explored.

4.4.2 Method of Generating Functions

The method of generating functions was developed by Euler, as an aid to solving complex equations involving sequences of numbers.

The solution to equation (4.9) can be represented as an ordered sequence of real numbers, $\{e_k\}$, $k = 0, 1, 2, ...$

In general, the generating function of a sequence of numbers

$$y_0, y_1, y_2, y_3, \cdots$$

is the power series

$$Y_s = y_0 + y_1 s + y_2 s^2 + y_3 s^3 + ... \tag{4.12}$$

Given that Y_s is a power series in s, the Taylor Series expansion of Y_s about $s = 0$ gives,

$$Y_s = Y_0 + Y_0' s + \frac{Y_0'' s^2}{2!} + ... + \frac{Y_0^n s^n}{n!} + ... \tag{4.13}$$

Equating coefficients of s in equation (4.12) with those in equation (4.13) gives

$$y_0 = Y_0; \quad y_1 = Y_0'; \quad y_2 = \frac{Y_0''}{2!}; \quad y_3 = \frac{Y_0'''}{3!}; \quad \ldots \quad ; \quad y_n = \frac{Y_0^n}{n!} \tag{4.14}$$

The coefficient of the n^{th} power of s is determined by differentiating equation (4.12) n times with respect to s about $s = 0$.

We begin by considering the simple case of $\mu = 1$ in equation (4.6), representing immediate ingestion of newly developed infective L3s. We proceed to the case where $\mu < 1$, representing the more realistic situation where only a proportion of newly developed infective L3s are ingested. Those remaining, may stay on pasture for a number of days, after which, if not ingested, they are assumed to perish.

Case 1 : Immediate Ingestion of Infective L3s ($\mu = 1$)

Consider equation (4.9), which is equivalent to equation (4.6) with $\mu = 1$,

$$e_{t+l_i} - Ce_t = 0 \tag{4.15}$$

where $C = \alpha^{\tau_i - 1} P_{12} P_{23} P_{34} \Theta_i$

The generating function of $\{e_k\}$, denoted E_s, is constructed in a similar way to that in (4.12). That is we define

$$E_s = e_0 + e_1 s + e_2 s^2 + e_3 s^3 + \ldots$$

The generating function for $\{e_{k+l_i}\}$ is therefore

$$\frac{E_s - \sum_{i=0}^{l_i - 1} e_i s^i}{s^{l_i}} = e_{l_i} + e_{l_i+1} s + e_{l_i+2} s^2 + \ldots + e_k s^{k-l_i} + \ldots$$

Substituting the generating functions for $\{e_k\}$ and $\{e_{k+l_i}\}$ into equation (4.15) yields

$$\frac{E_s - \sum_{i=0}^{l_i - 1} e_i s^i}{s^{l_i}} - CE_s = 0 \tag{4.16}$$

Collecting like terms results in

$$E_s = \frac{\sum_{i=0}^{l_i-1} e_i s^i}{1 - Cs^{l_i}} \tag{4.17}$$

If it is assumed that initial egg deposition on the pasture occurs only on day zero, and is e_0, then $\sum_{i=0}^{l_i-1} e_i s^i = e_0$.

The Taylor Series Expansion of equation (4.17) about $s = 0$ will yield the sequence $\{e_k\}$ as the coefficients of the k^{th} power of s, $k = 0, 1, 2, ...$

$$\begin{aligned} E_s = e_0 \quad &+ \quad e_0 C s^{l_i} + e_0 C^2 s^{2l_i} + e_0 C^3 s^{3l_i} + e_0 C^4 s^{4l_i} + e_0 C^5 s^{5l_i} + e_0 C^6 s^{6l_i} \\ &+ \quad e_0 C^7 s^{7l_i} + ... + O(s^{513}) \end{aligned} \tag{4.18}$$

as required.

For this particular model, with $\mu = 1$, and an initial population level determined e_0, eggs will appear on pasture every l_i days. In between these times, the pasture should be free of eggs in this age group.

When the power of s in the Taylor Series Expansion of (4.17), is a multiple of l_i, the associated coefficient is non-zero, the actual value depending on the values of C. That is

- if $C > 1$ the population will grow from its initial value without constraint,
- if $C < 1$, the population will eventually die out, and
- if $C = 1$, the population will remain in a steady state.

For example, if l_1, the generation time for FF individuals is 27 days, say, the number of newly voided FF eggs on pasture on day 162 can be found by differentiating (4.17) 162 times with respect to s about $s = 0$, and taking the coefficient of s^{162} as the result. That is

$$E_s^{162}|_{s=0} = e_0 C^6 s^{162} \tag{4.19}$$

whereas the number of newly voided FF eggs on pasture on day n, where n mod $l_i \neq 0$ can be seen from equation (4.18) to be zero.

Case 2 : Introducing a Host Ingestion Rate To the Basic Model ($\mu < 1$)

When $0 < \mu < 1$, only a proportion of the parasites on pasture on any day are ingested by the host. We assume that those remaining may spend up to $m = 3$ days on the pasture before being ingested, after which they die. This alters equation (4.9) to give, in standard form

$$e_{t+l_i+2} - \mu C\left[e_{t+2} + (1-\mu)se_{t+1} + (1-\mu)^2 s^2 e_t\right] = 0 \tag{4.20}$$

where C is defined above.

If the generating function for e_k is E_s, the generating function for e_{k+l_i+2} is

$$\frac{E_s - \sum_{i=0}^{l_i+1} e_i s^i}{s^{l_i+2}} \tag{4.21}$$

it follows that the generating function for e_{k+2} is

$$\frac{E_s - e_0 - e_1 s}{s^2} \tag{4.22}$$

and similarly, the generating function for e_{k+1} is

$$\frac{E_s - e_0}{s} \tag{4.23}$$

Substitution of equations (4.21) (4.22) and (4.23) into equation (4.20) gives

$$\frac{E_s - \sum_{i=0}^{l_i+1} e_i s^i}{s^{l_i+2}} - \mu C\left[\frac{E_s - e_0 - e_1 s}{s^2} + (1-\mu)\frac{E_s - e_0}{s} + (1-\mu)^2 E_s\right] = 0 \tag{4.24}$$

Multiplying (4.24) through by s^{l_i+2} and collecting like terms yields

$$E_s = \frac{\sum_{i=0}^{l_i+1} e_i s^i - s^{l_i}\mu C\left[e_0 + e_1 s + (1-\mu)e_0 s\right]}{\left[1 - s^{l_i}\mu C\left[1 + (1-\mu)s + (1-\mu)^2 s^2\right]\right]} \tag{4.25}$$

This is the generating function for the sequence generated by the difference equation in (4.20). In the same way as before (4.25) is expanded about $s = 0$ to obtain the egg numbers on pasture daily.

4.4.3 Using the Generating Function E_s to Explore the Impact on the Population Dynamics of Variation in Free-living Development Time Between Genotype Groups

A generating function is developed here that models patterns of egg deposition on pasture over a typical grazing season. The development times are hypothetical, and have been chosen to illustrate the method of generating functions rather than to provide any realistic biological insights. The generating function for a fast developing population, FF is outlined here. It is assumed that development time from the egg to infective L3 stage is 10 days, with up to an additional three days spent on pasture before ingestion or death. Intra-host development to the adult stage is assumed to take 16 days. Thus, $l_1 = 27$ days.

The generating function for such a population is therefore,

$$\begin{aligned} E_s &= \sum_{i=0}^{26} e_i s^i \\ &+ [\mu C e_0]\, s^{27} \\ &+ [\mu C(1-\mu) e_0]\, s^{28} \\ &+ \left[\mu C(1-\mu)^2 e_0\right] s^{29} \\ &+ \ldots \\ &+ \left[(\mu C)^2 e_0\right] s^{54} \\ &+ \left[2(\mu C)^2(1-\mu) e_0\right] s^{55} \\ &+ \left[3(\mu C)^2(1-\mu)^2 e_0\right] s^{56} \\ &+ \left[2(\mu C)^2(1-\mu)^3 e_0\right] s^{57} \\ &+ \left[(\mu C)^2(1-\mu)^4 e_0\right] s^{58} \\ &+ O(s^{59}) \end{aligned} \tag{4.26}$$

where $C = \alpha^9 P_{12} P_{23} P_{34} \Theta_1$.

Figure 4.2 shows how descendants of eggs voided onto pasture on a single day, that is, day zero, will be distributed temporally in the future.

New eggs are expected to appear on pasture on days 27, 28 and 29 as a result of the initial egg deposition on day zero, provided $\mu < 1$. A proportion, μ, of those eggs on day zero that develop to L3, will be ingested immediately by a host,

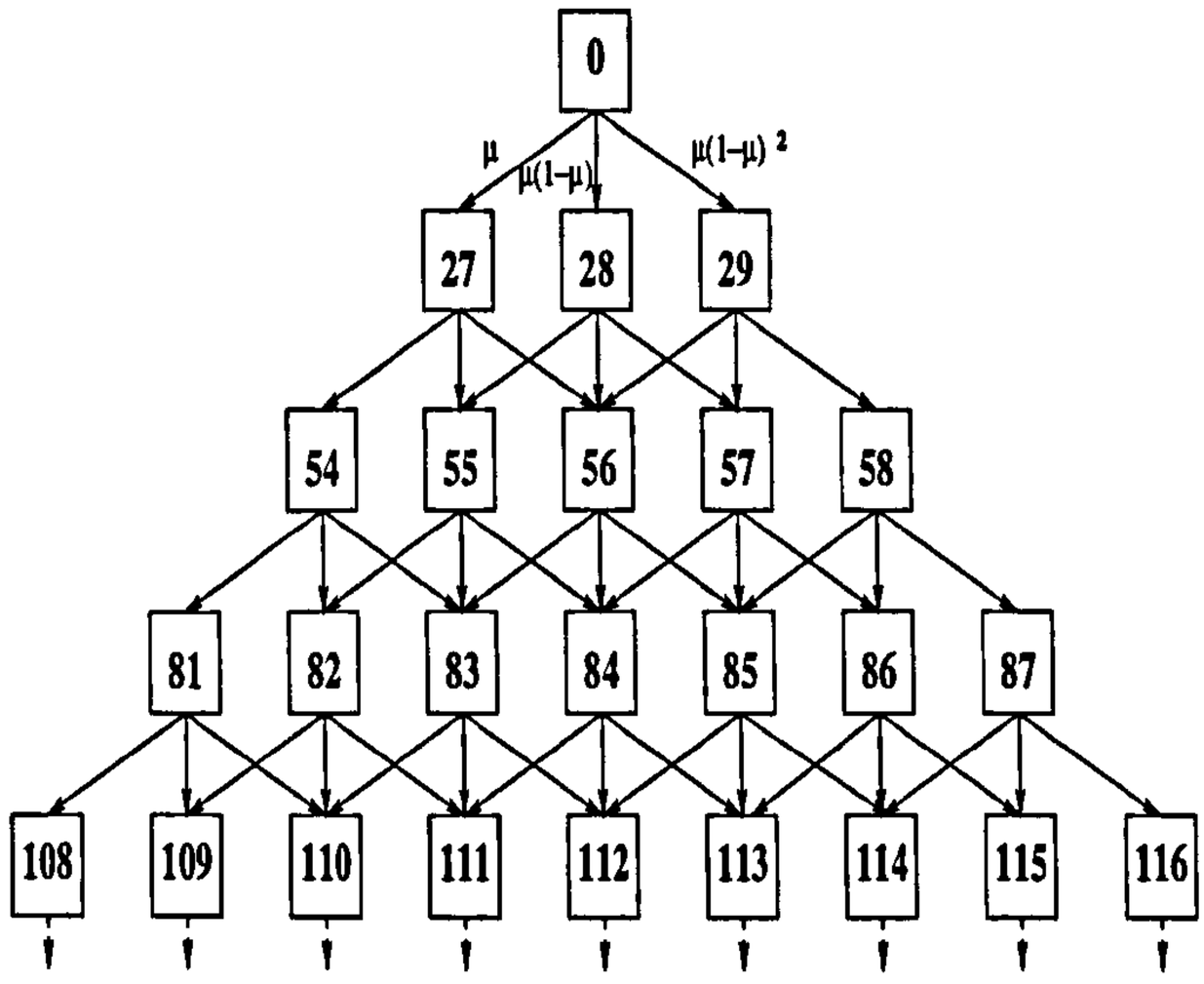

Figure 4.2: Flow diagram for emergence times of nematode eggs following equation (4.6).

become adult and produce offspring who will be deposited onto pasture on day 27. Of the proportion of infective L3 remaining on pasture, $(1-\mu)$, a proportion μ will be ingested the following day, will reach maturity within the host and produce offspring that will be deposited on pasture on day 28. Finally, of the proportion of L3 remaining on pasture on the third day of being in the infective stage, $(1-\mu)^2$, μ will be ingested and will subsequently produce offspring to be deposited on pasture on day 29 (having developed to adults and mated). Those infective L3s remaining on pasture, derived from the initial batch on day zero are assumed to die.

Those new eggs on days 27, 28 and 29 will take at least 27 days to complete their life cycle. Hence the next "batch" of new eggs will begin to appear on pasture on day 54. A proportion, μ of those eggs on day 27 that develop to L3 and are immediately ingested by a host, become adult and produce offspring who will emerge onto pasture on day 54. Those eggs on day 27 that develop to L3, but are not ingested until a day later will subsequently produce offspring that emerge as eggs on pasture on day 55. In addition to this, eggs on day 28, that develop to L3 and are immediately ingested by a host will subsequently produce offspring that emerge as eggs on day 55. A proportion, μ, of those eggs on day 27 that develop to L3, and remain uningested on pasture until the third day will now be ingested and will be expected to appear on pasture on day 56.

The first term of equation (4.26) is simply e_0, as initial contamination of the pasture occurs only on day zero. Taking a single time point on the tree in Figure

4.2, for example day 56, an explanation of the derivation of the numbers of eggs in age group one is given. If C contains mortality, fecundity and transition parameters, the number of newly voided eggs on day 56 will be

$$\mu(1-\mu)^2 Ce_{27} + \mu(1-\mu)Ce_{28} + \mu Ce_{29}$$

On days 27, 28 and 29, the numbers of new eggs, respectively is μCe_0, $\mu(1-\mu)Ce_0$ and $\mu(1-\mu)^2 Ce_0$. Substituting these into the equation for day 56 gives

$$3(\mu(1-\mu)C)^2 e_0 \qquad (4.27)$$

which is equivalent to the coefficient of the 56^{th} power of s in (4.26).

The model, as shown in equation (4.26) provides the flexibility of variable time delays and multiple initial contamination sources. Figure 4.2 is a simple realisation of the model developed for explanatory purposes.

Models for *medium* and *slow* developers are similarly constructed with adjustments being made to the time lags, l_i.

4.4.4 The Limiting Behaviour of the Non-Mixing Population Using Matrix Algebra

Matrix Notation

Conveniently, the linear difference equations in the previous section can be represented in matrix notation. Separate transition matrices are constructed for the genotype groups due to the assumption of no interaction between individuals from different genotype groups. The dynamics of the FF population are given here as an example, the structure for the remaining two populations being similar but requiring more space.

Consider the sub-population of individuals with FF genotype, where changes in population numbers are represented by the following equation

$$\mathbf{n}_{FF}(t+1) = \mathbf{B}_{FF}\mathbf{n}_{FF}(t) \qquad (4.28)$$

where

$\mathbf{n}_{FF}(t)$ and $\mathbf{n}_{FF}(t+1)$ are the population state vectors at time t and $t+1$, respectively and $\mathbf{B}_{FF}$ is the state transition matrix. A simple example is given here to illustrate how population dynamics can be modelled using matrix algebra techniques. The numerical values chosen in this example are unrealistically short- they serve only to illustrate the method and are in no way to be interpreted as biologically meaningful.

Example

It is assumed that eggs spend three days in development to the infective L3 stage, that is, $\tau_1 = 3$. Once infective, the parasites may spend up to $m = 3$ days free-living on pasture where they may be ingested by a host on any one of these days. Intra-host development is assumed to last $h = 2$ days after which the parasites become sexually mature, mate and produce offspring. Free-living and intra-host development times here are unrealistically short, however, for explanatory purposes, we shall forfeit realism for clarity.

The transition matrix is

$$\mathbf{B}_{FF} = \begin{pmatrix} 0 & 0 & 0 & 0 & 0 & 0 & 0 & 0 & \Theta_1 \\ \alpha & 0 & 0 & 0 & 0 & 0 & 0 & 0 & 0 \\ 0 & \alpha & 0 & 0 & 0 & 0 & 0 & 0 & 0 \\ 0 & 0 & P_{12} & 0 & 0 & 0 & 0 & 0 & 0 \\ 0 & 0 & 0 & (1-\mu) & 0 & 0 & 0 & 0 & 0 \\ 0 & 0 & 0 & 0 & (1-\mu) & 0 & 0 & 0 & 0 \\ 0 & 0 & 0 & \mu & \mu & \mu & 0 & 0 & 0 \\ 0 & 0 & 0 & 0 & 0 & 0 & P_{23} & 0 & 0 \\ 0 & 0 & 0 & 0 & 0 & 0 & 0 & P_{34} & 0 \end{pmatrix} \tag{4.29}$$

with an associated state vector

$$\mathbf{n}(t) = [e_0, e_1, e_2, L3_1, L3_2, L3_3, ..., Ad]$$

When no mixing occurs between genotypes at reproduction, convergence of the population is assured if the birth terms in the model balance the death terms.

From equation (4.6), convergence to a steady state egg population size will occur when

$$E_{t+l_i+2} = E_{t+2} = E_{t+1} = E_t = \hat{E}$$

That is,

$$\hat{E}_i = \mu\alpha^{\tau_i-1}P_{12}P_{23}P_{34}\Theta_i\hat{E}_i\left[1+(1-\mu)+(1-\mu)^2\right]$$

$$\hat{E}_i\left[1-\mu\alpha^{\tau_i-1}P_{12}\theta_i\left[1+(1-\mu)+(1-\mu)^2\right]\right]=0 \tag{4.30}$$

this results in the condition for convergence of the sequence generated by the difference equation

$$e_{t+l_i+2}-\mu C\left[e_{t+2}+(1-\mu)e_{t+1}+(1-\mu)^2e_t\right]=0 \tag{4.31}$$

where $C=\mu\alpha^{\tau_i-1}P_{12}P_{23}P_{34}\Theta_i$ as before, to be

$$\Theta_i=\frac{1}{\mu\alpha^{\tau_i-1}P_{12}\left[1+(1-\mu)+(1-\mu)^2\right]} \tag{4.32}$$

Using the matrix notation above and some fundamental theorems of matrix properties (Caswell, 1989), the limiting behaviour of such a population can be evaluated.

The solution to the projection equation in (4.28), from Caswell (1989), is

$$n_t=\sum_i c_i\lambda_i^t\mathbf{w_i} \tag{4.33}$$

where the c_is are coefficients dependent on n_0,

λ_is are the eigenvalues of **B**, and

$\mathbf{w_i}$ are right eigenvectors of **B**.

The long term behaviour of n_t as t increases will depend on the eigenvalues λ_i in (4.33), as they are raised to higher and higher powers of t.

The *Perron-Frobenius Theorem* defines the dominant eigenvalue, denoted by λ_1, to be that eigenvalue of **B** that is largest in magnitude. This eigenvalue determines the ergodic properties of population growth in this system.

This is the basis for the *Strong Ergodic Theorem* (Caswell, 1989), where from equation (4.33), given that the eigenvalues are ordered in decreasing magnitude, λ_1 is the dominant eigenvalue. Dividing both sides of (4.33) by λ_1 gives

$$\frac{n_t}{\lambda_1^t}=c_1\mathbf{w_1}+c_2\left(\frac{\lambda_2}{\lambda_1}\right)^t\mathbf{w_2}+c_3\left(\frac{\lambda_3}{\lambda_1}\right)^t\mathbf{w_2}+\ldots \tag{4.34}$$

Taking the limit as $t \to \infty$, and assuming that $\mathbf{B}$ is a primitive matrix so that strictly $\lambda_1 > \lambda_2$ then

$$\lim_{t\to\infty} \frac{n_t}{\lambda_1^t} = c_1 \mathbf{w_1} \tag{4.35}$$

This means that the future behaviour of the population n_t is dependent on the magnitude of the dominant eigenvalue λ_1. Its associated eigenvector, $\mathbf{w_1}$, is the stable population structure. Hence multiplication of $\mathbf{B_{FF}}$ by $\mathbf{w_1}$ is analogous to scalar multiplication.

4.4.5 The Rate of Convergence of Population Vector n

The rate of convergence of the population vector n is determined by the ratio of the moduli of the first two eigenvalues. This ratio is called the Damping Ratio, and is denoted by ρ

$$\rho = \frac{|\lambda_1|}{|\lambda_2|} \tag{4.36}$$

From equation (4.34), it is clear that the greater λ_1 is in relation to λ_2, the more rapid convergence to a stable distribution will be.

λ_2, the second largest eigenvalue of $\mathbf{B}$, provides information on the approach to convergence. If λ_2 and λ_3 are complex conjugates, the approach is likely to be oscillatory.

4.5 A Numerical Analysis of the Effect of Variable Development Time Within a Population

The models presented so far are very simple linear models of nematode population dynamics and assume no mixing between development groups.

The following section uses hypothetical parameter estimates of the vital rates of a population described by the model in equation (4.6) to demonstrate the powerful mathematical modelling techniques outlined previously.

Here we are interested in the impact on nematode population dynamics when the length of time the free-living stages spend on pasture is dependent on the genotype of the individual.

A numerical simulation model written in the Pascal programming language was developed to examine the effect of varying development times on a nematode population free-living on pasture. Effectively, the life cycle of the parasite, as described in Figure 4.1 was translated into programming code where population numbers were updated daily based on specific survival, ingestion and fecundity parameters. The results from the simulation program could then be compared to the results obtained from the numerical solution of the matrix equation.

For illustrative purposes, the vital rates, α, μ, P_{12}, P_{23} and P_{34}, have been chosen so that each population modelled will reach a steady state distribution, irrespective of development time on pasture. This is exercised by simply choosing values for μ, α, τ_i, P_{12} arbitrarily and then employing equation (4.32) to determine the number of new additions to the population, Θ_i, required to balance those leaving.

The assumption that the population converges to a steady state is made in order that the effect of altering development times within groups could be investigated. If this assumption was not satisfied the model could exhibit all sorts of undetermined behaviour that would make a comparative analysis difficult.

Parameter Values For the Non-Mixing Model

For simplicity, it is assumed that the only source of mortality occurs during the free-living phase of the life cycle, where a daily survival rate of $\alpha = 0.9$ is assumed. In conjunction with this, it is assumed that any infective individuals not ingested within three days, $m = 3$, of becoming infective also perish.

Transitions between life stages, P_{12} (egg to L3), P_{23} (L3 to intra-host), and P_{34} (intra-host to adult), are assumed to occur with certainty (that is, they all equal one). Intra-host development time is genotype independent and is assumed to take $h = 16$ days.

These values in no way represent reality, they have been chosen to illustrate the impact of variable development time on the population dynamics of a typical nematode population.

4.6 Results

Equation (4.35) shows that the ultimate fate of a population with a non-negative, primitive projection matrix B and initial population vector $\mathbf{n_0}$, is dependent on the dominant eigenvalue λ_1 and its associated eigenvector $\mathbf{w_1}$. That is, the population vector $\mathbf{n_t}$ will approach a stable population structure, proportional to $\mathbf{w_1}$, as $t \to \infty$. The actual population numbers are determined by multiplying $\mathbf{w_1}$ by the coefficient c_1, determined by initial conditions.

Using the parameter values outlined in the last section, the population will reach a steady state genotype distribution provided the dominant eigenvalue of the transition matrix is unity, that is, $\lambda_1 = 1$. For the simple non-mixing model, it was discovered that for a stable population structure to exist, some form of genotype-dependent regulator had to be in operation. As mortality of the free-living stages, α, was fixed, this regulator was chosen to be the fecundity of female parasites, denoted by Θ_i.

In order to eliminate bias, initial population numbers in each of the genotype groups were the same.

A simple example of the effect of development time on the stable population structure follows.

Example

In the first instance, assuming all other parameters take the values assigned previously, the development times from egg to L3 for FF, FS and SS genotypes are assumed to be $\tau_1 = 1$ day, $\tau_2 = 2$ days and $\tau_3 = 4$ days, respectively. This provides a very simple illustration of the dynamics of the model. The next step is to introduce a more realistic set of time delays into the model that reflect typical time delays experienced in the field (see chapter 2). These are, for FF, FS and SS genotypes, respectively, $\tau_1 = 10$ day, $\tau_2 = 17$ days and $\tau_3 = 28$ days.

We shall outline model construction and analysis for the simple case and then present the results of the more realistic case graphically.

Eigen Analysis

Case 1: $\tau_1 = 1,\ \tau_2 = 2,\ \tau_3 = 4$

We shall display the transition matrices, state vectors and mathematical analysis for the FF genotype group. Analysis of the FS and SS genotype groups is similar.

Changes in FF population numbers are represented by the following projection equation

$$\mathbf{n}_{\mathbf{FF}}(t+1) = \mathbf{B}_{\mathbf{FF}}\mathbf{n}_{\mathbf{FF}}(t) \tag{4.37}$$

The projection matrices and state vectors for this particular system are derived by substituting into the matrix in 4.29, the numerical parameter values discussed in the previous section

$$\mathbf{B}_{\mathbf{FF}} = \begin{pmatrix} 0 & 0 & 0 & 0 & 0 & 0 & 1.143 \\ 1 & 0 & 0 & 0 & 0 & 0 & 0 \\ 0 & 0.5 & 0 & 0 & 0 & 0 & 0 \\ 0 & 0 & 0.5 & 0 & 0 & 0 & 0 \\ 0 & 0.5 & 0.5 & 0.5 & 0 & 0 & 0 \\ 0 & 0 & 0 & 0 & 1 & 0 & 0 \\ 0 & 0 & 0 & 0 & 0 & 1 & 0 \end{pmatrix} \tag{4.38}$$

$$\mathbf{n}_{\mathbf{FF}}(t) = [e_0, L3_1, L3_2, L3_3, .., Ad]_t$$

Transition matrices and state population vectors for FS and SS populations are similarly constructed, but are not given here explicitly due to space restrictions.

In each case Θ_i, the fecundity of female parasites, has been calculated in order that $\lambda_1 = 1$. The eigenvector, $\mathbf{w_1}$ associated with the dominant eigenvalue represents the stable population structure that the state vector $\mathbf{n}(t)$ approaches as $t \to \infty$.

The dominant eigenvalue of the transition matrix, $\mathbf{B_{FF}}$, in (4.38) is known to be unity. The eigenvector, $\mathbf{w_1}$, associated with λ_1 is found by solving

$$\mathbf{B_{FF}w_1} = \lambda_1\mathbf{w_1} \tag{4.39}$$

In other words, this eigenvector satisfies the condition that matrix multiplication is equivalent to scalar multiplication. Numerically, for the FF population,

$$\mathbf{w_1} = [0.262613, 0.262613, 0.131306, 0.06565, 0.22979, ..., 0.22979, 0.22979]$$

Simulation Model

Alternatively, numerical simulation of the population dynamics over a long period of time produces the population vector, $\mathbf{n}^*$, that results from the computer program of the life cycle run for a long period of time (over 100000 time units). The steady state population vector for those individuals with FF genotypes was

$$\mathbf{n}^* = [539.46, 539.46, 270.23, 135.62, 472.16, ..., 472.16, 472.16]$$

The equation

$$\lim_{t\to\infty} \frac{\mathbf{n}^*}{\lambda_1^t} = c_1 \mathbf{w_1} \tag{4.40}$$

is satisfied, in this case, when $c_1 = 2054$, and is determined from initial conditions.

Figures 4.3, 4.4 and 4.5 provide graphical illustrations of the results of a numerical simulation of actual population numbers using the simulation model written in Pascal, and the results from a numerical simulation of the matrix model.

The Pascal simulation model was run for a period of 100000 time units or until the population had converged to some equilibrium distribution, the results of which are plotted as a solid black line on Figures 4.3, 4.4 and 4.5. These points are measured from the left-hand y-axis of each plot representing actual population numbers. Equation (4.37) was solved numerically on MAPLE and the resulting eigenvector, $\mathbf{w_1}$ elements plotted as open red circles. The right hand y-axis, represented the relative population structure at equilibrium.

The x-axis represents the life stages within the nematode life cycle.

The red circles lie directly on the solid black lines which suggests that the elements of the eigenvector associated with the dominant eigenvalue, λ_1 are in direct proportion to the equilibrium population vector obtained from the numerical simulation of the life cycle, verifying that indeed

$$\lim_{t\to\infty} \frac{\mathbf{n}^*}{\lambda_1^t} = c_1 \mathbf{w_1} \tag{4.41}$$

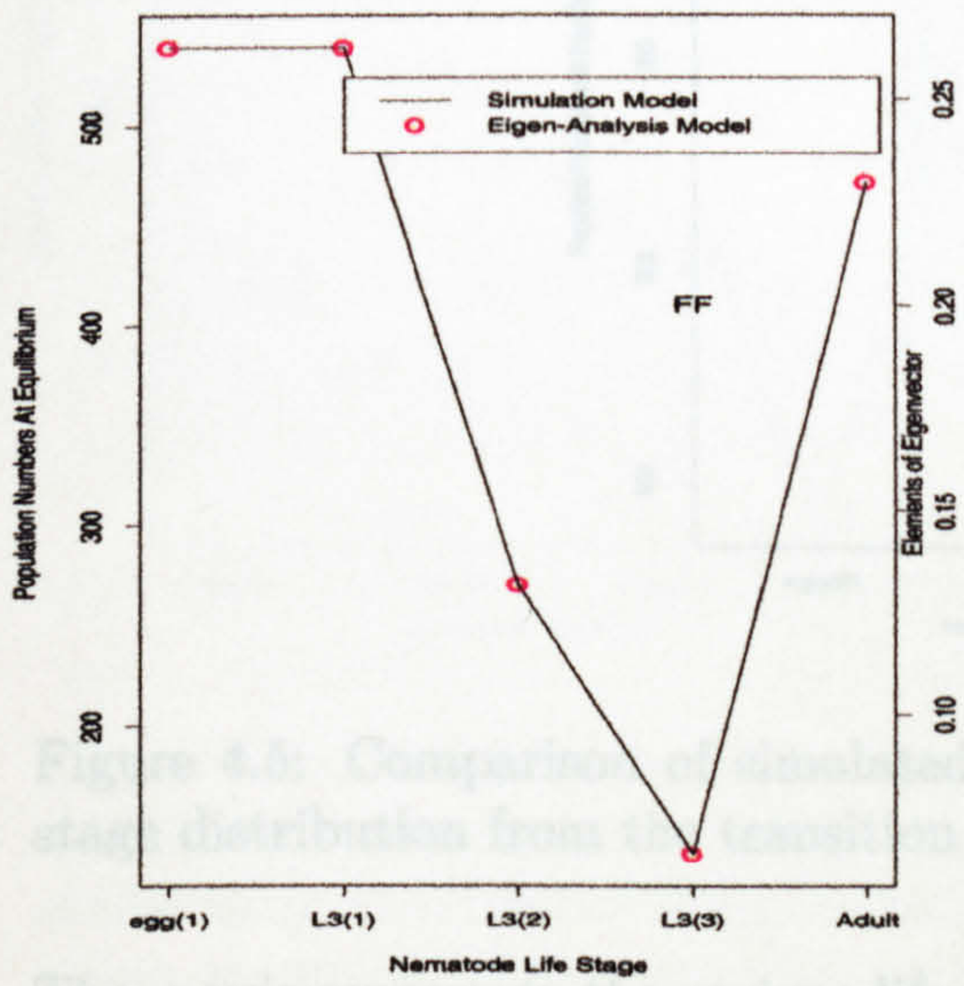

Figure 4.3: Comparison of simulated equilibrium population numbers and stable stage distribution from the transition matrix for FF population, $\tau_1 = 1$ day.

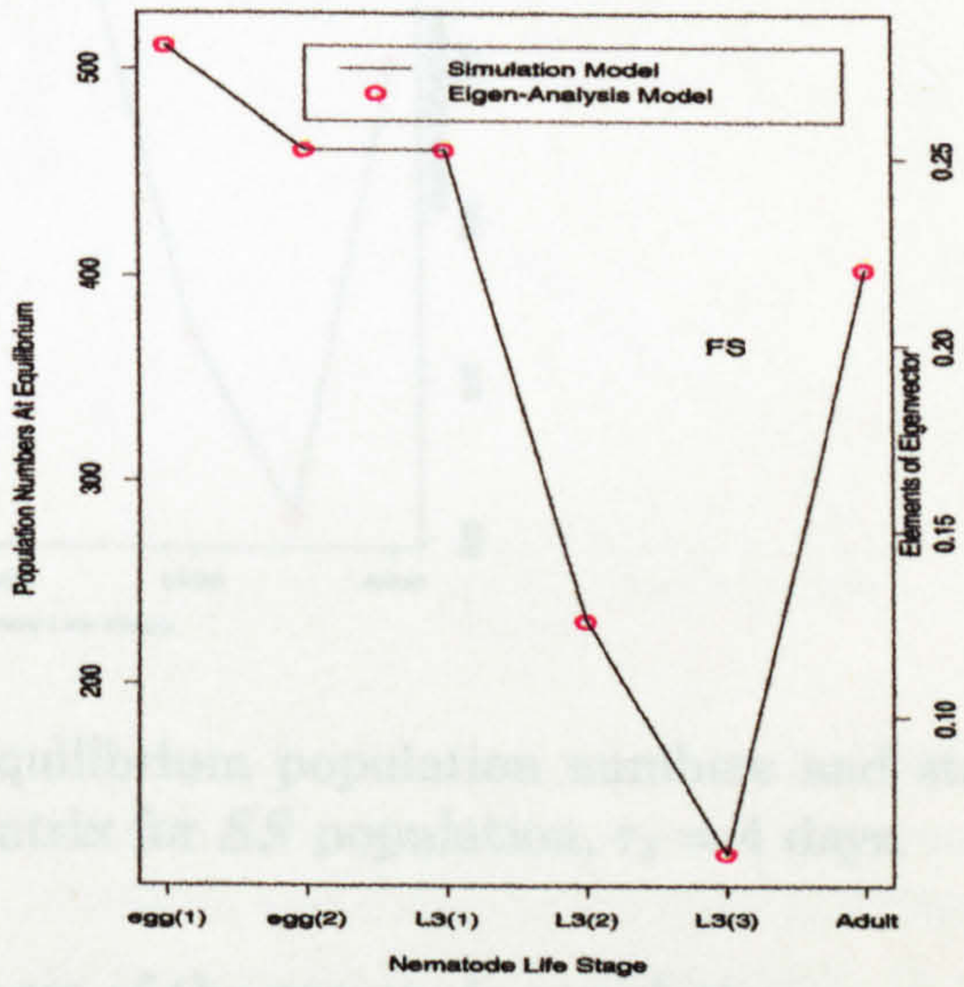

Figure 4.4: Comparison of simulated equilibrium population numbers and stable stage distribution from the transition matrix for FS population, $\tau_2 = 2$ days.

Case 2 : $\tau_1 = 10$, $\tau_2 = 17$, $\tau_3 = 28$

A more realistic case is now presented, where the time in development from the egg to L3 stage is, for FF, FS and SS, respectively, 10, 17 and 28 days. Again, transition matrices and state vectors were formed using the same survival, ingestion and transition probabilities as were used for the first case above. Fecundities were calculated from equation (4.32). The simulation model was run and the eigenvectors calculated using equation (4.39). The results from both analyses were then compared. Both $\mathbf{n}^*$ and $\mathbf{w_1}$ are presented graphically for FF, FS and SS groups in Figures 4.6, 4.7 and 4.8, respectively.

As before, the solid black line represents the equilibrium population numbers obtained from the simulation model and the open red circles are the elements of the eigenvector corresponding to the dominant eigenvalue of the transition matrix.

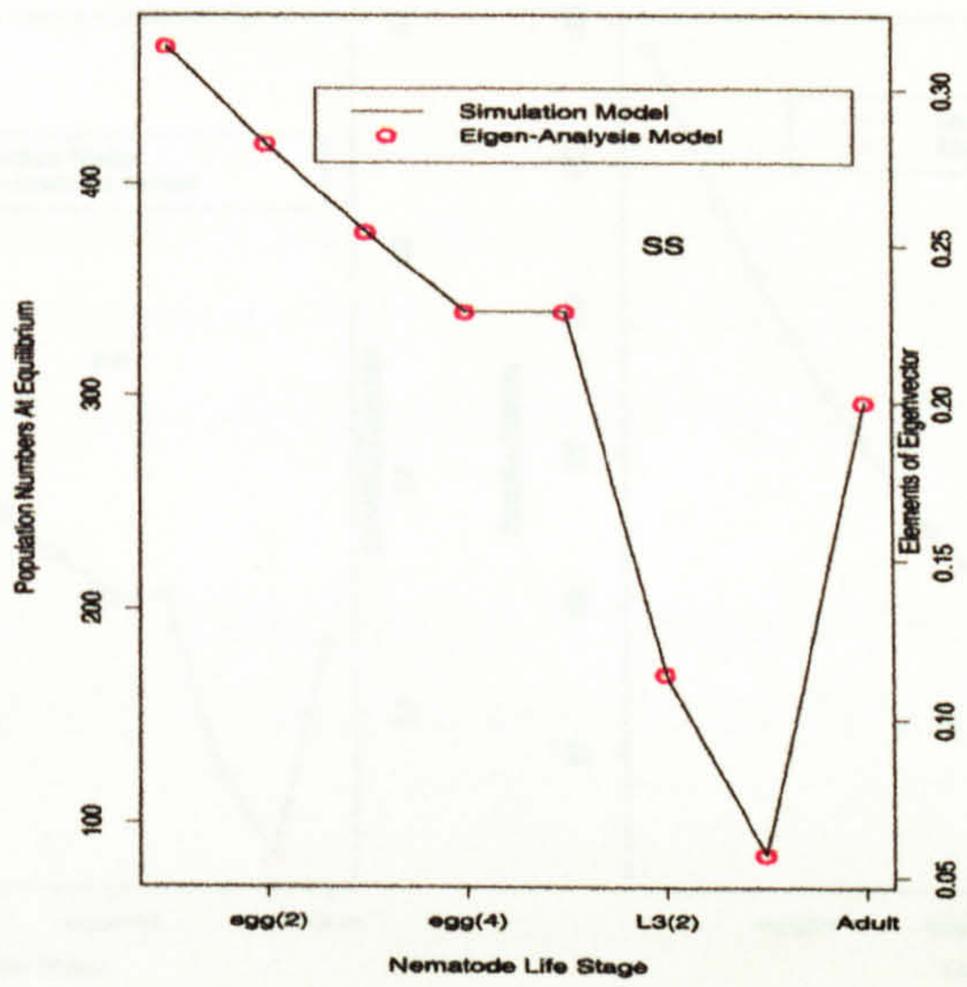

Figure 4.5: Comparison of simulated equilibrium population numbers and stable stage distribution from the transition matrix for SS population, $\tau_3 = 4$ days.

The x-axis represents the various life stages of the nematode population.

For all three populations, FF, FS and SS, the red circles lie entirely on the solid black lines. It therefore can be concluded that indeed

$$\lim_{t\to\infty} \frac{\mathbf{n}^*}{\lambda_1^t} = c_1 \mathbf{w_1} \tag{4.42}$$

4.7 Conclusion

Three models of the life cycle of *T. circumcincta* assuming no mixing occurs between development groups have been presented in the first part of this Chapter.

The first model used the technique of generating functions to describe changes in population numbers over time, given the appropriate vital rates of the population. This is a very simple but elegant method of solving quite complex linear difference equations and has the added advantage that information on population numbers can be retrieved very quickly with little effort particularly when the time frame is short.

The particular model developed for *T. circumcincta* is very flexible and allows for variable time delays and multiple initial contamination sources to be incorporated

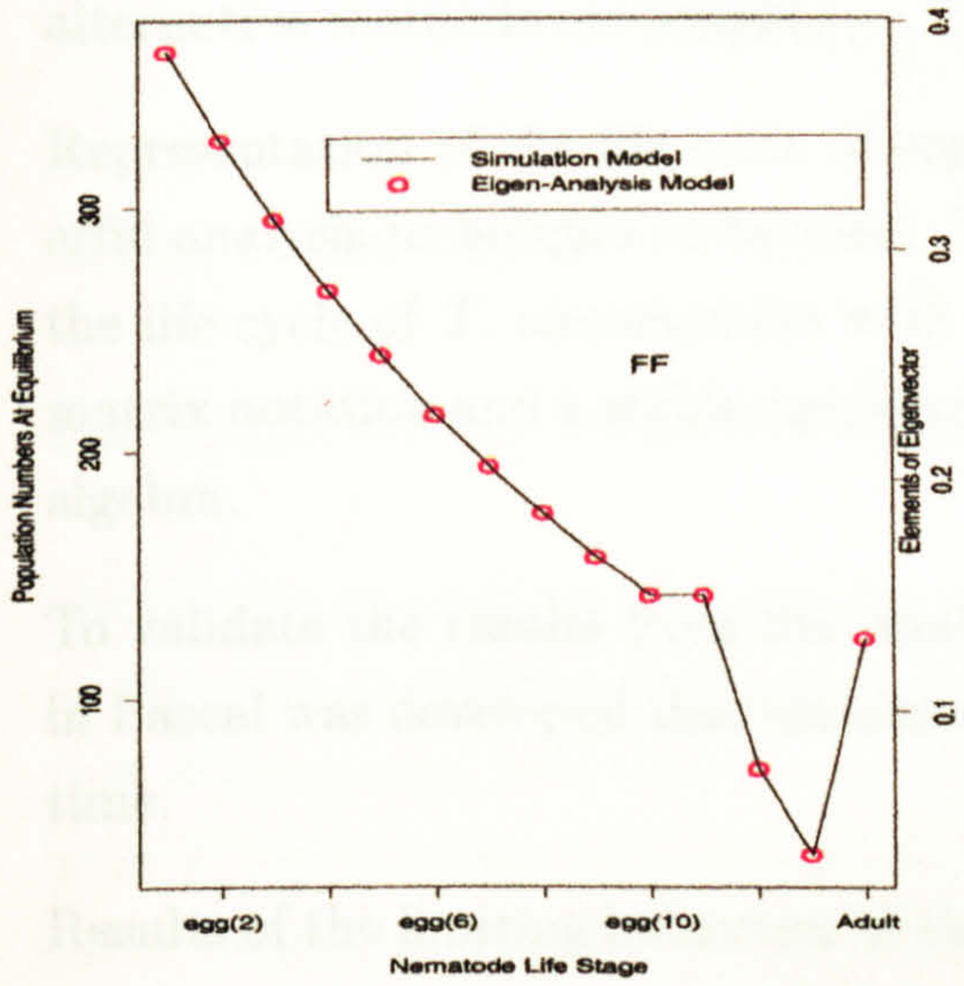

Figure 4.6: Comparison of simulated equilibrium population numbers and stable stage distribution from the transition matrix for FF population, $\tau_1 =$ 10 days.

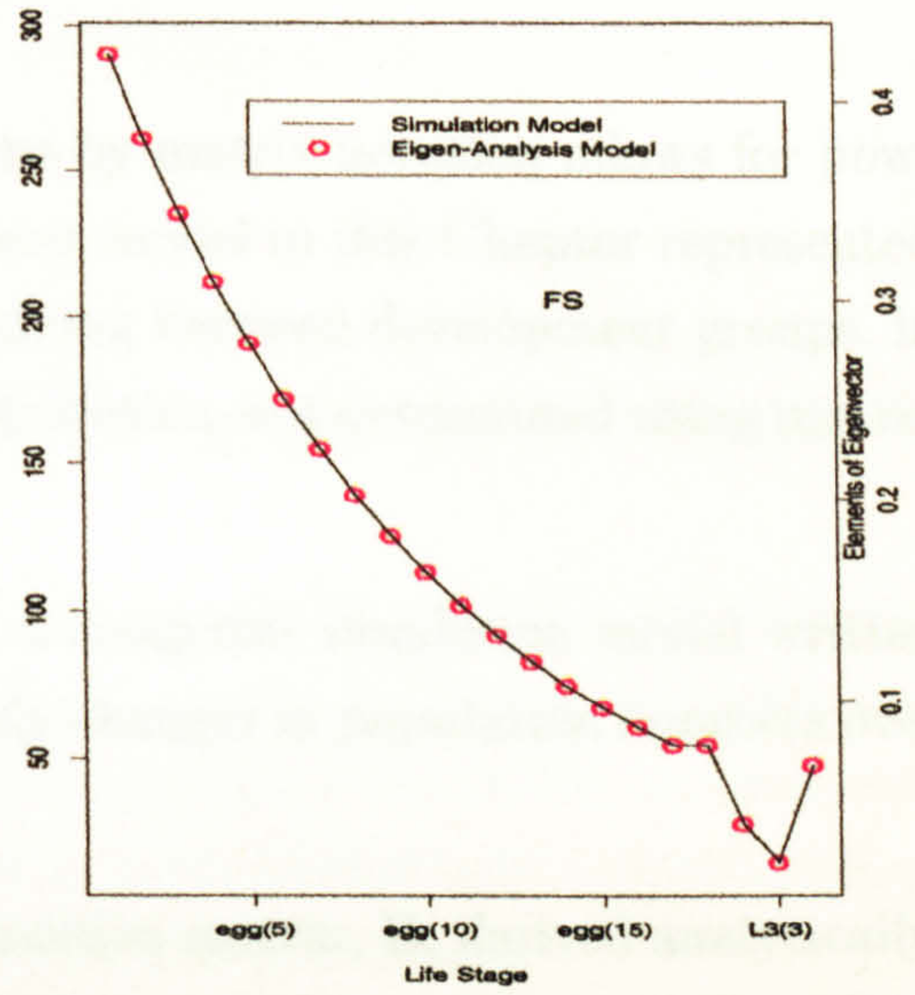

Figure 4.7: Comparison of simulated equilibrium population numbers and stable stage distribution from the transition matrix for FS population, $\tau_2 =$ 17 days.

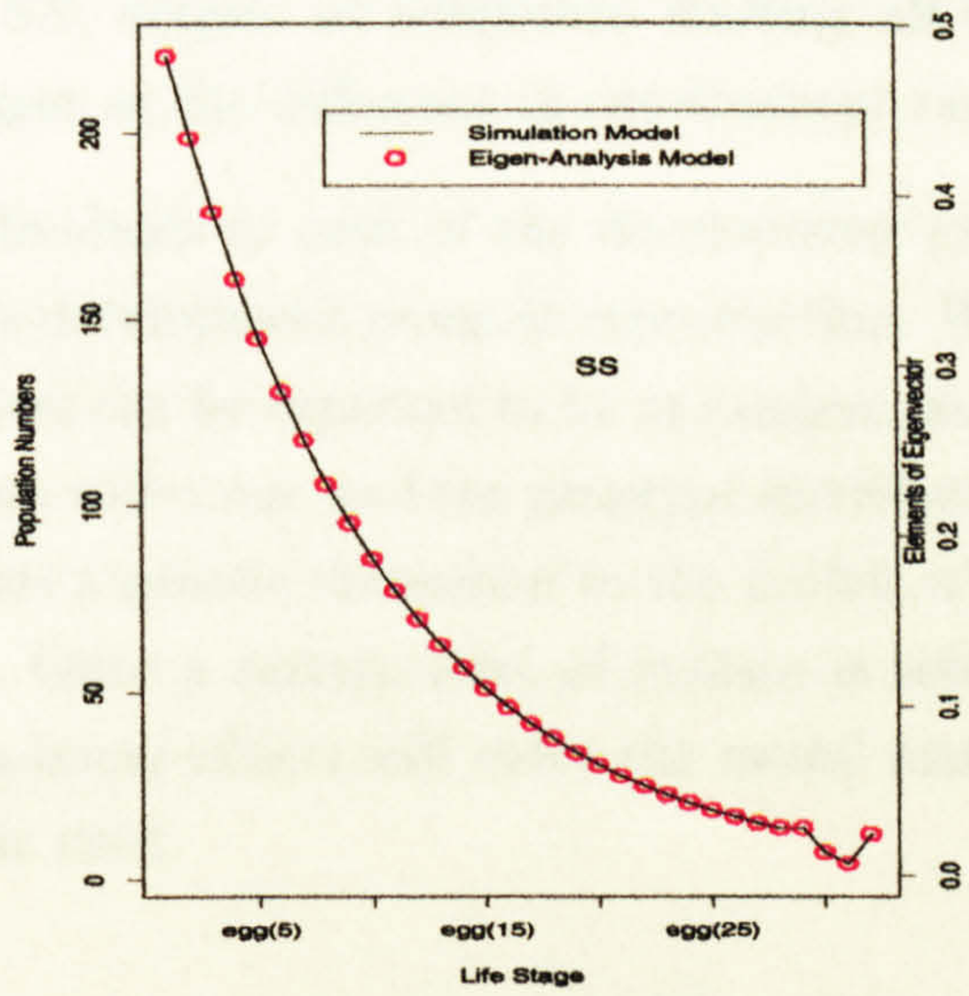

Figure 4.8: Comparison of simulated equilibrium population numbers and stable stage distribution from the transition matrix for SS population, $\tau_3 = 28$ days.

into the general framework. This method is ideal when examining the behaviour of a population within a single season, for example.

Determining long term or equilibrium behaviour of a population is possible using

this method of analysis, however, the computing power involved is high and so alternative methods are sought.

Representation of the life cycle of organisms by matrix notation allows for powerful analysis techniques to be used. The next model in this Chapter represented the life cycle of *T. circumcincta* with no mixing between development groups, in matrix notation and a stable age/stage distribution was determined using matrix algebra.

To validate the results from this analysis, a computer simulation model written in Pascal was developed that simulated daily changes in population numbers over time.

Results of the limiting behaviour of the transition matrix, **B**, derived analytically, were compared to the output from the simulation model having run it for a long period of time.

For each development group, FF, FS and SS, the analytical results were in total agreement with the simulated results. Not surprising was the discovery that those individuals who spent less time free-living on pasture, that is, the FF genotypes, would equilibrate at higher numbers than those who were slower to develop on pasture, say FS or SS, despite all subgroups starting off with equal numbers. This effect was stronger as the difference in development rates increased.

Realistically, the individuals in each of the development groups do not confine themselves to a single development group at reproduction. Within a host, mating between adult parasites can be expected to be at random, and so segregation and recombination of genes will occur, and the genotype distribution in the population will change. This adds a genetic dimension to the model, which will be explored in the next section. Once a certain level of realism is achieved, however, it is quite likely that non-linear effects will enter the model and non-linear methods of analysis need to be used.

4.8 The Life Cycle of *T. circumcincta* With Random Mixing Of Genotypes

The Mixing Model

Introducing A Genetic Component to the Basic Model

Consider a population in which the members are divided into groups according to the rate at which they develop during their free-living phase. It is assumed that development is conferred by two alleles at a single locus on the chromosome, with F representing *fast* development, and S, *slow* development. This results in three genotype groups, FF, FS and SS within the population.

The stochastic matrix, **F**, below, contains the probabilities that a parent of genotype j produces an offspring of genotype i, $\mathbf{F_{j,i}}$, for all $i, j = 1, 2, 3$.

For example, consider the probability that an offspring has genotype FF, given one parent, say the mother, has genotype FF

Pr{an offspring has genotype FF | it's mother has genotype FF}

The offspring will have inherited one of the F alleles from the mother with a probability of 1. The second F allele must come from the father with a probability f, which is the frequency of the F allele in the male population (assuming the sex ratio is 1:1). Therefore

Pr{an offspring has genotype FF | it's mother has genotype FF} $= \mathbf{F_{1,1}} = f$

This value is entered into the following matrix along with the other probabilities that are similarly calculated

	FF	FS	SS
FF	f	s	0
FS	$\frac{f}{2}$	$\frac{1}{2}$	$\frac{s}{2}$
SS	0	f	s

where, s is the frequency of the S gene in the male population and $f + s = 1$.

The frequency of the gene conferring fast development, f, at time t, is determined to be

$$\mathbf{F_{1,1}}(t) = \frac{Ad_1(t) + Ad_2(t)/2}{Ad_1(t) + Ad_2(t) + Ad_3(t)} \tag{4.43}$$

where $Ad_1(t)$, $Ad_2(t)$ and $Ad_3(t)$ are the number of adults in each genotype group at time t, the equations having been presented in the previous section.

Nematodes can only reproduce within a host. Therefore the incorporation of a genetic component into the model affects only equation (4.1) in the preceding section. This equation now becomes

$$E_{i,1}(t+1) = \Theta_i P_{34} \sum_{j=1}^{3} Ad_j(t)\mathbf{F_{j,i}}(t) \tag{4.44}$$

where $\mathbf{F_{j,i}}(t)$ is the probability that an adult of genotype j produces an offspring of genotype i at time t,

P_{34} is the transition probability from adult to egg stage, and

Θ_i is the fecundity of female worms.

Progress through the free-living stages of the life cycle is exactly as before as no mixing of genotypes occurs outwith the host. This leads to the genetic analogue of equation (4.6),

$$\begin{aligned} E_{i,1}(t) &= P_{12}P_{23}P_{34}\mu\Theta_i \sum_{j=1}^{3} \alpha^{\tau_j - 1}\mathbf{F_{j,i}}(t-1) \\ &\times \left[E_{j,1}(t-(\tau_j-1)-h-2)\right. \\ &+ E_{j,1}(t-\tau_j-h-2)(1-\mu)s \\ &\left. + E_{j,1}(t-(\tau_j+1)-h-2)((1-\mu)s)^2\right] \end{aligned} \tag{4.45}$$

where $\mathbf{F_{j,i}}(t)$ has been defined above.

This model is shown diagrammatically in Figure 4.9.

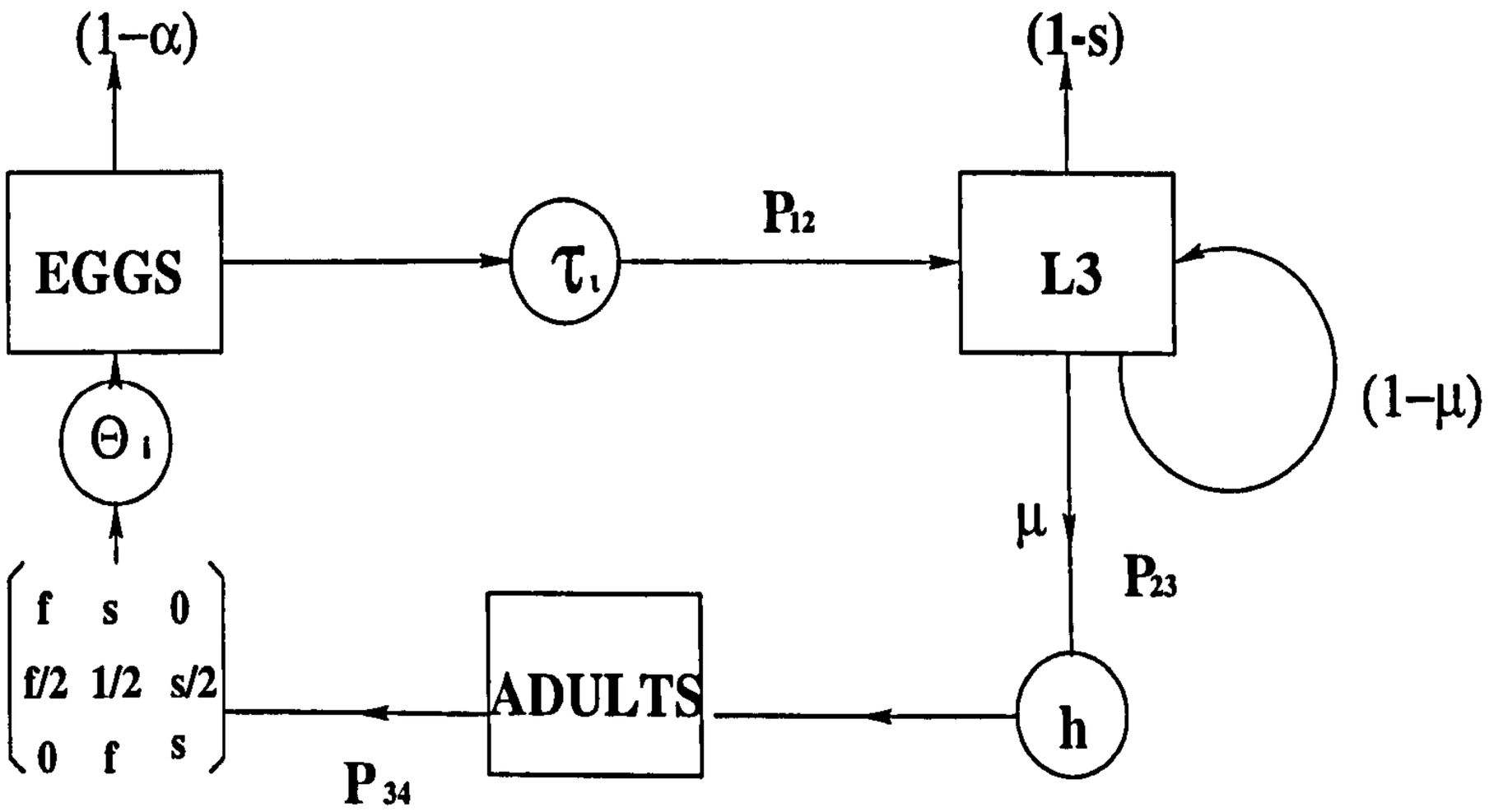

Figure 4.9: Flow diagram for life cycle of a typical nematode population with three life stages with random mixing of genotypes FF, FS and SS.

Biological interpretation of equation (4.45)

The explanation of this equation is somewhat more involved than that for the non-genetic equation. For example, the number of eggs of genotype FS at time t is equal to the number of eggs of genotype FF at time $(t-(\tau_1-1)-h-2)$, $(t-\tau_1-h-2)$ and $(t-(\tau_1+1)-h-2)$ days ago that developed to L3 and were immediately ingested, ingested after one day as L3 and ingested after two days as L3, respectively, by a host, became adults, mated and produced FS offspring plus the number of FS eggs at time $(t-(\tau_2-1)-h-2)$, $(t-\tau_2-h-2)$ and $(t-(\tau_2+1)-h-2)$ days ago that developed to L3 and were immediately ingested, ingested after one day as L3 and ingested after two days as L3, respectively, by a host, became adults, mated and produced FS offspring plus the number of SS eggs at time $(t-(\tau_3-1)-h-2)$, $(t-\tau_3-h-2)$ and $(t-(\tau_3+1)-h-2)$ days ago that developed to L3 and were immediately ingested, ingested after one day as L3 and ingested after two days as L3, respectively, by a host, became adults, mated and produced FS offspring.

This model is quite complex. It has three life stages, two time delays and two multiplier functions with three sub-populations moving through it. As a result of mixing between the genotype groups at reproduction, the model now consists of non-linear components, representing interaction between the groups. Consequently, the methods of analysis applied to the non-mixing model in the previous sections cannot be used here. Instead, the only available method of analysis for

non-linear systems is a local linearization analysis (or neighbourhood stability analysis), of the model at equilibrium. The equilibria of a non-linear system need not be a constant value, stable limit cycles, where the population numbers cycle within well defined boundaries may exist (May, 1974). The local stability of the equilibrium configuration, whether it be an equilibrium point, or a limit cycle is ensured if all eigenvalues of the Jacobian matrix, **A**, lie in a circle on the complex plane. The Jacobian matrix, or community matrix ($\mathbf{A_{i,j}}$), describes the effect of subgroup i on subgroup j at or near a point of equilibrium. From the characteristic equation derived from the determinant of $(\mathbf{A} - \lambda I)$, conditions for the stability of the model can be determined and a stability boundary can be sketched in terms of the parameters of the model.

The model developed here is analogous to a three species interaction model with multiple time delays. Successful local stability analyses have been done on interacting species with uniform time delays (for a general review, see Nisbet and Gurney, 1982; May, 1974), however, in our case, the generation times of different interacting species (or groups), are not identical in length. This adds an additional element of complexity to an already complex model. For the sake of brevity and since such an analysis as described above would be very time consuming, the genetic component of the model was examined in isolation as a preliminary analysis.

4.9 Extension of the Chiang Matrix to Incorporate Non-Uniform Generation Times

Consider a simple scenario where individuals are categorised into one of three groups according to their genotype for speed of development. These individuals are assumed to be single stage organisms that spend a specific period of time in maturation, after which they enter the gene pool, reproduce and are subsequently distributed amongst the genotype groups according to the probabilities in the matrix 4.8. Figure 4.10 is a graphical depiction of the above scenario.

Numbers of individuals in each genotype group over time are described by the following set of (non-linear) difference equations,

$$FF_{t+1} = FF_{t-\tau_1} f_{t-\tau_1} + \frac{FS_{t-\tau_2} f_{t-\tau_1}}{2}$$

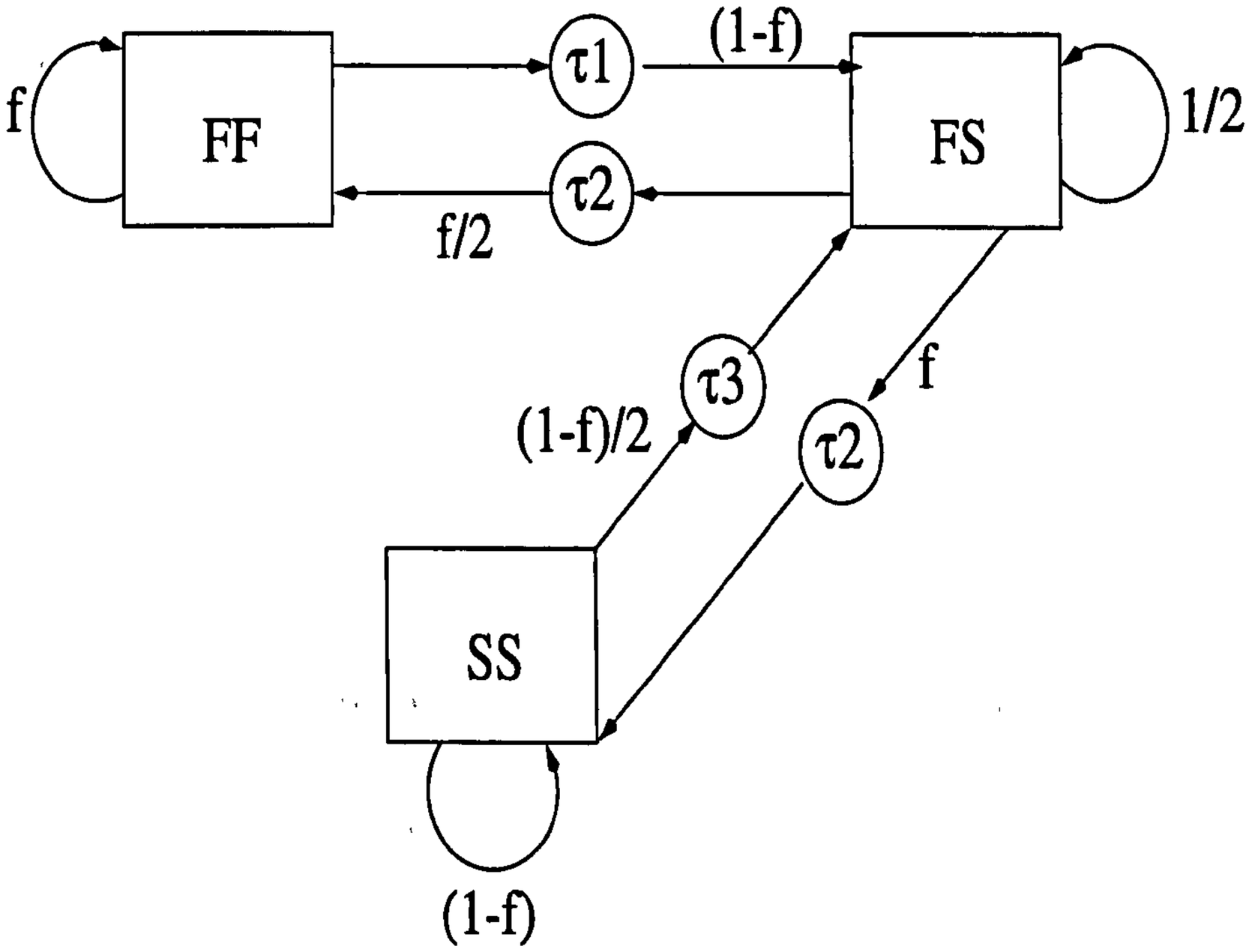

Figure 4.10: Flow diagram for life cycle of a single life staged organism.

$$\begin{aligned} FS_{t+1} &= FF_{t-\tau_1} s_{t-\tau_1} + \frac{FS_{t-\tau_2}}{2} + SS_{t-\tau_3} f_{t-\tau_1} \\ SS_{t+1} &= \frac{FS_{t-\tau_2} s_{t-\tau_1}}{2} + SS_{t-\tau_3} s_{t-\tau_1} \end{aligned} \tag{4.46}$$

where

$f(t-\tau_1)$ is the frequency of the gene conferring fast development at time $(t-\tau_1)$, given in full in equation (4.43), and $s = 1 - f$.

This is a closed system with replacement, that is, there is no mortality and each individual is replaced by a single individual at reproduction. The aim here is to investigate whether an equilibrium genotype distribution exists when generation times are non-uniform.

An equilibrium genotype distribution exists where

$$\begin{aligned} FF_{t+1} &= FF_{t-\tau_1} = \widehat{FF} \\ FS_{t+1} &= FS_{t-\tau_2} = \widehat{FS} \\ SS_{t+1} &= SS_{t-\tau_3} = \widehat{SS} \end{aligned} \tag{4.47}$$

Substituting the expressions in equation (4.47) into (4.46), and solving simultaneously gives the equilibrium genotype distribution, at any one time point, to

be

$$\begin{aligned} \widehat{FF} &= \frac{\widehat{FS}^2}{4\widehat{SS}} \\ \widehat{FS} &= \widehat{FS} \\ \widehat{SS} &= \widehat{SS} \end{aligned} \tag{4.48}$$

If the frequency of the F gene in the population is f and the frequency of the S, is s where $f + s = 1$, then when development times are equal for each development group, after one generation of mating, the genotype distribution, $FF : FS : SS$, follows the Hardy-Weinberg equilibrium $f^2 : 2fs : s^2$ (Strickberger, 1976). In our case, when the development times vary between genotype groups, an equilibrium genotype distribution, as in equation (4.48) is obtained.

This simple genetic model was simulated over time in ITERATOR (©STAMS) for four different sets of time delays, assuming that initial numbers in each genotype group were the same. A further two runs were simulated to look at the effect of initial f gene frequency on the outcome of the model. The aim was to investigate the nature of the genotype distribution equilibrium.

4.10 Results

The development times for each genotype differ, in that FF genotypes are assumed to spend fewer days on pasture than FS genotypes who in turn are assumed to spend fewer days on pasture than the SS genotypes. These times were varied for different runs of the model.

Figures 4.11, 4.12, 4.13 and 4.14 give the results from four different runs of the simulation model, each run corresponding to different time delays, but all starting at the same initial size, $FF_0 = FS_0 = SS_0 = 10000$. Table 4.1 gives the different time delays used in each of the four simulations.

All populations eventually converge to the steady state distribution in equation (4.48), with the time until convergence being longer as generation time increases.

At any one time point, individuals will be distributed throughout the age classes within each genotype group. For example if FS individuals have a generation time of 3 days, say, at any one time point, there will be FS individuals in age

Table 4.1: Time delays for FF, FS and SS genotype groups.

Figure	τ_1	τ_2	τ_3
4.11	1	2	4
4.12	10	17	28
4.13	1	2	3
4.14	10	20	30

classes 1, 2 and 3 respectively.

For each simulation run when the numbers at the final time point are summed over each age class within each genotype group, it is evident that the total population size has been retained. In addition the numbers in each genotype group at equilibrium for each simulation are in the ratio $f^2 : 2fs : s^2$, where f is the frequency of the gene for fast development, F, and $s = 1 - f$ (see Table 4.2). In other words, these preliminary results suggest that despite non-uniform generation times within a population, the initial gene frequency is conserved over time.

Table 4.2: Equilibrium genotype distribution for non-uniform generation times.

Figure	Time Delay	FF_0:FS_0:SS_0	FF^*:FS^*:SS^*	f_0	f^*
4.11	1,2,4	10000:10000:10000	7500:15000:7500	0.5	0.5
4.12	10,17,28	10000:10000:10000	7500:15000:7500	0.5	0.5
4.13	1,2,3	10000:10000:10000	7500:15000:7500	0.5	0.5
4.14	10,20,30	10000:10000:10000	7500:15000:7500	0.5	0.5
-	1,2,4	1000:20:50	953.694:112.6125:3.6937	0.943	0.943
-	1,2,4	100:500:2000	50.9376:598.125:1950.94	0.1346	0.1346

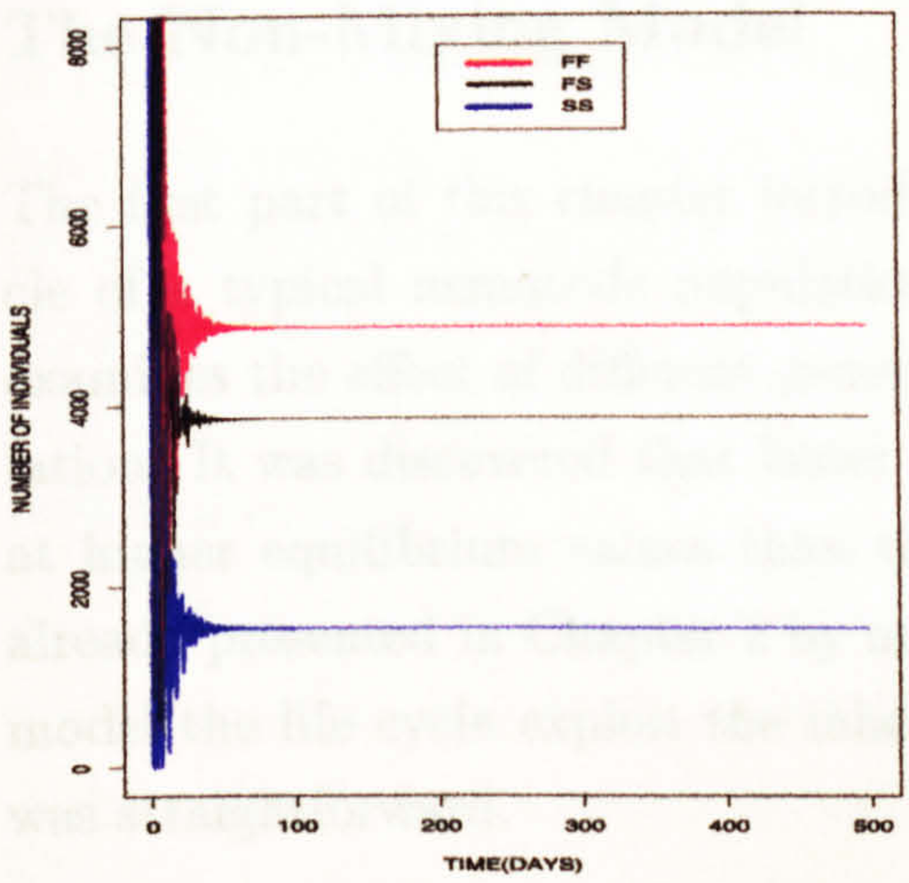

Figure 4.11: Population numbers over time for the single-staged organism, with generation times, $\tau_1 = 1$ day, $\tau_2 = 2$ days and $\tau_3 = 4$ days for FF, FS and SS genotypes respectively.

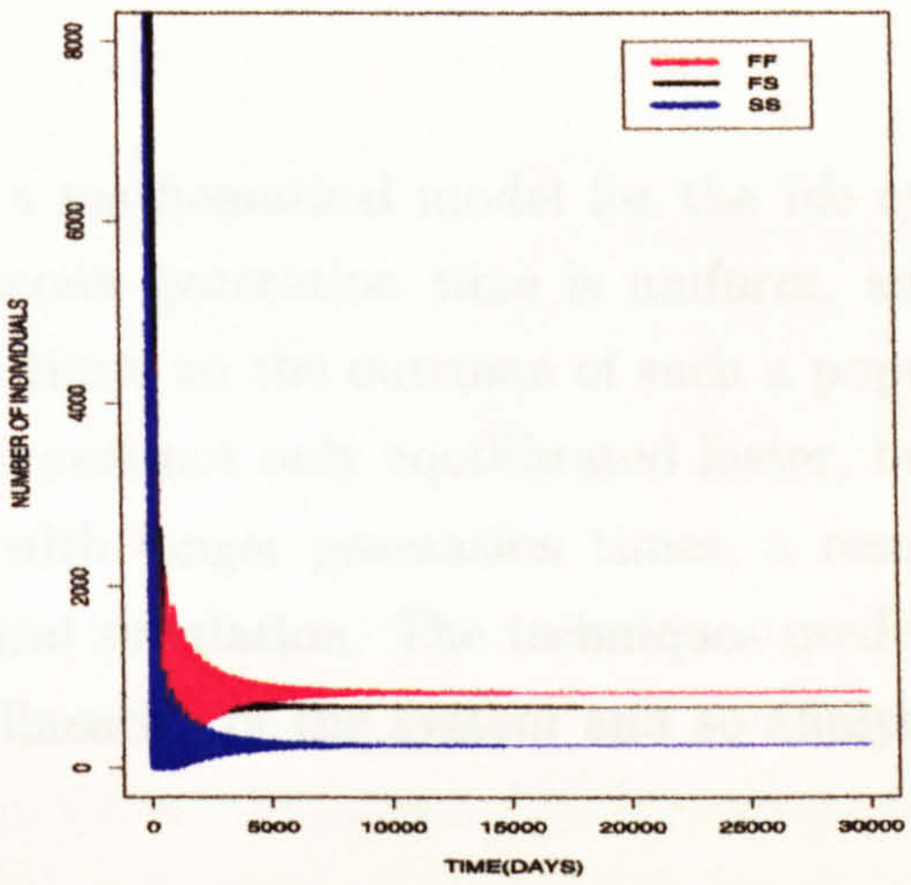

Figure 4.12: Population numbers over time for the single-staged organism, with generation times, $\tau_1 = 10$ days, $\tau_2 = 17$ days and $\tau_3 = 28$ days for FF, FS and SS genotypes respectively.

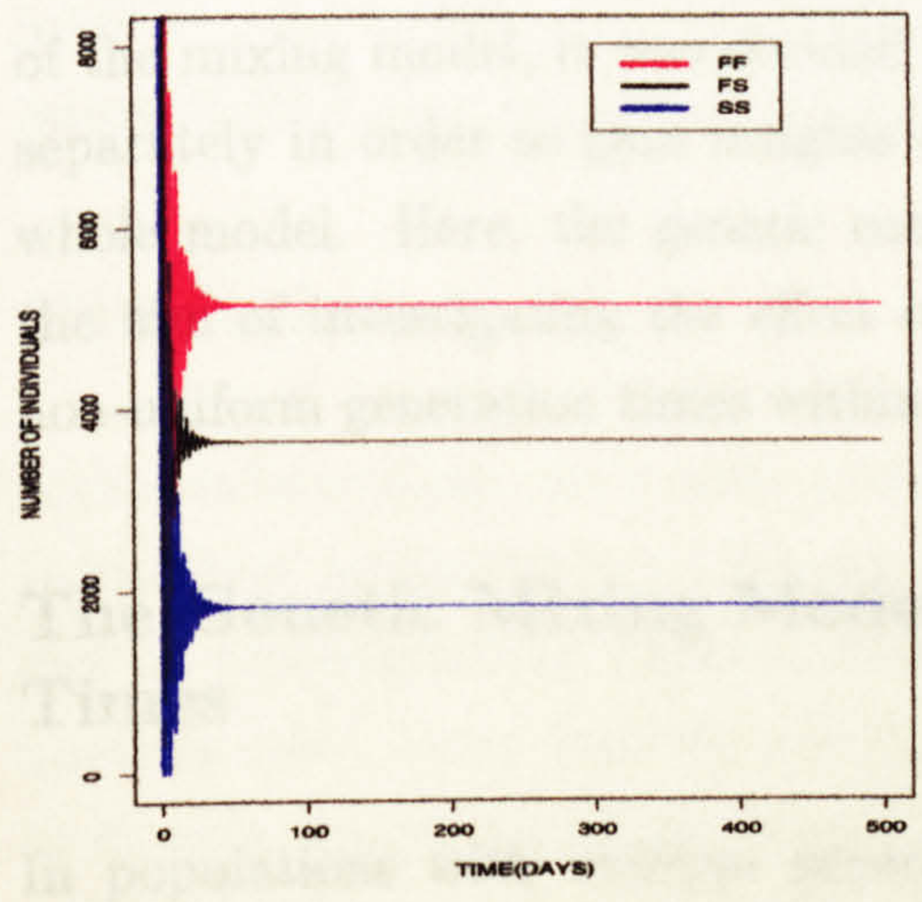

Figure 4.13: Population numbers over time for the single-staged organism, with generation times, $\tau_1 = 1$ day, $\tau_2 = 2$ days and $\tau_3 = 3$ days for FF, FS and SS genotypes respectively.

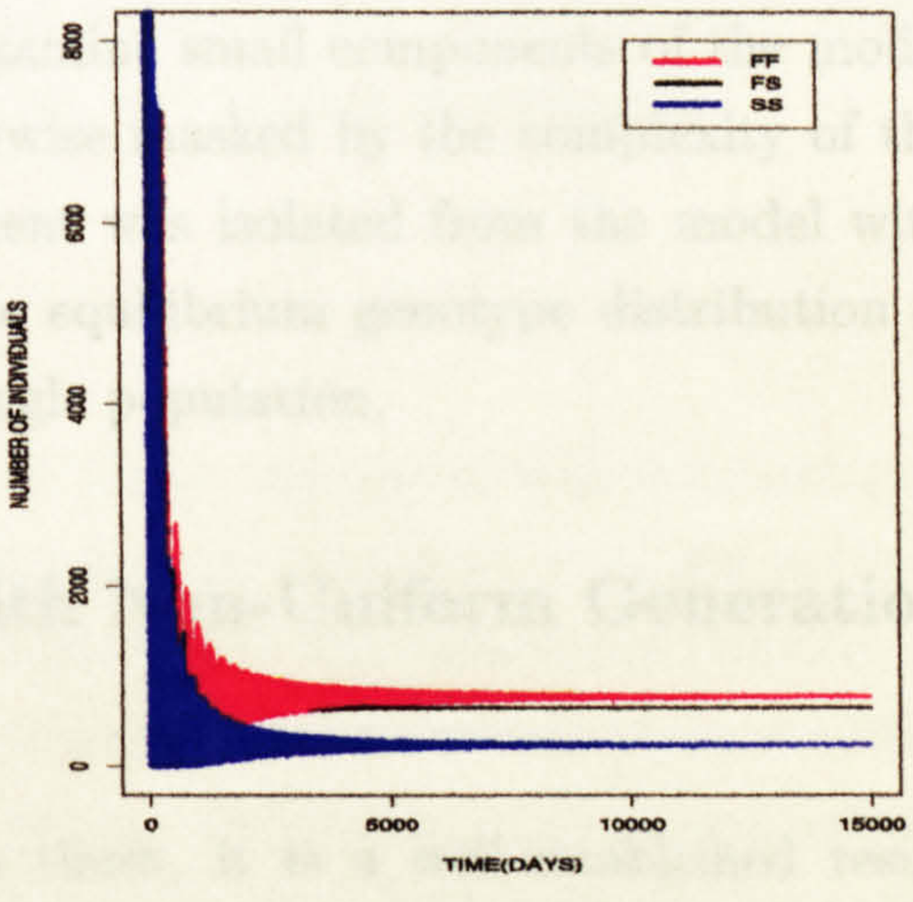

Figure 4.14: Population numbers over time for the single-staged organism, with generation times, $\tau_1 = 10$ day, $\tau_2 = 20$ days and $\tau_3 = 30$ days for FF, FS and SS genotypes respectively.

4.11 Conclusion

The Non-Mixing Model

The first part of this chapter introduces a mathematical model for the life cycle of a typical nematode population wherein generation time is uniform, and examines the effect of different generation times on the outcome of such a population. It was discovered that faster developers not only equilibrated faster, but at higher equilibrium values than those with longer generation times, a result already presented in Chapter 2 by numerical simulation. The techniques used to model the life cycle exploit the inherent linearity of the system and so analysis was straightforward.

The Mixing Model

The assumption that individuals within each genotype group were confined to that group at reproduction was relaxed in the second half of the chapter and a model incorporating genetic mixing of genotypes at reproduction was proposed. The population being modelled now had non-uniform development times, which meant that generations were no longer distinct, a feature distinguishing nematode worms from insect species. The mixing model is non-linear. Due to the complexity of the mixing model, it was decided to examine small components of the model separately in order to gain insights otherwise masked by the complexity of the whole model. Here, the genetic component was isolated from the model with the aim of investigating the effect on the equilibrium genotype distribution of non-uniform generation times within a single population.

The Genetic Mixing Model with Non-Uniform Generation Times

In populations with uniform generation times, it is a well-established result (Strickberger, 1976), that, provided individuals within a population mate at random, if the frequency of a specific gene at a single locus on the chromosome, is f, say, the genotype distribution of the next generation will be in the ratio

$$f^2 : 2fs : s^2$$

This ratio is called the Hardy Weinberg equilibrium, where, effectively, the gene frequency is conserved from generation to generation.

In populations with non-uniform generation times where development rate is conferred by two alleles at a single locus on the chromosome, it appears from these preliminary results that such a population will also reach an equilibrium genotype distribution similar to the Hardy Weinberg equilibrium, only the population numbers are now distributed amongst age classes rather than all individuals being in the same stage.

As this is a closed system with replacement, there is an intrinsic assumption that births equal deaths. So provided that this is the case, then in any population with non-uniform generation times, an equilibrium genotype distribution exists.

Having determined the outcome of the genetical mixing of a population with non-uniform generation times, the model could now be reconstructed with the results of this analysis in mind, and as was mentioned earlier, a stability boundary sketched in terms of other parameters such as fecundity, mortality and ingestion rates.

Both the mixing and non-mixing models described in this chapter are discrete, deterministic representations of a complex biological system where change is continuous and some events occur at random. When there are multiple time delays, however, and members of the population are within an age class structure, deterministic difference equations lend themselves well to such phenomena.

Conclusions

Methods of analysis are readily available for linear systems as was demonstrated in the first section of this Chapter. Unfortunately, very few biological systems can be represented by linear models. Furthermore, few non-linear methods of analysis exist, those that do consist of examining the behaviour of populations at or near points of equilibrium after perturbing the system. The computational difficulties that arise when analysing such models have been outlined here, and it is necessary to point out that transient behaviour of the system far away from equilibria may be of interest when examining nematode population dynamics.

It is recognised that this model focuses in detail on the free-living dynamics of nematode parasites. The dynamics of the intra-host stage is equally as important and must be given due consideration, particularly with respect to host induced

population regulatory mechanisms known to operate when high adult worm burdens are being harboured within the host.

In this Chapter, no account has been taken of environmental influences on the free-living development of nematode parasites. Factors such as temperature, relative humidity, etc govern the rate at which individuals develop whilst free-living on pasture. Considering the temperature-dependent development rate data in Chapter 2, generally at the start and end of a typical grazing season, temperatures are quite low, therefore, development times are quite long. As summer approaches, the development time decreases to a minimum at the height of summer, then slowly begins to increase as autumn approaches.

An interesting addition to the final model in this chapter would be the inclusion of a seasonality function, which could be in the form of a parabola, that would alter the free-living development times according to the temperature the parasites would be exposed to at different times of the year.

Chapter 5

Modelling The Genetics of Resistance within a Parasite Population

5.1 Introduction

The widespread and sporadic use of compounds designed to eradicate pests has resulted in the selection for drug resistant strains of organism. In this Chapter we shall discuss the problems of resistance with respect to ecto- and endo-parasites. Current insecticide and anthelmintic resistance models are reviewed and a mathematical framework is presented to model the evolution of drug resistance in a nematode population in a bid to identify the major factors influencing the growth of resistance.

5.2 Current Models of Drug Resistance

5.2.1 Insecticide Resistance

In 1972, Georghiou reported over 300 cases of insecticide resistance since the introduction three decades previously of modern organic pesticides. In 1986, just a decade later, that number had risen to 447. The sporadic use of these chemicals in an uncontrolled manner has led to the acceleration of resistance in insect populations, with a growing trend towards the development of multiple and cross resistance.

Having identified the major genetic, biological and operational factors influencing

insecticide resistance, Georghiou and Taylor (1977a,b) developed mathematical models to explore the effect of these factors on the growth and evolution of resistance.

Around the same time Comins (1977) presented a mathematical model of insecticide resistance. He introduced the concept of migration into and out of an insect population as a means of controlling resistance. It was discovered that if drug-susceptible individuals were introduced into the population, the evolution of resistance may be delayed. Taylor and Georghiou (1979) use a system of coupled difference equations to describe changes in the frequency of the gene conferring resistance, and changes in the population size in an insect population exposed to insecticide. The authors re-examined the novel technique of controlling insecticide resistance via the inward migration of insecticide-susceptible strains initially explored by Comins (1977). Their approach differed to that of Comins (1977) in that the migrant pool is assumed to be unaffected by the outward migration of resistant strains from the population. In making this assumption, Taylor & Georghiou (1979), with their model, successfully achieved control of resistance and population numbers simultaneously provided the migration rate was high and the resistant allele recessive.

More recently, similar modelling techniques have been used to explore the phenomenon of multiple resistance and the effect of mixtures of compounds on the progression of insecticide resistance (Mani, 1985). In this study Mani (1985) assessed the effect of administering mixtures of insecticide as opposed to sequential treatment of an insect population. This was mathematically more challenging as a two-locus instead of a single-locus modelling approach was taken which involved considering linkage disequilibrium and recombination factors . It was concluded that the use of mixtures will delay the onset of resistance in a population, quite drastically when the recombination factor, r, is above a certain specified threshold.

Roush (1990) reviews the genetics and management of insecticide resistance and considers whether the lessons learned by entomologists may be usefully applied to similar problems associated with internal parasites, particularly nematodes. A great many similarities exist between both disciplines. As a result, preventative measures can be undertaken to avoid making the same mistakes that were made two decades ago in the insect domain.

5.2.2 Anthelmintic Resistance

Simulation Models

Models, such as those developed by Gettinby *et al* (1989) for *T. circumcincta* , and Barnes and Dobson for *T. colubriformus* (1995), simulate the evolution of resistance in a specific parasite population using the relevant epidemiological, climatic and genetic factors at a particular site. These models are very complex and so are unable to provide simple analytical results on how resistance evolves in a population.

Analytical Models

Smith (1990) proposed a drug resistance model that was generic to most direct life cycle nematode populations with overlapping generations, undergoing some form of selective drug treatment. A system of deterministic differential equations was developed to model changes in the genotype distribution of free-living parasites and sexually mature adults in a typical nematode population. The equations incorporated many of the important biological aspects of a parasite population undergoing intensive drug treatment, including host ingestion rate, fecundity of female parasites and mortality of free-living parasites. In addition, a genetic component that determined the genotype distribution of the offspring population given the parent population genotype distribution after drug treatment was incorporated into the model. Analytical results were obtained for the pre-treated population, where equilibrium gene frequencies were found by imposing a heterozygote advantage on the mortality of the free-living stages. The effect of treatment on this population was explored by numerical simulation, and it was concluded that sequential treatment using different anthelmintics was less effective at delaying the onset of resistance than simultaneous treatment with mixtures.

5.3 Difference Equation Models for the Evolution of Drug Resistance in Parasite Populations

This Chapter presents a pair of models for the evolution of drug resistance in a parasite population in a bid to identify the major factors influencing the growth of resistance in a population.

5.3.1 Genetic Component of the Models

It is assumed that resistance is conferred by two alleles at a single locus on the chromosome, with R and S representing the resistant and susceptible alleles respectively. This results in three genotypes, denoted by RR, RS and SS. The frequency of the R gene in generation t is denoted p_t and the frequency of the S gene in generation t is denoted q_t, where $p_t + q_t = 1$. Of those parasites exposed to an anthelmintic, all RR genotypes will survive, a proportion, $1-h$, of the RSs will survive and all SSs will be killed. The value of h determines the relative dominance of the R allele, $(0 \leq h \leq 1)$. That is, if $h = 0$, the R gene is fully dominant; if $h = 1$, the S gene is fully dominant; if $0 < h < 1$, there is partial dominance.

Mating between parasites within the host is assumed to be at random. After a single generation of mating, the resultant genotype distribution in the offspring population is in the Hardy-Weinberg ratio. That is, if the frequency of the gene conferring resistance in the population before reproduction is p_t and the frequency of the susceptible gene in the population is q_t, where $q_t = 1 - p_t$, in the following generation, the offspring genotype distribution will be in the ratio $p_t^2 : 2p_tq_t : q_t^2$ $(RR : RS : SS)$ (Strickberger, 1976).

5.3.2 Host-Pasture Model (HP Model)

In a single generation, it is assumed that a proportion, α, of the population on pasture will be ingested by a single host. Once inside the host, these parasites are exposed to an anthelmintic. Those surviving treatment will mate and produce offspring which will be deposited onto the pasture. Meanwhile, those individuals not ingested by the host will remain on the pasture and will decrease over time due to natural mortality, at a rate $1-\beta$. The proportion of the original population

surviving on pasture is therefore $(1-\alpha)\beta$. This is illustrated in Figure 5.1.

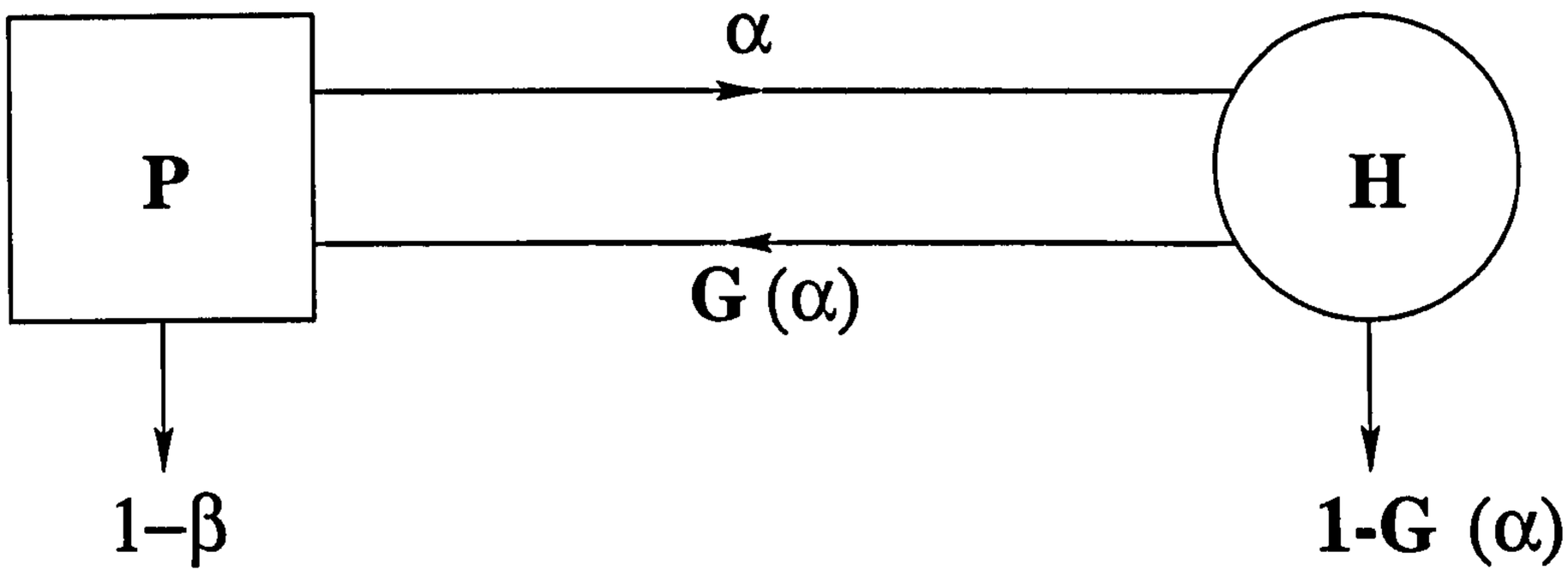

Figure 5.1: Flow Diagram for Host-Pasture Model depicting the flow of parasites from pasture to host undergoing drug treatment, with offspring returning to the pasture after a single generation.

It follows that the proportion of individuals from the population that survive treatment within the host will be

$$\bar{w}_t(H) = \alpha\left[p_t^2 + 2p_t\left(1-p_t\right)\left(1-h\right)\right] \tag{5.1}$$

The proportion of individuals from the population that survive on the pasture is

$$\bar{w}_t(P) = \left(1-\alpha\right)\beta \tag{5.2}$$

Let the number of individuals that would have survived if the animal was not dosed, and natural mortality was zero, be N_t. Thus the frequency of the R gene in the subsequent generation is

$$p_{t+1} = \frac{f\alpha\left[p_t^2 + p_t\left(1-p_t\right)\left(1-h\right)\right] + \left(1-\alpha\right)\beta p_t}{f\bar{w}_t(H) + \bar{w}_t(P)} \tag{5.3}$$

The change in population numbers is modelled using the simple relationship

$$N_{t+1} = N_t\left(\bar{w}_t(P) + f\bar{w}_t(H)\right) \tag{5.4}$$

where f is the fecundity of female worms.

5.4 Analysis of the HP Model

Equilibrium occurs when the gene frequency and population size are unchanging. That is, when

$$\Delta p_t = p_{t+1} - p_t = 0$$

and

$$\Delta N_t = N_{t+1} - N_t = 0$$

5.4.1 Gene Frequency Equilibrium

The gene frequency is unchanging where

$$\Delta p_t = \frac{f\alpha\left[p_t^2 + p_t\left(1-p_t\right)\left(1-h\right)\right] + \left(1-\alpha\right)\beta\left[p_t\right]}{f\bar{w}_t(H) + \bar{w}_t(P)} - p_t \;=\; 0 \qquad (5.5)$$

$$f\alpha\left[p_t^2 + p_t\left(1-p_t\right)\left(1-h\right)\right] + \left(1-\alpha\right)\beta\left[p_t\right] \;=\; p_t\left[f\bar{w}_t(H) + \bar{w}_t(P)\right] \qquad (5.6)$$

$$f\alpha\left(2h-1\right)p_t^3 + f\alpha\left(2-3h\right)p_t^2 - f\alpha\left(1-h\right)p_t \;=\; 0 \qquad (5.7)$$

Dividing equation (5.7) by $f\alpha$ results in a cubic equation in p_t

$$p_t\left[\left(2h-1\right)p_t^2 + \left(2-3h\right)p_t - \left(1-h\right)\right] = 0 \qquad (5.8)$$

the roots of which represent the equilibrium gene frequencies, p_0^*, p_1^* and p_2^*. These are given by

$$p_0^* = 0$$

$$p_1^*, p_2^* \;=\; \frac{3h-2 \pm \sqrt{\left(2-3h\right)^2 - 4\left(2h-1\right)\left(h-1\right)}}{2\left(2h-1\right)} \qquad (5.9)$$

and so one root is

$$p_1^* \;=\; \frac{4h-2}{4h-2} = 1 \qquad (5.10)$$

and the other is

$$p_2^* = \frac{h-1}{2h-1} \tag{5.11}$$

By definition,

$$0 \leq p_1^*, p_2^* \leq 1$$

From equation (5.10), it is clear that $p_1^* = 1$ satisfies this condition. For p_2^* to satisfy this condition,

$$0 \leq \frac{h-1}{2h-1} \leq 1$$

Given that $0 \leq h \leq 1$, the only reasonable value that h can take is $h = 1$. Substitution of $h = 1$ into (5.11), gives the second root of equation (5.9) to be $p_2^* = 0$, representing the trivial solution to equation (5.9). A value of $h = 1$ represents complete recessiveness of the R gene.

5.4.2 Population Size Equilibrium

The equilibrium population size under the HP model is calculated by setting $\Delta N_t = 0$ and so

$$\Delta N_t = N_{t+1} - N_t = 0 \tag{5.12}$$

$$N_t \bar{w}_t(P) + N_t \bar{w}_t(H) f - N_t = 0 \tag{5.13}$$

This means that either

$$N^* = 0 \tag{5.14}$$

or that

$$\bar{w}_t(P) + \bar{w}_t(H) f - 1 = 0 \tag{5.15}$$

$N^* = 0$ is the trivial equilibrium for this system. An alternative equilibrium exists only when (5.15) is satisfied. If this is the case, N^* can effectively take one of an infinite number of possible values. Expanding equation (5.15) gives

$$(2h-1)\alpha f p_t^2 + (2-2h)\alpha f p_t + (1-\alpha)\beta - 1 = 0 \tag{5.16}$$

This result suggests that conditional on there being a gene frequency equilibrium (or equilibria), p_1^*, p_2^*, that can be substituted into the final equation in (5.16), a population size equilibrium will exist provided equation (5.16) is satisfied.

Equilibrium Population Size with $p_1^* = 1$

Substituting $p_1^* = 1$ into equation (5.16) reveals that a non-trivial population size equilibrium will exist provided

$$f\alpha = 1 - (1 - \alpha)\beta$$

That is to say that once a population has reached the gene frequency equilibrium of $p_1^* = 1$, the size of the population will reach equilibrium provided the incomers to the population equal those leaving the population each generation.

Equilibrium Population Size with $p_2^* = 0$

Substitution of $p_2^* = 0$ into equation (5.16) demonstrates that for an equilibrium population size to exist,

$$(1 - \alpha)\beta = 1$$

When the population is fully susceptible, an equilibrium population size will be reached only if the proportion of individuals that remain on pasture and survive is 1.

Given that α and β must both lie between 0 and 1, the only valid solution of this equation is $\alpha = 0$ and $\beta = 1$. This corresponds to no parasites being ingested by a host and 100% survival on the pasture. Clearly if any member of this population leaves the pasture and enters a host, it will be killed by the anthelmintic drug.

Effectively, once $p^* = 1$ has been reached, the process defined in equation (5.4) becomes a simple birth death process where an infinite number of steady state population sizes exist provided births equal deaths. Otherwise, if $\alpha f > 1 - (1 - \alpha)\beta$ the population will increase monotonically, and if $\alpha f < 1 - (1 - \alpha)\beta$ the population will decrease to below 1 and become extinct. The second case reported above is looked on as the trivial case and will not be pursued further.

5.4.3 A Neighbourhood Stability Analysis of the Gene Frequency Equilibria

The equilibrium state or fixed point, p^*, is said to be stable if all initial values in some neighbourhood are attracted to it, (Mickens, 1990).

Let p^* be a fixed point of equation (5.3). We consider the behaviour of states in some neighbourhood of $p_t = p^*$, that is

$$p_t = p^* + \rho_t \tag{5.17}$$

where ρ_t is assumed to be very small. On substitution of equation (5.17) into equation (5.3), and expansion of equation (5.3) about p^* we get

$$\begin{aligned} \rho_{t+1} + p^* &= F(p^* + \rho_{t+1}) \\ &= F(p^*) + F'(p^*)\rho_t + \frac{1}{2}F''(p^*)\rho_t^2 + \frac{1}{6}F'''(p^*)\rho_t^3 + ... \end{aligned} \tag{5.18}$$

which leads to

$$\rho_{t+1} = F'(p^*)\rho_t + \frac{1}{2}F''(p^*)\rho_t^2 + \frac{1}{6}F'''(p^*)\rho_t^3 + ... \tag{5.19}$$

Discarding terms of second order or more results in

$$\rho_{t+1} = F'(p^*)\rho_t \tag{5.20}$$

the solution of which is

$$\rho_t = \rho_0 \left[F'(p^*)\right]^t \tag{5.21}$$

The stability of p^* is therefore determined by the sign of the first derivative of equation (5.3) about this point.

Equation (5.3) becomes

$$F(p_t) = \frac{f\alpha\left[p_t^2 + p_t\left(1 - p_t\right)\left(1 - h\right)\right] + \left(1 - \alpha\right)\beta p_t}{f\bar{w}_t(H) + \bar{w}_t(P)} \tag{5.22}$$

It follows that

$$F'(p^*) = \frac{f\alpha(1-h)+(1-\alpha)\beta}{f\alpha+(1-\alpha)\beta} \tag{5.23}$$

In order for $p^* = 1$ to be stable, the RHS of equation (5.23) must be less than one. This means that $f\alpha h > 0$. Since f, α and h are all positive parameters, this condition holds for all p^*. For p^* to be unstable, $F'(p^*) > 1$, this would result in $-f\alpha h > 0$, which under the circumstances in this model, is not possible.

5.5 Numerical Simulation of the HP Model

5.5.1 Frequency of the Gene Conferring Resistance

It has been determined that under normal circumstances, the frequency of the gene conferring resistance, R, will always reach 1 eventually, provided $p_0 > 0$, independent of N, the population size.

The HP Model was simulated for eleven different parameter sets using ITERATOR (©STAMS), a numerical solutions package for difference equations, to determine the effect of the parameters on the evolution of resistance. The parameter values are given in Table 5.1. The parameter values were chosen to reflect the entire range of possible values. For the ingestion rate, α, initial R gene frequency, p_0, survival rate, β and proportion of heterozygotes killed by the drug, h, possible values ranged from zero to one. We chose a minimum, a maximum and an intermediate value for each parameter. For f, the fecundity of female parasites, values of 10, 100 and 1000 were chosen.

Initial Gene Frequency p_0

Figure 5.2(a) demonstrates the effect of initial gene frequency on the evolution of resistance in a typical parasite population. Provided that $p_0 > 0$, a fully resistant population will always evolve. At low initial gene frequencies, growth to resistance appears to be sigmoidal. However, when the gene frequency is initially high or in the mid values, growth to resistance is exponential in nature. We can explain this by recalling the principles of segregation and recombination of genetic material at reproduction (Strickberger, 1976). When the frequency of the R allele is initially low, after one generation, provided the population mixes at

Table 5.1: Table of parameter values chosen to illustrate the behaviour of the HP model using numerical simulation.

Simulation	p_0	α	β	**f**	**h**
1	0.1	0.1	0.9	100	1
2	0.4	0.1	0.9	100	1
3	0.9	0.1	0.9	100	1
4	0.1	0.4	0.9	100	1
5	0.1	0.9	0.9	100	1
6	0.1	0.1	0.1	100	1
7	0.1	0.1	0.5	100	1
8	0.1	0.1	0.9	10	1
9	0.1	0.1	0.9	1000	1
10	0.1	0.1	0.9	100	0.75
11	0.1	0.1	0.9	100	0.25

random, the majority of R alleles are to be found in the heterozygotes. According to Mendellian principles of segregation, the mating combination $RS \times RS$ yields a probability of 0.5 of producing an R allele, whereas the combination of $RR \times RR$ has a probability of 1 of producing an R allele. Therefore the R gene frequency will grow more slowly when the majority of the R alleles are within heterozygotes rather than within the homozygotes.

Ingestion Rate, α

The rate at which the host ingests parasites will have an effect on the rate at which a fully resistant population evolves, as it is only the ingested proportion that can reproduce and contribute their genetic material to future generations. It is clear from Figure 5.2(b) that the higher the fraction of the population that is ingested at any one time, the quicker resistance evolves.

Survival Rate, β

Figure 5.2(c) illustrates the effect of varying survival on the pasture. A high survival rate on pasture will lead to full resistance much slower than a low survival

rate. If fewer parasites are available to the host, fewer will reproduce, and so it will take longer for resistance to evolve in a population. As the survival rate decreases, the rate at which the population becomes fully resistant increases.

Fecundity of Female Worms, f

In this model, the fecundity of the female worms is assumed to be uniform irrespective of genotype. Figure 5.3(a) shows the effect on the R gene frequency over time that varying the egg output of female parasites from 10 to 100 to 1000, respectively will have. Reducing fecundity from 1000 to 100 and 100 to 10 eggs per female respectively has a very different effect on the rate at which the population converges to resistance. Fecundities of 1000 and 100 lead to very similar behaviour of the model. However a fecundity of 10 eggs per female has a dramatic effect on the dynamics of the R gene frequency, and convergence to resistance is notably slower.

Proportion of heterozygotes killed by the drug, h

The dominance of the R gene is the only factor in this model that is at least partially under the control of the experimenter. Provided that the dominance of the gene conferring resistance is dependent on the dose of anthelmintic, the parameter, h, the proportion of heterozygotes killed by the drug, can be adapted. Figure 5.3(b) demonstrates the effect that this parameter has on the system. Consider three populations where $h = 1$, $h = 0.75$ and $h = 0.25$, respectively. In the first population, the drug kills all heterozygotes, in the second, the drug kills 75% of the heterozygotes and in the third population, the drug kills 25% of the heterozygotes. In all three populations the R gene frequency is initially low, ($p_0 = 0.1$). This means that the majority of the R genes are to be found in heterozygotes. Resistance in the first population will evolve slower than in the other two populations, whilst the R gene frequency is low. In fact the higher the h value, the slower resistance will proceed provided the initial R gene frequency is low. Recall that when the R gene frequency is initially low, there will be a greater number of heterozygotes than homozygote RRs if mating is at random (Strickberger,1976). This increases the chances of an RSxRS mating rather than a RRxRR or RRxRS. The latter mating combinations producing on average a higher proportion of R genes than the former mating combination. Once the R gene frequency has reached some critical level in the population, there is a greater

number of RR homozygotes now than heterozygotes which results in more R genes being introduced to the population than before.

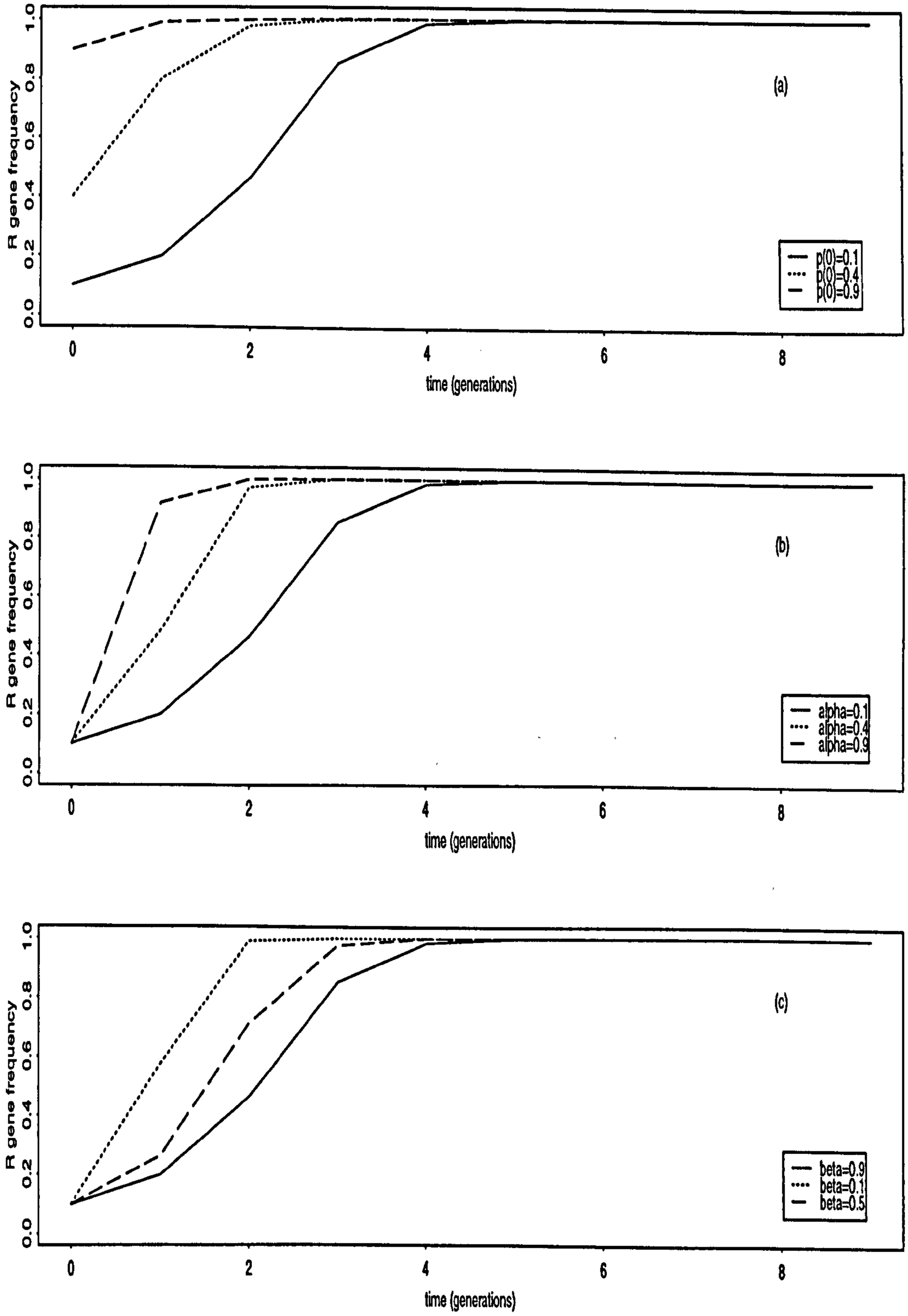

Figure 5.2: Changes in the frequency of the R gene over time for the HP model, when (a) the initial gene frequency, p_0, is varied;(b) the ingestion rate, α, is varied; and (c) the survival rate, β, is varied.

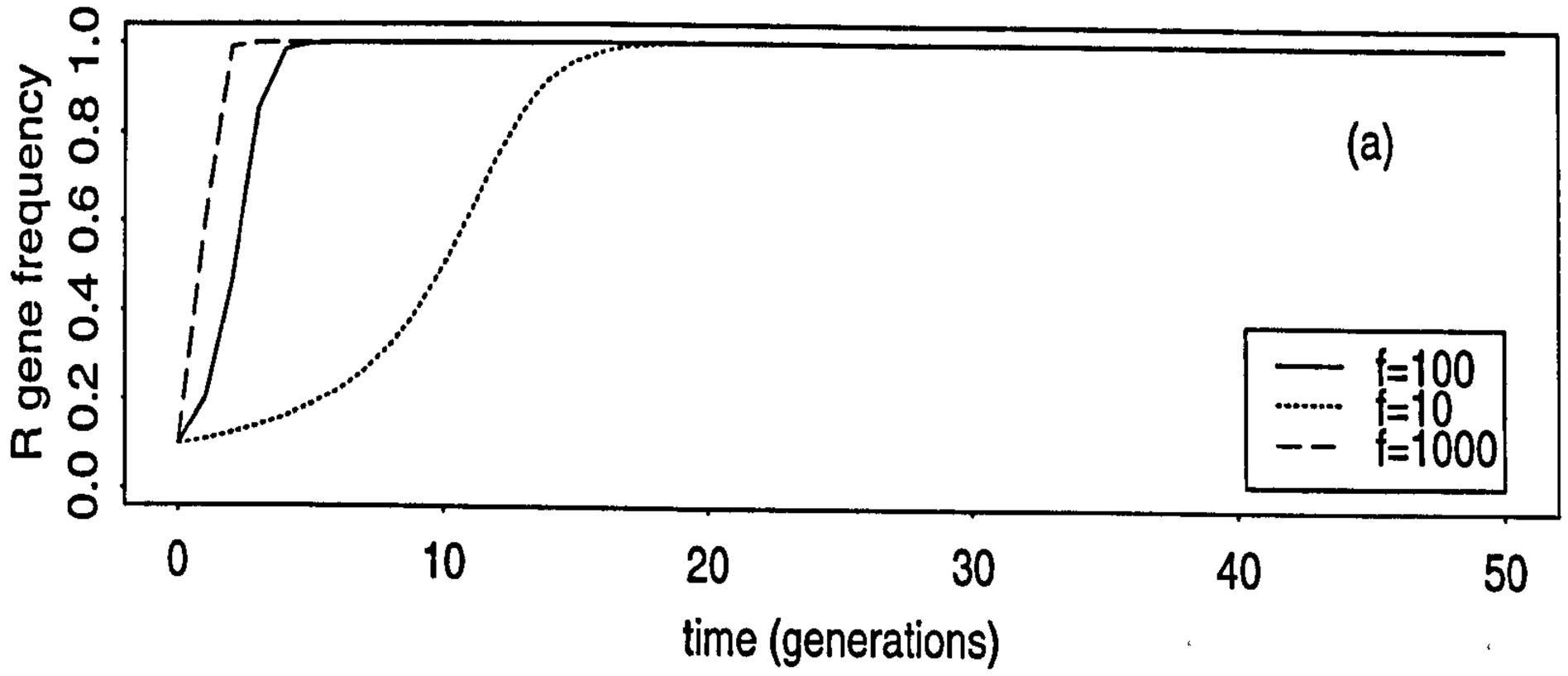

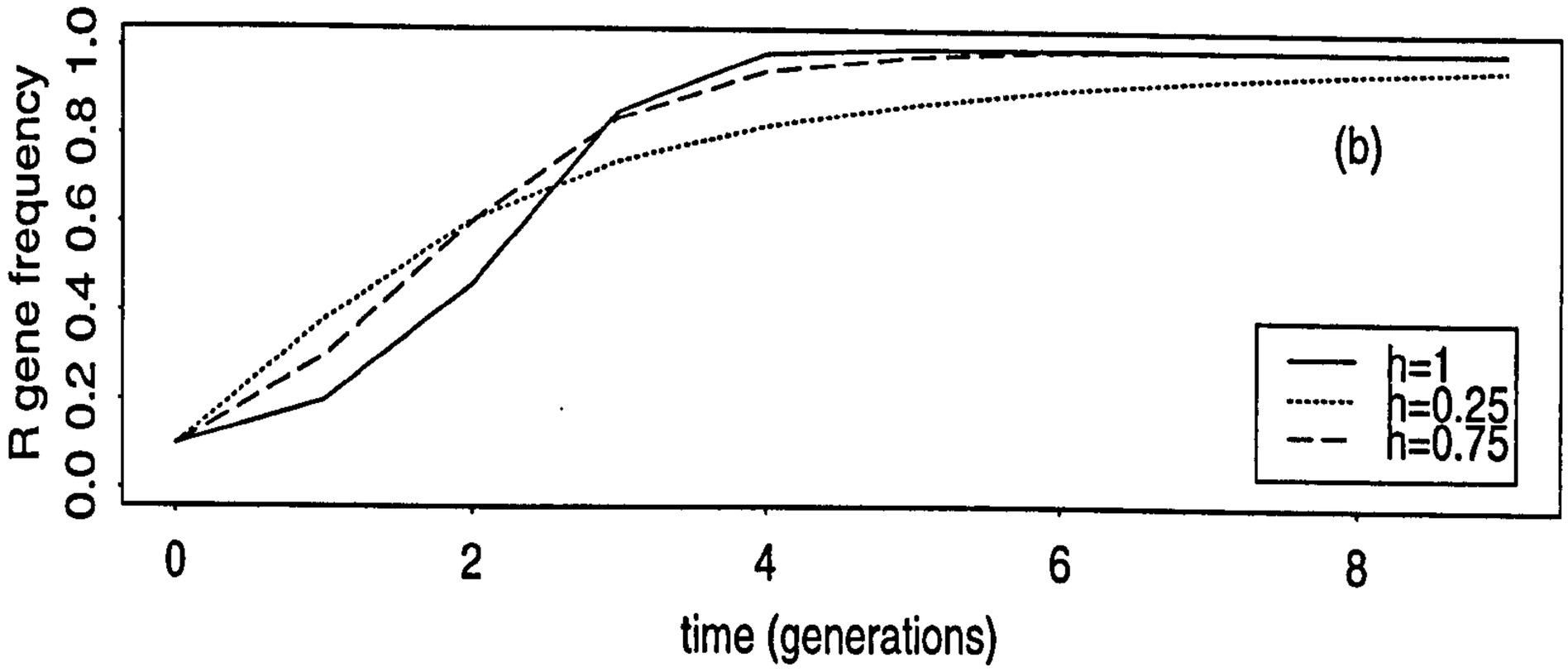

Figure 5.3: Changes in the frequency of the R gene over time for the HP model, when (a) the fecundity of female worms, f, is varied; and (b) the proportion of heterozygotes that are killed by the drug, h, is varied.

5.5.2 Population Size

Figure 5.4 shows the behaviour of the population size over time for four different starting conditions, $N_0 = 1000000, 500000, 100000, 10000$. Provided $f\alpha = 1-(1-\alpha)\beta$, the condition for population size equilibrium, the steady state values will depend only on the starting conditions. The steady state values of populations with initial population sizes of 1E6, 5E5, 1E5 and 1E4, respectively, are 245.848, 122.924, 24.5848 and 2.45848, respectively. In other words, the equilibrium population size is directly proportional to the initial population size, since we have a very simple population growth function that does not contain any regulatory mechanism such as host immunity. However, there are suggestions that density dependent effects will not affect the results.

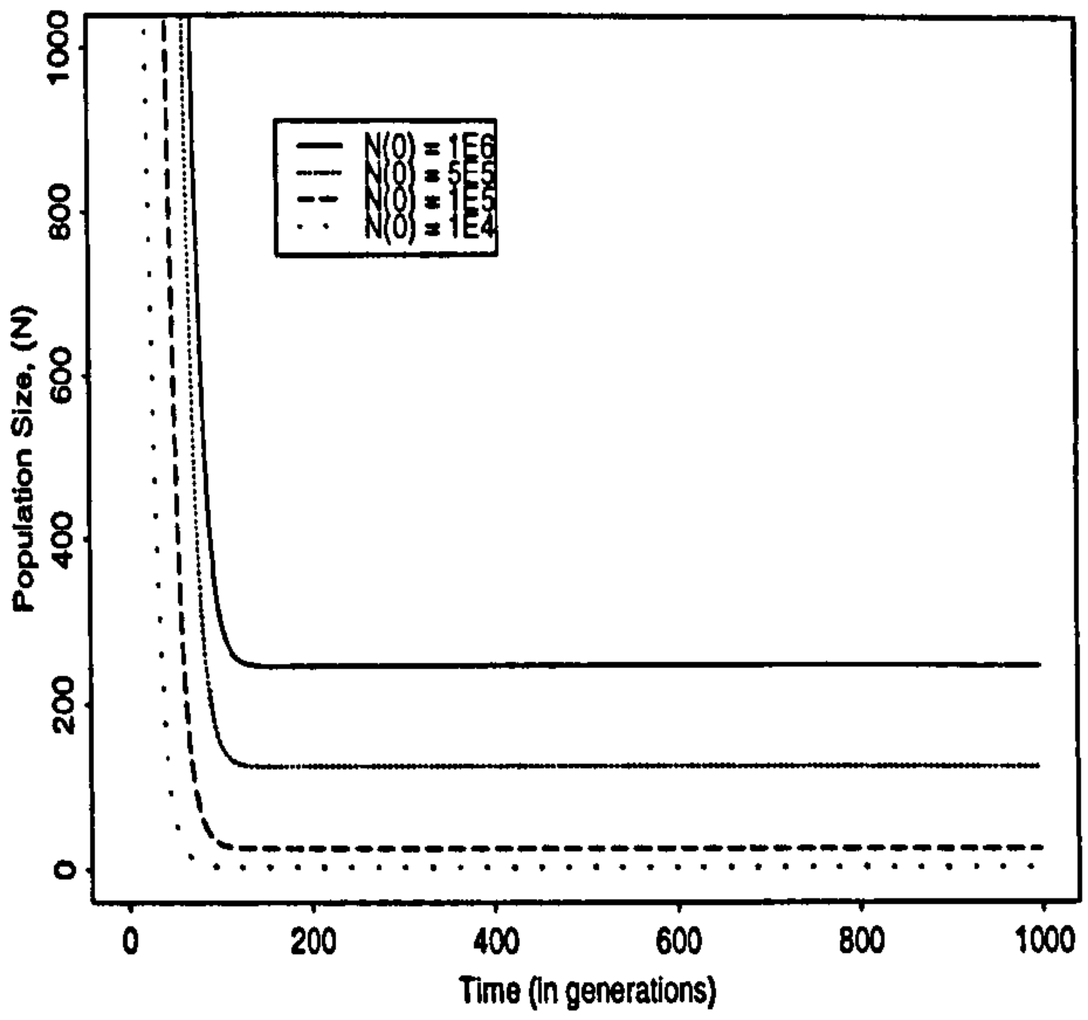

Figure 5.4: Trajectory of population sizes when $f\alpha = 1-(1-\alpha)\beta$ for different starting conditions.

5.6 Host-Pasture-Refugia Model (HPR Model)

Refugia are areas where parasites avoid exposure to drug treatment. For nematode populations, there are two forms of refugia. Those parasites that remain on pasture, uningested by a host, are said to be in refugia as they are avoiding exposure to the drug. Similarly those parasites ingested by a host that manage to avoid treatment by concealing themselves in areas of the abomasum inaccessible to the drug are also said to be in refugia. Refugia of the former kind has

already been modelled in the previous section where a fraction of the free-living population remain on pasture whilst the remainder are ingested by a host and are exposed to the drug.

Refugia of the latter kind is modelled here by assuming that a fixed proportion of the parasites ingested by the host are not exposed to the anthelmintic. That proportion is denoted by μ. It is assumed that those individuals entering refugia only do so for a single time period. This model is presented diagrammatically in Figure 5.5.

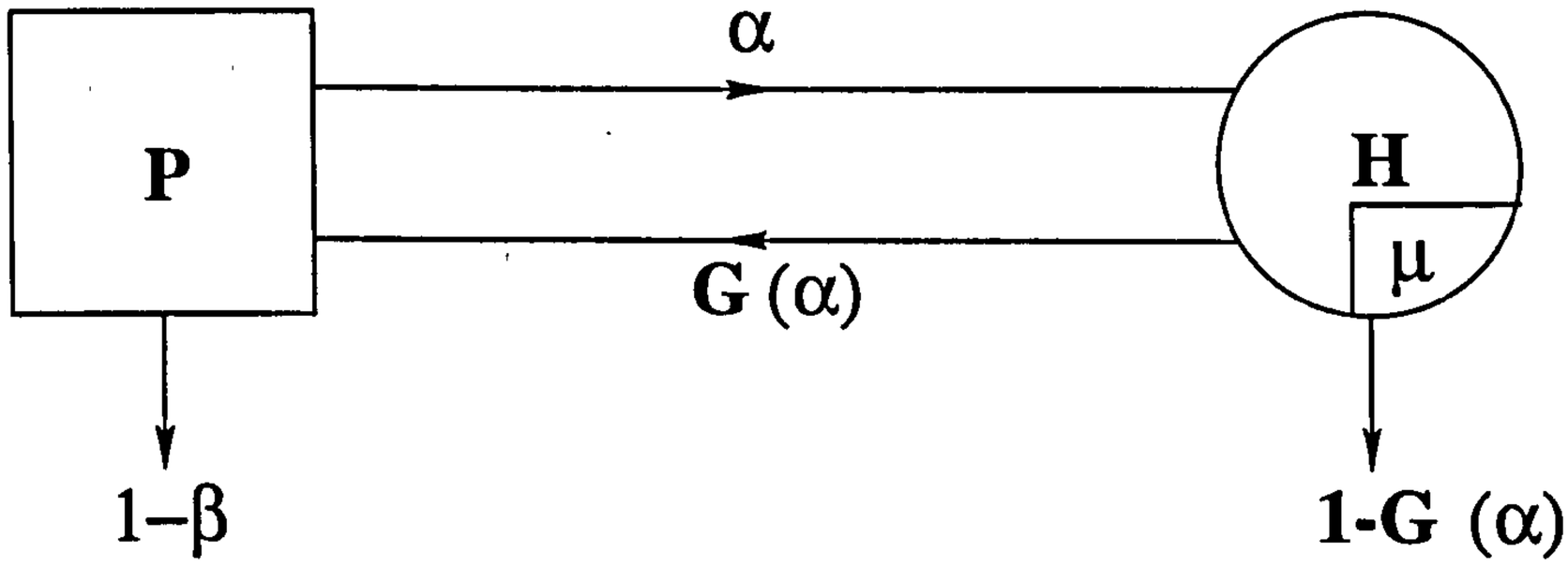

Figure 5.5: Flow Diagram for Host-Pasture-Refugia Model depicting the flow of parasites from the pasture to the host with a proportion of parasites entering refugia once inside the host.

If the R allele frequency in generation t is p_t, then, the proportion of individuals that undergo and survive treatment is now

$$\bar{w}_t(H)' = \alpha(1-\mu)\left[p_t^2 + 2p_t(1-p_t)(1-h)\right]$$

As before, α is the ingestion rate of the host, β, the survival of free-living parasites, and $1-h$, the proportion of heterozygotes that survive treatment.

It follows that the proportion of parasites that are returned to free existence by the host after one generation is

$$\bar{w}_t(H) = f\left[\bar{w}_t(H)' + \alpha\mu\right]$$

assuming that all those in refugia survive and reproduce successfully.

The proportion of individuals that survive mortality on pasture is again

$$\bar{w}_t(P) = (1-\alpha)\beta$$

The frequency of the R gene in the subsequent generation is now

$$p_{t+1} = \frac{f\alpha(1-\mu)[p_t^2 + p_t(1-p_t)(1-h)] + (f\alpha\mu + (1-\alpha)\beta)p_t}{\bar{w}_t(H) + \bar{w}_t(P)} \tag{5.24}$$

and the population size after one generation is

$$N_{t+1} = N_t[\bar{w}_t(P) + \bar{w}_t(H)] \tag{5.25}$$

5.7 Analysis of the HPR Model

5.7.1 Gene Frequency Equilibrium

The gene frequency under these conditions will be in equilibrium when

$$\Delta p_t = \frac{f\alpha(1-\mu)[p_t^2 + p_t(1-p_t)(1-h)] + (f\alpha\mu + (1-\alpha)\beta)[p_t]}{p_t(\bar{w}_t(H) + f\alpha\mu + \bar{w}_t(P))} - p_t = 0 \tag{5.26}$$

which simplifies to

$$f\alpha(1-\mu)(2h-1)p_t^3 + f\alpha(1-\mu)(2-3h)p_t^2 + f\alpha(1-\mu)(h-1)p_t = 0 \tag{5.27}$$

Dividing equation (5.27) throughout by $f\alpha(1-\mu)$ gives a cubic equation in p_t

$$p_t\left[(2h-1)p_t^2 + (2-3h)p_t - (1-h)\right] = 0 \tag{5.28}$$

with roots p_0^*, p_1^* and p_2^*, that represent the equilibrium gene frequencies. These are

$$p_0^* = 0$$

$$p_1^*, p_2^* = \frac{3h - 2 \pm \sqrt{(2-3h)^2 - 4(2h-1)(h-1)}}{(2h-1)} \tag{5.29}$$

From this it is clear that

$$p_1^* = 1 \tag{5.30}$$

irrespective of h, and

$$p_2^* = 0 \tag{5.31}$$

if and only if $h = 1$.

These are identical to the roots obtained for the HP model in the previous section. This suggests that the inclusion of refugia into the model has no effect on the equilibria. From equation (5.29), it is clear that only the parameter h has any effect on the equilibria.

Therefore, under these conditions, where a small fraction of the population may enter an area inaccessible to the drug, prior to treatment, ultimately, the population will become fully resistant, irrespective of the rate of ingestion (α), proportion in refugia (μ), survival rate (β) or fecundity (f), provided $p_0^* \neq 0$.

5.7.2 Population Size Equilibrium

An equilibrium population size, if it exists, can be calculated as follows

$$\Delta N_t = N_{t+1} - N_t = 0 \tag{5.32}$$

$$N_t(\bar{w}_t(P) + (\bar{w}_t(H) + \alpha\mu) f) - N_t = 0 \tag{5.33}$$

$$f\alpha(1-\mu)(2h-1)p_t^2 + f\alpha(1-\mu)(2-2h)p_t + \beta(1-\alpha) + f\alpha\mu - 1 = 0 \tag{5.34}$$

When the non-trivial equilibrium gene frequency, $p_1^* = 1$, has been reached, the population size will go into equilibrium only if $f\alpha = 1 - (1-\alpha)\beta$, representing a balance of birth and death terms.

5.7.3 A Neighbourhood Stability Analysis of the Fixed Points in the HPR Model

The stability of the steady state $p^* = 1$ in the HPR model is determined in a similar way to the stability of the fixed point in the HP model. The behaviour of states in some neighbourhood of $p^* = 1$ is investigated by perturbing the equilibrium by a small quantity, ρ_t, such that

$$p_t = p^* + \rho_t \tag{5.35}$$

The system will return to its fixed state, if

$$\lim_{t\to\infty} \rho_t = 0 \tag{5.36}$$

and the fixed point will be stable. As in Section 5.4.3, we consider

$$F_{HPR} = \frac{f\alpha\,(1-\mu)\,[p_t^2 + p_t\,(1-p_t)\,(1-h)] + (f\alpha\mu + (1-\alpha)\,\beta)\,p_t}{\bar{w}_t(H) + \bar{w}_t(P)} \tag{5.37}$$

The first derivative of equation (5.37) about p^*, according to equation (5.23) must be less than one if p^* is to be a stable point,

$$F'_{HPR} = \frac{f\alpha(1-\mu)(1-h) + f\alpha\mu + (1-\alpha)\beta}{f\alpha + (1-\alpha)\beta} \tag{5.38}$$

It follows that $F'_{HPR} < 1$ if and only if $\mu < 1$, indicating that provided 100% of parasites do not avoid exposure to the drug, $p^* = 1$ will be a (locally) stable fixed point. Selection for resistant strains could not occur if none of the parasites were exposed to the drug.

5.8 Numerical Solution of the HPR Model

A series of plots have been produced to illustrate the effects of varying the parameter values on the growth and evolution of resistance for the HPR model.

Similar patterns are observed in this model when the parameters are varied as were observed under the HP model, and are shown in Figures 5.6 (a), (b) and (c) for initial R gene frequency, p_0, ingestion rate α, and survival rate, β, respectively,

and Figure 5.7 (a) and (b) for fecundity, f and the proportion of heterozygotes killed by the drug, h

In this section we shall discuss the effect of refugia on the resistance status of a population.

Proportion of the ingested population entering refugia, μ

The same parameter values were used in the simulation of the HPR model that were used in the HP model (Table 5.1). However, unless otherwise stated, it is now assumed that 50% of individuals enter areas of refugia each generation. Figure 5.7(c) illustrates the effect of varying that proportion in a population.

From Figure 5.7(c), the rate at which the population converges to resistance is decreased when a proportion, ($\mu = 0.1$), of the ingested population go into refugia. When this proportion is increased to $\mu = 0.9$, meaning that 90% of the parasites ingested avoid contact with the anthelmintic and can go onto reproduce regardless of genotype, the result is still a fully resistant population. However, as can be seen from Figure 5.7(c), the evolution of resistance under these circumstances is much slower due to the sigmoidal shape of the growth curve compared to the other two curves, representing 50% and 10% in refugia, respectively.

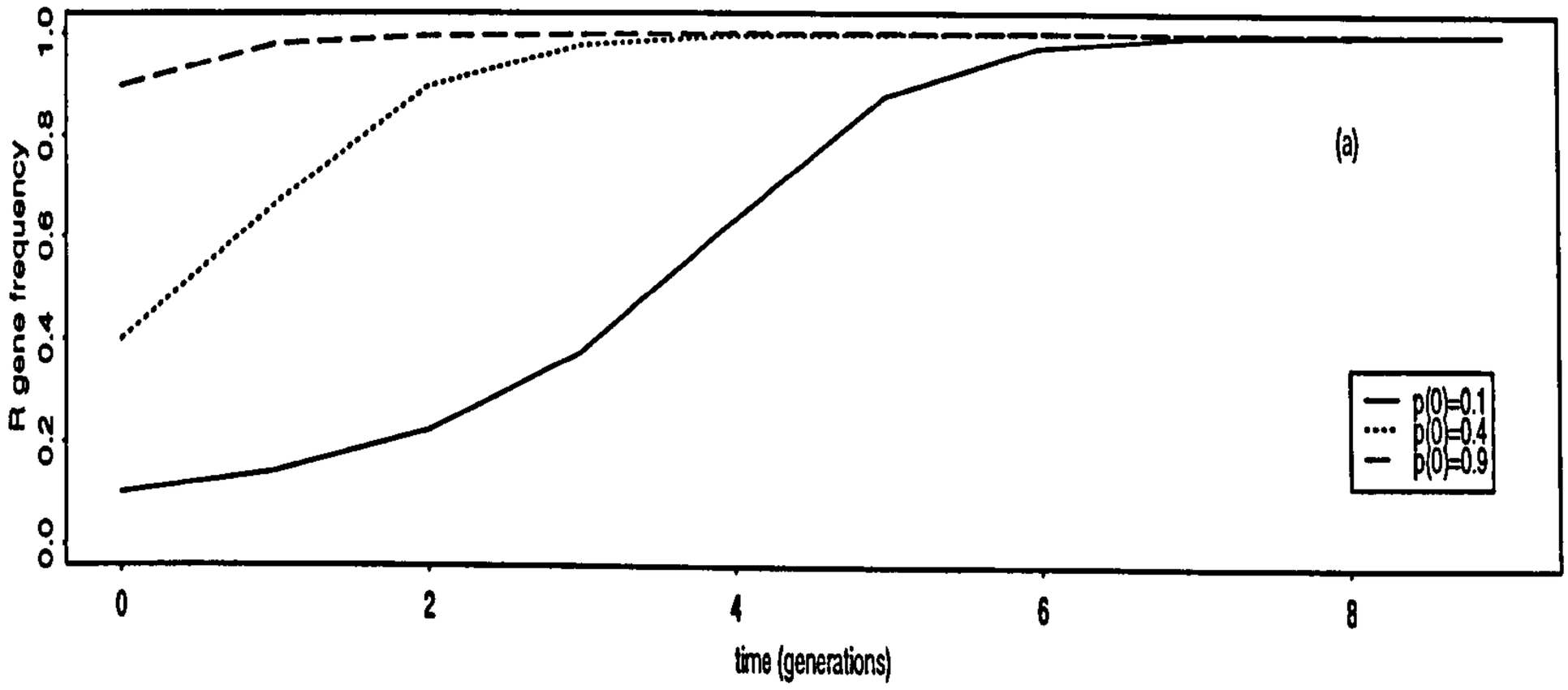

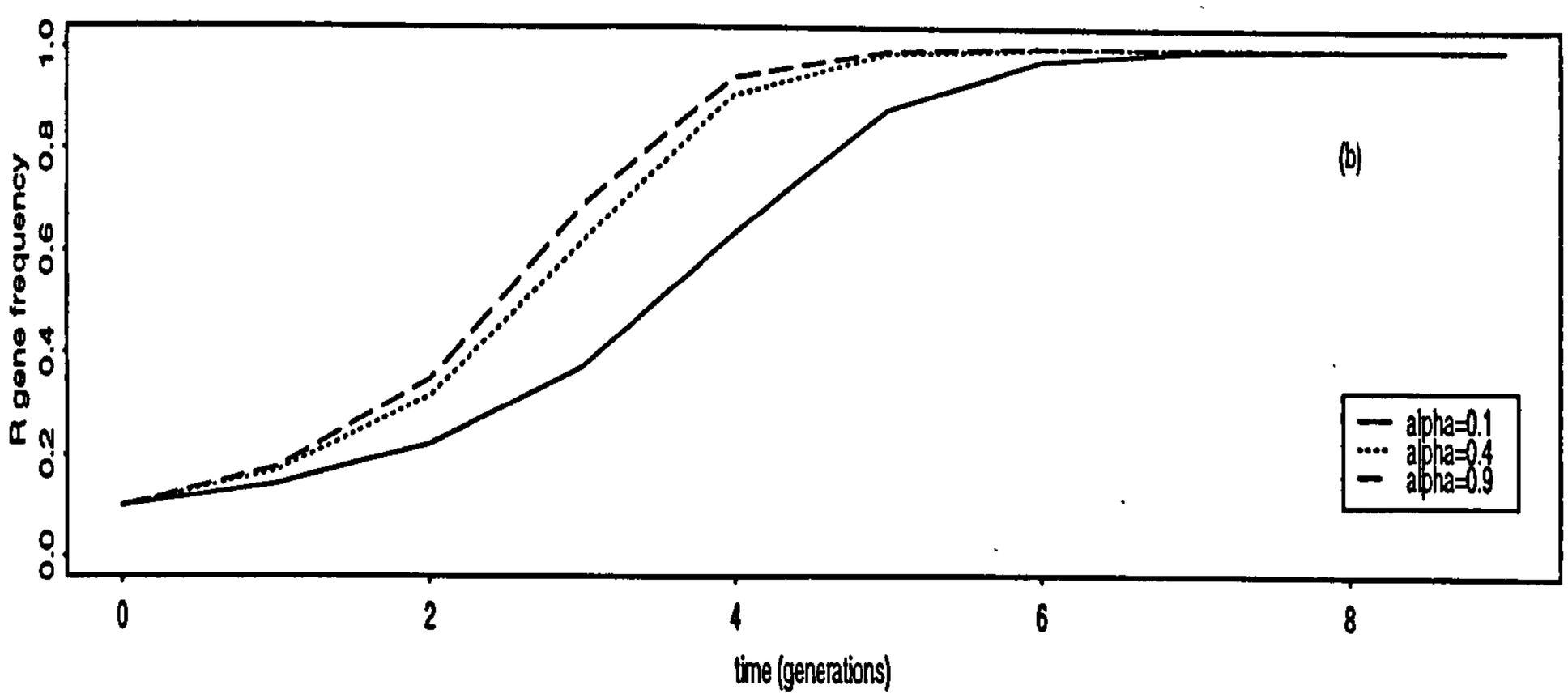

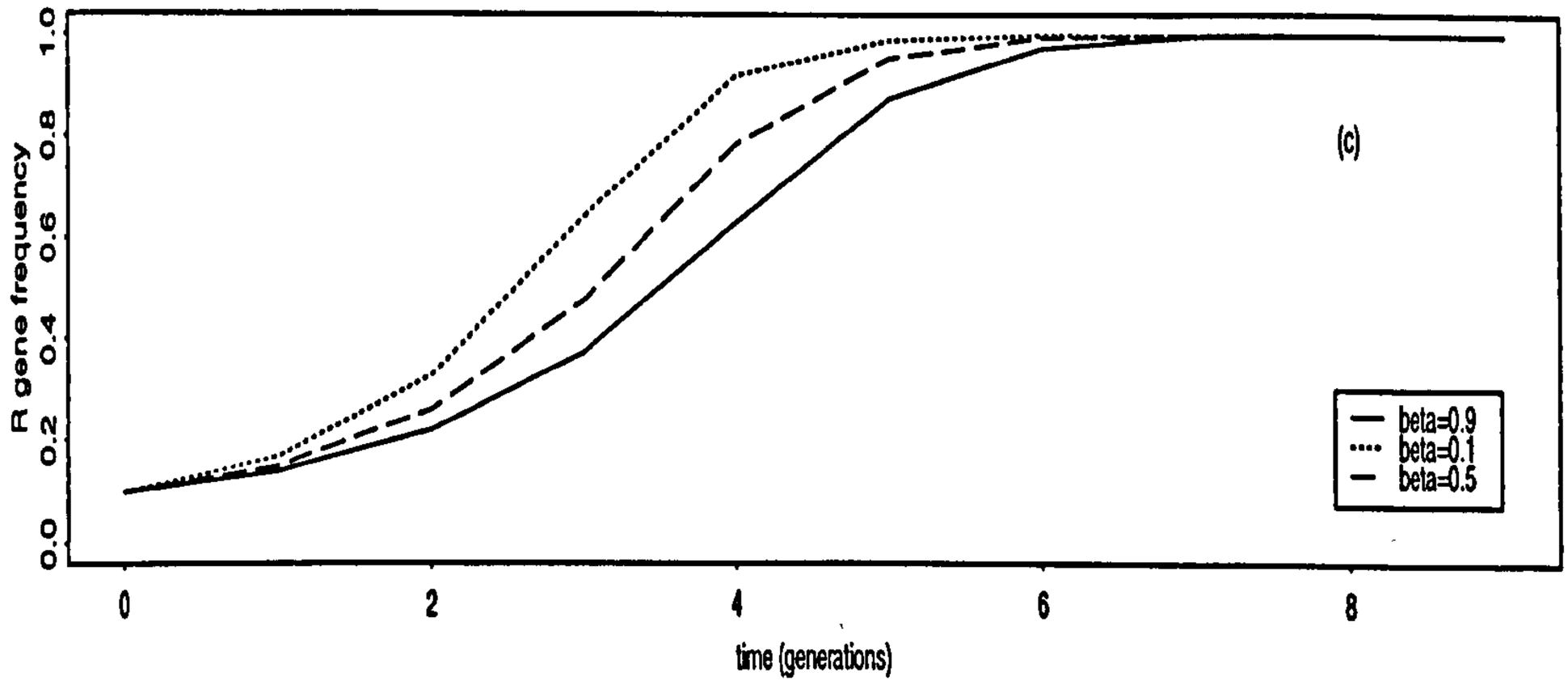

Figure 5.6: Changes in the frequency of the R gene over time for the HPR model when (a) the initial gene frequency, p_0, is varied;(b) the ingestion rate, α, is varied;(c) the survival rate, β, is varied.

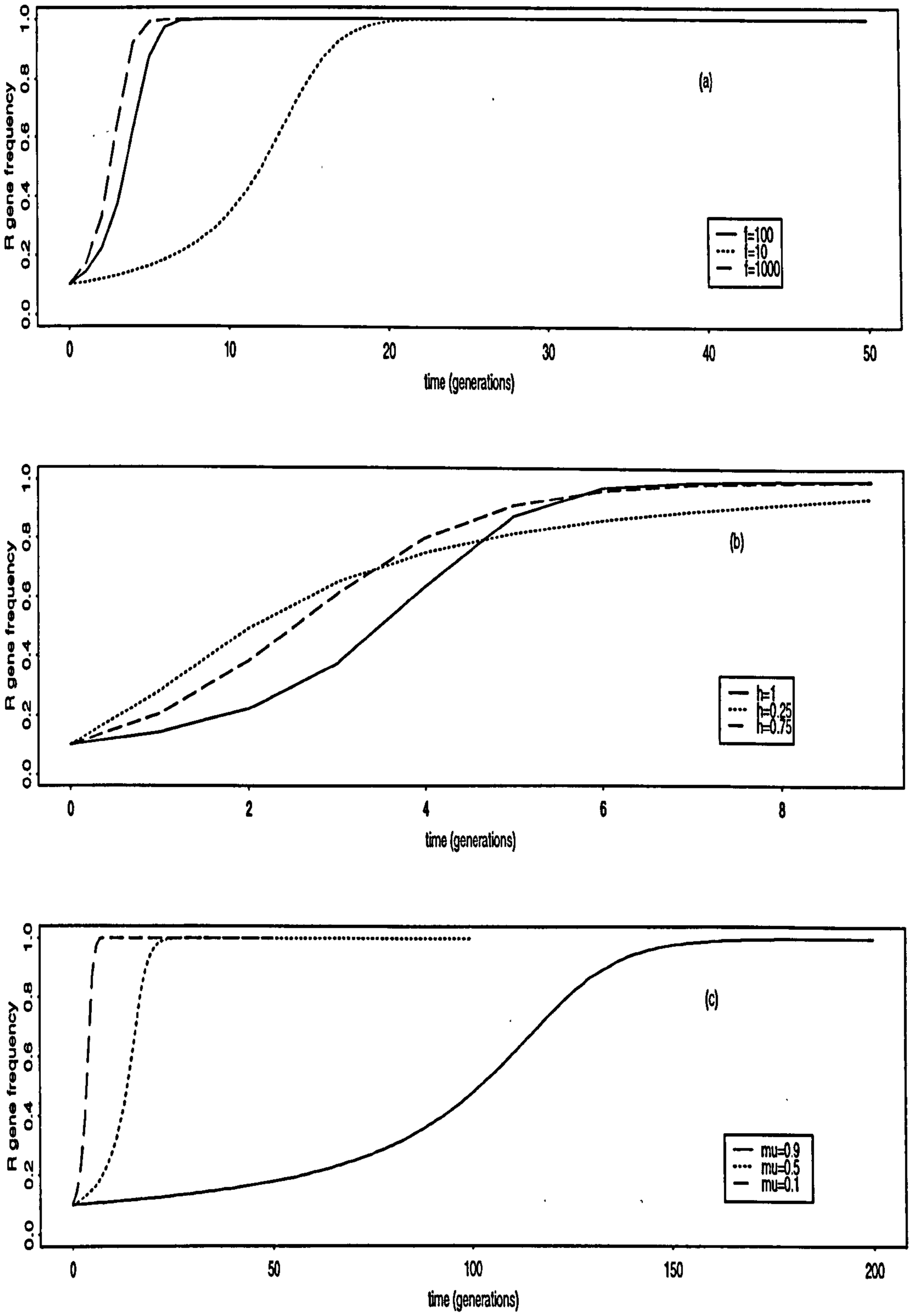

Figure 5.7: Changes in the frequency of the R gene over time for the HPR model when (a) the fecundity of female worms, f, is varied;(b) the proportion of heterozygotes killed by the drug, h, is varied;(c) the proportion of the ingested population in refugia, μ, is varied.

5.9 Exploring the Rate of Convergence to Resistance under the HP and the HPR Models

Analyses of the previous two models suggest that a fully resistant population will evolve provided no measures are taken to control the dissemination of resistance throughout the population. From the numerical simulations of the HP and HPR models, the rate at which a population converges to resistance varies considerably with changing parameter values.

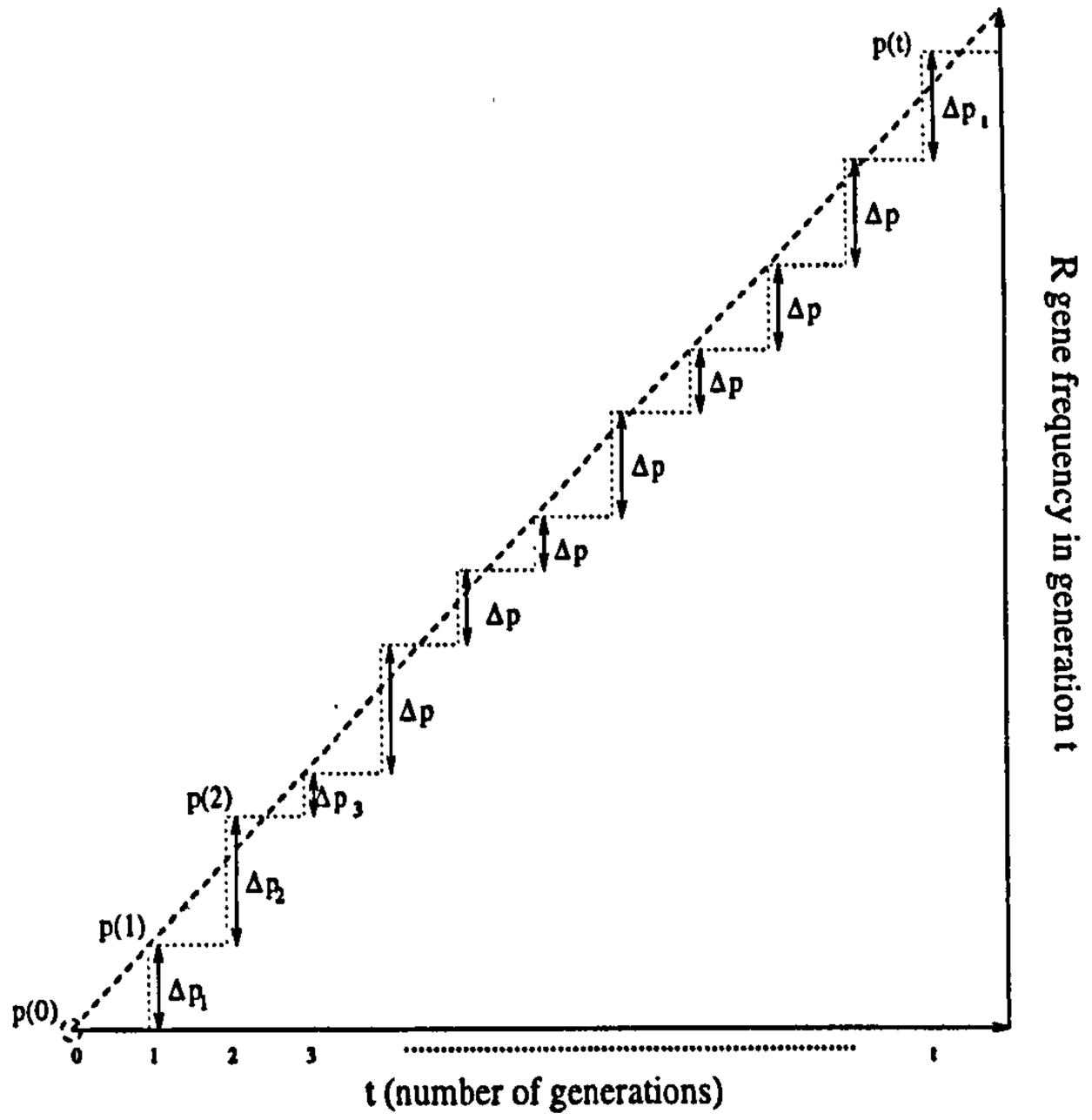

Figure 5.8: Representation of the change in gene frequency

Figure 5.8 shows the progress of anthelmintic resistance in a population with time. Geometrically, it is possible to determine how many time units it takes to reach a gene frequency of p_t from an initial gene frequency of p_0 by simply counting along the x-axis the appropriate number of time steps.

For example, in one time unit, the gene frequency changes by $\Delta p_i = p_{i+1} - p_i$. In two time units, the gene frequency changes by $\Delta p_i + \Delta p_{i+1}$. It follows that in t time units, the gene frequency will change by $\sum_{i=1}^{t} \Delta p_i$. So that after t time points, the new gene frequency will be

$$p_t = p_0 + \sum_{i=1}^{t} \Delta p_i$$

(5.39)

If we replace $\sum_{i=1}^{t} \Delta p_{ti}$ in equation (5.39) with some average value, $t\bar{\Delta}p_t$, then (5.39) becomes

$$p_t - p_0 = t\bar{\Delta}p_t \tag{5.40}$$

The quantity $\frac{p_t - p_0}{t}$ is the gradient of the slope in Figure 5.8 that begins at p_0 and ends at p_t. We can use the approximation

$$\frac{dp_t}{dt} \approx \bar{\Delta}p_t$$

For the HP model, the time t that it takes to reach a gene frequency of p_t from an initial value of p_0 is

$$\begin{aligned} \bar{\Delta}p_t &= p_{t+1} - p_t \\ &= \frac{f\alpha\left[(1-2h)p_t^3 + (3h-2)p_t^2 + (1-h)p_t\right]}{\bar{w}_t(H) + \bar{w}_t(P)} \end{aligned} \tag{5.41}$$

This can be approximated by

$$\frac{dp_t}{dt} \approx \frac{f\alpha\left[(1-2h)p_t^3 + (3h-2)p_t^2 + (1-h)p_t\right]}{\bar{w}_t(H) + \bar{w}_t(P)} \tag{5.42}$$

Similarly for the HPR model

$$\frac{dp_t}{dt} \approx \frac{f\alpha(1-\mu)\left[(1-2h)p_t^3 + (3h-2)p_t^2 + (1-h)p_t\right]}{\bar{w}_t(H) + \bar{w}_t(P) + f\alpha\mu} \tag{5.43}$$

For explanatory purposes, the complexity of both equations is reduced by assuming that $h = 1$, that is, the susceptible allele is fully dominant, and hence all heterozygotes are killed by the drug. And so for the HP model:

$$\frac{dp_t}{dt} \approx \frac{f\alpha p_t^2\left[1 - p_t\right]}{f\alpha p_t^2 + (1-\alpha)\,\beta} \tag{5.44}$$

and again for the HPR model

$$\frac{dp_t}{dt} \approx \frac{f\alpha(1-\mu)p_t^2[1-p_t]}{f\alpha(1-\mu)p_t^2 + f\alpha\mu + \beta(1-\alpha)} \tag{5.45}$$

Conveniently, equations (5.44) and (5.45) can be solved to give the time, t, in generations for the gene frequency to change from p_0 to p_t . The solution to equation (5.44) is

$$t_{HP} \approx \frac{(1-\alpha)\beta}{f\alpha}\left[ln\left[\frac{p_t}{p_0}\right] + ln\left[\frac{p_0-1}{p_t-1}\right] + \frac{1}{p_0} - \frac{1}{p_t}\right] + ln\left[\frac{1-p_0}{1-p_t}\right] \tag{5.46}$$

and for the HPR model , equation (5.45)

$$t_{HPR} \approx \frac{f\alpha\mu + (1-\alpha)\beta}{f\alpha(1-\mu)}\left[ln\left[\frac{p_t}{p_0}\right] + ln\left[\frac{p_0-1}{p_t-1}\right] + \frac{1}{p_0} - \frac{1}{p_t}\right] + ln\left[\frac{1-p_0}{1-p_t}\right] \tag{5.47}$$

Examination of the terms outside the brackets in equations (5.46) and (5.47) shows how each of the model parameters affect the time taken to reach significant levels of resistance. For both models, the higher the survivorship on pasture, β, the longer it will take for 100% resistance to evolve. This is because if more parasites survive on pasture, the ratio of free-living to parasitic stages will be higher than if the survival rate was lower on the pasture, and so the relative proportion of R genes will decrease as β is increased. The higher the ingestion rate α, the quicker resistance will evolve. Clearly this is because those individuals ingested by a host will undergo selection due to drug treatment whereas those remaining on pasture do not. For the HP model, increasing the fecundity leads to a reduction in the time until 100% resistance evolves. This effect is not the same in the HPR model, however when refugia is incorporated into the model.

A comparison can now be made between the analytical results and the results from the numerical simulation using ITERATOR(©STAMS). Table 5.2 gives the time taken for the gene frequency to reach a value of p_t from an initial value of p_0, using numerical simulation and the analytical equation derived above for both the HP and HPR models.

Table 5.2: Table of times to significant resistance derived analytically, equations (5.46) and (5.47), and by simulation in ITERATOR.

Model	p_0	p_t	ITERATOR	ANALYTICAL
HP	0.1	0.99997	201	202.8
HPR	0.1	0.99997	225	226.7
HP	0.4	0.99997	117	119.6
HPR	0.4	0.99997	130	133.5
HP	0.9	0.99997	80	82.3
HPR	0.9	0.99997	89	91.5

5.10 Discussion

The two models presented in this Chapter serve as the starting block for a series of models designed to investigate the evolution and control of drug resistance within a parasite population. We have assumed that

- changes to the population structure occur at discrete points in time, in this case, generations,
- all parasites on pasture are in the same life stage, irrespective of the time spent on the pasture,
- once ingested by a host the parasites become adults,
- treatment occurs post reproduction,
- mating occurs at random, therefore offspring are produced in Hardy-Weinberg equilibrium, (Strickberger, 1976),
- the ingestion, mortality and refugia rates are genotype independent, and
- the parasite-host system involves only a single host.

A continuous time model for the evolution of anthelmintic resistance in a typical nematode population was developed by Smith in 1990 to deal with the direct life

cycles of these parasites and overlapping generations. Unfortunately, no analytically tractable mechanism was provided in this model to determine changes in gene frequency after administration of treatment. As a result, the equations were solved numerically.

This made it impossible to derive general qualitative insights into how patterns of resistance might develop over time as any inferences that are made from numerical methods of solution usually cannot be extrapolated outwith the scope of the numerical solution.

Changes in the frequency of the resistance gene coupled with changes in the overall population size were modelled using a system of non-linear difference equations. Steady state gene frequencies and population sizes were obtained and the (local) stability of these fixed points determined. The HP and HPR models describe the dynamics of a typical nematode population undergoing selective drug therapy. Combined, they incorporate many of the important factors governing the speed of dissemination of resistance throughout a parasite population.

Results from the models indicate that provided the gene pool initially contains some R genes, that is, $p_0 > 0$, eventually the entire population will become resistant to the drug. This result holds irrespective of the values of the model parameters, α, β, μ, h or f.

This provides strong evidence that managing existing problems by simply altering the vital rates may slow down the evolution of resistance, but will not stop it altogether. Clearly interventionist measures must be employed if we are to totally suppress resistance in a population.

A stability analysis of the fixed points in the models revealed local stability of the equilibria.

The change in population size is represented here by a very simple equation. In this model, control of parasite numbers on pasture can only be achieved if the additions to the population, that is births, balance those that are removed from the population, once that population has become fully resistant. This would be a difficult control strategy to implement, as first, the population numbers would have to be low, and secondly to maintain the equilibrium strict control over births and deaths would have to be taken which would in practice be impossible. It is widely known that density dependent mechanisms act on the population to regulate numbers when parasite levels are high. Recently, host issues have

been addressed by Roberts (1991, 1992), however, examining the effect on the evolution of anthelmintic resistance within a heterogeneous host population has yet to be addressed.

Time To Significant Resistance

The analytical expression derived to determine the time taken for the gene frequency to reach p_t from an initial value of p_0 for both the HP and HPR models appears to be a good approximation to the real time generated from the simulation model, differing by at most two generations. When a fraction of the ingested population enter refugia in the HPR model, the equilibrium behaviour of the entire population does not change from that in the HP model. However, the time taken for the population to converge to the steady state gene frequency increases by a factor

$$\frac{\mu}{1-\mu}\left[1+\frac{(1-\alpha)\beta}{f\alpha}\right]$$

From this, we can explore the effect of biologically meaningful parameters on the time to 100% resistance and through this make recommendations on the optimal methods of impeding the dissemination of resistance.

The time to significant resistance is minimised by reducing mortality on pasture, $1-\beta$, slowing down the rate of host ingestion of parasites, α, and increasing the proportion of individuals entering refugia in any one generation, μ.

We have shown in this Chapter that when no measures are taken to control resistance, even when initial resistance levels in a population are very low, the entire population will become resistant in time. We have provided a means of determining how long under present circumstances it would take for resistance to evolve in a population and have examined ways in which the dissemination of resistance could be slowed down whilst research is continuing on alternative methods of resistance control.

Chapter 6

The Effect of Immigration on the Evolution of Anthelmintic Resistance In a Parasite Population

6.1 Introduction

The introduction of a new host onto pasture brings with it the danger of inadvertently introducing resistant strains of parasite into the established worm population. In this chapter we examine the effect on a nematode population when an influx of migrants with RR genotypes enter the pasture.

6.2 The Resistant Immigrants Model (RIM Model)

Synthesis of this model proceeds from that of the HP and HPR models in the previous Chapter. Of the proportion of the population ingested by a host, α, a proportion, μ go into refugia and avoid exposure to the anthelmintic. Those not in refugia are treated with an anthelmintic and survive according to the dose of drug administered and the genetic composition of the parasite population. Of the population remaining on pasture, a proportion $1-\beta$, die from natural mortality. In addition, in each generation, it is assumed that a number, r, of RR genotypes are introduced as migrants onto pasture. A diagrammatic representation of the flow of parasites to and from the pasture is given in Figure 6.1.

If the frequency of the R allele in generation t is p_t, and all susceptible homozy-

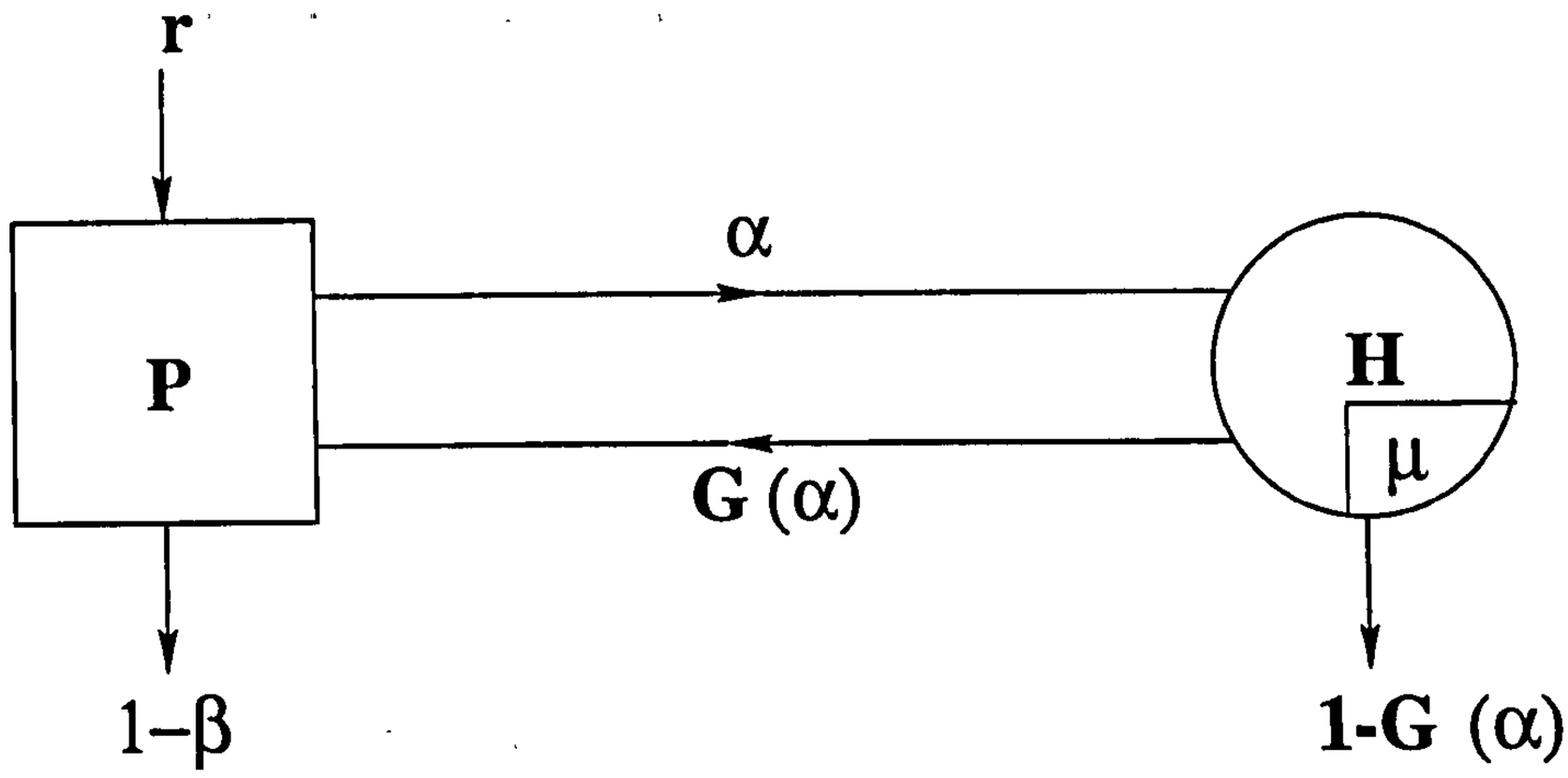

Figure 6.1: Flow diagram of Resistant Immigrants Model depicting the flow of parasites from pasture to host undergoing treatment with an anthelmintic drug, with a constant input of r RR immigrants being introduced to the pasture each generation.

gotes and a proportion h of the heterozygotes are killed by the anthelmintic and mating between those remaining is at random, it follows that the proportion of individuals that are expelled onto the pasture by the host after one generation will be

$$\bar{w}_t(H) = f\alpha(1-\mu)\left[p_t^2 + 2p_t(1-p_t)(1-h)\right] + f\alpha\mu \tag{6.1}$$

Again, the proportion of individuals that survive mortality on the pasture, assuming that the mortality rate is the same for each genotype, is

$$\bar{w}_t(P) = (1-\alpha)\,\beta \tag{6.2}$$

If the number of resistant genotypes entering the population as migrants in a single generation is r, then the frequency of the R gene in the subsequent generation will be

$$p_{t+1} = \frac{N_t\left[f\alpha(1-\mu)\left[p_t^2 + p_t(1-p_t)(1-h)\right] + \left[f\alpha\mu + (1-\alpha)\beta\right]p_t\right] + r}{N_t\left[\bar{w}_t(H) + \bar{w}_t(P)\right] + r} \tag{6.3}$$

Changes in population size over time are described by the following simple equation

$$N_{t+1} = N_t\left[\bar{w}_t(H) + \bar{w}_t(P)\right] + r \tag{6.4}$$

where the population size in generation t is N_t.

6.3 Analysis of the RIM Model

As with the HP and HPR models in the previous chapter, the existence of non-linear components within the model leads to an analysis of the stability of the system in the vicinity of the equilibrium points.

6.3.1 Gene Frequency Equilibrium

A gene frequency equilibrium will be reached when $\Delta p = p_{t+1} - p_t = 0$

$$\frac{N_t\left[f\alpha(1-\mu)\left[p_t^2 + p_t(1-p_t)(1-h)\right] + \left[f\alpha\mu + (1-\alpha)\beta\right]p_t\right] + r}{N_t\left[\bar{w}_t(H) + \bar{w}_t(P)\right] + r} - p_t = 0 \tag{6.5}$$

When simplified, the following cubic in p_t is obtained

$$\begin{aligned} &[N_t f\alpha(1-\mu)(2h-1)] \quad p_t^3 \\ +&[N_t f\alpha(1-\mu)(2-3h)] \quad p_t^2 \\ +&[r - N_t f\alpha(1-\mu)(1-h)] \quad p_t \quad -r = 0 \end{aligned} \tag{6.6}$$

The roots of this cubic will yield three equilibrium gene frequencies.

Cardano's Formula (Abramowitz and Stegun, 1970) gives the solution of the general normalised cubic equation

$$x^3 + bx^2 + cx + d = 0 \tag{6.7}$$

to be

$$\begin{aligned} x_1 &= -\frac{b}{3} + \gamma - \frac{p}{3\gamma} \\ x_2 &= -\frac{b}{3} + \omega\gamma + \frac{\omega^2 p}{3\gamma} \\ x_3 &= -\frac{b}{3} + \omega^2\gamma + \frac{\omega p}{3\gamma} \end{aligned} \tag{6.8}$$

where ω is either root of the equation

$$x^2 + x + 1 = 0$$

and γ is any value of

$$\left(-\frac{q}{2} \pm \sqrt{\frac{q^2}{4} + \frac{p^3}{27}}\right)^{\frac{1}{3}} \tag{6.9}$$

where

$$q = \frac{2b^3}{27} - \frac{bc}{3} + d$$

and

$$p = c - \frac{b^2}{3}$$

The discriminant, Δ^2, of this cubic equation is

$$\Delta^2 = \frac{q^2}{4} + \frac{p^3}{27} \tag{6.10}$$

If

- $\Delta^2 < 0$ there exists three real roots,
- $\Delta^2 > 0$ exactly one real root exists, and
- $\Delta^2 = 0$ the roots are repeated.

The three roots, p_0^*, p_1^* and p_2^* are determined to be

$$p_0^* = 1$$

and

$$p_1^*, p_2^* = \frac{Nf\alpha(1-\mu)(h-1) \pm \sqrt{(Nf\alpha(1-\mu)(h-1))^2 - 4rNf\alpha(1-\mu)(2h-1)}}{2Nf\alpha(1-\mu)(2h-1)} \tag{6.11}$$

The gene frequencies, p_0^*, p_1^* and p_2^*, by definition must lie between zero and one. p_0^* satisfies this condition. The remaining two roots of equation (6.6) must be examined to determine their validity. For $0 \leq p_1^*, p_2^* \leq 1$,

$$0 \leq \frac{Nf\alpha(1-\mu)(h-1) \pm \sqrt{(Nf\alpha(1-\mu)(h-1))^2 - 4rNf\alpha(1-\mu)(2h-1)}}{2Nf\alpha(1-\mu)(2h-1)} \leq 1 \tag{6.12}$$

For both roots to be positive (that is, ≥ 0), both the numerator and denominator in equation (6.11) must be of equal sign. The denominator in (6.11) is positive only if $h > \frac{1}{2}$, however, the numerator is positive only if $h < \frac{1}{2}$, (assuming that $r, N, f > 0$ and $0 \leq \alpha, \mu, h \leq 1$). Under these conditions, the numerator and denominator will never be of equal sign and so the roots, p_1^* and p_2^* will never be positive. A similar case exists when both the numerator and denominator are negative. This means that the only valid root of equation (6.6) is $p_0^* = 1$.

In populations described by the RIM model, where immigrants introduced onto pasture have the RR genotype, intensive drug treatment will result in 100% resistance, provided $p_0 \neq 0$ and $r > 0$.

6.3.2 Population Size Equilibrium

The population size will reach a steady state when $\Delta N_t = N_{t+1} - N_t = 0$, that is, where

$$N_{t+1} = N_t [\bar{w}_t(H) + \bar{w}_t(P)] + r \tag{6.13}$$

which results in the following quadratic in p_t

$$\begin{aligned} [f\alpha(1-\mu)(2h-1)] \quad & p_t^2 \\ +[f\alpha(1-\mu)(2-2h)] \quad & p_t \\ +\left[f\alpha\mu + (1-\alpha)\beta - 1 + \frac{r}{N_t}\right] \quad & = 0 \end{aligned} \tag{6.14}$$

In the previous section, it was shown that an equilibrium R gene frequency of one would result in populations described by the RIM model. On substitution of $\hat{p}_1 = 1$ into equation (6.14), it is clear that the population size will equilibrate at

$$N^* = \frac{r}{1 - (f\alpha + (1-\alpha)\beta)} \tag{6.15}$$

This represents a balance between additions to the population and deaths out of it due to natural mortality. No individuals are killed by the drug as the population consists of RR individuals only.

The value at which the population size equilibrates, given by equation (6.15), must be positive, that is, $N^* > 0$. It is assumed that $r > 0$ and so the denominator $1 - (f\alpha + (1-\alpha)\beta) > 0$, therefore, $f \leq \frac{1-(1-\alpha)\beta}{\alpha}$. Effectively, this means that additions to the population, $f\alpha$, must be less than or equal to the number leaving the population due to mortality, $1 - (1-\alpha)\beta$ so that the introduction of new individuals can still occur.

6.3.3 A Neighbourhood Stability Analysis of the Fixed Points in the RIM Model

At equilibrium, a population described by the RIM model will be fully resistant with $p^* = 1$, and will have reached a steady state population size of $N^* = \frac{r}{1-(f\alpha+(1-\alpha)\beta)}$, provided $p_0 > 0$.

The stability properties of the fixed points,

$$\bar{x} = f(\bar{x}, \bar{y}),$$

$$\bar{y} = g(\bar{x}, \bar{y})$$

of a coupled difference equation,

$$x_{k+1} = f(x_k, y_k)$$

$$y_{k+1} = g(x_k, y_k)$$

are determined by the partial derivatives of the functions

$$f(x_k, y_k)$$

and

$$g(x_k, y_k)$$

evaluated at the fixed points, (Mickens, 1990). For the RIM model,

$$\begin{aligned} p^* &= f(p^*, N^*) \\ N^* &= g(p^*, N^*) \end{aligned} \tag{6.16}$$

are solutions to the coupled difference equation

$$f = p_{t+1} = \frac{N_t\left[f\alpha(1-\mu)\left[p_t^2 + p_t(1-p_t)(1-h)\right] + \left[f\alpha\mu + (1-\alpha)\beta\right]p_t\right] + r}{N_t\left[\bar{w}_t(H) + \bar{w}_t(P)\right] + r} \tag{6.17}$$

and

$$g = N_{t+1} \quad = \quad N_t\,[\bar{w}_t(H) + \bar{w}_t(P)] + r \tag{6.18}$$

The behaviour of the solution in a neighbourhood of the fixed points, $(\frac{r}{1-(f\alpha+(1-\alpha)\beta)}, 1)$ is investigated here.

The stability of the fixed points requires that

$$\begin{aligned} \lim_{t\to\infty} \rho_t &= 0 \\ \lim_{t\to\infty} \eta_t &= 0 \end{aligned} \tag{6.19}$$

where

$$p_t = p^* + \rho_t \tag{6.20}$$

and

$$N_t = N^* + \eta_t \tag{6.21}$$

assuming that ρ_t and η_t represent infinitesimal perturbations away from the equilibrium.

Substituting equations (6.20) and (6.21) into equation (6.17) and linearising the resultant equation, discarding all second order terms and higher, gives

$$\begin{aligned} \rho_{t+1} &= A_{11}\rho_t + A_{12}\eta_t \\ \eta_{t+1} &= A_{21}\rho_t + A_{22}\eta_t \end{aligned} \tag{6.22}$$

where

$$\begin{aligned} A_{11} &= \frac{\partial f}{\partial p}\Big|_{p=p^*;N=N^*} \\ A_{12} &= \frac{\partial f}{\partial N}\Big|_{p=p^*;N=N^*} \\ A_{21} &= \frac{\partial g}{\partial p}\Big|_{p=p^*;N=N^*} \\ A_{22} &= \frac{\partial g}{\partial N}\Big|_{p=p^*;N=N^*} \end{aligned} \tag{6.23}$$

The characteristic equation that is formed on substitution of the second equation in equation (6.22) into the first is

$$m^2 - \phi m + \gamma = 0 \tag{6.24}$$

where $\phi = A_{11} + A_{22}$ and $\gamma = A_{11}A_{22} - A_{12}A_{21}$.

Since

$$|m_{1,2}| = \frac{\phi \pm \sqrt{(\phi^2 - 4\gamma)}}{2} < 1 \tag{6.25}$$

$$1 + \gamma > \phi \tag{6.26}$$

Because $\gamma = m1.m2$ and $|m_{1,2}| < 1$, it follows that

$$\phi < 1 + \gamma < 2 \tag{6.27}$$

Equation (6.27) defines the condition for stability.

For the RIM model

$$\begin{aligned} A_{11} &= f\alpha(1 - h(1-\mu)) + (1-\alpha)\beta \\ A_{12} &= 0 \\ A_{21} &= \frac{2rf\alpha(1-\mu)h}{1 - (f\alpha + (1-\alpha)\beta)} \\ A_{22} &= f\alpha + (1-\alpha)\beta \end{aligned} \tag{6.28}$$

Hence

$$\phi = f\alpha(1 - h(1-\mu)) + (1-\alpha)\beta + f\alpha + (1-\alpha)\beta \tag{6.29}$$

and

$$\gamma = (f\alpha(1 - h(1-\mu)) + (1-\alpha)\beta)(f\alpha + (1-\alpha)\beta) \tag{6.30}$$

The following two subsections present conditions that satisfy the stability criteria in equation (6.27).

Condition 1: $1 + \gamma < 2$

This condition is satisfied if

$$[f\alpha(1 - h(1-\mu)) + (1-\alpha)\beta]\,[f\alpha + (1-\alpha)\beta] + 1 < 2 \tag{6.31}$$

Equation (6.31) is a quadratic equation in f, the fecundity of female parasites. Note that the coefficient of f^2, $1-h(1-\mu)$, in equation (6.31) is positive. Therefore, provided the fecundity lies between the roots of

$$[f\alpha(1-h(1-\mu))+(1-\alpha)\beta]\,[f\alpha+(1-\alpha)\beta]-1=0 \tag{6.32}$$

condition 1 will be satisfied.

Condition 2: $1+\gamma > |\phi|$

This condition is satisfied if

$$(1+\gamma)^2 > \phi^2 \tag{6.33}$$

which, after some simple algebra results in the same quadratic as in equation (6.32) with identical conditions for stability, that is, provided f lies between the roots of

$$[f\alpha(1-h(1-\mu))+(1-\alpha)\beta]\,[f\alpha+(1-\alpha)\beta]-1=0 \tag{6.34}$$

the condition that $(1+\gamma)^2 > \phi^2$ is satisfied.

Provided that the condition imposed on f in order that the population size equilibrium is valid, that is, $f \leq \frac{1-(1-\alpha)\beta}{\alpha}$, has a common interval with the condition for local stability, see equations (6.32) and (6.34), the equilibrium point $(\frac{r}{1-(f\alpha+(1-\alpha)*\beta)}, 1)$ will be at least locally stable.

Global Stability

Examining the trajectory plane of population size with R gene frequency in Figure 6.2, there is some evidence that this equilibrium point may be globally stable. A population originating in any valid region of the $N-p$ plane, is attracted to the equilibrium point, $(\frac{r}{1-(f\alpha+(1-\alpha)*\beta)}, 1)$, provided the fecundity, f is within the regions defined by equations (6.32) and (6.34).

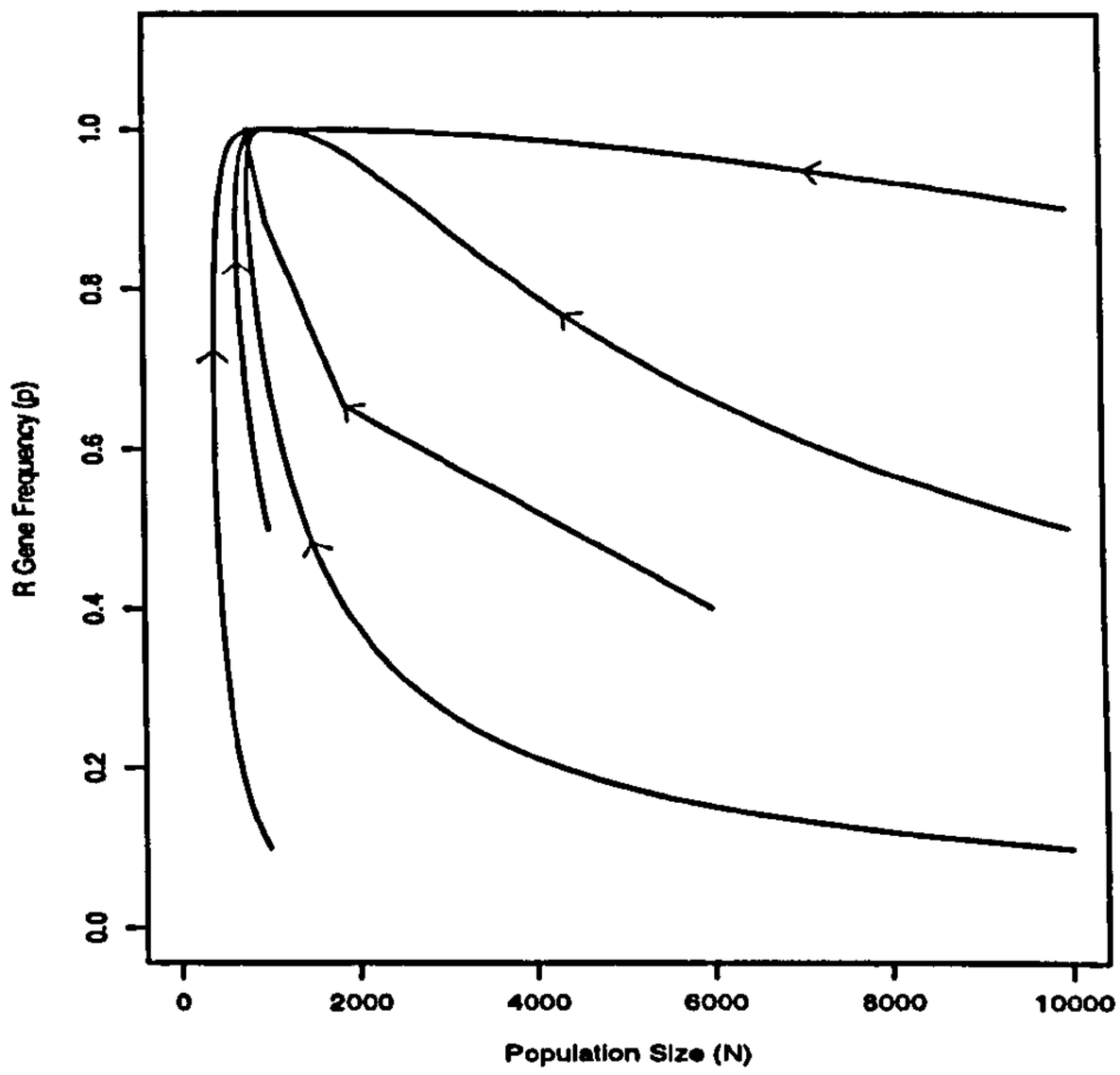

Figure 6.2: Trajectory of R gene frequency (p), and population size, (N), from an initial population size, N_0 and R gene frequency, p_0 under circumstances where (N^*, p^*) is a stable point.

Theoretically, a fixed point or set of fixed points is globally stable if a function, called a Lyapunov function, $L(N_1, N_2)$, exists such that

1. $L(N_1^*, N_2^*) = 0$;
2. $L(N_1, N_2) > 0$ for all $(N_1, N_2) \neq (N_1^*, N_2^*)$;
3. $\frac{dL}{dt} \leq 0$ with equality only if $(N_1, N_2) = (N_1^*, N_2^*)$.

There is no available method for choosing an appropriate Lyapunov function, which restricts the use of this technique in determining global stability. In addition, it is argued that even when a Lyapunov function is obtained, biological insights from it are often obscured (Renshaw, 1993).

6.4 The Dynamics of a Nematode Population Described by the RIM Model

The RIM model was simulated over time using a computer program written in the Pascal programming language, under a range of different conditions to provide an insight of the transient as well as the long term behaviour of this particular system. Each of the model parameters was varied one at a time with all others remaining constant and the behaviour of the population over time under these different conditions is shown in Figures 6.3 - 6.14.

6.4.1 Results

From the previous sections, it was determined analytically that irrespective of parameter values, every individual within the modelled population will have RR genotype after a period of time (which is determined by the parameter values). However, certain conditions must hold before the population size equilibrates. Figures 6.3 - 6.14, illustrate these results for the various different parameter sets. The first plot in each pair illustrates the change in gene frequency over time, the second, the change in population size over time.

The parameter estimates have been chosen to illustrate the behaviour of the RIM model. The numeric values reflect the range of possible values that each parameter could take.

Initial Gene Frequency, p_0

From Figure 6.3, it is clear that varying the initial R gene frequency from 0.1 to 0.5 to 0.9 alters the rate at which the population converges to resistance. The time to full resistance decreases as the initial gene frequency is increased.

Host Ingestion Rate, α

Figure 6.5 shows that by increasing the host ingestion rate, α, a fully resistant population will develop in a shorter time, as a higher proportion of the population are undergoing selective drug treatment. The ingestion rate α, influences the value at which the population size, N, equilibrates. It therefore also influences the fecundity threshold; below which a population size equilibrium value exists;

above which, the population size grows unconstrained. It follows that when α is changed, f, the fecundity threshold changes, and hence N^* changes accordingly. This explains why for different values of α in Figure 6.6, the population size converges to different equilibria.

Mortality Rate, $1-\beta$

Similarly, an increasing mortality rate, $1-\beta$, on pasture leads to a fully resistant population in a shorter time (Figure 6.7). Again, the value for β influences the fecundity threshold and hence the equilibrium population size, N^*. When the mortality rate is high, that is, β is low, a higher population size equilibrium value is reached compared with high values of β meaning low mortality rates. This is clearly demonstrated in Figure 6.8.

The Proportion of heterozygotes killed by the drug, h

Recall that when the initial R gene frequency is low, the majority of the R genes are to be found in the heterozygotes. Growth of the R gene frequency is more rapid when h is low as fewer R genes are being destroyed by the drug. However, as the R gene frequency exceeds a certain level, the majority of the R genes are now to be found in homozygotes, which means that the majority of S genes are to be found in the heterozygotes and therefore a high h value will lead to the S genes being killed off faster than a low h value. This results in the R gene frequency growing faster after a certain level under a high h value rather than a low h value as is evident in Figure 6.9. The population size equilibrium is unchanged by changing h, however the time taken to reach equilibrium is affected by h.

Number of immigrants, r

Figures 6.11 and 6.12 demonstrate the effect that the inward migration of resistant genotypes to the population will have on the rate at which the population converges to resistance and a steady state population size. As the number of immigrants increases, the time until a fully resistant population develops decreases. From Figure 6.12, the value at which the population equilibrates, N^*, is directly proportional to the migration rate.

Proportion in refugia, μ

Finally, Figure 6.13 illustrates the effect that varying the proportion of the ingested population that go into refugia will have on the evolution of anthelmintic resistance. The higher the proportion of parasites that go into refugia, the longer it will take for a fully resistant population to evolve. The population size converges to the same equilibrium, (see Figure 6.14), for all possible values of μ, the approach to this equilibrium is markedly different for values of μ less than $\frac{1}{2}$ than for values of μ greater than $\frac{1}{2}$.

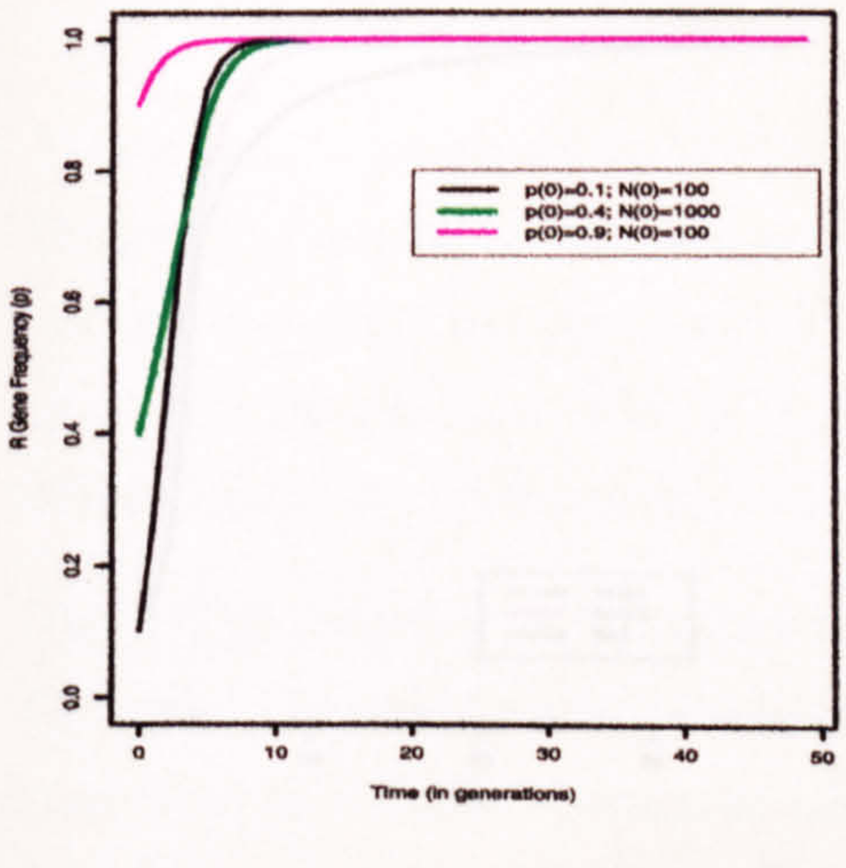

Figure 6.3: Trajectory of gene frequency altering initial conditions.

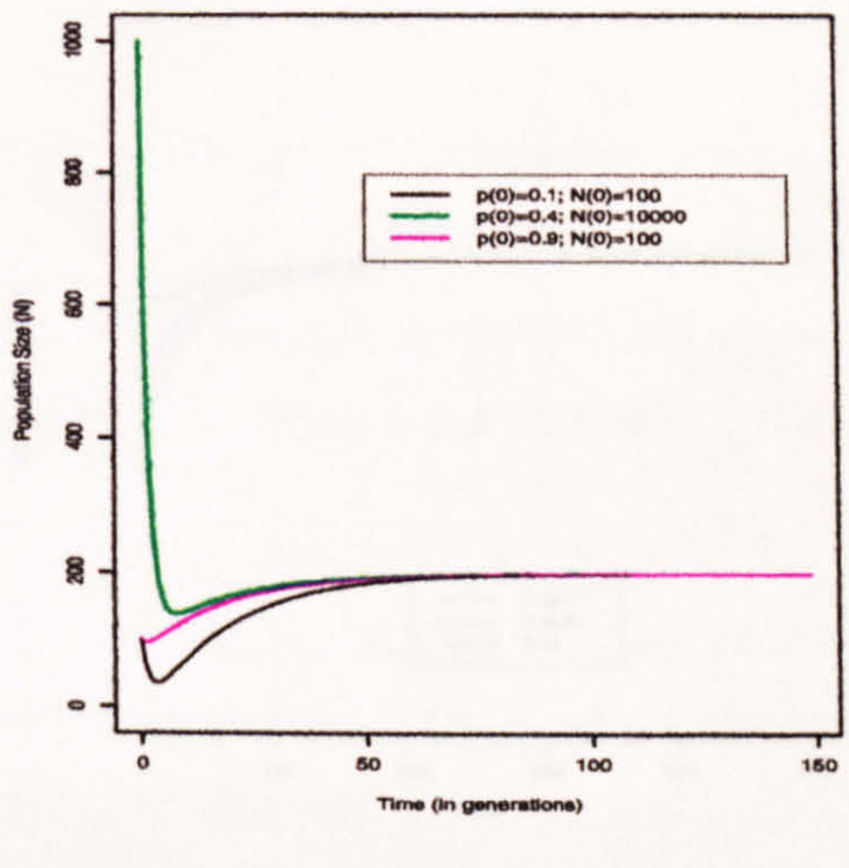

Figure 6.4: Trajectory of population size altering initial conditions.

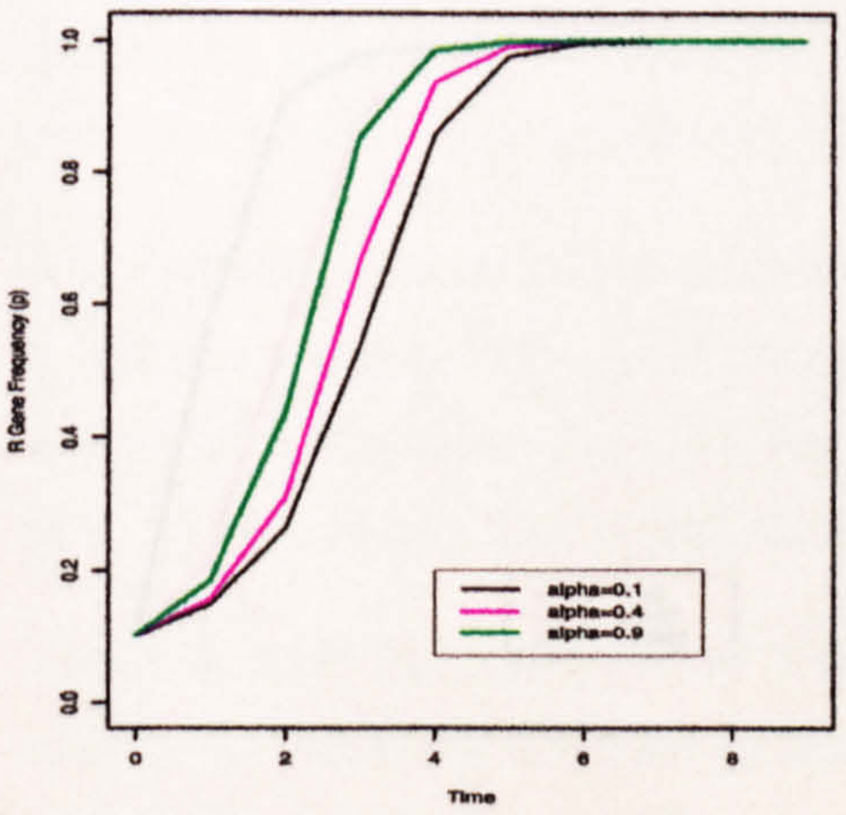

Figure 6.5: Trajectory of gene frequency altering the ingestion rate.

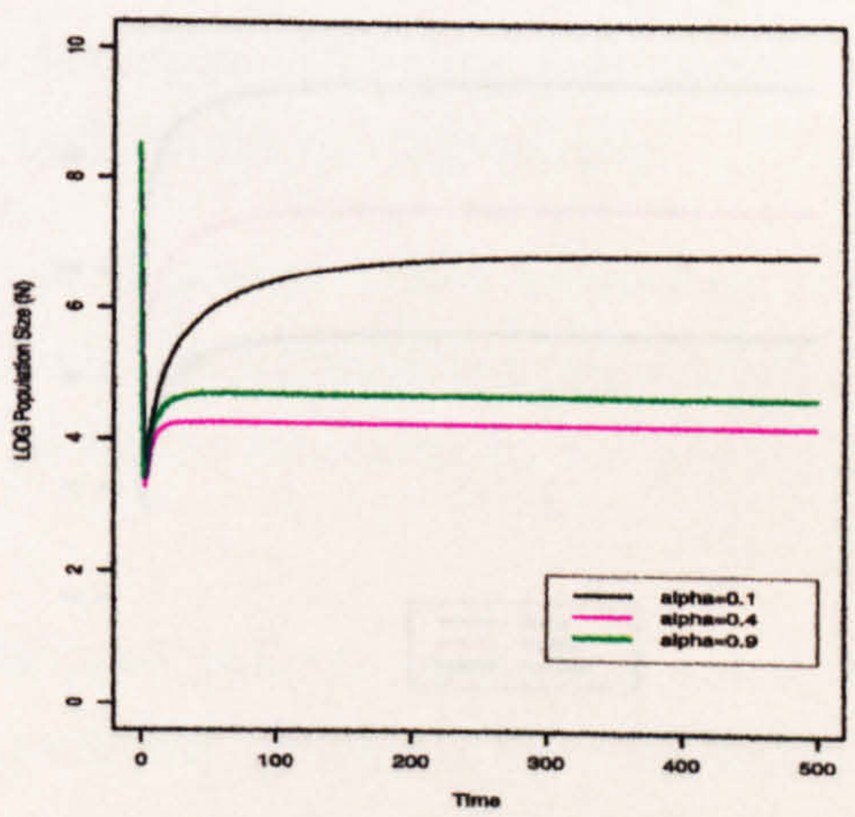

Figure 6.6: Trajectory of population size altering the ingestion rate.

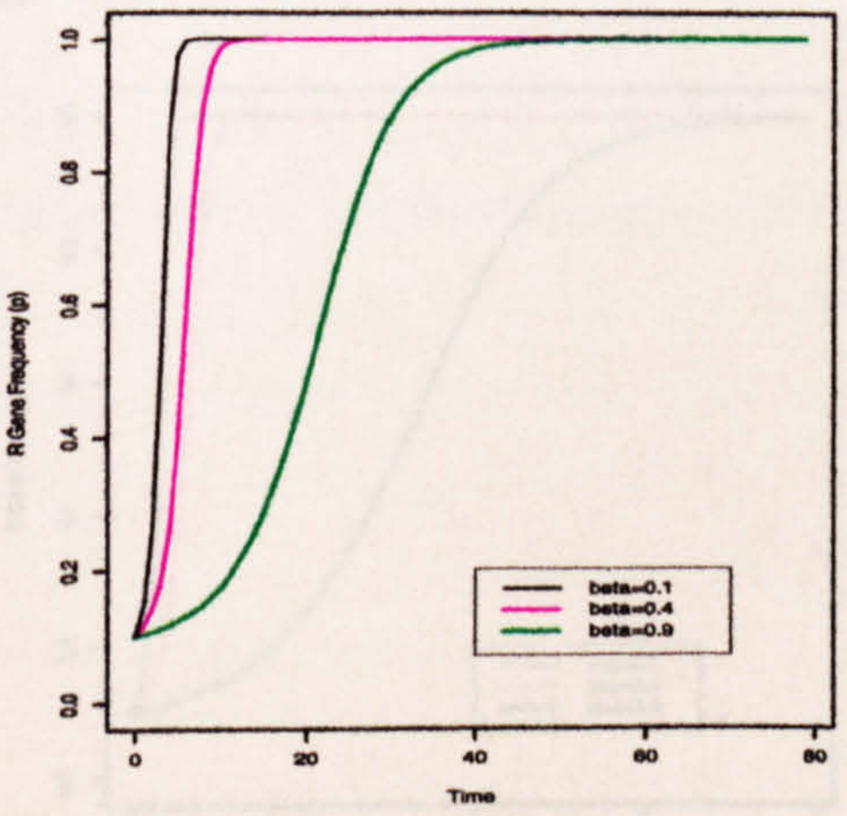

Figure 6.7: Trajectory of gene frequency altering altering survival rate.

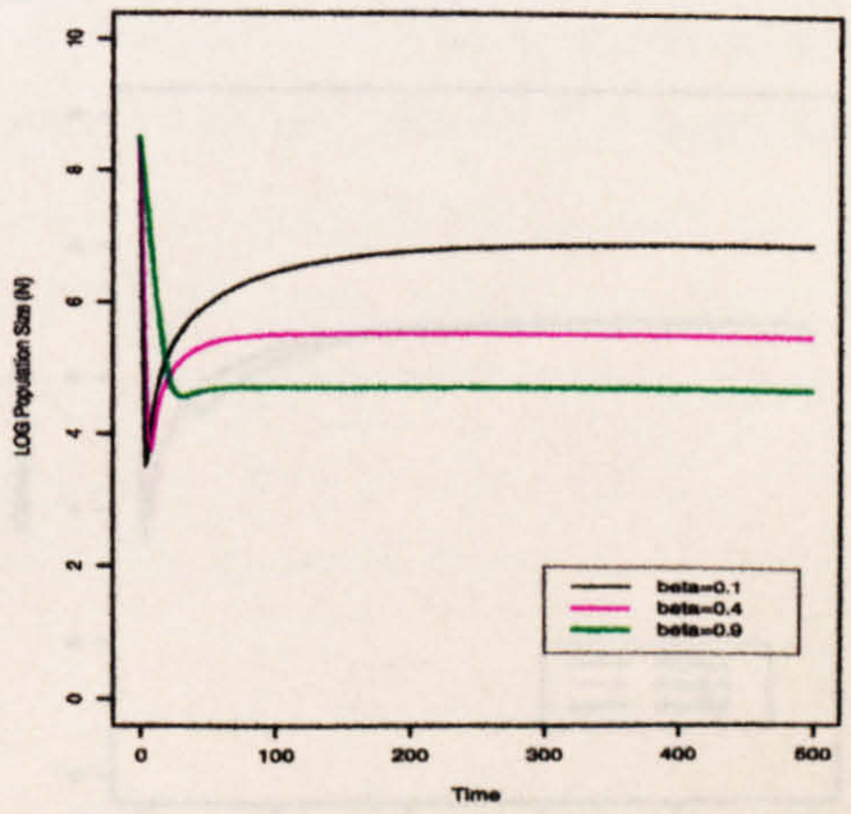

Figure 6.8: Trajectory of population size altering altering survival rate.

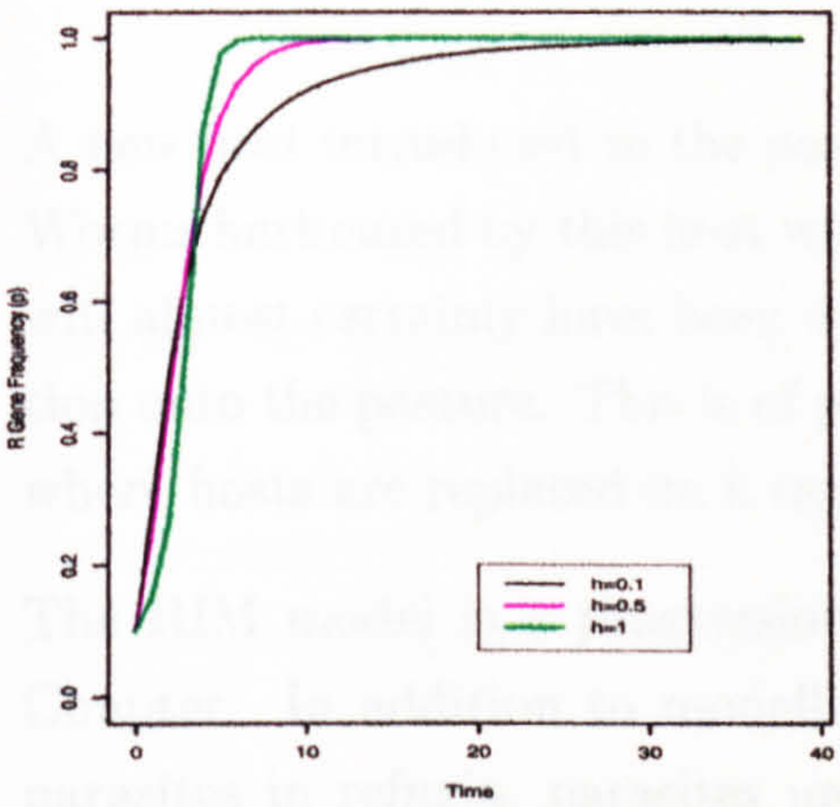

Figure 6.9: Trajectory of gene frequency altering h.

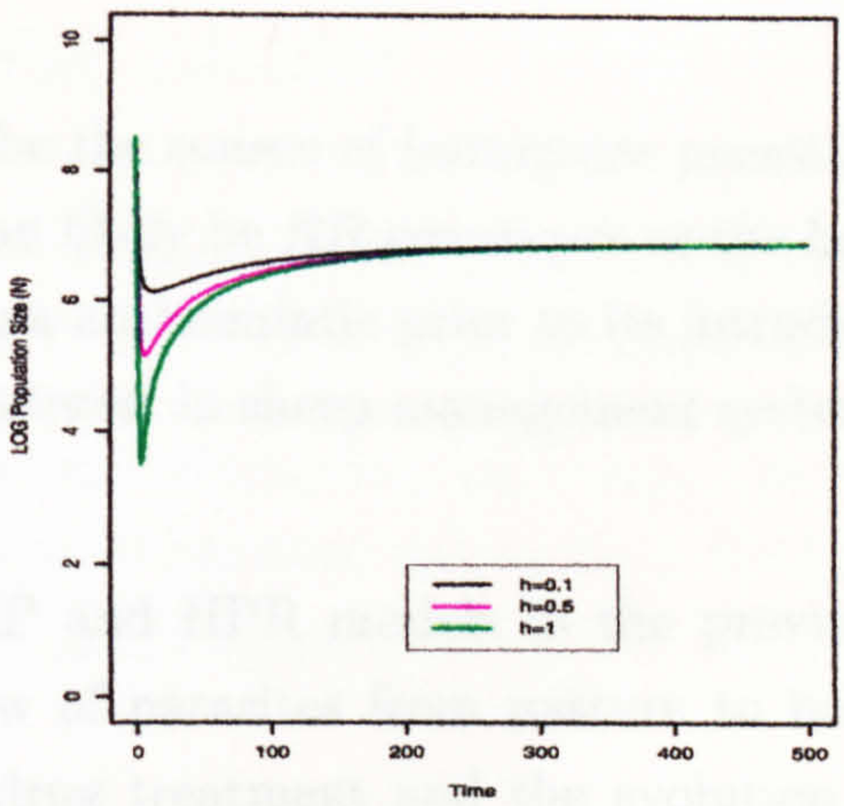

Figure 6.10: Trajectory of population size altering h.

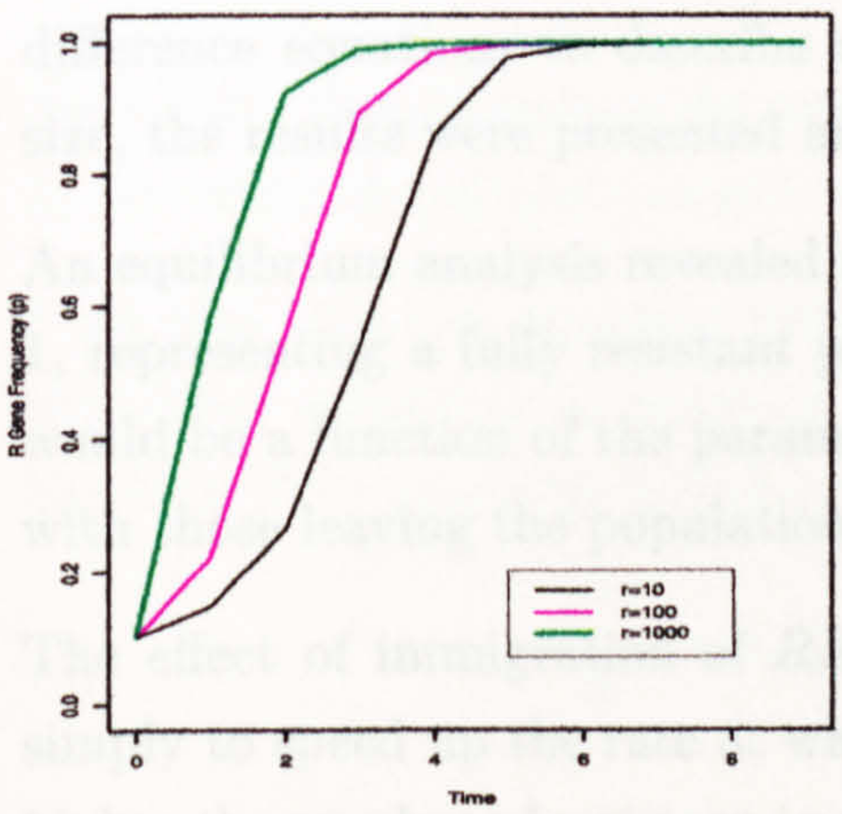

Figure 6.11: Trajectory of gene frequency altering the number of migrants.

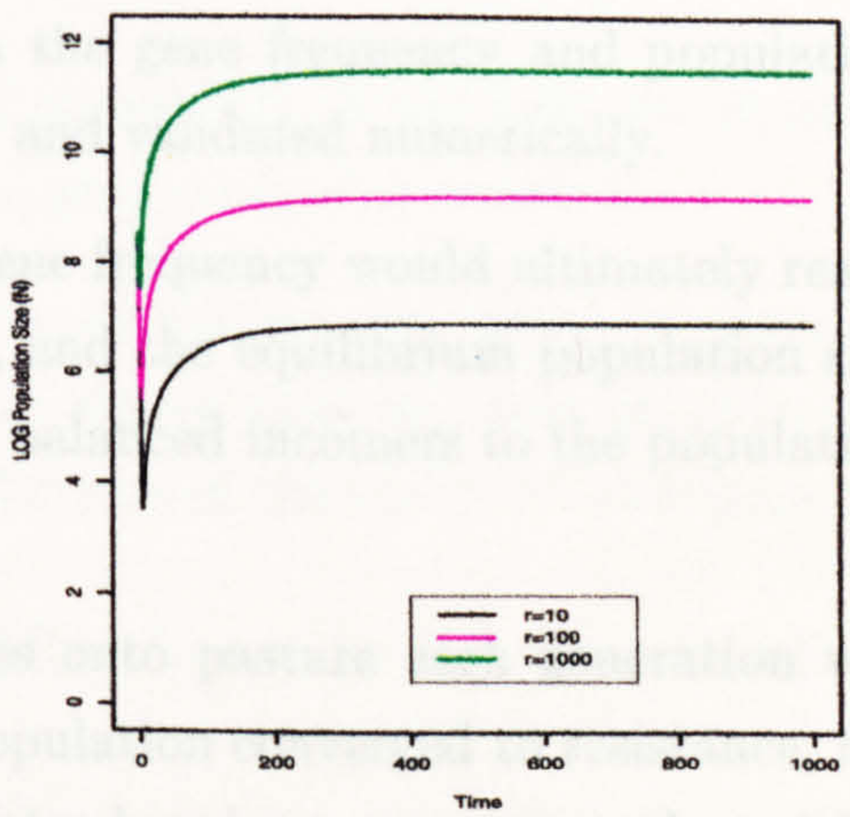

Figure 6.12: Trajectory of population size altering the number of migrants.

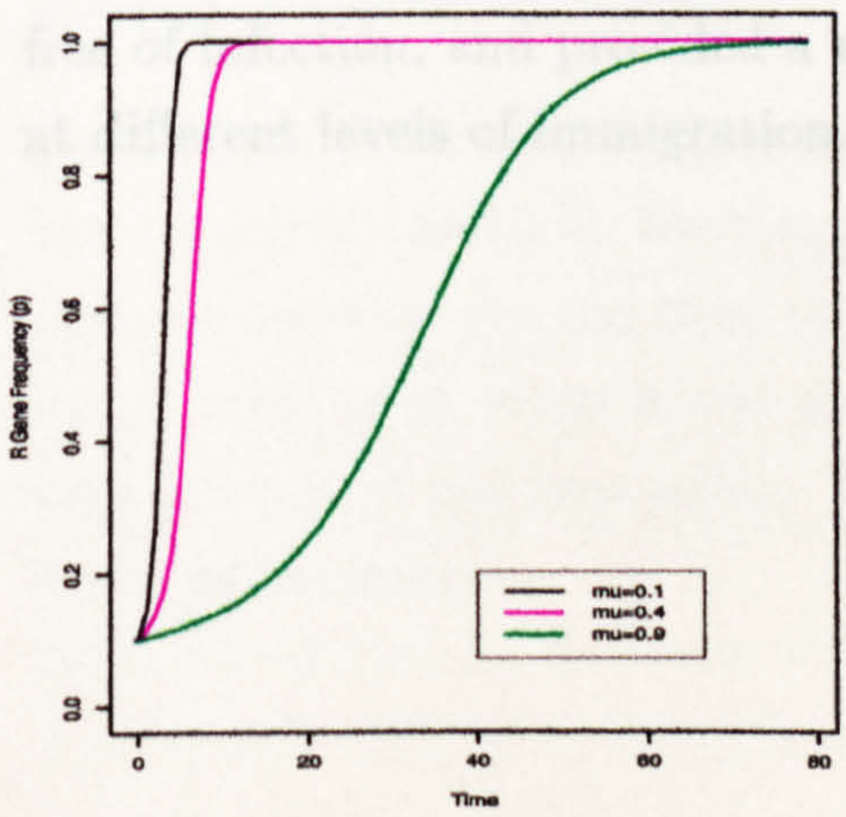

Figure 6.13: Trajectory of gene frequency altering the proportion in refugia.

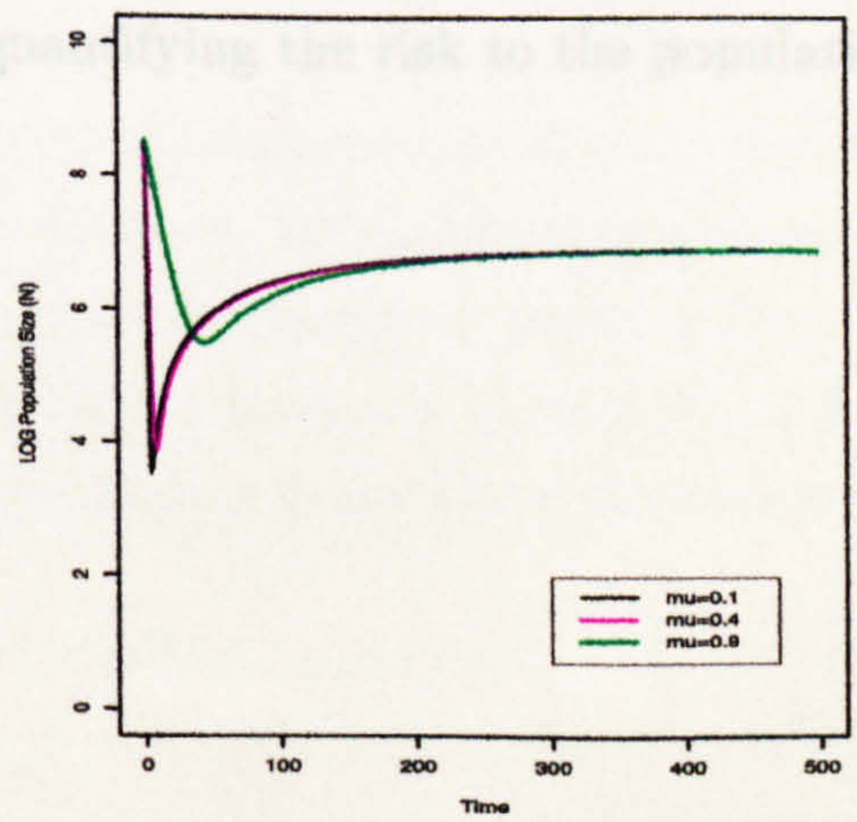

Figure 6.14: Trajectory of population size altering the proportion in refugia.

6.5 Exploring the Rate of Convergence to Resistance under the RIM Model

Given that a fully resistant population will eventually evolve, it is of interest to examine the time taken for resistance to reach a critical level in the population.

In Chapter 5 the change in gene frequency in one generation, $\Delta p_t = p_{t+1} - p_t$ was approximated by $\frac{dp_t}{dt}$ and the resulting differential equation solved for t, the time for the gene frequency to reach p_t from an initial frequency of p_0. For the RIM model,

$$\frac{dp_t}{dt} \approx \frac{N_t f \alpha (1-\mu)\left[p_t^2 - p_t^3\right] + r(1-p_t)}{N_t\left[\bar{w}(H) + \bar{w}(P)\right] + r} \tag{6.35}$$

Note here, that to reduce the mathematical complexity, h has been set equal to 1, representing complete recessiveness of the gene conferring resistance.

Note also that this equation contains N, the population size, which is changing with time according to equation (6.4). This means that we must consider the fact that N is changing in this equation. The rate of change of N with time is

$$\frac{dN}{dt} = N_t\left[\bar{w}_t(H) + \bar{w}_t(P) - 1\right] + r \tag{6.36}$$

In order to determine the time taken for the gene frequency to reach p_t from an initial level of p_0, when the initial population size was N_0 and the final population size is N_t, the two differential equations, (6.35) and (6.36) must be solved simultaneously. The existence of transcendental as well as single order factors prevents a tractable solution .

Fortunately in the last chapter the simulated model approximated quite well the exact analytic results for time to significant resistance. Here, obtaining a tractable analytic solution for the time taken for the gene frequency to reach p_t from an initial value of p_0 when initial and final population sizes are N_0 and N_t, will be very difficult, if not impossible. The use of simulation under these circumstances becomes necessary.

6.6 Conclusion

A new host introduced to the pasture may be the source of immigrant parasites. Worms harboured by this host will more than likely be RR genotypes as the host will almost certainly have been dosed with an anthelmintic prior to its introduction onto the pasture. This is of particular interest in sheep management systems where hosts are replaced on a regular basis.

The RIM model is a progression of the HP and HPR models in the previous Chapter. In addition to modelling the flow of parasites from pasture to host, parasites in refugia, parasites undergoing drug treatment and the evolution of resistance in a population, it also incorporates immigration of RR genotypes onto the pasture. This is a very useful addition to the model when we wish to examine the contribution of a new host to the resistance status in the population. Using difference equations to describe changes in the gene frequency and population size, the results were presented analytically and validated numerically.

An equilibrium analysis revealed that the gene frequency would ultimately reach 1, representing a fully resistant population, and the equilibrium population size would be a function of the parameters that balanced incomers to the population with those leaving the population.

The effect of immigration of RR genotypes onto pasture each generation was simply to speed up the rate at which the population converged to resistance, the higher the number of resistant immigrants introduced per generation, the quicker resistance evolved.

This chapter highlighted the dangers of introducing new hosts onto pasture particularly when they had been dosed with an anthelmintic and were assumed to be free of infection, and provided a means of quantifying the risk to the population at different levels of immigration.

Chapter 7

The Control of Resistance by the Inward Migration of Susceptible Individuals

7.1 Introduction

In Chapter 5, a basic model of the evolution of anthelmintic resistance in a parasite population with a direct life cycle was constructed. This model was used to identify primary factors influencing the outcome of an intensive drug programme on such a population. The model was extended to incorporate areas of refugia in the host and an expression for the time to significant resistance was formulated.

In this Chapter, the model is used to explore a novel method of controlling drug resistance in the field.

Biological control of anthelmintic resistance through the inward migration of susceptible strains of nematode has been proposed by Van Wyk (1990). The idea is that under a controlled situation, resistant strains of parasite are replaced by susceptible ones. Provided sufficient numbers of SS genotypes are introduced onto pasture and mating is at random, individuals with RR genotypes are more likely to mate with the SS migrants than with each other. This has the effect of reducing the number of RR offspring in the subsequent generation.

Here, we extend the previous models by introducing s susceptible migrants onto the pasture each generation in a bid to explore the novel method of resistance control.

7.2 The SIM Model

Here, the structure of the model in Chapter 5 is expanded. Provision is made within the model for s susceptible parasites to be introduced onto the pasture in each generation. The SIM model is illustrated in figure 7.1.

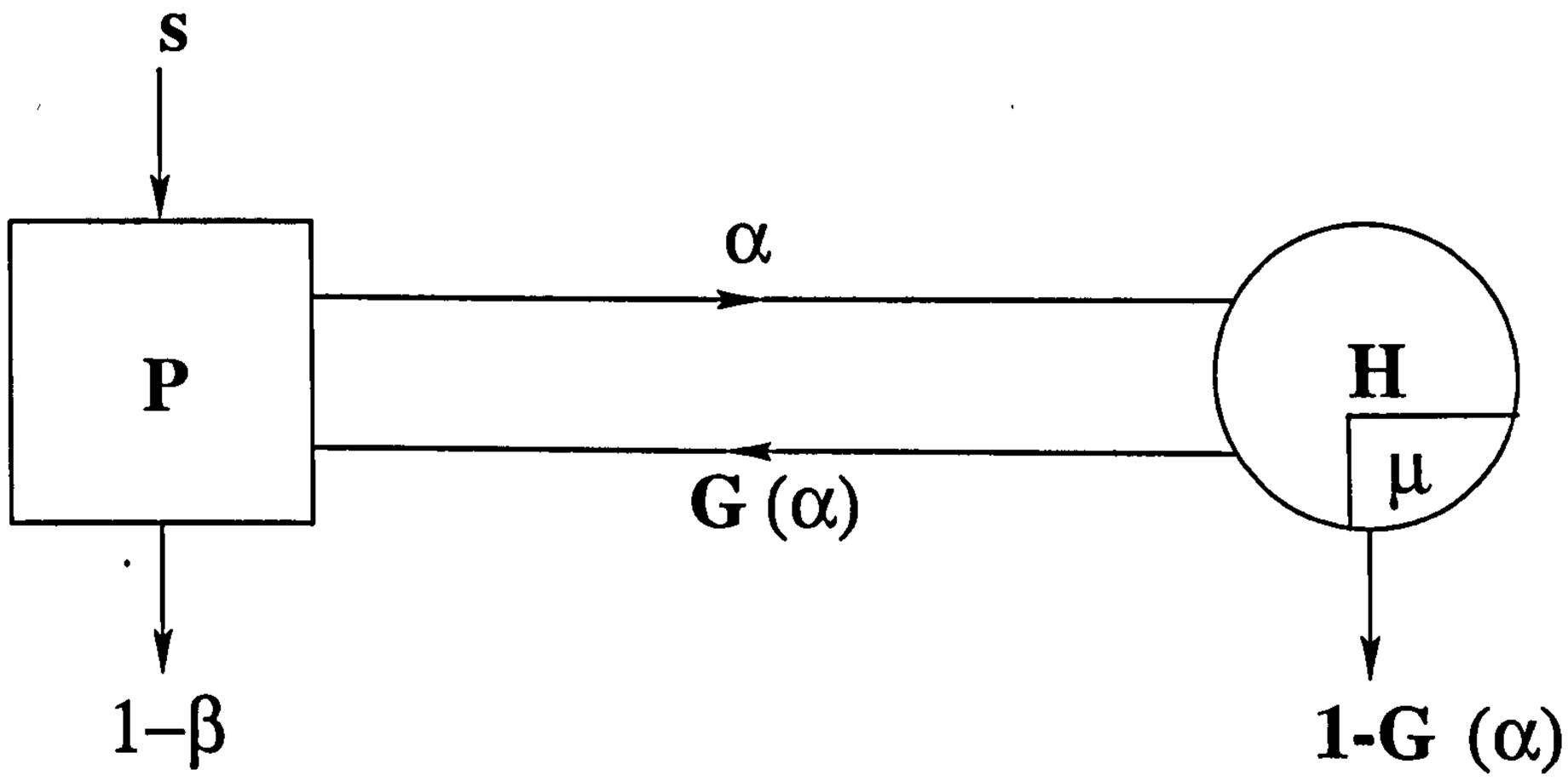

Figure 7.1: Flow diagram of Susceptible Immigrants Model illustrating the flow of parasites from host to pasture undergoing anthelmintic treatment, with a constant input of s susceptible (SS) genotypes onto pasture.

Therefore

$$\bar{w}_t(H) = f\alpha(1-\mu)\left[p_t^2 + 2p_t(1-p_t)(1-h)\right] + f\alpha\mu \tag{7.1}$$

and

$$\bar{w}_t(P) = (1-\alpha)\,\beta \tag{7.2}$$

The gene frequency in generation $t+1$ becomes

$$p_{t+1} = \frac{N_t\left[f\alpha(1-\mu)\left[p_t^2 + p_t(1-p_t)(1-h)\right] + \left[f\alpha\mu + (1-\alpha)\beta\right]p_t\right]}{N_t\left[\bar{w}_t(H) + \bar{w}_t(P)\right] + s} \tag{7.3}$$

and the population size in generation $t+1$ is

$$N_{t+1} = N_t\,[\bar{w}_t(H) + \bar{w}_t(P)] + s \tag{7.4}$$

7.3 Equilibrium Analysis of the SIM Model

At equilibrium, both the gene frequency and population size are unchanging. That is,

$$\Delta p_t = p_{t+1} - p_t = 0 \tag{7.5}$$

and

$$\Delta N_t = N_{t+1} - N_t = 0 \tag{7.6}$$

Substituting equation (7.3) into (7.5) yields a cubic equation in p_t as follows

$$p_t\left((2h-1)p_t^2 + (2-3h)p_t + \left[\frac{s}{N_t f\alpha(1-\mu)} - (1-h)\right]\right) \;=\; 0 \tag{7.7}$$

It is easy to see that one root of this equation, is $p_0^* = 0$.

The remaining two roots of this equation p_1^* and p_2^* are

$$p_1^*, p_2^* = \frac{(3h-2) \pm \sqrt{h^2 - \frac{(8h-4)s}{N_t f\alpha(1-\mu)}}}{2(2h-1)} \tag{7.8}$$

Substitution of equation (7.4) into (7.6) results in

$$(2h-1)p_t^2 + (2-2h)p_t + \left[\frac{f\alpha\mu + (1-\alpha)\beta - 1}{f\alpha(1-\mu)} + \frac{s}{N_t f\alpha(1-\mu)}\right] = 0 \tag{7.9}$$

The roots of equation (7.9), $\hat{p}_1$ and $\hat{p}_2$, represent those gene frequencies that equilibrate the population size

$$\hat{p}_1, \hat{p}_2 = \frac{(2h-2) \pm \sqrt{(2-2h)^2 - 4(2h-1)\left[\frac{f\alpha\mu+(1-\alpha)\beta-1}{f\alpha(1-\mu)} + \frac{s}{N_t f\alpha(1-\mu)}\right]}}{2(2h-1)} \tag{7.10}$$

Of interest here are the circumstances under which the population will equilibrate at zero resistance and 100% resistance, respectively.

Complete eradication of resistance from worm populations on pasture is proving a very difficult goal to achieve. Instead, we are now forced to examine possible methods of impeding the dissemination of resistance throughout the parasite population. This requires determining circumstances under which the population will equilibrate somewhere between zero and 100% resistance.

7.3.1 Boundary Equilibria

In this section we shall first examine the circumstances under which the population remains free of resistance and then determine circumstances under which the population will become fully resistant.

The two cases outlined above will be discussed here. The subsequent section will deal with the existence of intermediate equilibria.

A Resistance Free Population

A resistance-free population exists when $p = 0$ and $N = \frac{s}{1-(f\alpha\mu+(1-\alpha)\beta)}$.

A Fully Resistant Population

The population will approach 100% resistance asymptotically as $N \to \infty$. That is,

$$\begin{aligned} \lim_{N\to\infty} p_{t+1} &= \frac{N_t\left[f\alpha(1-\mu)\left[p_t^2 + p_t(1-p_t)(1-h)\right] + \left[f\alpha\mu + (1-\alpha)\beta\right]p_t\right]}{N_t\left[\bar{w}(H) + \bar{w}(P)\right] + s} \\ &= 1 \end{aligned} \tag{7.11}$$

This point is obtained by substituting $p = 1$ into equation (7.7) and solving for N. If, alternatively, we substituted $p = 1$ into equation (7.9), the equilibrium population size obtained would be negative. The population will get larger and larger as 100% resistance is reached, and will never realistically become negative. Equilibria outwith these boundaries may exist, but are biologically meaningless and will not be pursued further here.

The two equilibria derived previously represent boundary equilibria for the SIM model. Either the population is resistance free and the population size remains constant, or resistance evolves and the population grows out of control. Ideally, it is hoped that a nematode population remains resistance free and the population size controlled. The existence of equilibria between these boundaries may identify a middle ground between full resistance and zero resistance.

7.3.2 Intermediate Equilibria

An internal, or intermediate equilibrium will exist if the cubic equation defined in equation (7.7) intersects with the quadratic in equation (7.9) in a valid region of the $N - p$ plane.

The roots of equation (7.7) are the equilibrium gene frequencies

$$\begin{aligned} p_0^* &= 0 \\ p_1^*, p_2^* &= \frac{3h - 2 \pm \sqrt{h^2 - \frac{4(2h-1)s}{Nf\alpha(1-\mu)}}}{2(2h-1)} \end{aligned} \tag{7.12}$$

and the roots of equation (7.9) are the gene frequencies that equilibrate population size

$$\hat{p}_1, \hat{p}_2 = \frac{2h - 2 \pm \sqrt{(2-2h)^2 - \frac{4(2h-1)(N(f\alpha\mu+(1-\alpha)\beta-1)+s)}{Nf\alpha(1-\mu)}}}{2(2h-1)} \tag{7.13}$$

We are interested in the point where the quadratic in equation (7.12) intersects with the quadratic in equation (7.13). This point, denoted by (N^*, p_I) is as follows

$$\hat{N} = \frac{f\alpha(1-\mu)sh^2}{[1-(f\alpha+(1-\alpha)\beta)]\,[f\alpha(\mu-1)h^2-[1-(f\alpha+(1-\alpha)\beta)]\,(2h-1)]} \tag{7.14}$$

and

$$p_I = 1 + \frac{(1-(f\alpha+(1-\alpha)\beta))}{f\alpha(1-\mu)h} \tag{7.15}$$

A few preliminary points of interest are noted here

(i) an increase in h, the proportion of heterozygotes killed by a drug, produces an increase in p_I. An increase in h corresponds to a greater number of heterozygotes, (RS), being killed by a drug. Given that all SSs exposed to the drug will be killed by it and all RRs survive treatment, a higher proportion of R genes in the population will survive leading to a higher gene frequency at which the population equilibrates,

(ii) as the proportion of the population that enter refugia, μ, increases, the gene frequency equilibrium decreases. This means that more SSs and RSs avoid treatment, thus survive to produce progeny contributing relatively more S genes to the gene pool in the next generation,

(iii) the number of immigrants introduced to the population each generation, s, occurs only in the numerator of $\hat{N}$, thus by increasing the number of immigrants per generation the value of $\hat{N}$ at which the population equilibrates increases by the same magnitude, and

(iv) the frequency at which the gene conferring resistance equilibrates is not affected by s.

7.4 Biological Significance of $(\hat{N}, p_I)$

For $(\hat{N}, p_I)$ to have practical significance in a biological population, it must lie in a valid region of the $N-p$ plane. That is,

(i) the population size equilibrium, $\hat{N}$, must be positive, and

(ii) the equilibrium gene frequency, p_I, must lie between zero and one.

7.4.1 $\hat{N} > 0$ (The population size must be positive)

The intersection of the gene frequency equilibrium and the gene frequency that equilibrates the population size was determined in the previous section to occur when

$$\hat{N} = \frac{f\alpha(1-\mu)sh^2}{[1-(f\alpha+(1-\alpha)\beta)]\,[f\alpha(\mu-1)h^2-[1-(f\alpha+(1-\alpha)\beta)]\,(2h-1)]} \tag{7.16}$$

$\hat{N}$ is positive, if both the numerator and denominator are of equal sign. Clearly this is true if and only if

(i) $f\alpha(1-\mu)sh^2 > 0$, and

(ii) $[1-(f\alpha+(1-\alpha)\beta)]\,[f\alpha(\mu-1)h^2-[1-(f\alpha+(1-\alpha)\beta)]\,(2h-1)] > 0$

since under no circumstances can the numerator be negative.

The first condition is satisfied provided $f, \alpha, s, h > 0$ and $\mu \neq 1$.

The second condition is satisfied in one of two ways. Either

Case 1

(i) $[1-(f\alpha+(1-\alpha)\beta)] > 0$, and

(ii) $[f\alpha(\mu-1)h^2-[1-(f\alpha+(1-\alpha)\beta)]\,(2h-1)] > 0$

or

Case 2

(i) $[1-(f\alpha+(1-\alpha)\beta)] < 0$ and

(ii) $[f\alpha(\mu-1)h^2-[1-(f\alpha+(1-\alpha)\beta)]\,(2h-1)] < 0$

Consider Case 2. It follows that if $[1-(f\alpha+(1-\alpha)\beta)] < 0$, then $f > \frac{1-(1-\alpha)\beta}{\alpha}$.

Provided this is the case for $\hat{N}$ to be positive part (ii) in Case 2, that is,

$$f\alpha(\mu-1)h^2 - 2\left[1-(f\alpha+(1-\alpha)\beta)\right]h + \left[1-(f\alpha+(1-\alpha)\beta)\right] < 0 \quad (7.17)$$

must be satisfied.

Thus, values of h are sought such that the quadratic in equation (7.17) is negative and $h \in (0,1)$. By setting equation (7.17) equal to zero, the roots, h_1 and h_2 are

$$h_1, h_2 = \frac{1-(f\alpha+(1-\alpha)\beta) \pm \sqrt{[1-(f\alpha+(1-\alpha)\beta]^2 - f\alpha(\mu-1)(1-(f\alpha+(1-\alpha)\beta)}}{f\alpha(\mu-1)} \quad (7.1$$

Since the coefficient of h^2 in (7.17) is negative (because $\mu < 1$), the quadratic will be negative whenever $h < h_1$ or $h > h_2$. We arbitrarily chose the positive root of equation (7.18). In order that $h \in (0,1)$, the following restrictions are imposed on f, the fecundity of female parasites

$$\frac{1-(1-\alpha)\beta}{\alpha} < f < \frac{1-(1-\alpha)\beta}{\alpha\mu} \quad (7.19)$$

Provided f lies within the interval defined above, any value of $h \in (0,1)$ will result in a positive value of $\hat{N}$. Alternatively, restrictions could be imposed on any of the other parameters. The choice of f was arbitrary. However, in this way the effect of different drug efficacies, h, can be investigated.

7.4.2 $0 \leq p_I \leq 1$ (The equilibrium gene frequency must lie between zero and one)

The intersection of p_1^*, p_2^* in equation (7.8) with $\hat{p}_1, \hat{p}_2$ in equation (7.10), occurs where $\hat{N} > 0$ provided

1. f, α, β, s, h, $\mu > 0$ and $\mu \neq 1$
2. $\frac{1-(1-\alpha)\beta}{\alpha} < f < \frac{1-(1-\alpha)\beta}{\alpha\mu}$

It is now necessary to determine the conditions under which the intersection will also occur in the valid region where $p_I \in (0,1)$ of the $N-p$ plane.

7.4.3 $p_I \geq 0$

From equation (7.15),

$$p_I = 1 + \frac{(1 - (f\alpha + (1-\alpha)\beta))}{f\alpha(1-\mu)h} \tag{7.20}$$

p_I is positive or zero, if

$$\frac{1 - (f\alpha + (1-\alpha)\beta}{f\alpha(1-\mu)h} \geq -1 \tag{7.21}$$

Since the denominator in equation (7.21) is positive (because $f, \alpha, \mu, h \geq 0$ and $\mu \neq 1$), the absolute value of the numerator must be less than $f\alpha(1-\mu)h$. That is

$$|1 - (f\alpha + (1-\alpha)\beta| \leq f\alpha(1-\mu)h \tag{7.22}$$

It follows that

$$(1 - (f\alpha + (1-\alpha)\beta)^2 \leq (f\alpha(1-\mu)h)^2 \tag{7.23}$$

Solving equation (7.23) results in the following quadratic in f

$$\alpha^2(1 - ((1-\mu)h)^2)f^2 - 2\alpha(1 - (1-\alpha)\beta)f + (1 - (1-\alpha)\beta)^2 \leq 0 \tag{7.24}$$

Provided the coefficient of f^2 in equation (7.24) is positive (which it is when $\mu < 1$), this quadratic will be negative between the roots of

$$\alpha^2(1 - ((1-\mu)h)^2)f^2 - 2\alpha(1 - (1-\alpha)\beta)f + (1 - (1-\alpha)\beta)^2 = 0 \tag{7.25}$$

Therefore, $p_I \geq 0$ if and only if

$$\frac{(1 - (1-\alpha)\beta)(1 - (1-\mu)h)}{\alpha(1 - ((1-\mu)h)^2} < f < \frac{(1 - (1-\alpha)\beta)(1 + (1-\mu)h)}{\alpha(1 - ((1-\mu)h)^2} \tag{7.26}$$

7.4.4 $p_I \leq 1$

The point of intersection of the gene frequencies, p_I, by definition, cannot exceed unity, therefore,

$$1 + \frac{1-(f\alpha+(1-\alpha)\beta)}{f\alpha(1-\mu)h} \leq 1$$

$$\frac{1-(f\alpha+(1-\alpha)\beta)}{f\alpha(1-\mu)h} \leq 0 \tag{7.27}$$

It follows that

$$f \geq \frac{1-(1-\alpha)\beta}{\alpha} \tag{7.28}$$

This results in the same condition imposed on f to ensure that $\hat{N} > 0$(see equation (7.19)).

7.4.5 Summary

A biologically meaningful intermediate equilibrium point, $(\hat{N}, p_I)$, will exist provided the following conditions are satisfied.

1. $\hat{N} > 0$

   (i) f, α, β, s, h, $\mu > 0$, and $\mu \neq 1$

   (ii) $\frac{1-(1-\alpha)\beta}{\alpha} < f < \frac{1-(1-\alpha)\beta}{\alpha\mu}$

2. $0 \leq p_I \leq 1$

   (i) f, α, β, s, h, $\mu > 0$, and $\mu \neq 1$

   (ii) $\frac{(1-(1-\alpha)\beta)(1-(1-\mu)h)}{\alpha(1-((1-\mu)h)^2} < f < \frac{(1-(1-\alpha)\beta)(1+(1-\mu)h)}{\alpha(1-((1-\mu)h)^2}$

The fecundity of female parasites, f, must satisfy both conditions in 1(ii) and 2(ii) above. Thus, there must exist some common region, $f \in (f_1, f_2)$ within

which f must lie for both conditions to be satisfied and the point of intersection to be valid. This region is found to be

$$f \in \left(\frac{1-(1-\alpha)\beta}{\alpha}, \frac{(1-(1-\alpha)\beta)(1+(1-\mu)h)}{\alpha(1-((1-\mu)h)^2} \right)$$

since

$$\frac{1-(1-\alpha)\beta}{\alpha} > \frac{(1-(1-\alpha)\beta)(1-(1-\mu)h)}{\alpha(1-((1-\mu)h)^2} \tag{7.29}$$

and

$$\frac{1-(1-\alpha)\beta}{\alpha\mu} < \frac{(1-(1-\alpha)\beta)(1+(1-\mu)h)}{\alpha(1-((1-\mu)h)^2} \tag{7.30}$$

7.5 A Numerical Study of The SIM Model

It has been established analytically that in a parasite population described by the SIM model, one of three outcomes is to be expected. Either resistance will evolve in the parasite population and the number of parasites will escalate beyond control, or the population will be resistance free and the number of parasites controlled. Alternatively, there are circumstances under which the frequency of the gene conferring resistance in a population will reach a steady state in conjunction with the population size which we denote by $(\hat{N}, p_I)$ and call it the intermediate equilibrium.

7.5.1 How Do Initial Conditions Affect The Outcome of a Population ?

The SIM model was numerically simulated using ITERATOR, (©STAMS), to illustrate the various possible outcomes of the model. Figures 7.2 and 7.3 are graphical descriptions of the resistance status and the population size, respectively, in a typical nematode population described by the SIM model over some period of time.

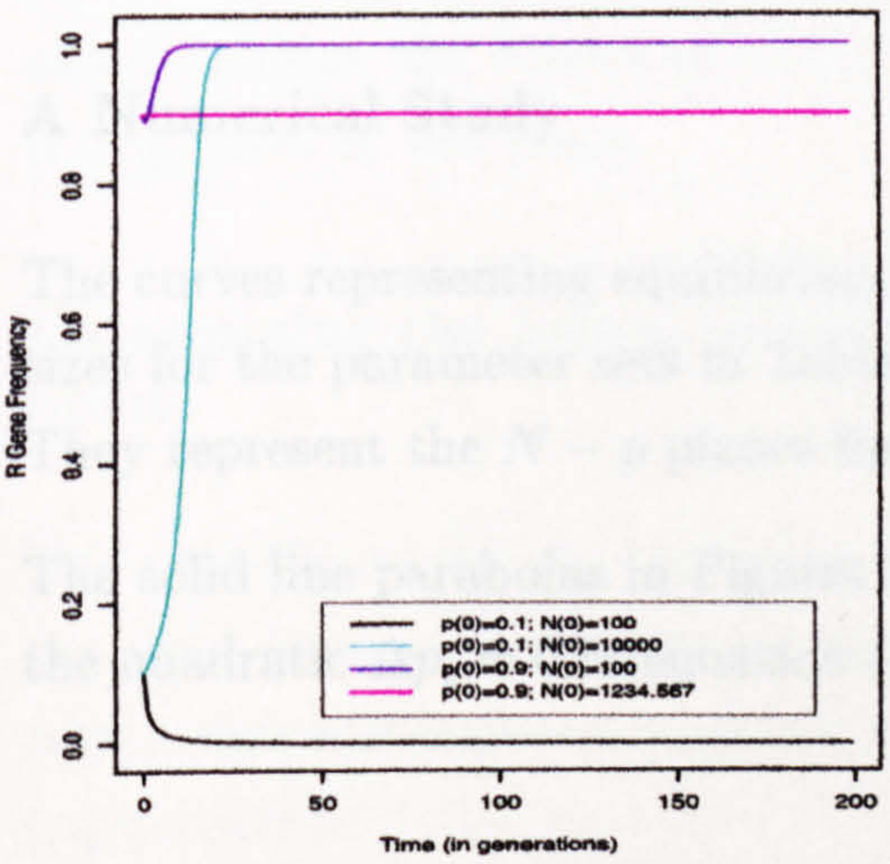

Figure 7.2: Changes in the R gene frequency over time for different starting conditions, shown in the legend.

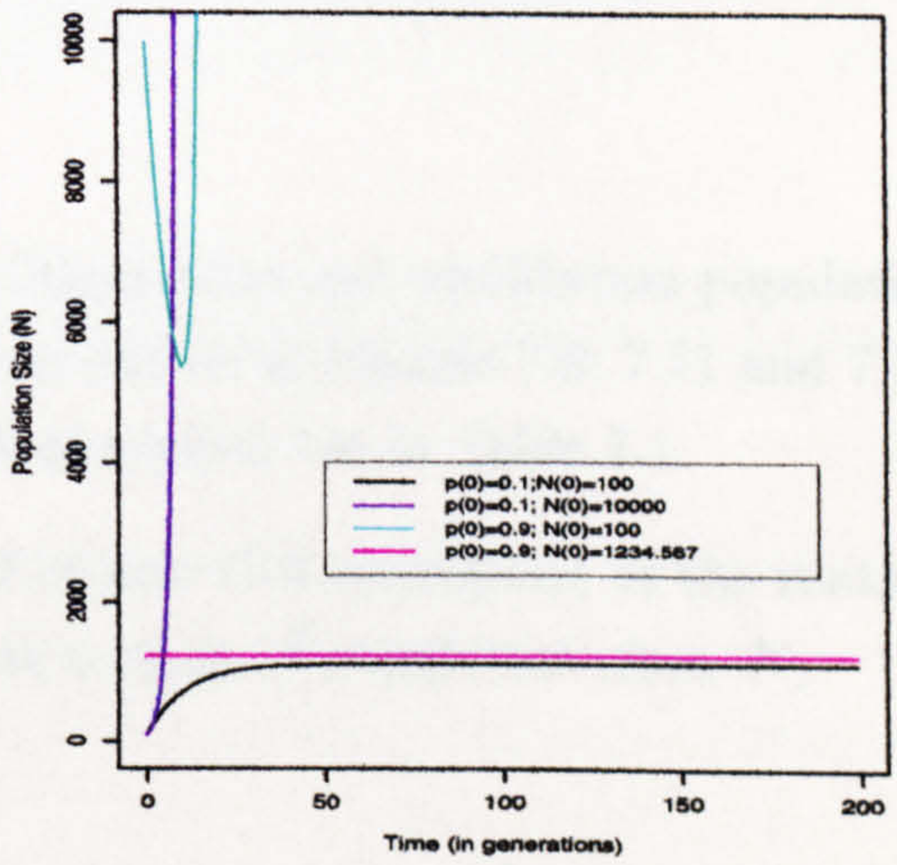

Figure 7.3: Changes in population size over time for different initial conditions shown in the legend.

Initial conditions are clearly important in determining the eventual outcome of a population. To investigate the effect of initial conditions on the fate of a population, all other parameters in the model were held constant as indicated in

parameter set 1 in Table 7.1, and various combinations of low and high initial gene frequency and population size, respectively, were simulated. A population with an initial R gene frequency of $p_0 = 0.1$ whose initial size is $N_0 = 100$ (the grey line in Figures 7.2 and 7.3), will become virtually resistance free with the population size reaching a steady state value of $\hat{N} = 1111.11$ within a few generations. In contrast, if the same population has initially $N_0 = 10000$ individuals to start with, (the aqua lines in Figures 7.2 and 7.3), within a few generations, that population will have become fully resistant and the population will have grown out of control. If, instead, the initial population size remains at $N_0 = 100$ but the initial R gene frequency is increased to $p_0 = 0.9$, (the purple lines in Figures 7.2 and 7.3), resistance evolves and there is a population explosion. Finally, the magenta trajectories shown in Figures 7.2 and 7.3 depict a population with initial gene frequency of $p_0 = 0.9$ and initial population size of $N_0 = 1234.567$. Here, the gene frequency and population size remain unchanged from inception of the population.

Thus there is some indication that under certain circumstances, resistance may be suppressed and population size controlled.

7.5.2 Can the population size be controlled and resistance suppressed by immigration of susceptible parasites?

A Numerical Study

The curves representing equilibrium gene frequencies and equilibrium population sizes for the parameter sets in Table 7.1 are shown in Figures 7.8, 7.11 and 7.14. They represent the $N - p$ planes for each parameter set in Table 7.1.

The solid line parabolas in Figures 7.8, 7.11 and 7.14 correspond to the roots of the quadratic $\Delta p_t = 0$ in equation (7.7) at a range of population sizes, N,

$$(2h-1)p_t^2 + (2-3h)p_t + \left[\frac{s}{N_t f \alpha (1-\mu)} - (1-h)\right] = 0 \qquad (7.31)$$

when all other parameters are held constant.

The broken line parabolas in Figures 7.8, 7.11 and 7.14 correspond to the roots of the quadratic $\Delta N_t = 0$,

Table 7.1: Parameter values assigned to the SIM model to illustrate the behaviour of the model over a spectrum of possible values.

Parameter Set	α	β	μ	**fecundity**	h	s
1	0.1	0.9	0.1	10	1	100
2	0.1	0.9	0.9	2	1	100
3	0.5	0.9	0.1	10	1	100
4	0.1	0.1	0.1	10	1	100

$$(2h-1)p_t^2 + (2-2h)p_t + \left[\frac{f\alpha\mu + (1-\alpha)\beta - 1}{f\alpha(1-\mu)} + \frac{s}{N_t f\alpha(1-\mu)}\right] = 0 \tag{7.32}$$

The intersection of these curves represents the intermediate equilibrium. Already established is the fact that initial conditions are important in determining the outcome of a population. Plotting p^* and $\hat{p}$ on the same plane means that we can determine the behaviour of the modelled population by the region in which it originates in this plane.

Determining the future behaviour of the population from its starting point

If the conditions derived previously and summarised in Section 7.4.5 are satisfied, the solid line parabolas will intersect with the broken line parabolas in a valid region that will represent population control and control of resistance within that population.

For populations originating in many of the regions on the $N - p$ plane, we can determine the eventual outcome of that population.

Consider the first parameter set in Table 7.1. The change in gene frequency and population size in such a population are depicted graphically in the surfaces in Figures 7.6 and 7.7 respectively. From Figure 7.6, it is clear that the gene frequency equilibrates where the curve of Δp_t cuts the x-axis. It can be seen

clearly from the plots of the surfaces that there are three such roots, p_0^*, p_1^*, p_2^* for each value of N. If we assume that $p_0^* < p_1^* < p_2^*$, then

(i) the gene frequency will decrease ($\Delta p_t < 0$), between p_0^* and p_1^* and above p_2^*,

(ii) the gene frequency will increase between p_1^* and p_2^* ($\Delta p_t > 0$).

The solid line in Figure 7.8 represents p_1^* and p_2^*, and the x-axis represents p_0^*. In other words, when the population is within the solid lined parabola, gene frequency will increase, whereas when the population is outwith the solid lined parabola, the gene frequency will decrease.

Similarly, the population size equilibrates where the curve of ΔN_t (shown in Figure 7.6 for parameter set 1 in Table 7.1), cuts the x-axis. Since ΔN_t is a quadratic equation, there are two roots, $\hat{p}_1$ and $\hat{p}_2$ for each value of N. The population size will decrease ($\Delta N_t < 0$), between $\hat{p}_1$ and $\hat{p}_2$, and will increase outwith these points. This translates into a reduction in population size when a population starts off within the broken lined parabola in Figure 7.8, and an increase in population size when the population starts outside this parabola.

Changing the values that the parameters of the model take results in different forms of the cubic and quadratic equations for Δp_t and ΔN_t, respectively and different forms of the parabolas. Figures 7.9 and 7.10 are the curves obtained when the parameter values in the second row of Table 7.1 are substituted into the model, with Figure 7.11 representing the roots of the equations where $\Delta p_t = 0$ and $\Delta N_t = 0$. Figures 7.12 and 7.13 result when parameter values in the third row of Table 7.1 are substituted into the model. The corresponding $N - p$ plane is given in Figure 7.14.

Arrows have been superimposed onto each $N - p$ plane in Figures 7.8, 7.11 and 7.14, indicating the direction of change of the population size and gene frequency over time.

Example

As an example, we consider the first parameter set in Table 7.1 that corresponds to the surfaces in Figures 7.6 and 7.7 and the $N - p$ plane in Figure 7.8.

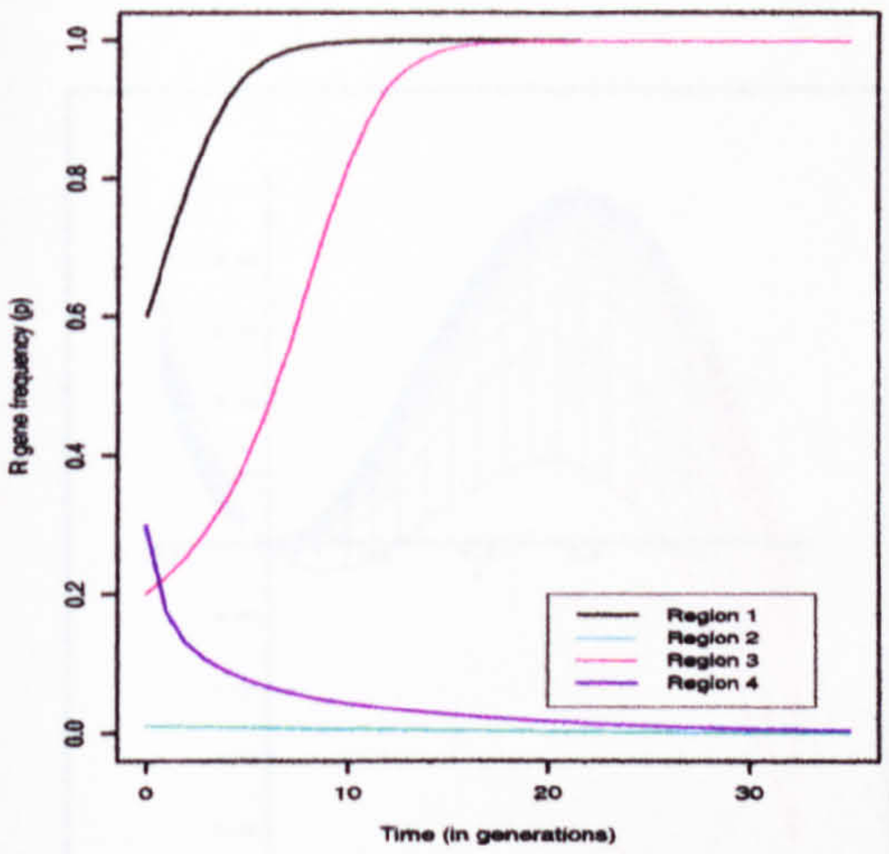

Figure 7.4: Changes in the R gene frequency over time for different starting conditions, shown in the legend.

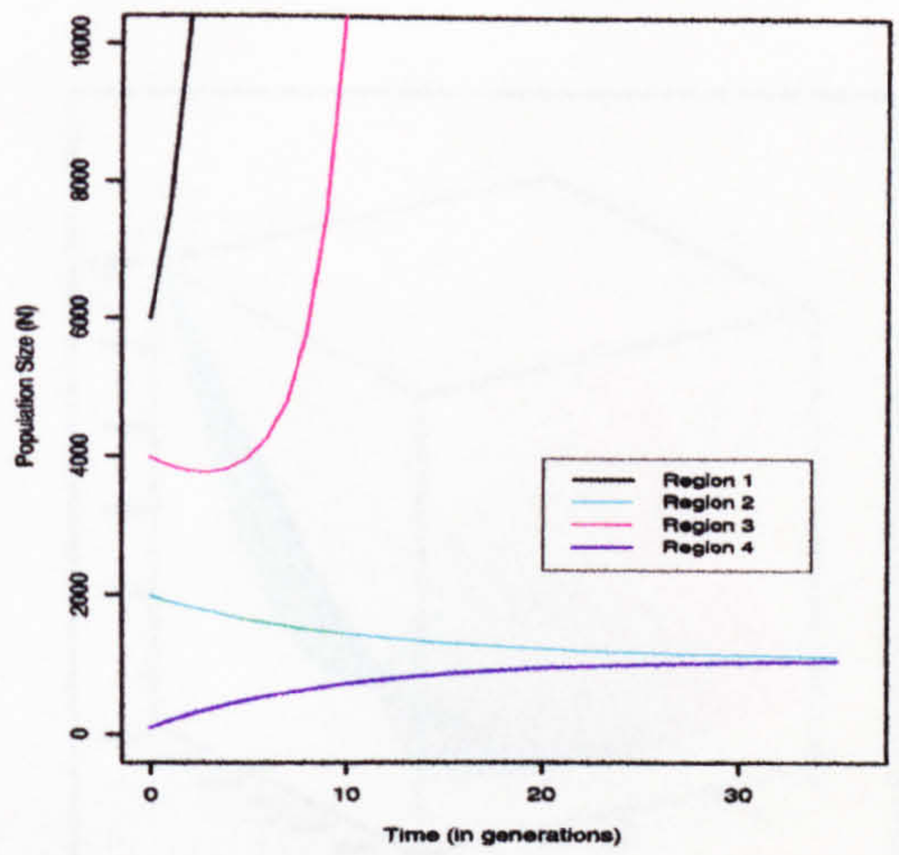

Figure 7.5: Changes in population size over time for different initial conditions shown in the legend.

Figures 7.4 and 7.5 show the trajectory of the R gene frequency and population size, respectively, when the population starts in one of the four regions labelled I-IV.

Results

A population whose initial gene frequency and population size lies in region I, for example (0.6,6000), will increase in size with a concomitant increase in gene frequency. This population will reach 100% resistance and its numbers will grow out of control. Conversely, a population originating in region II (0.01,2000), will be contained and resistance eradicated. Unless disturbed into any of the other regions, a population originating in region III (0.2,4000), will experience an increase in gene frequency and decrease in population size (as indicated by the arrows in Figure 7.8). A population originating somewhere in region IV above the dotted line (0.3,100), will have an initial decrease in gene frequency and increase in population size. By the nature of the dynamics of populations starting in either region III or IV above the dotted line, the eventual behaviour cannot be conclusively determined as it is easy for such a population to enter into another region and assume the behaviour of a population originating in that region. Finally, a population starting at the point of intersection of p^* and $\hat{p}$ will remain at this point indefinitely.

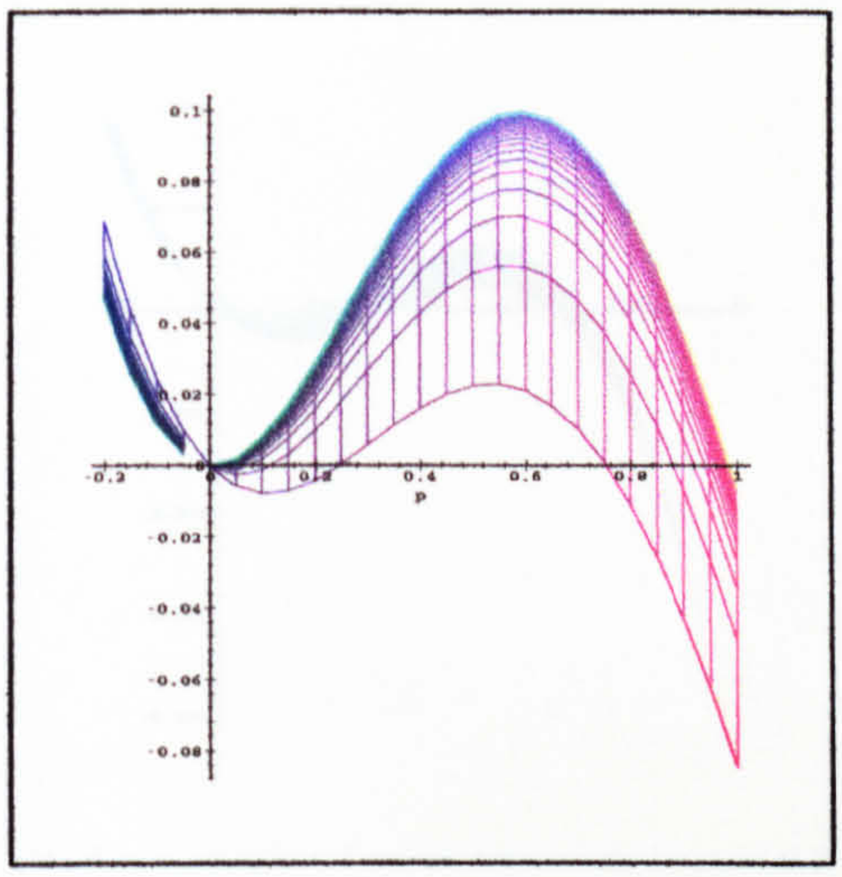

Figure 7.6: Surface representing the change in gene frequency, Δp_t, as a function of initial gene frequency and population size for parameter set 1 in Table 7.1.

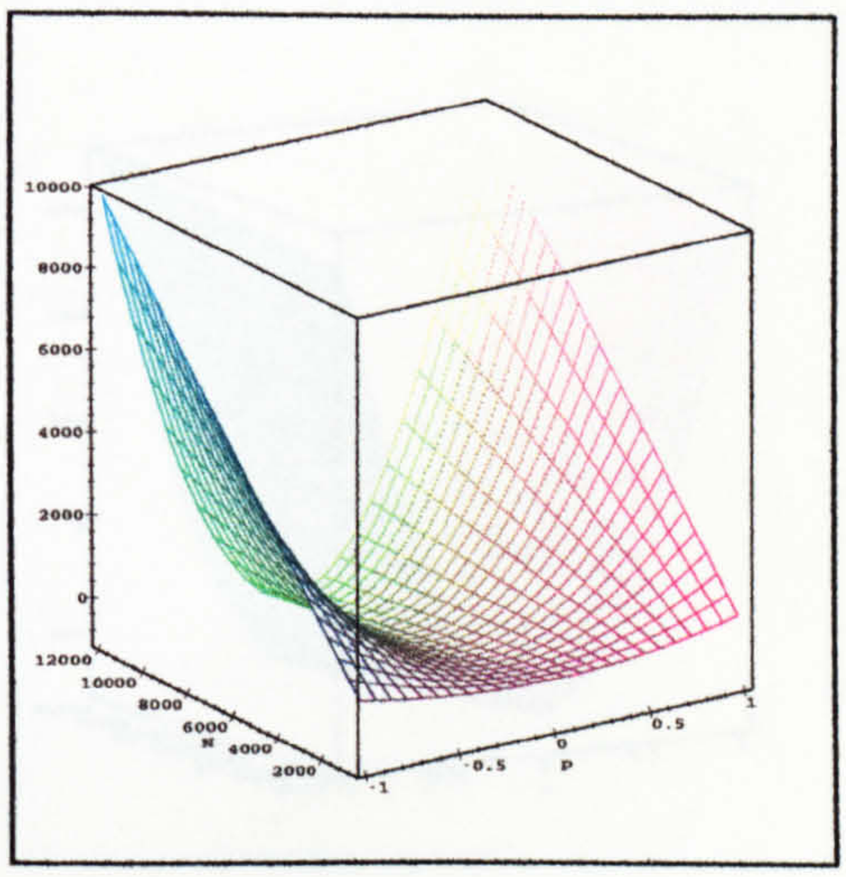

Figure 7.7: Surface representing the change in population size, ΔN_t, as a function of initial gene frequency and population size for parameter set 1 in Table 7.1.

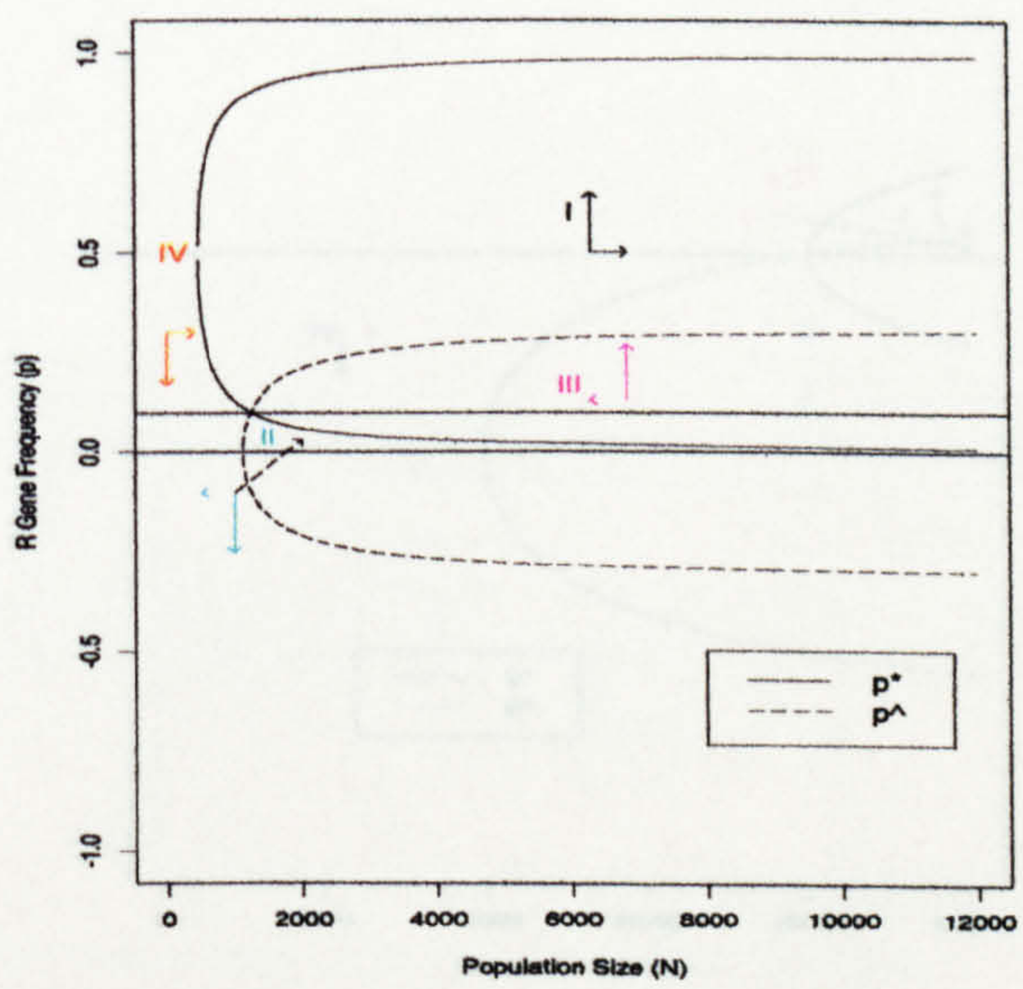

Figure 7.8: $N - p$ plane for parameter set 1 in Table 7.1 with p^* and $\hat{p}$ representing equilibrium gene frequency and equilibrium population size respectively, with an intersection point of $(0.1, 1234.567)$.

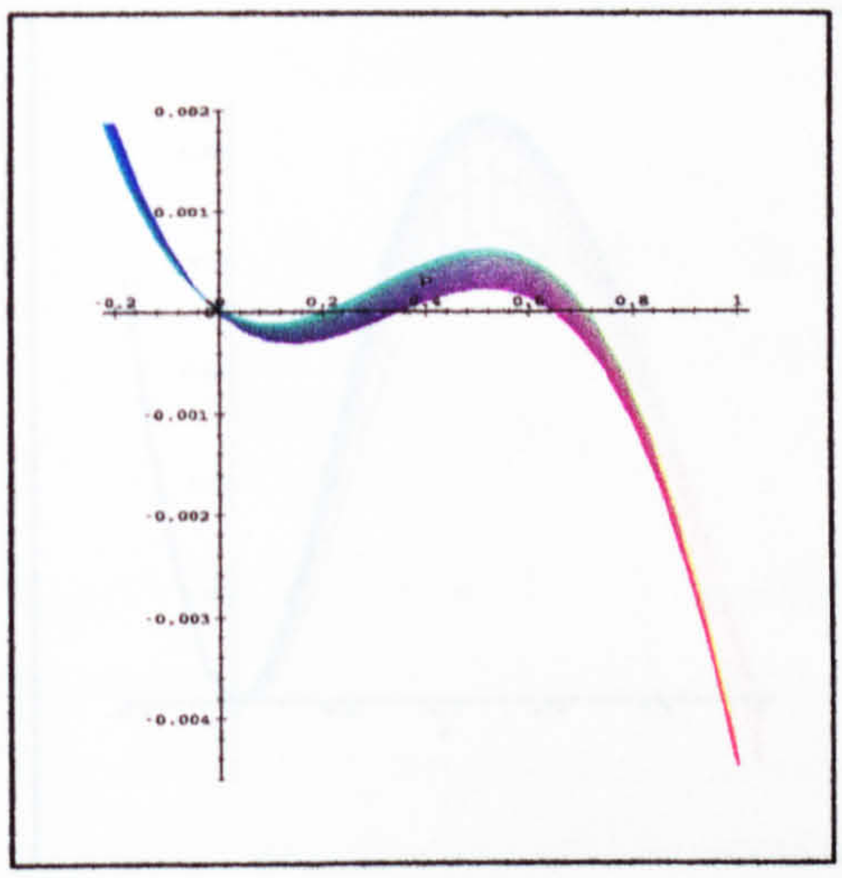

Figure 7.9: Surface representing the change in gene frequency, Δp_t, as a function of initial gene frequency and population size for parameter set 2 in Table 7.1.

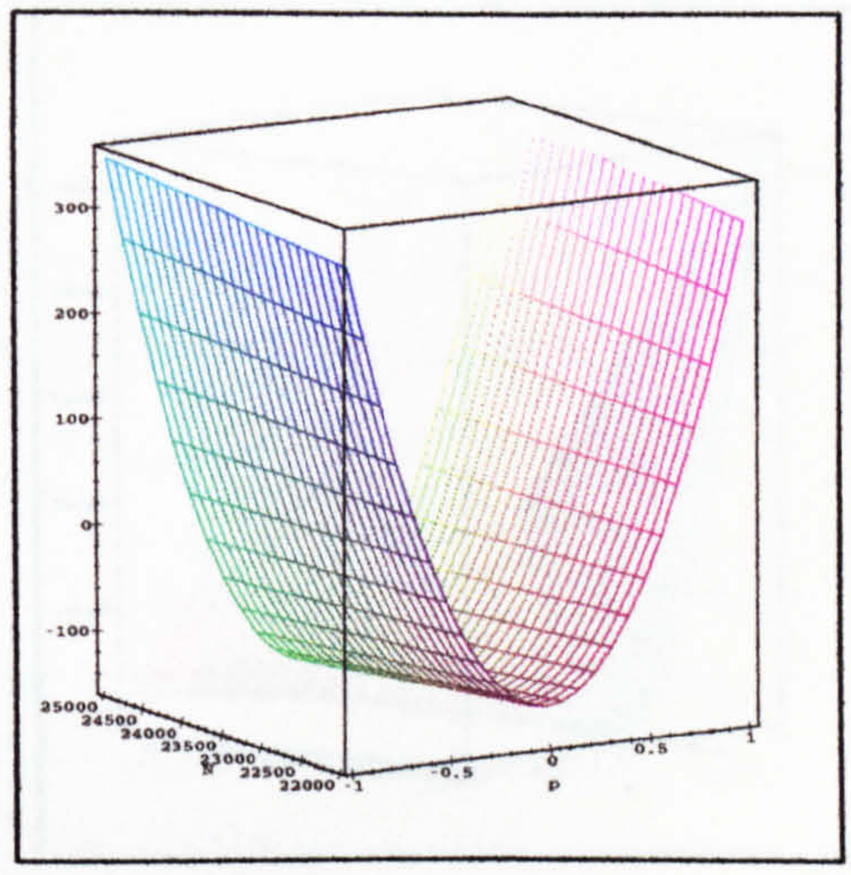

Figure 7.10: Surface representing the change in population size , ΔN_t,as a function of initial gene frequency and population size for parameter set 2 in Table 7.1.

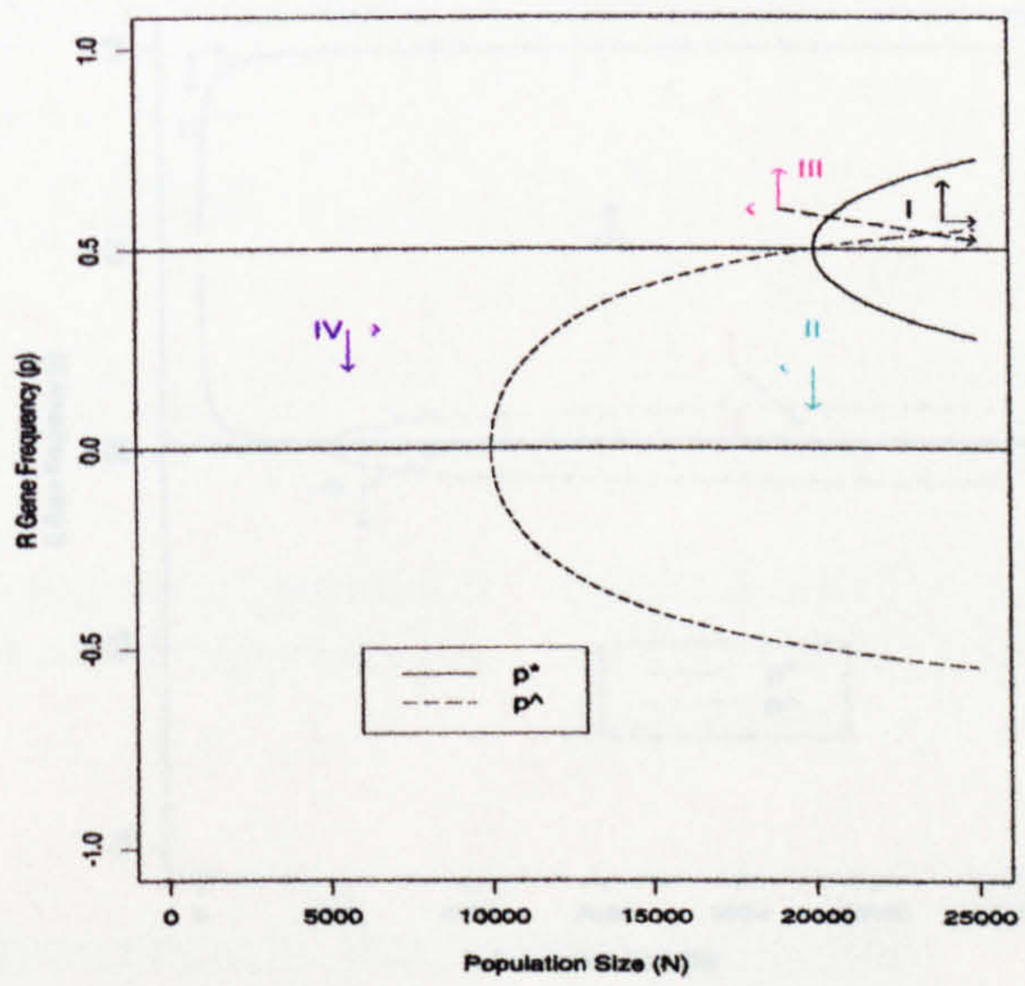

Figure 7.11: $N-p$ plane for parameter set 2 in Table 7.1 with p^* and $\hat{p}$ representing equilibrium gene frequency and equilibrium population size respectively, with an intersection point of $(0.5, 20000)$.

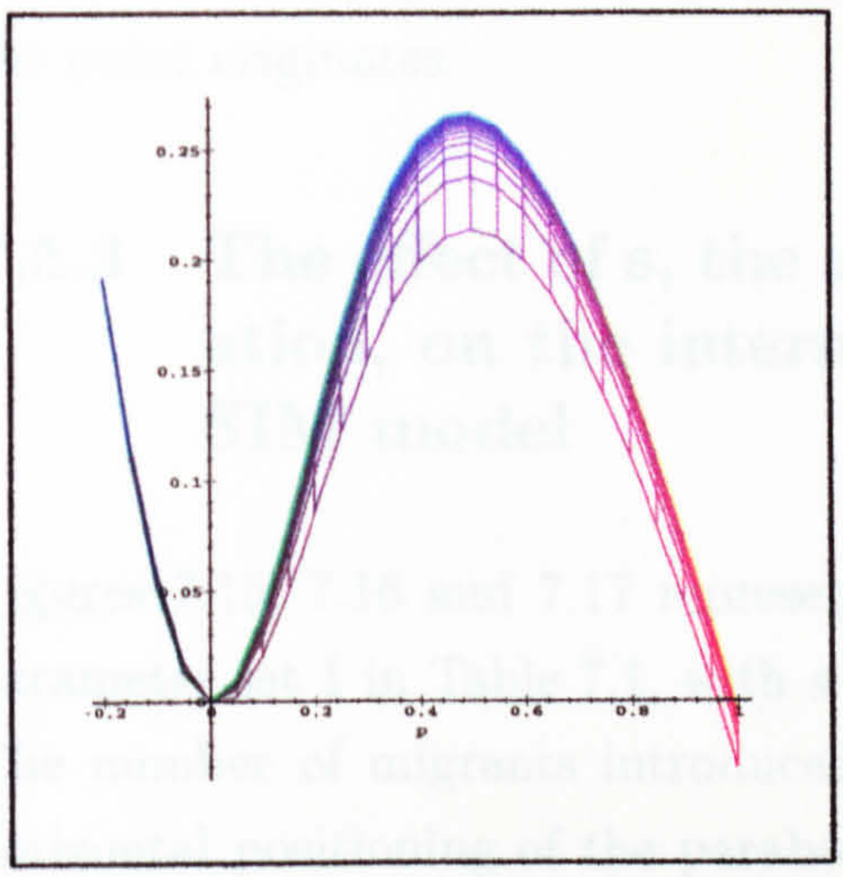

Figure 7.12: Surface representing the change in gene frequency, Δp_t, as a function of initial gene frequency and population size for parameter set 3 in Table 7.1.

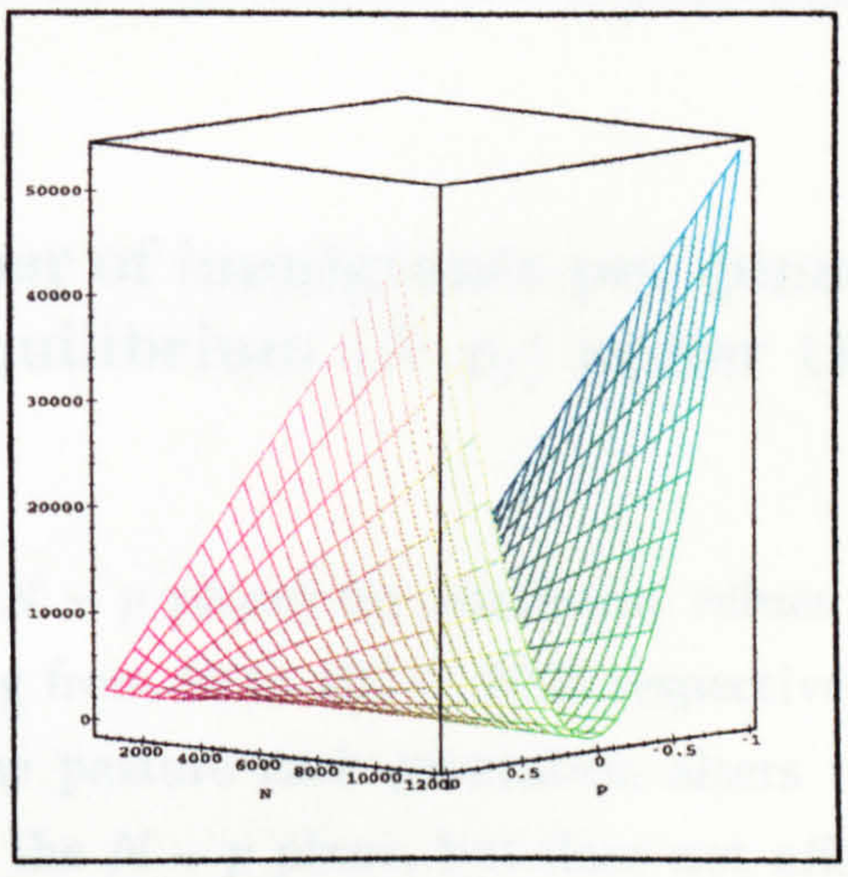

Figure 7.13: Surface representing the change in population size, ΔN_t, as a function of initial gene frequency and population size for parameter set 3 in Table 7.1.

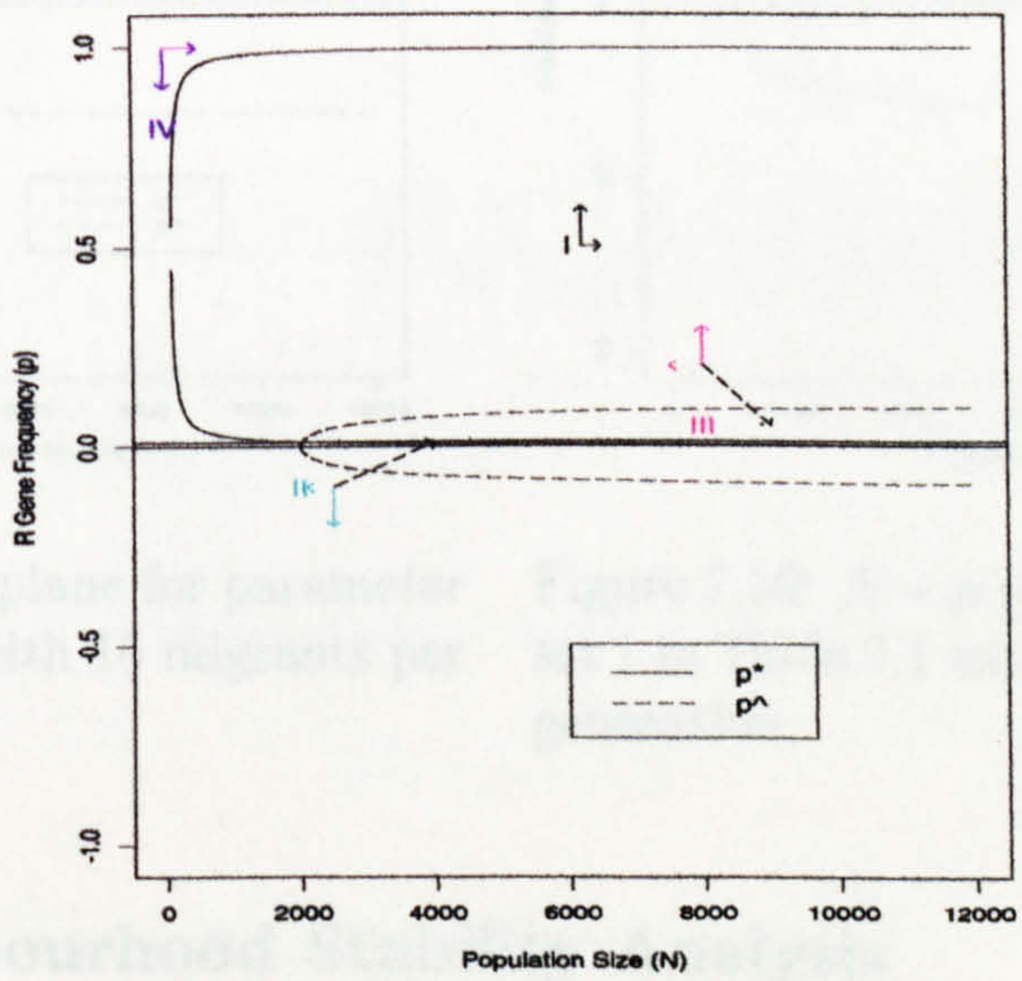

Figure 7.14: $N-p$ plane for parameter set 3 in Table 7.1 with p^* and $\hat{p}$ representing equilibrium gene frequency and equilibrium population size respectively, with an intersection point of $(0.01, 2022.47)$.

Consequently, for any arbitrarily chosen set of initial conditions, the outcome of that particular population is determined by the region in the $N-p$ plane where the point originates.

7.5.3 The effect of s, the number of immigrants per generation, on the internal equilibrium $(\hat{N}, p_I)$ under the SIM model

Figures 7.15, 7.16 and 7.17 represent the $N-p$ planes for numerical values in parameter set 1 in Table 7.1, with s varying from 10 to 100 to 1000 respectively. The number of migrants introduced to the pasture each generation alters the horizontal positioning of the parabolas on the $N-p$ plane, but does not affect the vertical placement of the parabolas. This means that as the immigration rate increases, the size at which the population equilibrates increases, but the equilibrium R gene frequency remains unchanged.

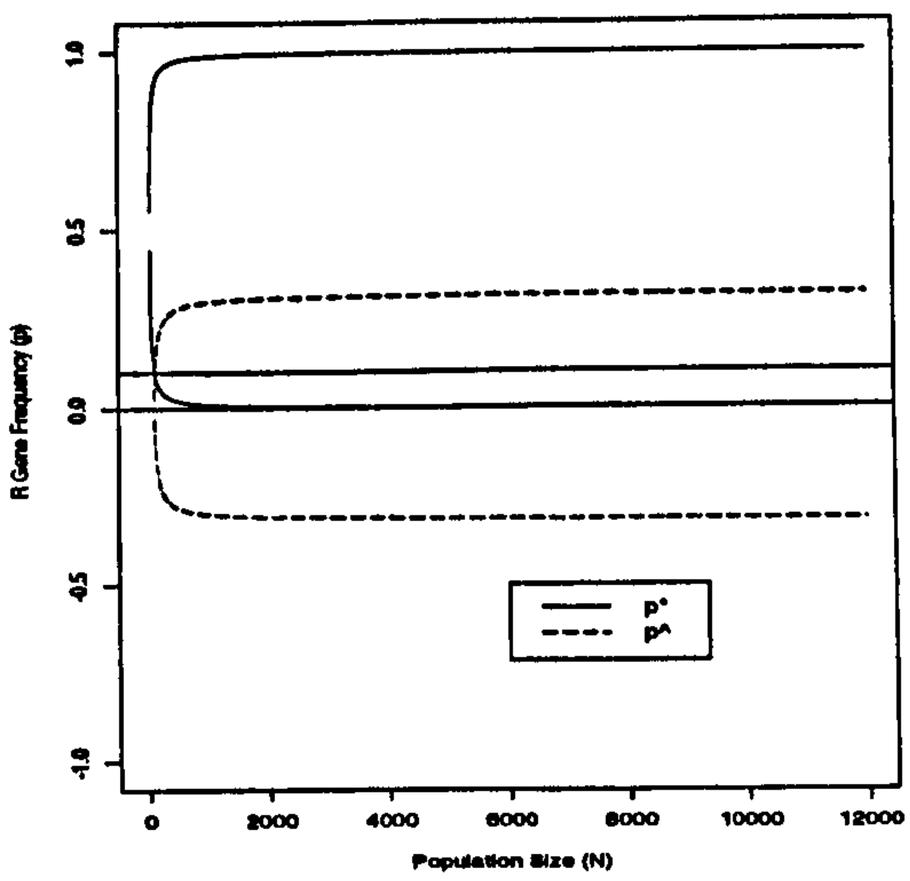

Figure 7.15: $N-p$ plane for parameter set 1 in Table 7.1 with 10 migrants per generation.

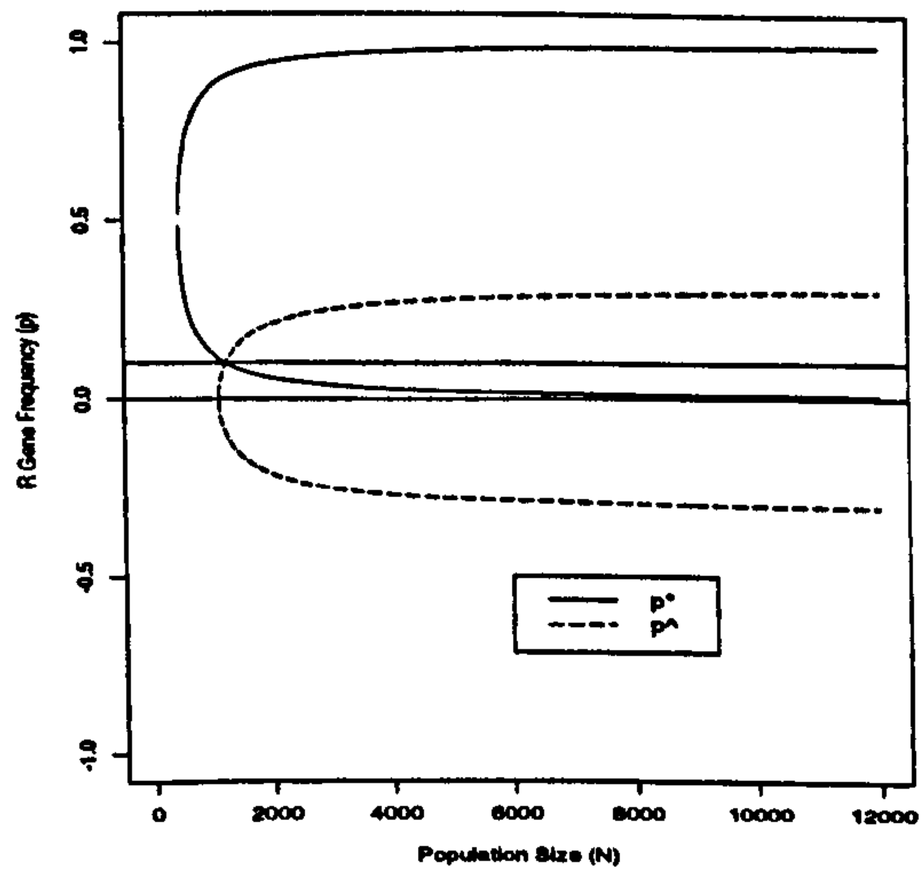

Figure 7.16: $N-p$ plane for parameter set 1 in Table 7.1 with 100 migrants per generation.

7.5.4 Neighbourhood Stability Analysis

Stability of the SIM Model

It has been shown that three points of equilibrium exist under the SIM model

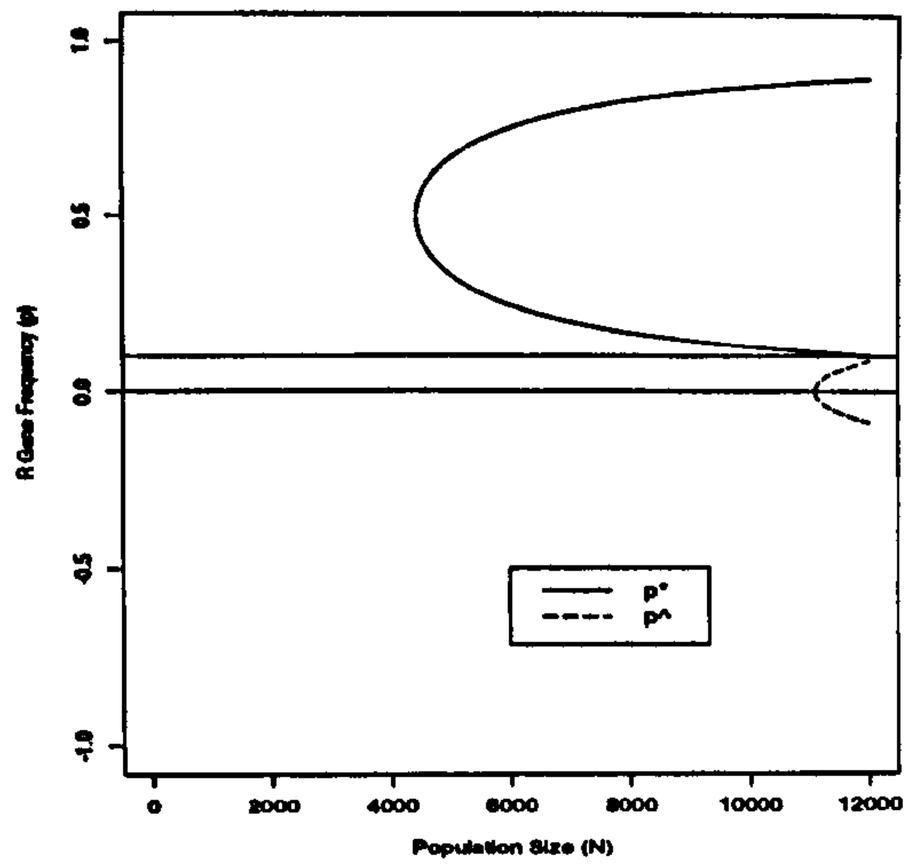

Figure 7.17: $N-p$ plane for parameter set 1 in Table 7.1 with 1000 migrants per generation.

(i) $p^* = 0,\ N^* = \frac{s}{(1-f\alpha\mu-(1-\alpha)\beta}$

(ii) $p^* \to 1$ as $N^* \to \infty$

(iii) $p^* = 1 + \frac{(1-(f\alpha+(1-\alpha)\beta))}{f\alpha(1-\mu)h},\ N^* = \frac{f\alpha(1-\mu)sh^2}{[1-(f\alpha+(1-\alpha)\beta)][f\alpha(\mu-1)h^2-[1-(f\alpha+(1-\alpha)\beta)](2h-1)]}$

In Chapter 6 we introduced the concept of stability of a two dimensional model. For the SIM model,

$$F_{SIM} = p_{t+1} = \frac{N_t\left[f\alpha(1-\mu)\left[p_t^2+p_t(1-p_t)(1-h)\right]+\left[f\alpha\mu+(1-\alpha)\beta\right]p_t\right]}{N_t\left[\bar{w}_t(H)+\bar{w}_t(P)\right]+s}$$

$$G_{SIM} = N_{t+1} = N_t\left[\bar{w}_t(H)+\bar{w}_t(P)\right]+s \tag{7.33}$$

The equilibria, (N^*, p^*) will be (locally) stable if

$$\phi < \gamma + 1 < 2$$

where

$$\phi = A_{11} + A_{22}$$

and

$$\gamma = A_{11}A_{22} - A_{12}A_{21}$$

A_{11}, A_{12}, A_{21}, and A_{22} are the partial derivatives of both equations in (7.33) with respect to p and N. That is

$$\begin{aligned} A_{11} &= \left.\frac{\partial F_{SIM}}{\partial p}\right|_{p=p^*;N=N^*} \\ A_{12} &= \left.\frac{\partial F_{SIM}}{\partial N}\right|_{p=p^*;N=N^*} \\ A_{21} &= \left.\frac{\partial G_{SIM}}{\partial p}\right|_{p=p^*;N=N^*} \\ A_{22} &= \left.\frac{\partial G_{SIM}}{\partial N}\right|_{p=p^*;N=N^*} \end{aligned} \tag{7.34}$$

and so

$$\begin{aligned} A_{11} &= \frac{N\left[f\alpha(1-\mu)\left(2p+(1-p)(1-h)-p(1-h)\right)+f\alpha\mu+(1-\alpha)\beta\right]}{N\left[f\alpha(1-\mu)\left(p^2+2p(1-p)(1-h)\right)+f\alpha\mu+(1-\alpha)\beta\right]+s} \\ &- \frac{N^2\left[f\alpha(1-\mu)\left(p^2+p(1-p)(1-h)\right)+\left(f\alpha\mu+(1-\alpha)\beta\right)p\right]}{\left[N\left[f\alpha(1-\mu)\left[p^2+2p(1-p)(1-h)\right]+f\alpha\mu+(1-\alpha)\beta\right]+s\right]^2} \\ &* \frac{f\alpha(1-\mu)+(1-\alpha)\beta\left[2p+s(1-p)(1-h)-2p(1-h)\right]}{\left[N\left[f\alpha(1-\mu)\left[p^2+2p(1-p)(1-h)\right]+f\alpha\mu+(1-\alpha)\beta\right]+s\right]^2} \end{aligned} \tag{7.35}$$

$$\begin{aligned} A_{12} &= \frac{f\alpha(1-\mu)\left[p^2+p(1-p)(1-h)\right]+\left(f\alpha\mu+(1-\alpha)\beta\right)p}{N\left[f\alpha(1-\mu)\left[p^2+2p(1-p)(1-h)\right]+\left(f\alpha\mu+(1-\alpha)\beta\right)\right]+s} \\ &- \frac{N\left[f\alpha(1-\mu)\left[p^2+p(1-p)(1-h)\right]+\left(f\alpha\mu+(1-\alpha)\beta\right)\right]}{\left[N\left[f\alpha(1-\mu)\left[p^2+2p(1-p)(1-h)\right]+f\alpha\mu+(1-\alpha)\beta\right]+s\right]^2} \\ &* \frac{\left[f\alpha(1-\mu)\left[p^2+2p(1-p)(1-h)\right]+f\alpha\mu+(1-\alpha)\beta\right]}{\left[N\left[f\alpha(1-\mu)\left[p^2+2p(1-p)(1-h)\right]+f\alpha\mu+(1-\alpha)\beta\right]+s\right]^2} \end{aligned} \tag{7.36}$$

$$A_{21} = Nf\alpha(1-\mu)\left[2p+2(1-p)(1-h)-2p(1-h)\right]$$

$$A_{22} = f\alpha(1-\mu)\left[p^2+2p(1-p)(1-h)\right]+f\alpha\mu+(1-\alpha)\beta \tag{7.37}$$

Evaluation of A_{11}, A_{12}, A_{21}, and A_{22} at the equilibria (p^*, N^*), increases the complexity of the equations quite drastically, and so we shall proceed with a numerical analysis of the stability of the fixed points

Table 7.2: Stability of equilibria in SIM Model for parameter values in Table 7.1.

Parameter Set	Equilibria			Stability
	Boundary		Intermediate	
	$(1, \infty)$	$(0, \frac{s}{(1-(f\alpha\mu+(1-\alpha)\beta)})$	$(p_I, \hat{N})$	
1	$(1, \infty)$	$(0, 1111.111)$	$(0.1, 1234.567)$	S/S/US
2	$(1, \infty)$	$(0, 10000)$	$(0.5, 20000)$	S/S/US
3	$(1, \infty)$	$(0, 2000)$	$(0.01, 2022.4719)$	S/S/US
4	$(1, \infty)$	$(0, 123.4567)$	$(0.9, 1234.567)$	S/S/US

It has been established that each population in Table 7.1 must approach or remain at one of three equilibria. Table 7.2 gives the three equilibria for each parameter set in Table 7.1, and shows which equilibrium points are (locally) stable (S), or not (US). A stable equilibrium point suggests that provided the population starts within the domain of attraction, it will always approach that equilibrium. Whereas, an unstable equilibrium suggests that unless the population starts exactly at that point, the population will end up approaching one of the other two equilibria, depending on which region the point is disturbed into. Table 7.2 shows that both boundary equilibria are stable within their domain of attraction, but that the intermediate equilibrium is unstable.

In conclusion, it appears that although an equilibrium does exist that represents population control and the concomitant suppression of resistance, the point is not stable which means that small perturbations about this point will not return the system to equilibrium. This suggests that the system must start off at this point at which it will remain provided nothing is done to upset the equilibrium. However, once perturbed, the population will enter into the domain of attraction for one of the boundary equilibria.

7.6 Discussion

The development of resistance to anthelmintics by the economically important species of nematode over the last two decades has many similarities with the development of insecticide resistance in insects since the start of the century (Roush, 1990).

Despite obvious differences in the life cycles of ecto- and endo-parasites and in the mechanisms of resistance, a great wealth of knowledge is being exchanged by both disciplines.

Currently, researchers are shifting the emphasis from documentation and monitoring of anthelmintic resistance to the task of controlling and managing resistance.

To date, there have been three different approaches proposed for controlling and managing resistance.

Chemical Control

The catastrophic effects as a result of excessive and sporadic use of chemical agents on nematode worms have been instrumental in creating a more responsible approach to resistance control. Coupled with a greater willingness to conform to strict control guidelines is the introduction of practical management models such as those of Barnes and Dobson (1995), Gettinby *et al* (1989) and Smith (1990), that provide decision support on alternative drug usage that optimises drug efficacy whilst impeding the evolution of drug resistance. There are a number of strategies adopted to impede the onslaught of mass resistance

(i) the sequential use of drugs involves using a drug with a specific mode of action until it becomes ineffective, then switching to another with an alternative mode of action,

(ii) drug rotation which involves alternating a variety of different drugs with different modes of action over a period of time, and finally,

(iii) drug mixtures where two or more drugs with different modes of action are administered simultaneously.

These may, at least in the short term, prolong the life of the highly effective drugs in use at the moment, and may play a significant role in the development

of new drugs. However, concern is mounting over the harmful effects of drugs in the environment as well as in the animal. Non-chemical methods of control are becoming a more realistic alternative to drug treatment as research effort in these fields increases.

Biological Control

Chemical control of anthelmintic resistance via sequential treatment, drug rotation or mixtures may extend the usefulness of these drugs into the next century. However as a long term strategy for the control or eradication of resistance, given that the development of new more effective drugs is becoming more costly and time consuming, may not be feasible. There is no option but to pursue other avenues of control. First introduced as a means of controlling insecticide resistance (Comins, 1977;Taylor and Georghiou, 1979), the technique of overwhelming a resistant strain of nematode worm with a susceptible strain was suggested as a means of suppressing anthelmintic resistance by Van Wyk (1990). So far, this method has only been experimentally tested on veld ram units in South Africa.

Two main problems have prevented widespread acceptance of this control method in the insect domain. The first of the problems is do to with the coverage of pesticide on pasture which is notoriously inconsistent and uneven, making it very difficult to ensure a high kill of the heterozygote genotypes (RS). The second problem is one of logistics-ensuring that a high proportion of the heterozygotes are killed whilst protecting the SS genotypes from pesticide exposure until after they have contributed their genetic material to the next generation, given that all individuals occupy the same area of pasture.

Fortunately, neither of these problems affect nematode populations. The dose of anthelmintics given to nematodes is more tightly controlled than the dose of insecticide given to insects, as drug treatment is confined to the site in the host where the majority of parasites ingested are harboured. Secondly, if it is assumed that treatment is administered post-reproduction, then the susceptible immigrants are able to fulfil their function prior to their eradication by the drug.

Under these circumstances, it appears that this novel method of control may have more success in the field of nematode resistance than it has had in the insect domain.

Genetical Control

The important role of the host in regulating worm population numbers has long been recognised (Anderson and May, 1991). Recently, attempts have been made to model the host-parasite relationship of *T. circumcincta* and its sheep host (Roberts, 1995; Roberts and Heesterbeek, 1995; Roberts and Dobson, 1995; Barnes and Dobson, 1995). These models are based on continuous time and incorporate host factors such as acquired immunity. Stear *at al* (1996) have recently identified a major gene for sheep resistance to *T. circumcincta* , which means effectively that worm-resistant sheep may be bred. Further research is necessary to optimise this strategy so that productivity is not impaired in the process.

Mathematical Implementation

A mathematical model has been developed in this chapter to explore the feasibility of biological control of resistance in nematode populations. The model is an extension of the models in Chapters 5 and 6. These were based on the model of insecticide resistance developed by Taylor and Georghiou (1979). A necessary extension to the insect models was the inclusion of a host into the system. Since treatment is administered to the parasitic stages, it follows that only the ingested proportion of the parasite population are exposed to the drug; those not ingested by the host remain on pasture untreated. Thus the target population of nematode parasites is smaller and easier to access than the target population of insects. A further extension to the model involved the creation of areas of refugia within the host where parasites were inaccessible to the drug, a phenomenon not yet fully understood but thought to have considerable impact on nematode population dynamics.

The SIM model in this chapter models anthelmintic resistance in a nematode population and investigates the possibility of control via the inward migration of susceptible strains.

We demonstrated in Chapters 5 and 6, that once a population contains even a small proportion of resistant strains, without intervention, the population will eventually become fully resistant. Flooding the pasture with susceptible strains of parasite re-introduces susceptibility to the population and improves the chances of the drug working on the population by exploiting the fact that these parasites

mate at random. We have shown, however that in the long term conservation of susceptibility and the concomitant control of parasite numbers by inward migration of susceptible strains is only possible under certain circumstances.

A graphical approach was adopted to illustrate the effect of this novel technique of resistance control. There existed one region in the $N - p$ plane, called region II, where control was possible if the population originated in that region. Within region II, the R gene frequency would decrease as would parasite numbers. Predictions could be made about the fate of a population originating in any of the other regions, however, region II was the only region that represented resistance and parasite numbers control, respectively. This region could be increased in area by altering the migration rate per generation, s, so that control of the population would be possible with larger initial parasite infection levels.

Van Wyk (1990) has called for the urgent attention of all researchers in this field to find alternate methods of control, as the use of anthelmintic compounds will not solve the problem of resistance alone. A great deal more research has to be undertaken on the alternative method suggested by these authors, both theoretically and practically.

Chapter 8

Discussion

In this thesis, the life cycle of *T. circumcincta* has been modelled from two different perspectives. First, the effect of environmental factors, in particular temperature, on the development rate of *T. circumcincta* free-living on pasture is examined. The impact of developmental variability on parasite infection levels in the field is then explored. Secondly, the parasitic stage of the nematode life cycle is investigated with respect to the growth and evolution of drug resistance within a typical nematode population. In particular, the effect of specific life history parameters on the growth and evolution of anthelmintic resistance is examined and a model to investigate the possible suppression or eradication of resistance is presented.

8.1 The Effect of Environmental Factors on the Life Cycle of *T. circumcincta*

Chapters 2, 3 and 4 present models of the life cycle of *T. circumcincta* referring specifically to the dynamics of the free-living stages. Three main points of discussion arose from this work.

8.1.1 Development Models

In Chapter 2, the need for a more accurate representation of the temperature development rate phenomena in free-living nematode worms was highlighted. Conventional models of nematode development (Paton, 1983) were shown to be inadequate at describing this phenomenon at high temperatures. Beyond an opti-

mum temperature, different biological mechanisms act on the organism, to those experienced by the organism at moderate temperatures and the developmental process is altered. A comparative analysis of a current temperature development rate model for nematodes (Paton, 1983) and the more sophisticated models for insect development (Stinner *et al*, 1974; Logan *et al*, 1976) was undertaken. It was concluded that the model of Logan *et al* (1976), whereby the assumed mechanisms controlling development are described within the model, by far gave the best description of the temperature-development rate relation. This model has many advantages. By comparing the Final Sums of Squares for each model with that of Logan *et al* (1976), it was clear that the fit to the data for all free-living life stages of *T. circumcincta* was best for this model. Furthermore, the biophysical properties of the model mean that biologists are provided with a greater understanding of the temperature dependent development response for a given species, (Wagner, 1984a). The flexibility of this modelling approach allows us to investigate various theories on the mechanisms of the heat denaturization effect on the development of organisms at high temperatures.

8.1.2 Developmental Variation

Having presented a usable model for the description of the temperature development rate phenomena in nematodes, the concept of developmental variability in response to temperature was introduced. Up until now, the dynamics of the free-living stages have been modelled under the assumption that development and survival on pasture is influenced by the environment, particularly temperature and hence patterns of infection can be predicted by climate. These models relate mean development time to temperature and so assume a uniform response within the population. No attempt has been made previously to examine the impact on the population dynamics of nematode parasites when we consider within-population variation in response to temperature.

Previously variation in emergence patterns had been attributed to climatic changes either geographically or temporally. In Chapter 3, using **Osterant**, it was suggested that variation in response to temperature between individuals in a population may account for a great deal of the observed variation in emergence patterns in the field. Consistently, differences in simulated emergence patterns of infective L3s in the field, between *fast*, *average* and *slow* developers were greater than simulated differences between locations or over years. These results serve as a primary indicator of possible alternative sources of variation in infection levels on

the pasture. It is accepted that climate governs free-living development and survival, what is being proposed here is that the genetic constitution of the nematode population is not uniform with respect to individual response to environmental stimuli, and that this genetic variation may be a significant source of observed variation.

Important oversights in the epidemiology of nematode parasites may occur as a result of ignoring those individuals who develop quicker or slower than average. Those individuals in the tails of the developmental distribution may be important contributors to infection levels in the subsequent season as they may be more likely to overwinter on pasture or inhibit within the host.

8.1.3 A Genetic Model Incorporating Multiple Time Delays

A life cycle model incorporating both free-living and intra-host development was proposed in Chapter 4. Combining complex developmental models with genetic rules for mating and reproduction could only be facilitated through computer simulation rather than mathematical analysis.

The genetic aspect of this model was investigated mathematically, however. A simple analytic model was formulated to explore the dynamics of a population of single stage organisms split into three genotype groups according to development rate: *fast*, *average* or *slow*. Of interest was the equilibrium genotype distribution of such a population that reproduced under the assumption of random mixing. Preliminary results indicate that a Hardy-Weinberg equilibrium exists for such a population with the individuals in each genotype group distributed throughout the age classes within that genotype group. Further analysis of this interesting result is now required.

8.2 Drug Resistance

The second half of this thesis addresses the issues of anthelmintic resistance in nematodes. A series of models were designed in Chapters 5 and 6 to explore the dissemination of resistant strains throughout a nematode population. A final model was presented in Chapter 7 to explore a novel method of controlling resistance not modelled previously. Important aspects of the nematode life cycle

were incorporated into these models. These were

(i) the host and pasture environment,

(ii) intra-host and free-living areas of refugia, and

(iii) immigration of resistant and susceptible strains onto pasture.

8.2.1 Describing the Dissemination of Resistance

Analyses of the models in Chapters 5 and 6 revealed that when no form of resistance control was in operation, the population would eventually become fully resistant, the time taken for significant resistance to build up being a directly measurable quantity derived from the original model equations. The effect of the various model parameters on the approach to 100% resistance is discussed with the general conclusions that low ingestion rate (α), high free-living mortality ($1-\beta$), low fecundity (f), a high proportion of ingested larvae entering refugia (μ), a low h value and a low rate of immigration of resistant strains (r), would result in the slowing down of the evolution of resistance.

8.2.2 Controlling the Dissemination of Resistance

At present, the rate of escalation of resistance world-wide is higher than the rate at which new anthelmintic drugs are being developed (Van Wyk, 1990). Practical measures are being taken to slow down the progress of resistance, particularly in Australia with national integrated pest management schemes (IPM) (Waller, 1993). Management of resistance via the careful use of anthelmintics is important in the short term, however, alternative methods of worm control need to be researched urgently. A great deal of experimental effort has gone into the development of alternative worm control programs including

(i) the selection for resistant hosts,

(ii) nematophagous fungi (Gronvold *et al*, 1993), and

(iii) conventional and novel vaccines.

In the meantime, until these methods become practical to use, we must focus on ways to retain susceptibility of the parasites to the drugs.

Barnes and Dobson (1995) explored two alternative methods of control: novel vaccines and nematophagous fungi, using the simulation model for *Trichostrongylus vitrinus*. The results were encouraging, both the vaccine and the fungi worked as well as or better than conventional worm control programs. The need for further research was emphasised, however.

In Chapter 7, a novel method of controlling the evolution of resistance is addressed. This method had initially been advocated for the control of insecticide resistance (Taylor and Georghiou, 1979), and later was suggested as a means of controlling anthelmintic resistance in nematode populations by Van Wyk (1990). To date, the biological control of resistant strains of nematode by replacing them with susceptible strains has never been considered in a mathematical model.

The novel method of controlling resistance by overwhelming the resistant strain by a susceptible one on pasture, exploits the Mendellian principle of segregation and recombination of genes at reproduction (Strickberger, 1976; Crow and Kimura, 1970). A mathematical model was formulated in Chapter 7 to investigate the feasibility of such an approach. Results from the model suggest that the deliberate introduction of parasites susceptible to the anthelmintic drug onto a pasture containing resistant strains may suppress and even reduce levels of resistance in the field. Provided initial population size and gene frequency are within a well-defined region on the $N - p$ plane, determined by parameters such as immigration levels, (s), proportion of heterozygotes killed by drug, (h), fecundity, (f), ingestion rate, (α) and proportion of individuals ingested that enter refugia, (μ), the dissemination of resistance through the population will be suppressed. This means that there are possibilities of halting the evolution of resistance in a population and controlling corresponding levels of parasitism in the field.

8.3 Future Course of Research

In the last 15 years, a great deal of progress has been made in the development of practical models for animal disease control. Subsequently these models have been adapted and used to investigate and explore the evolution of resistance in parasite populations of sheep. This thesis has addressed certain issues relating to the nematode life cycle and drug resistance that many of the previous models had not considered, such as developmental variability and novel methods of resistance control.

In Chapter 2 , the importance of within-population variability in development rates was highlighted. It is recommended that future data collection focuses on the entire distribution of development times rather than on mean population behaviour. This would provide the data needed in Chapter 3 to evaluate the contribution of individuals in the tails of the developmental distribution to subsequent infection levels in the field, particularly with respect to the succeeding seasons infection levels as a result of overwintered and inhibited larvae.

Many of the current models of anthelmintic resistance focus on the progression of resistance and methods of controlling the dissemination of resistance using conventional resistance control methods, such as drug rotation, pasture switching and drug mixtures. Few attempts are being made to explore alternative methods. Now is the time to rigorously test alternative methods, both experimentally and practically, whilst the resistance management schemes are still effective. Mathematical models must be used in this process to save time and money and direct future research efforts.

Bibliography

Abrami, G., (1972). Optimum mean temperature for plant growth calculated by a new method of summation. *Ecology*, **53**, 893-900.

Abramowitz, M. and Stegun, I.A., (1970). A Handbook of Mathematical Functions. Dover Publications Inc., New York.

Allen, J.C., (1976). A modified sine wave method for calculating day-degrees. *Ibid.*, **5**, 388-396.

Anderson, R.M. and May, R.M., (1991). *Infectious diseases of humans: dynamics and control.* Oxford University Press, Oxford.

Andrewartha, H.G. and Birch, L.C., (1954). The Distribution and Abundance of Animals. University of Chicago Press, Chicago, Illinoi.

Arnold, C.Y., (1960). Maximum-minimum temperatures as a basic for computing heat units. *Proc. Am. Soc. Hort. Sci.*, **76**, 682-692.

Bailey, N.T.J., (1975). The Mathematical Theory of Infectious Diseases. Griffin, London.

Barger, I.A., (1982). Helminth parasites and animal production. In: Biology and Control of Endoparasites. (Eds. L.E.A. Symons, A.D.Donald and J.K. Dineen), pp. 133-135. Academic Press, Sydney.

Barnes, E.H. and Dobson, R.J., (1995). Worm control and anthelmintic resistance-Adventures with a model. *Parasitology Today*, **11**, 56-63.

Baskerville, G.L. and Emin, P., (1969). Rapid estimation of heat accumulation from maximum and minimum temperatures. *Ecology*, **50**, 514-517.

Britt, D.P., (1982). Benzimadazole-resistant nematodes in Britain. *Veterinary Record*, **110**, 343-344.

Caswell, H., (1989). Matrix Population Models, Sinauer Associates Inc.

Cawthorne, R.J.G. and Cheong, F.H., (1984). Prevalence of anthelmintic resistant nematodes in sheep in south-east England. *Veterinary Record*, **114**, 562-564.

Chiang, C.L., (1980). An Introduction to Stochastic Processes and their Applications. Robert E. Krieger Publishing Company, Huntington, New York.

Coles, G.C., (1992). Survey of anthelmintic resistant nematodes. *Veterinary Record*, **131**, 20.

Comins, H.N., (1977). The development of insecticide resistance in the presence of migration. *Journal of Theoretical Biology*, **64**, 177-197.

Coyne, M.J. and Smith, G., (1992). The Development and mortality of free-living stages of *Haemonchus contortus* in laboratory culture. *International Journal of Parasitology*, **22**, 641-650.

Crofton, H.D., (1963). Nematode parasite populations in sheep and on pasture. Technical Communication No. 25. Commonwealth Bureau of Helminthology.

Crofton, H.D., (1965). Ecology and biological plasticity of sheep nematodes.1. The effect of temperature on the hatching of eggs of some nematode parasites of sheep. *Cornel Veterinarian*, **55**, 242-250.

Crow, J.F.K., & Kimura, M., (1970). An introduction to population genetics. Harper and Row.

Evans, P., (1988). Anthelmintic Resistance: Studies on Sheep Flocks in the North-East of England. Ph.D Thesis, University of Newcastle upon Tyne.

Georghiou, G.P., (1972). The evolution of resistance to pesticides. *Annual Review of Ecological Systems*, **3**, 133-168.

Georghiou, G.P. and Taylor, C.E., (1977). Genetic and biological influences in the evolution in insecticide resistance. *Journal of Economic Entomology*, **70**, 319-323.

Georghiou, G.P. and Taylor, C.E., (1977). Operational influences in the evolution of insecticide resistance. *Journal of Economic Entomology*, **70**, 653-658.

Gettinby, G., Hope-Cawdery, M.J. and Grainger, J.N.R., (1974). Forecasting the incidence of fascioliasis from climatic data. *International Journal of Biomete-*

orology, **18**, 319-323.

Gettinby, G., Bairden, K., Armour, J. and Benitex-Usher, C., (1979). A prediction model for bovine ostertagiasis. *Veterinary Record*, **105**, 57-59.

Gettinby, G. and McClean, S, (1979). A Matrix formulation of the life cycle of liver fluke. *Proceedings of the Royal Irish Academy*, **79B**, 155-167.

Gettinby, G., Soutar, A., Armour, J. and Evans, P., (1989). Anthelmintic resistance and the control of ovine ostertagiasis: A drug action model for genetic selection. *International Journal for Parasitology*, **19**, 369-376.

Gordon, H.M., (1948). The epidemiology of parasitic diseases with special reference to studies with nematode parasites of sheep. *The Australian Veterinary Journal*, 17-45.

Grenfell, B., Dietz, K. and Roberts, M., (1995). Modelling the immuno-epidemiology of macroparasites in wildlife host populations. In: Ecology of Infectious Diseases in Natural Populations (Ed. B.Grenfell & A. Dobson).

Gronvold, J., Wolstrup, J., Nansen, P. and Henriksen, S.A., (1993). Nematode-trapping fungi against parasitic cattle nematodes. *Parasitology Today*, **9**, 137-140.

Gulland, F.M.D., (1991). The Role of Parasites in the Population Dynamics of Soay Sheep on St. Kilda. Ph.D Thesis. Girton College, University of Cambridge.

Harte, J., (1988). Consider a spherical cow: A course in environmental problem solving. University Science Books.

Hazelby, C.A., Probert, A.J., Rowlands, D.AP.T., (1994). Anthelmintic resistance in nematodes causing parasitic gastroenteritis of sheep in the UK. *Journal of Veterinary Pharmacological Therapy*, **17**, 245-252.

Heesterbeek, and Roberts, M.G., (1995). Threshold quantities for helminth infections. *Journal of Mathematical Biology*, **33**, 415-434.

Hong, C., Hunt, K.R., Harris, T.J., Coles, G.C., Grimshaw, W.T.R. and McMullin, P.F., (1992). A survey of benzimadazole resistant nematodes in sheep in three counties of southern England. *Veterinary Record*, **131**, 5-7.

Hope-Cawdery, M.J., Gettinby, G. and Grainger, J.N.R., (1978). Mathematical models for predicting the prevalence of liver fluke disease and its control from

biological and meteorological data. In: Weather and Parasitic Animal Disease (Ed. T.E. Gibson). World Meteorological Organisation, Geneva, WMO-Tech. Note. 159, 21-28.

Isham, V., (1995). Stochastic models of host-macroparasite interaction. *Annals of Applied Probability*, **5**, to appear.

Jackson, F., (1989). Studies on the epidemiology of *Trichostrongylus vitrinus*(Loos 1905). Ph.D Thesis. Napier Polytechnic.

Kates, K.C., (1965). Ecological aspects of helminth transmission in domesticated animals. *American Zoologist*, **5**, 95-130.

Krogh, A., (1914). On the influence of the temperature on the rate of embryonic development. *Z Allg. Physiol.*, **16**, 163-177.

Leathwick, D.M., Barlow, N.D. and Vlassoff, A., (1992). A model for nematodiasis in New Zealand lambs. *International Journal for Parasitology*, **22**, 789-799.

Lefkovitch, L.P., (1965). The study of population growth in organisms grouped by stages. *Biometrics*, **21**, 1-18.

LeJambre, L.F., (1977). Resistance of selected lines of *T. circumcincta* to thiabendazole, morantel and levamisol. *International Journal of Parasitology*, **7**, 473-479.

Leslie, P.H., (1945). On the use of matrices in certain population mathematics. *Biometrika*, **33**, 183-212.

Levine, N.D., (1963). Weather, climate and the bionomics of ruminant nematode larvae. *Advances in Veterinary Science*, 8, 215-261.

Lewis, E.R., (1977a). Network models in population biology. Springer-Verlag, Berlin.

Logan, J.A., Wollkind, D.J., Hoyt, S.C. and Tanigoshi, L.K., (1976). An analytic model for description of temperature dependent rate phenomena in arthropods. *Environmental Entomology*, **5**, 1133-1140.

Mani, G.S., (1985). Evolution of resistance in the presence of two insecticides. *Genetics*, **109**, 761-783.

May, R.M., (1974). Stability and Complexity in Model Ecosystems. Princetown

University Press.

McBride, E.B., (1970). Obtaining Generating Functions. Springer Tracts in Natural Philosophy, Volume 21.

Michel, J.F., Cawthorne, R.J.G., Anderson, R.M., Armour, J., Clarkson, M.J. and Thomas, R.J., (1982). Resistance to anthelmintics in Britain: Husbandry practices and selective pressure. In *Facts and Reflections IV: Resistance of Parasites to Anthelmintics.* pp 41-50. Central Veterinary Institute, Lelystad, The Netherlands.

Mickens, R.E., (1990). Difference Equations: Theory and Applications. Van Nostrand Reinhold, New York.

Nisbet, R.M. and Gurney, W.S.C., (1982). Modelling Fluctuating Populations. John Wiley & Sons Ltd.

Ollerenshaw, C.B., (1974). Forecasting liver fluke disease. In: The Effects of Meteorological Factors Upon Parasites. *Symposium of the British Society of Parasitology*, **12** 33-52.

Ollerenshaw, C.B. and Rowlands, W.T., (1959). A method of forecasting the incidence of fascioliasis in Anglesey. *Veterinary Record*, **71**, 591-598.

Pandey, V.S., Chaer, A. and Dakkak, A., (1993). Effect of temperature and relative humidity on survival of eggs and infective larvae of *Ostertagia circumcincta*. *Veterinary Parasitology*, **49**, 219-227.

Paton, G., (1983). Mathematical models for the prediction and control of ovine parasitic gastro-enteritis. Ph.D Thesis, University of Strathclyde.

Paton, G., Thomas, R.J. and Waller, P.J., (1984). A prediction model for parasitic gastro-enteritis in lambs. *International Journal of Parasitology*, , .

Precht, H., (1973). Temperature and Life. Springer Verlag, Berlin.

Press, W.H., Flannery, B.P., Teukolsky, S.A. and Vetterling, W.T., (1992). Numerical Recipes in Pascal. Cambridge University Press.

Prichard, R.K., Hall, C.A., Kelly, J.D., Martin, I.C.A. and Donald, A.D. , (1980). The problem of anthelmintic resistance in nematodes. *Australian Veterinary Journal.*, **56**, 239-250.

Prichard, R.K., (1994). Anthelmintic Resistance. *Veterinary Parasitology*, **54**,

259-268.

Regniere, J., Rabb, R.L. and Stinner, R.E., (1981). *Popillia japonica*: Simulation of temperature-dependent development of the immatures, and prediction of adult emergence. *Environmental Entomology*, **10**, 290-296.

Renshaw, E., (1993). *Modelling biological populations in space and time.* Cambridge University Press, Cambridge.

Revie, C.W., Reid, S.W.J., Irwin, T., Mellor, D.J., Love, S. and Gettinby, G., (1994). Eqwise and the development of diagnostic aids in equine coughing. *International Journal of Applied Expert Systems*, **2:3**, 175-190.

Roberts, M.G. and Grenfell, B.T., (1991). The population dynamics of nematode infection of ruminants: Periodic perturbations as a model for management. *IMA Journal of Mathematics Applied in Medicine & Biology*, **8**, 83-93.

Roberts, M.G. and Grenfell, B.T., (1992). The population dynamics of nematode infection of ruminants: The effect of seasonality in the free-living stages. *IMA Journal of Mathematics Applied in Medicine & Biology*, **9**, 29-41.

Roberts, M.G., (1995). A pocket guide to host-parasite models. *Parasitology Today*, **11**, 172-177.

Roberts, M.G. and Dobson, A.P., (1995). The population dynamics of communities of parasitic helminths. *Mathematical Biosciences*, **126**, 191-214.

Roberts, M.G. and Heesterbeek, (1995). The dynamics of nematode infections of farmed ruminants. *Parasitology*, **110**, 493-502.

Roush, R.T., (1990). Genetics and management of insecticide resistance: Lessons for resistance in internal parasites? In: Resistance of Parasites to Antiparasitic Drugs (ICOPA). (Ed. J.C. Boray, P.J. Martin, and R.T. Roush).

Salih, N.E. and Grainger, J.N.R., (1981). The effect of constant and changing temperatures on the development of the eggs and infective larvae of *T. circumcincta* . *Journal of Thermal Biology*, **7**, 35-38.

Sanderson, E.D. and Peairs, L.M., (1913). The relation of temperature to insect life. *N.H. Coll. Agric. Exp. Stn. Tech. Bull.*, **7**.

Scott, M.E. and Smith, G., (1994). Parasitic and Infectious Diseases. Academic Press.

Scott, E.W., McKellar, Q.A., Armour, J., Coop, R.L., Jackson, F. and Mitchell, G.B.B., (1990). Incidence of anthelmintic resistance in Scotland, UK. In: Resistance of Parasites to Antiparasitic Drugs (ICOPA). (Ed. J.C. Boray, P.J. Martin, and R.T. Roush).

Sevacherian, V., Stern, V.M. and Mueller, A.J., (1977). Heat accumulation for timing *Lygus* control measures on a safflower-cotton complex. *Journal of Econ.omic Entomology*, **70**, 399-402.

Sharpe, P.J.H. and DeMichele, D.W., (1977). Reaction Kinetics of poikilotherm development. *Journal of Theoretical Biology*, **64**, 649-670.

Smith, G., (1990). A mathematical model for the evolution of anthelmintic resistance in a direct life cycle nematode parasite. *International Journal for Parasitology*, **20**, 913-921.

Smith, G. and Grenfell, B.T., (1994). Modelling of parasite populations-gastrointestinal nematode models. *Veterinary Parasitology*, **54**, 127-143.

Soulsby, E.J.L., (1969). Helminths, arthropods and protozoa of domesticated animals. Bailliere, Tindall.

Stear, M.J., Bairden, K., Bishop, S.C., Buitkamp, J., Duncan, J.L., Gettinby, G., McKellar, Q.A., Park, M., Reid, S.W.J., and Murray, M., (1996). The genetic basis of resistance to *Ostertagia circumcincta* in lambs. In Press.

Stinner, R.E., Gutierrez, A.P. and Butler, G.D., (1974). An algorithm for temperature-dependent growth rate simulation. *Canadian Entomologist*, **106**, 519-524.

Strickberger, M.W., (1976). Genetics. Collier Macmillan Publishers, London.

Taylor, E.L., (1938). Observations on the bionomics of strongyloid larvae in pastures. *The Veterinary Record*, **50**, 1265-1272.

Taylor, H.M., (1968). Some models in epidemic control. *Mathematical Biosciences*, **3**, 383-398.

Taylor, C.E. and Georghiou, G.P., (1979). Suppression of insecticide resistance by alteration of gene dominance and migration. *Journal of Economic Entomology*, **72**, 105-109.

Taylor, M.A. and Hunt, K.R., (1989). Anthelmintic Drug Resistance in the UK. *Veterinary Record*, **125**, 143-147.

Taylor, M.A., (1990). Anthelmintic resistance in nematodes in the UK and Ireland. In: Resistance of Parasites to Antiparasitic Drugs (ICOPA). (Ed. J.C. Boray, P.J. Martin, and R.T. Roush).

Thomas, R.J., (1982). The ecological basis for parasite control. *Veterinary Parasitology*, **11**, 9-24.

Thomas, R.J. and Starr, J.R., (1978). Forecasting the peak of gastro-intestinal nematode infection in lambs. *Veterinary Record*, **103**, 465-468.

Threkeld, W.L., (1934). The life history of *T. circumcincta*. *Virginia Agricultural Experimental Station Technical Bulletin*, **52**, 1-21.

Thrusfield, (1995). Veterinary epidemiology. 2nd edition. Blackwell Science Ltd., Oxford.

Urquhart, G.M., Armour, J., Duncan, J.L., Dunn, A.M. and Jennings, F.W., (1991). Veterinary Parasitology. Longman Scientific and Technical.

Van Wyk, J.A., (1990). Occurrence and dissemination of anthelmintic resistance in South Africa, and management of resistant worm strains. In: Resistance of Parasites to Antiparasitic Drugs (ICOPA). (Ed. J.C. Boray, P.J. Martin, and R.T. Roush).

Wagner, T.L., Wu, H., Sharpe, P.J.H., Schoolfield, R.M., and Coulson, R.N., (1984a). Modelling insect development rates: a literature review and application of biophysical model. *Annals of the Entomological Society of America*, **77**, 208-225.

Waller, P.J., Dobson, R.J., Donald, A.D. and Thomas, R.J. (1981). Populations of strongyloid nematode infective stages in sheep pastures: Comparison between direct pasture sampling and tracer lambs as estimators of larval abundance. *International Journal of Parasitology*, **11**, 359-367.

Waller, P.J., (1993). Towards sustainable nematode parasite control of livestock. *Veterinary Parasitology*, 48, 295-309.

Waller, P.J., (1994). The development of anthelmintic resistance in ruminant livestock. *Acta Tropica*, **56**, 233-243.

Williamson, M., (1972). The Analysis of Biological Populations. Arnold, London.

Young, R.R., Anderson, N., Overend, D., Tweedie, R.L., Malafant, K.W.J. and Preston, G.A.N., (1980). The effect of temperature on the time to hatching of

eggs of the nematode *T. circumcincta* . *Parasitology*, 81, 477-491.